

UNIVERSIDADE DE LISBOA
FACULDADE DE CIÊNCIAS
DEPARTAMENTO DE FÍSICA



Effects of EEG-neurofeedback training on brain functional connectivity

Pedro Miguel Gonçalves Gomes

Mestrado em Engenharia Biomédica e Biofísica

Dissertação orientada por:
Prof. Gina Caetano
Prof. Alexandre Andrade

Preface

The work presented in this thesis was performed at the Evolutionary Systems and Biomedical Engineering Lab of the Institute for Systems and Robotics at Instituto Superior Técnico, between September 2021 and September 2022, on the basis of data formerly acquired with guidance from Prof. Gina Caetano, Dr. Athanasios Vourvopoulos, Prof. Patrícia Figueiredo and Prof. Agostino Rosa, and under the supervision of Prof. Gina Caetano and Prof. Alexandre Andrade.

Acknowledgments

I want to thank to all my supervisors for the help and expertise that they shared with me during this project, especially professor Gina Caetano whom week after week dedicated her time to guide me and help me to overcome every difficulty that I've faced. Together we created the solutions for every obstacle and we're able to reach this point.

Also, I want to thank my family, friends, and girlfriend for all the support. This has been a hard-fought year, yet the best of my life thanks to all of them.

Resumo

O neurofeedback (NF) consiste em medir a atividade cerebral, usando técnicas como a eletroencefalografia (EEG) ou a imagem por ressonância magnética funcional (fMRI), e apresentar ao participante, em tempo real, uma representação de um padrão de atividade de interesse, enquanto lhe é pedido para manipular essa mesma representação através da autorregulação da atividade cerebral (Sitaram et al., 2017). As bases neurofisiológicas desta técnica ainda não são conhecidas na sua totalidade, apesar de vários estudos terem demonstrado que o treino através de NF tende a reorganizar as redes cerebrais. Posto isto, existem poucos estudos que tentam comparar a influência da utilização de diferentes modalidades sensoriais de apresentação do “feedback” nos resultados do treino por NF em EEG, e os poucos estudos existentes não investigam possíveis efeitos nas métricas de conectividade funcional do cérebro.

Neste projeto, pretendemos avaliar o efeito da utilização de diferentes modalidades de “feedback” no treino de NF através EEG (EEG-NF) para o incremento da amplitude relativa da banda alfa superior no canal Cz, e investigar se existe um efeito significativo nos padrões de conectividade funcional do cérebro. Para esse fim, será efetuada a análise de dados previamente recolhidos em 20 participantes saudáveis que realizaram quatro sessões de treino por EEG-NF, que visava incrementar a densidade espectral na banda alfa superior, e que utilizaram diferentes modalidades de feedback (visual, realidade virtual (VR), e auditiva). Os dados de EEG foram pré-processados, com remoção de artefactos através de análise de componentes independentes. Adicionalmente, duas técnicas de re-referenciação do sinal EEG foram utilizadas para comparação posterior, sendo estas a re-referenciação para a média de todos os canais EEG, e a re-referenciação através da aplicação de um Laplaciano de Superfície com parâmetro de rigidez de valores 4 e 3, respetivamente. A avaliação dos resultados foi efetuada a diversos níveis, com a análise: i) das variações intra-sessão da amplitude relativa da banda alfa superior no canal Cz, ii) da distribuição topológica da banda alfa superior no decorrer do treino, iii) das variações intra-sessão dos padrões de conectividade funcional da banda alfa superior, utilizando a parte imaginária da coerência como métrica de conectividade, e iv) por fim, em termos de uma análise de redes, que visava avaliar a importância de nodos de rede, verificada através das métricas como *betweenness centrality* e *força*, da atividade segregada, verificada através da métrica de *transitividade*, e da atividade integrada, verificada através de métricas como *caminho característico* e *eficiência global* da rede cerebral.

Relativamente aos resultados para a análise espectral e topológica, encontram-se correlações estatisticamente significativas entre o valor da amplitude relativa da banda alfa superior e o número de set, em todos os grupos, principalmente nas duas primeiras sessões, sendo cada set composto por 6 trials com duração de 30 segundos. Posto isto, não são registadas diferenças estatisticamente significativas intra-sessão, isto é, do set 1 para o set 5 de cada sessão. Para a análise topológica, não se realizaram testes de significância, mas é possível visualizar uma acentuação da amplitude relativa da banda alfa superior em zonas parietais/occipitais, e é também possível verificar que o treino realizado, não afetou somente a banda de interesse mas também a banda theta, cuja atividade não focal diminuiu, a banda alfa inferior, cuja amplitude relativa parece incrementar. Relativamente aos resultados da análise de conectividade, os mesmos sugerem que o treino de EEG-NF para o incremento da banda alfa superior resulta num incremento mais pronunciado nas fases iniciais do treino, isto é, nas duas primeiras sessões de treino. Este incremento é representado pelo do número de canais que apresentam conectividade funcional com a zona parietal central, com canais como o Pz, e com a zona parietal direita, CP6, P4, entre outros, independentemente da modalidade de feedback, ou seja, para a generalidade dos “Learners”. De facto, os próprios canais parietais direitos, P4, P8, CP6, TP10 aumentam de forma estatisticamente significativa a conectividade entre eles. Isto parece indiciar a criação de um complexo

focado na zona parietal direita. Em todas as modalidades, à exceção da VR, verifica-se ainda um aumento significativo intra-sessão da *transitividade* e *eficiência global* enquanto uma diminuição estatisticamente significativa intra-sessão é observada para a métrica *caminho característico*. Posto isto, a metodologia de neurofeedback no contexto experimental que foi implementado, parece promover a atividade cerebral segregada, isto é, a atividade que resulta de uma atividade cerebral mais localizada, e também integrada, isto é, que resulta da integração da atividade de áreas cerebrais dispersas. A não existência de variações significativas na modalidade VR não parece estar relacionada com a modalidade em si, mas sim devido a uma menor amostra do respetivo grupo. Assim, futuramente será necessário aumentar a amostra, pelo menos para este grupo, por forma a poderem ser extraídos resultados significativos da análise do mesmo. Interessantemente, e independentemente do método de re-referenciação utilizado, enquanto para o grupo do treino NF para a modalidade visual se observa a partir da terceira sessão de treino a estabilização do número de conexões funcionais entre os diferentes elétrodos, ou seja deixa de haver um crescimento acentuado da transitividade e da eficiência global com diminuição simultânea do caminho característico, para o grupo do treino NF com a modalidade auditiva a generalidade dos incrementos verificados, estão presentes em todas as sessões, incluindo a última sessão.

No referente ao estudo sobre o método de re-referenciação dos dados EEG, com interesse específico na utilização de um Laplaciano de superfície comparativamente à simples utilização da média dos sinais EEG, a análise topológica das diferentes bandas cerebrais confirma que a utilização do Laplaciano de superfície contribuiu para aumento da resolução espacial dos dados de EEG, uma vez que atenuou para as diferentes bandas a amplitude relativa da atividade periférica, ou seja não focal, que estará relacionada com frequências espaciais mais baixas. Relativamente à análise da conectividade funcional intra-sessão, verifica-se que a aplicação do Laplaciano se reflete na mudança das configurações de variações de conexões funcionais no cérebro, nomeadamente eliminando determinados aumentos estatisticamente significativos, por exemplo para a sessão 1 dos “Learners”, após a aplicação do Laplaciano de superfície, o incremento da conectividade funcional entre Pz e O2 deixa de ser estatisticamente significativo. Possivelmente, isto poderá estar relacionado com uma eliminação de conexões espúrias. Também na análise de redes, a aplicação do Laplaciano afeta a configuração dos dados e outputs embora não se consiga precisar uma relação causa efeito. Posto isto, a variação da própria configuração do Laplaciano, no que se refere à rigidez do mesmo, de parâmetro $m=4$ para $m=3$, não se traduz em resultados tão diferentes, pese embora algumas alterações notadas na análise de redes. De facto, para análise de conectividade funcional, os heatmaps resultantes da aplicação de Laplaciano de superfície com $m=4$, são exatamente iguais aos heatmaps resultantes da aplicação de Laplaciano de superfície com $m=3$. Quanto à análise de redes, nomeadamente nas métricas de *transitividade*, *caminho característico* e *eficiência global*, se verificarmos os gráficos e tabelas apresentadas, apesar de serem notados ligeiros desvios quer nas curvas quer em valores de correlação ou variação intra-sessão, o nível de significância é quase sempre atingido, independentemente da rigidez do Laplaciano aplicado, para a mesma sessão. Posto isto, não é possível reportar claramente uma relação causa-efeito vantajosa decorrente da aplicação do Laplaciano de superfície nos dados aqui tratados. De facto, reitera-se que, pela análise topológica se confirma que este possa estar associado a um filtro espacial, mas nas restantes análises não se consegue confirmar se este “melhorou ou não” os nossos dados.

Palavras-Chave

EEG; Neurofeedback; Banda Alfa Superior; Conectividade Funcional; Modalidade de Feedback Sensorial; Análise de Redes.

Abstract

Neurofeedback (NF) consists in measuring brain activity and presenting a real-time representation of a brain activity pattern of interest to an individual, while instructing him to manipulate the feedback representation through self-regulation. The neurophysiological basis for NF remains to be fully elucidated, whereas several studies support that NF training tends to reorganize the brain networks. Only a handful of studies compare how different feedback sensory modalities affect the outcomes of EEG-based NF training, and none of them analyzes such effect on the functional connectivity or network metrics.

In this project, we evaluate how using different feedback modalities on the EEG-based NF-training will affect the brain's functional connectivity, by analyzing previously collected data from a total of 20 healthy subjects, who underwent four sessions of upper-alpha (UA) band EEG-based NF training, with different feedback modalities (visual, auditory, or virtual reality (VR)). The EEG data was preprocessed and re-referenced with three different methods for posterior comparison, the common average reference (avgREF), and spline lines Surface Laplacian with stiffness parameters equals 4 and 3. The data were evaluated in terms of: i) the within-sessions' variations of the relative amplitude of the UA at the Cz channel, ii) relative band amplitude topological distribution across sets and sessions, iii) the within-sessions' variations of the UA functional connectivity patterns, computed with the imaginary part of coherency, and iv) an UA band network analysis of the metrics *betweenness centrality*, *strength*, *transitivity*, *charpath* and *global efficiency*.

Our results suggest that the UA EEG-based NF-training is associated with an early increment of functional connections with channels over parietal areas (e.g. Pz), independently of the feedback sensory modality. All the modalities, except the VR, which had a reduced sample, verify statistically significant intra-session increases in the *transitivity* and *global efficiency*, while showing statistically significant intra-session decreases of the *charpath*, suggesting that this protocol promotes both clustered and integrated brain activity. While for the visual NF-training group the third session seems to be a breakthrough point, where the number of functional connections stabilize, for the auditory NF-training group longer lasting "variations" are reported. Through the topological analysis we confirm that the application of Laplacian leads to higher spatial resolutions on the EEG data. Regarding the connectivity analysis and network analysis, we note that the application of the Surface Laplacian creates different values when compared to the avgREF data, yet no advantageous outcome can be reported.

Keywords

EEG; Neurofeedback; Upper-Alpha Band; Functional Connectivity; Feedback Sensory Modality, Network Analysis.

Declaration

I declare that this document is an original work of my own authorship and it fulfills all the requirements of the Code of Conduct and Good Practices of the Universidade de Lisboa.

Contents

1	Introduction	1
1.1	Context and Motivation.....	1
1.2	Thesis Outline.....	2
1.3	Electroencephalography	2
1.3.1	Neurophysiological Basis.....	3
1.3.2	Brain Waves	4
1.3.3	Electrode Placement	5
1.3.4	EEG Common Artifacts	6
1.4	Functional Connectivity	8
1.4.1	Concepts and Basis.....	8
1.4.2	EEG and Functional Connectivity.....	8
1.4.2.1	Algorithms for Functional Connectivity	9
1.4.2.2	Network Analysis: Introduction	12
1.4.2.3	Limitations	13
1.4.2.4	Surface Laplacian	14
1.4.3	Connectivity Context: Diseases and Related Phenomena	17
1.5	Neurofeedback.....	19
1.5.1	Concepts	19
1.5.2	Basis	19
1.5.3	Neurofeedback Loop	20
1.5.3.1	Data Acquisition.....	20
1.5.3.2	Data Preprocessing	21
1.5.3.3	Feature Selection and Extraction.....	21
1.5.3.4	Feedback.....	22
1.5.3.5	Learners	22
1.5.4	Independence of the NF-training.....	23
1.6	Applications.....	23
1.6.1	Alpha and Upper-Alpha Neurofeedback.....	23
1.6.2	Neurofeedback and Functional Connectivity	24
1.6.3	Neurofeedback Sensory Modalities and Functional Connectivity	26
1.7	Objectives.....	27
2	Methods.....	29
2.1	Subjects	29
2.2	Neurofeedback Protocol	29

2.2.1	Protocol Design	29
2.2.2	Feedback.....	30
2.2.3	Surveys	32
2.3	Signal Acquisition and Equipment Setup.....	32
2.4	Data Preprocessing	33
2.5	Assessment of the training effects.....	34
2.5.1	Spectral Analysis.....	34
2.5.2	Functional Connectivity Analysis	35
2.5.2.1	Choice of Metric and Time Design for Functional Connectivity Analysis	35
2.5.2.2	Functional Connectivity Evolution.....	36
2.5.2.3	Network Analysis	36
3	Results	38
3.1	Spectral Analysis: Results	38
3.1.1	Learner vs non-Learner	38
3.1.2	Per-Set Cz Channel RAUA Evolution	39
3.1.3	Topological Changes.....	41
3.2	Functional Connectivity Analysis: Results	44
3.2.1	Functional Connectivity Evolution.....	44
3.2.2	Network Analysis	53
3.2.2.1	<i>Transitivity</i>	53
3.2.2.2	<i>Charpath</i> and <i>GE</i>	56
4	Discussion	61
4.1	Spectral Analysis.....	61
4.1.1	Learners vs Non-Learners	61
4.1.2	Per-Set Cz Channel RAUA Evolution	61
4.1.3	Topological Changes.....	62
4.2	Functional Connectivity Analysis	63
4.2.1	Functional Connectivity Evolution.....	63
4.2.2	Network Analysis	65
4.2.2.1	<i>Betweenness Centrality</i>	65
4.2.2.2	<i>Strength</i>	65
4.2.2.3	<i>Transitivity</i>	65
4.2.2.4	<i>Charpath</i> and <i>GE</i>	66
4.2.2.5	Modality Comparison.....	67
4.2.2.6	Surface Laplacian Application	68
5	Conclusion.....	70

6	References	72
7	Appendix	85
7.1	Preliminary Study: Choice of FC metric and time	85
7.2	Spectral Analysis.....	88
7.2.1	Learners vs <i>Non-Learners</i>	88
7.2.2	Per-Set Cz Channel RAUA Evolution	90
7.2.3	Topological Changes.....	92
7.3	Functional Connectivity Analysis	96
7.3.1	Functional Connectivity Evolution.....	96
7.3.2	Network Analysis	102
7.3.2.1	Betweenness Centrality	102
7.3.2.2	Strength	114
7.3.2.3	Transitivity	126
7.3.2.4	Charpath	128
7.3.2.5	GE.....	130

List of Figures

Figure 1.1 - The spatial Scales of current generation, with respective time scales (adapted from (le Van Quyen, 2011)).....	4
Figure 1.2- 10/20 Electrode Placement System. Adapted from (Rojas et al., 2018).....	6
Figure 1.3 - Grid example for the finite difference method—adapted from (Hjorth, 1975).	15
Figure 1.4 - Neurofeedback data acquisition techniques - adapted from (Thibault et al., 2016)	20
Figure 2.1 - Time design of a NF training session	30
Figure 2.2 - Visual feedback presented to the subjects. (Left) When the Cz-RAUA is below the threshold, the sphere color is red and the radius is smaller. (Right) When the Cz-RAUA is above the threshold, the sphere color is white and the radius is bigger. Adapted from (Bucho et al., 2019).	31
Figure 2.3 - Auditory feedback modulation. thr = threshold. Red curves: the dashed represents the perceived and the solid represents the actual noise volume. Gray curves: the dashed represents the perceived and the solid represents the actual music volume. Adapted from (Bucho et al., 2019).	31
Figure 2.4 - VR feedback presented to the Subjects. Top row: particle system changes size, middle row: particle system changes rotation speed, bottom row: camera approaches particle system with changing speed. Adapted from (Berhanu, 2019).....	32
Figure 2.5 - Electrode positioning system used for the experiment	33
Figure 3.1 - Median Per-Set RAUA for the Cz Channel for each sensory modality (rows) and for each re-referencing method (columns). Error bars represent the inter-quartile interval.....	39
Figure 3.2 – Median relative power spectral density values across the Sets for the Session 1 for the Visual NF-training group and avgREF.	41
Figure 3.3 – Median Values of the Session 1 vs Session 4 for the Visual NF-training group and avgREF.....	41
Figure 3.4 - Median values across the Sets for the Session 1 for the VR NF-training group and avgREF.....	42
Figure 3.5 - Median Values of the Session 1 vs Session 4 for the VR NF-training group and avgREF.	42
Figure 3.6 - Median values across the Sets for the Session 1 for the Auditory NF-training group and avgREF.....	43
Figure 3.7 - Median Values of the Session 1 vs Session 4 for the Auditory NF-training group and avgREF.....	43
Figure 3.8 - Changes in Functional Connectivity within session. Results are shown for the Visual NF-training group with avgREF, when comparing changes in ImC between Set 1 and Set 5, in each NF-training session. Red: increases; Blue: decreases; *: $p < 0.05$ (corrected for multiple comparisons). The green boxes highlight specific patterns of connectivity changes.	45
Figure 3.9 - Changes in Functional Connectivity within session. Results are shown for the Visual NF-training group with SL4, when comparing changes in ImC between Set 1 and Set 5, in each NF-training session. Red: increases; Blue: decreases; *: $p < 0.05$ (corrected for multiple comparisons) The green boxes highlight specific patterns of connectivity changes.	46
Figure 3.10 - Changes in the Functional Connectivity within session. Results are shown for the Visual NF-training group with SL3, when comparing ImC values between Set 1 and Set 5. Red: increases;, Blue: decreases, *: $p < 0.05$ (corrected for multiple comparisons). The green boxes highlight specific patterns of connectivity changes.	47
Figure 3.11 - Changes in the Functional Connectivity within session for the Learners of all the NF-training groups (visual, auditory, and VR). Results are shown for the avgREF, when comparing ImC values between Set 1 and Set 5. Red: increases;, Blue: decreases, *: $p < 0.05$ (corrected for multiple comparisons). The green boxes highlight specific patterns of connectivity changes.....	50

Figure 3.12 - Changes in the Functional Connectivity within session for the Learners of all the NF-training groups (visual, auditory, and VR). Results are shown for the SL4, when comparing ImC values between Set 1 and Set 5. Red: increases;, Blue: decreases, *: $p < 0.05$ (corrected for multiple comparisons). The green boxes highlight specific patterns of connectivity changes.....	51
Figure 3.13 - Changes in the Functional Connectivity within session for the Learners of all the NF-training groups (visual, auditory, and VR). Results are shown for the SL3, when comparing ImC values between Set 1 and Set 5. Red: increases;, Blue: decreases, *: $p < 0.05$ (corrected for multiple comparisons). The green boxes highlight specific patterns of connectivity changes.....	52
Figure 3.14 - Median transitivity (orange dots) and interquartile range (blue bars), per-set across the four NF-training sessions. Rows: NF-training modality. Columns: data re-referentiation method. Yellow stars mark sessions where the Wilcoxon Rank Sum Test with H_0 denotes that the median Transitivity is greater in set 5 than in the set 1. (Significance threshold reached for p -value < 0.05 & no correction for multiple comparisons)	53
Figure 3.15 - Median GE (orange dots) and interquartile range (blue bars), per-set across the four NF-training sessions. Yellow stars mark sessions where the Wilcoxon Rank Sum Test with H_0 denotes that the median GE is greater in set 5 than in the set 1. (Significance threshold reached for p -value < 0.05 & no correction for multiple comparisons)	56
Figure 3.16 - Median Charpath (orange dots) and interquartile range (blue bars), per-set across the four NF-training sessions. Yellow stars mark sessions where the Wilcoxon Rank Sum Test with H_0 denotes that the median charpath is lower in set 5 than in the set 1. (Significance threshold reached for p -value < 0.05 & no correction for multiple comparisons).....	57
Figure 7.1 - Per-Epoch wPLI computation.....	85
Figure 7.2 - Per-Block wPLI computation	85
Figure 7.3 - Per-Set wPLI computation.....	86
Figure 7.4 - Per-Epoch ImC computation	86
Figure 7.5 - Per-Block ImC computation.....	87
Figure 7.6 - Per-Set ImC computation	87
Figure 7.7 - Per-Block RAUA at Cz channel for Visual NF-training group.....	88
Figure 7.8 - Per-Block RAUA at Cz channel for VR NF-training group.....	88
Figure 7.9 – Per-Block RAUA at Cz channel for Auditory NF-Training group.....	89
Figure 7.10 - Per-Set RAUA at Cz channel for the Visual NF-training group	90
Figure 7.11 - Per-Set RAUA at Cz channel for the VR NF-training group	90
Figure 7.12 - Per-Set RAUA at Cz channel for the Auditory NF-training group	91
Figure 7.13 - Median values across the Sets for the Session 1. Learners of the Visual NF-training group with SL4.....	92
Figure 7.14 - Median Values of the Session 1 vs Session 4. Learners of the Visual NF-training group with SL4.....	92
Figure 7.15 - Median values across the Sets for the Session 1. Learners of the VR NF-training group and SL4	92
Figure 7.16 - Median Values of the Session 1 vs Session 4. Learners of the VR NF-training group and SL4	93
Figure 7.17 - Median values across the Sets for the Session 1. Learners of the Auditory NF-training group and SL4	93
Figure 7.18 - Median Values of the Session 1 vs Session 4. Learners of the Auditory NF-training group and SL4.....	93
Figure 7.19 - Median values across the Sets for the Session 1. Learners of Visual NF-training group and SL3	94

Figure 7.20 - Median Values of the Session 1 vs Session 4. Learners of Visual NF-training group and SL3	94
Figure 7.21 - Median values across the Sets for the Session 1. Learners of the VR NF-training group and SL3	94
Figure 7.22 - Median Values of the Session 1 vs Session 4. Learners of the VR NF-training group and SL3	95
Figure 7.23 - Median values across the Sets for the Session 1. Learners of the Auditory NF-training group and SL3	95
Figure 7.24 - Median Values of the Session 1 vs Session 4. Learners of the Auditory NF-training group and SL3	95
Figure 7.25 - Changes in Functional Connectivity within session. Results are shown for the VR NF-training group with avgREF, when comparing changes in ImC between Set 1 and Set 5, in each NF-training session. Red: increases; Blue: decreases; *: $p < 0.05$ (corrected for multiple comparisons)...	96
Figure 7.26 - Changes in Functional Connectivity within session. Results are shown for the VR NF-training group with SL4, when comparing changes in ImC between Set 1 and Set 5, in each NF-training session. Red: increases; Blue: decreases; *: $p < 0.05$ (corrected for multiple comparisons)...	97
Figure 7.27 - Changes in Functional Connectivity within session. Results are shown for the VR NF-training group with SL3, when comparing changes in ImC between Set 1 and Set 5, in each NF-training session. Red: increases; Blue: decreases; *: $p < 0.05$ (corrected for multiple comparisons)...	98
Figure 7.28 - Changes in Functional Connectivity within session. Results are shown for the Auditory NF-training group with avgREF, when comparing changes in ImC between Set 1 and Set 5, in each NF-training session. Red: increases; Blue: decreases; *: $p < 0.05$ (corrected for multiple comparisons)	99
Figure 7.29 - Changes in Functional Connectivity within session. Results are shown for the Auditory NF-training group with SL4, when comparing changes in ImC between Set 1 and Set 5, in each NF-training session. Red: increases; Blue: decreases; *: $p < 0.05$ (corrected for multiple comparisons).	100
Figure 7.30 - Changes in Functional Connectivity within session. Results are shown for the Auditory NF-training group with SL3, when comparing changes in ImC between Set 1 and Set 5, in each NF-training session. Red: increases; Blue: decreases; *: $p < 0.05$ (corrected for multiple comparisons).	101
Figure 7.31- Betweenness Centrality per Set for the Session 1, with avgREF data.....	102
Figure 7.32 - Betweenness Centrality per Set for the Session 2 – avgREF	103
Figure 7.33 - Betweenness Centrality per Set for the Session 3 – avgREF	104
Figure 7.34 - Betweenness Centrality per Set for the Session 4 – avgREF	105
Figure 7.35 - Betweenness Centrality per Set for the Session 1 – SL4 data	106
Figure 7.36 - Betweenness Centrality per Set for the Session 2 – SL4 data	107
Figure 7.37 - Betweenness Centrality per Set for the Session 3 – SL4 data	108
Figure 7.38 - Betweenness Centrality per Set for the Session 4 – SL4 data	109
Figure 7.39 - Betweenness Centrality per Set for the Session 1 – SL3 data	110
Figure 7.40 - Betweenness Centrality per Set for the Session 2 – SL3 data	111
Figure 7.41 - Betweenness Centrality per Set for the Session 3 – SL3 data	112
Figure 7.42 - Betweenness Centrality per Set for the Session 4 – SL3 data	113
Figure 7.43 - Strength per Set for the Session 1, with avgREF data.....	114
Figure 7.44 - Strength per Set for the Session 2 – avgREF.....	115
Figure 7.45 - Strength per Set for the Session 3 – avgREF.....	116
Figure 7.46 - Strength per Set for the Session 4 – avgREF.....	117
Figure 7.47 - Strength per Set for the Session 1 – SL4 data.....	118
Figure 7.48 -Strength per Set for the Session 2 – SL4 data	119
Figure 7.49 - Strength per Set for the Session 3 – SL4 data	120

Figure 7.50 - Strength per Set for the Session 4 – SL4 data	121
Figure 7.51 - Strength per Set for the Session 1 – SL3 data	122
Figure 7.52 - Strength per Set for the Session 2 – SL3 data	123
Figure 7.53 - Strength per Set for the Session 3 – SL3 data	124
Figure 7.54 - Strength per Set for the Session 4 – SL3 data	125
Figure 7.55- Per-Set Transitivity for the Visual NF-training group.....	126
Figure 7.56 - Per-Set Transitivity for the VR NF-training group.....	126
Figure 7.57 - Per-Set Transitivity for the Transitivity NF-training group.....	127
Figure 7.58 - Per-Set Charpath for the Visual NF-training group.....	128
Figure 7.59 - Per-Set Charpath for the VR NF-training group.....	128
Figure 7.60-Per-Set Charpath for the Auditory NF-training group.....	129
Figure 7.61 - Per-Set GE for the Visual NF-training group	130
Figure 7.62 - Per-Set GE for the VR NF-training group	130
Figure 7.63 - Per-Set GE for the Auditory NF-training group.....	131

List of Tables

Table 3.1 - Learners vs Non-Learners for the Visual NF-training Group.....	38
Table 3.2 - Learners vs Non-Learners for the VR NF-training Group.....	38
Table 3.3 - Learners vs Non-Learners for the Visual NF-training Group.....	38
Table 3.4 - Spearman Correlation between RAUA per-set and Set Number, for the Cz channel. H0: Correlation coefficient is positive (Significance threshold reached for p-value < 0.05 & no correction for multiple comparisons)	40
Table 3.5 - Wilcoxon Signed Rank test - H0: The median of the IntraA1 list is greater than 0. (Significance threshold reached for p-value < 0.05 & no correction for multiple comparisons).....	40
Table 3.6 – Spearman’s Correlation Between Set Transitivity and Set Number - H0: Correlation coefficient is positive. (Significance threshold reached for p-value < 0.05 & no correction for multiple comparisons)	55
Table 3.7 Wilcoxon Rank Sum Test P-values - H0: The median transitivity is greater in Set 5 than in the set 1. (Significance threshold reached for p-value < 0.05 & no correction for multiple comparisons)	55
Table 3.8-Spearman’s Correlation Between Set Charpath and Set Number - H0: Correlation coefficient is negative. (Significance threshold reached for p-value < 0.05 & no correction for multiple comparisons)	59
Table 3.9 - Wilcoxon Rank Sum Test P-values - H0: The median Charpath is greater in set 1 than in the set 5. (Significance threshold reached for p-value < 0.05 & no correction for multiple comparisons)	59
Table 3.10 - Spearman’s Correlation Between Set GE and Set Number - H0: Correlation coefficient is positive. (Significance threshold reached for p-value < 0.05 & no correction for multiple comparisons)	60
Table 3.11 -Wilcoxon Rank Sum Test P-values - H0: The median GE is greater in set 5 than in the set 1. (Significance threshold reached for p-value < 0.05 & no correction for multiple comparisons).....	60

List of Abbreviations

AD: Alzheimer's Disease	18
ADHD: Attention Deficit Hyperactivity Disorder	2, 4, 18, 24, 25
avgREF: common average Re-referenced.....	vi, 33, 34, 38, 40, 41, 42, 43, 47, 52, 53, 55, 56, 57, 60, 61, 62, 63, 65, 66, 67, 103, 104, 114, 115, 116
BOLD: Blood Oxygenation Level Dependent	18
CCA: Canonical Correlation Analysis	21
CSD: Current Source Density	15
DMN: Default-Mode Network.....	18
ECG: Electrocardiogram	6
EEG-NF: treino de Neurofeedback através de EEG	iii
EOG: Electrooculogram.....	6, 21
FFT: Fast Fourier Transform.....	29
fMRI: functional Magnetic Resonance Imaging.....	iii, 1, 8, 17, 18, 21
fNIRS: Functional Near-Infrared Spectroscopy	1, 21
<i>GE: Global Efficiency</i>	ix, x, xii, xiv, xv, 13, 25, 35, 36, 55, 56, 57, 65, 66, 67, 69, 129, 130
HADS: Hospital Anxiety And Depression.....	31
IAB: Individual Alpha Band	25, 28
IAF: Individual Alpha Frequency	5, 29, 34
ICA: Independent Component Analysis.....	6, 16, 21, 33
MCI: Mild Cognitive Impairment	18
MDD: Major Depressive Disorder.....	18
MEG: Magnetoencephalography	1, 8, 21
NF: Neurofeedback	iii, vi, 2, 12, 19, 22, 23, 24, 25, 28, 35, 37, 41, 42, 47, 52, 53, 56, 57, 60, 61, 63, 64, 69, 70, 87, 88, 89, 90, 125, 126, 127, 129, 130
OCD: Obsessive Compulsive Disorder	18
PCA: Principal Component Analysis	21
PLI: Phase Lag Index	11
PTSD: Post-Traumatic Stress Disorders	18, 26
RSS: Residual Sum of Squares	16
SF-36: 36-Item Short Form Survey.....	31
SL: Surface Laplacian	14, 15, 16, 27, 33, 38, 40, 41, 42, 47, 52, 53, 55, 60, 61, 64, 65, 66, 67, 69, 70, 81
SL3: Surface Laplacian with m=3;...	xi, xii, xiii, xiv, 33, 39, 41, 43, 47, 53, 56, 57, 61, 62, 65, 67, 93, 94, 109, 110, 111, 112, 122, 123, 124
SL4: Surface Laplacian with m=4;...	xi, xii, xiii, 33, 39, 41, 43, 47, 53, 56, 57, 61, 62, 65, 67, 91, 92, 105, 106, 107, 108, 117, 118, 119, 120
SZ: Schizophrenia	18
UA: Upper-Alpha.....	vi, 25, 28
VR: Virtual Reality	iii, iv, vi, 1, 2, 19, 25, 27, 28, 30, 31, 34, 35, 37, 38, 41, 47, 53, 56, 60, 61, 63, 65, 66, 67, 69, 70, 87, 89, 125, 127, 129

1 Introduction

This Master Thesis proposes to investigate the effect of sensory feedback modality, in a protocol of electroencephalography (EEG) based neurofeedback (NF), on estimated metrics of brain functional connectivity.

In this Section, a theoretical introduction is presented, which not only features the fundamentals behind this project, these being the EEG, Functional Connectivity, and Neurofeedback fundamentals, with the respective applications, but also features some of the premises, context, and motivations behind this work. At the end of the section, we will clearly state the objectives of this Master Thesis project.

1.1 Context and Motivation

“Neurofeedback is a kind of biofeedback, which teaches self-control of brain functions to subjects by measuring brain features and providing a feedback signal. (Marzbani et al., 2016)”.

The NF technique relies on an almost instantaneous loop that enables the user to perceive his/her brain activity, such that, he/she can adapt and reach the desired performance (Hammond, 2007). The brain activity can be detected with imaging techniques such as EEG, functional magnetic resonance imaging (fMRI), magnetoencephalography (MEG) and functional near-infrared spectroscopy (fNIRS) (Lakshmi et al., 2014), and the feedback can be given to the user through auditory, visual, and virtual-reality (VR) information, among other modalities (Marzbani et al., 2016). Neurofeedback training relies on associative learning, also referred to as operant conditioning or reinforcement learning, that sums up the power of the reinforcement and says that a behavior, when rewarded, tends to be promoted and maintained, while when punished, tends to be extinguished (Sherlin et al., 2011). In many NF protocols, while a subject registers a desired brain pattern, a positive reward reinforcer is displayed as feedback, while in case the objective is not attained a positive punisher reinforcer is displayed as feedback. Although the neurophysiological basis for the outcomes observed from NF-training remain to be fully elucidated, this technique offers a non-pharmacological, non-invasive, non-dependency inducing, and with almost no side effects, way of strengthening the brain circuitry and enhancing “brain performance” (Hammond, 2007). For instance, positive results have been shown for cognitive enhancement (Loriette et al., 2021), physical rehabilitation (T. Wang et al., 2018) and therapy/symptom relieving (Niv, 2013), registering high effectiveness in the improvement of clinical outcome in the context of abnormal connectivity related conditions, such as stroke patients, neurodegenerative disorder patients, ADHD populations, among others. Hence, it has been suggested that NF-training promotes the reorganization of brain functional paths.

There are two major frameworks that try to explain the mapping of the brain function. The first perspective posits that each specific area in the brain cortex is specialized in a function. This can be referred to as the brain segregation framework since it is based on the functional segregation over key cortical areas. The second perspective states that a single function involves several areas of the brain cortex. This can be referred to as the brain integration framework, since the brain function is defined based on the functional integration of several specific areas (Friston, 2011).

With the above said, Functional Connectivity (FC) can be defined as the temporal coincidence of spatially distant neurophysiological events (Eickhoff & Müller, 2015a), which reflects processes of functional integration that can be measured by techniques such as fMRI, EEG and MEG (Eickhoff & Müller, 2015a). Over the years, this has been studied and related to several diseases like attention

deficit/hyperactivity disorder (ADHD), (Cao et al., 2009a), Schizophrenia (SZ) (Damaraju et al., 2014a), among others. Such a concept has gained momentum and currently there are NF studies that already include FC analyzes on their post-hoc processing (Shtark et al., 2018), or even target such concept-related metrics during the NF training (Bauer et al., 2020).

Despite the burgeoning interest in NF training, a lack of guidelines for the design of NF protocols is evident, and more pronounced in electrophysiology-based studies. Conscious of this limitation, and aiming to tackle it, researchers have recently defined a set of guidelines (Enriquez-Geppert, 2017) and a subsequent consensus-derived checklist (Ros, 2020). Yet, many other factors remain to be clarified, such as the effect on the NF outcome of the different sensory modalities of the feedback. For example, in the context of the upper-alpha (UA) EEG-based NF-training, only few studies have tackled the influence of sensory modalities, such as comparing both the influence of auditory and visual feedback modalities in the outcomes of the NF-training (Bucho et al., 2019). Furthermore, and as far as we are aware of, no studies have yet consistently compared the effect of sensory modality for the EEG-based UA NF-training with simultaneous evaluation of related changes in FC. These are major motivational factors for the work developed in this project. The aim is to answer the following question, “Is there, for EEG-based NF, a specific functional connectivity outcome, and does it depend on the sensory modality?”

Researching this topic may represent a step further in understanding the underlying neural mechanisms of NF-training, thus paving the way for optimization of protocols in clinical context, as for pathophysiologies associated with abnormal FC patterns (Damaraju et al., 2014a; Hull et al., 2017; Zhang et al., 2020). To answer this, we will analyze and evaluate, the changes in FC during an UA EEG-based NF protocol, with data collected using visual (2-dimensional screen display), auditory, and VR (visual) feedback modalities.

1.2 Thesis Outline

This thesis is composed by 5 sections. The first is the “Introduction”, where all the concepts, fundamentals, and literature related to Electroencephalography, Functional Connectivity and Neurofeedback are disclosed. Then, in the second section “Methods”, the methodology deployed in this thesis is explained in detail, including both the preprocessing and analysis pipelines. In the third section “Results”, we expose all the results from the different analyses performed in scope of this project. This is followed by the “Discussion” section, where the results are evaluated and compared with the most recent scientific findings. This report ends with a “Conclusion”, in which the findings are briefly summarized while addressing some of its limitations and prospects.

1.3 Electroencephalography

According to Olejniczak (Olejniczak, 2006), EEG can be defined as a “graphic representation of the difference in voltage between two cerebral locations plotted over time”. In other words, the EEG is an electrophysiological technique that records the electrical activity from the human brain. This technique is characterized by a high temporal resolution since it provides a real time registration of brain electric activity in the order of the millisecond. The electrical activity can be registered invasively and non-invasively thanks to volume conduction of the electrical potentials generated by the neurons, even at deeper locations. (Olejniczak, 2006; Rutkove, 2007). Equivalently, this means that the recorded signal

of the EEG, in particular if captured in a non-invasive scalp measurement, is largely dependent from the electrically conductive properties of the pathway tissues. As addressed latter, this volume conduction is one of the main limitations of the EEG technique as it results in a low spatial resolution, due to the fact that the activity will spread through the surrounding tissues, without any specificity on the direction (Nunez et al., 1994).

1.3.1 Neurophysiological Basis

Concerning the neurophysiological basis of the EEG recordings, for neuronal activity to be measured it is necessary to fulfill both a specific duration of activity and amplitude. These conditions are met when a large assembly of neurons produce temporally and spatially organized activity (Schomer & Lopes da Silva, 2012). This type of activity can not be obtained from pre-synaptic activity, or simply action potentials, which results from changes in the neurons membrane potential due to the flux of ions, and create a current that sharply decays as long as the distance to the source increases (Hämäläinen et al., 1993). Instead, EEG signals are generated at the post-synaptic level, where, through to the binding of neurotransmitters released by a large group of pre-synaptic neurons, where both excitatory and inhibitory pre-synaptic potentials are summed up temporally, such that the post-synaptic potentials are longer in time. So, for the post-synaptic activity, as opposite to the pre-synaptic one, the requirement of the duration can be fulfilled (Kirschstein & Köhling, 2009). Yet, EEG temporal summation is not enough to ensure detection of neuronal activity using EEG, it is also necessary for the activity to have enough strength to be detectable on the scalp surface, a condition that can be fulfilled with spatial summation of the underlying neuronal activity. These specific conditions exist when large assemblies of cortical pyramidal neurons are activated. These cells have their apical dendrites perpendicularly oriented to the cortical surface and parallel to each other's (Kirschstein & Köhling, 2009), such that during the periods of neuronal activity, the longitudinal components of the produced currents, parallel to the neuronal membrane, sum up, while the components perpendicular to the membrane cancel each other, thus creating a primary current parallel to the neuronal membrane. Additionally, during such activity periods, magnetic fields are created around the neuronal membrane (Schomer & Lopes da Silva, 2012) that will sum to the current field potentials that are created. Hence, a great enough amplitude of activity is created such that it can be detected in the EEG. To wrap up what was formerly detailed, the EEG technique captures mostly post-synaptic potentials, with the measured activity being proportional to the degree of temporal and spatial synchronism among the cortical pyramidal neurons (Olejniczak, 2006; Louis et al., 2016).

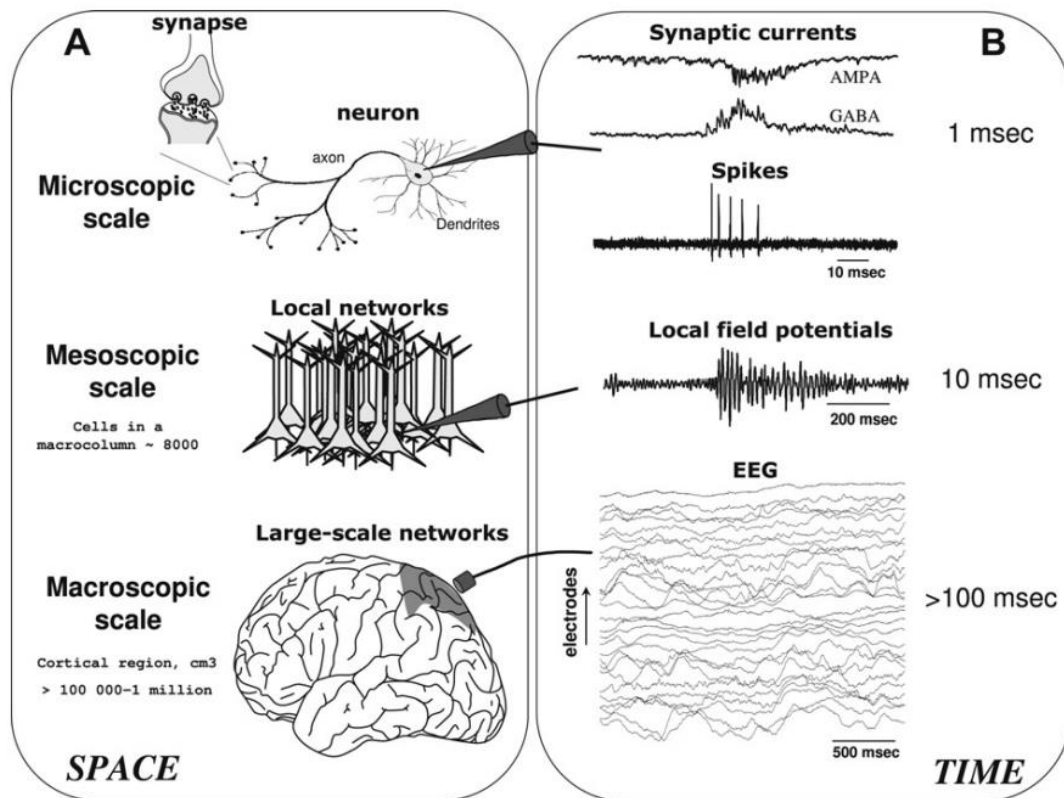


Figure 1.1 - The spatial Scales of current generation, with respective time scales (adapted from (le Van Quyen, 2011))

1.3.2 Brain Waves

Concerning the EEG data, there are specific electrical brain patterns that can be verified. These are called brain waves and differ in frequency and amplitude, which in non-invasive EEG scalp measurement are up to 200 μV (He & Lin, 2013). These brain waves tend to reflect the state of the individual and sometimes can have pathological relevance. One example is the quite controversial evaluation of the EEG Theta/Beta Ratio in the context of ADHD (Arns et al., 2013).

The first pattern, hence with lower frequency content, relates to the delta rhythm, which contains frequencies between 0.5 and 4 Hz and is highly associated with deep stages of sleep (Purves et al., 2001).

Then, from 4 to 8 Hz (Schacter, 1977) there are the theta waves, which are related to sleepy and hypnotic states. Also, several reports demonstrate the association of the theta waves with cognition (Klimesch, 1999), as for example in memory (Herweg et al., 2020; Klimesch, 1999), with specific hippocampal theta waves (Kragel et al., 2020; Zhang & Jacobs, 2015).

From 8 to 12 Hz, there are the alpha waves. These, in a relaxed condition are mainly seen in the parietal/occipital area (Groppe et al., 2013), and are largely dependent on the eye-open vs eye-closed state of the subject (Barry et al., 2007). They are more prominent under an eye-closed state, as it is hypothesized that under an eye-open state desynchronization occurs among the occipital generators (Gómez-Ramírez et al., 2017). Usually related to a relaxed or resting state (Abhang et al., 2016), these brain waves have also been reported as reflecting cognitive and memory performance (Klimesch, 1999;

Klimesch et al., 1993). In fact, the prominence of the alpha waves has been often reported as attention dependent. During attentive periods, reduced alpha activity has been reported (Shaw, 1996), whereas during inattentive periods higher alpha activity was noted (Groppe et al., 2013). Concerning these alpha waves, Klimesch et al. (1999) defined a “center of gravity” of the band. With the premise that both, the power of the band was not linear but instead “subject subjective”, and that there is a subdivision in the band concerning the cognitive functions—the author proposed that this center of gravity would be defined as the frequency, within the band, with maximum power. This individual alpha frequency (IAF) would be the threshold for the subdivision in lower-alpha and upper-alpha, with the lower-alpha band being the frequencies below the IAF and the upper-alpha band being the frequencies over the IAF in the alpha band (Klimesch, 1999).

From 13 to 35 Hz, there are the beta waves, which are low amplitude waves related to a wakeful alert, anxiety, attentive state (Abhang et al., 2016). Again, in this band, a subdivision is made between lower-beta, from 13 to 20 Hz, and upper-beta, higher than 20 Hz, with the lower-beta being affected by mental activity, and the upper-beta band being more related to intense mental activity, anxiety, and containing the sensorimotor rhythm (Thakor & Sherman, 2013).

Frequencies above 35 Hz (Abhang et al., 2016) belong to the gamma band, which is not often measured in non-invasive EEG (Groppe et al., 2013). Also, there are reports that such band is involved in attention, working memory, and long-term memory processes (Malik & Amin, 2017).

1.3.3 Electrode Placement

As non-invasive EEG involves the placement of electrodes in the scalp, several positioning systems were created. The standard one is the 10/20 System, which describes the head surface locations of the electrodes by measuring the relative locations between cranial landmarks (Jurcak et al., 2007). Specifically, the four anatomical landmarks used as reference are the nasion, a depression between the eyes just above the nasal bridge, the inion, “*highest point in the midline of the protuberance of the occipital bone*” (Mecarelli, 2019), and two preauricular points, “*depressions at the root of the zygoma just anterior to the tragus*” (Jurcak et al., 2007; Sazgar & Young, 2019). Then, the adjacent electrodes are placed in intervals of 10 percent of the total distance of the lines that unite the nasion and inion, and in intervals of 20 percent of the total distance of the lines that unite both preauricular points (Mecarelli, 2019). The purpose of a standard electrode positioning is to allow reproducibility among studies, by maintaining the relative position on the scalp, diminishing the bias caused by the subjects different head sizes (Jurcak et al., 2007). In the nomenclature of the electrodes positioning, it is first defined the scalp position, frontal with F, fronto-polar with Fp, temporal with T, Central with C, parietal with P, occipital with O, and then the side/specific location with a z or a number, that can be odd or even. The odd numbers refer to the left hemisphere, even numbers to the right-hemisphere, and finally the letter “z” designates midline (Mecarelli, 2019; Sazgar & Young, 2019). In total, in the standard positioning system there are 21 electrodes (Jurcak et al., 2007). Other electrode placement systems exist, as, for example, 10/5 and the 10/10. These will differ regarding the percentage of the intervals that are used to calculate the relative position between channels over the lines that unite the preauricular references, respectively 5% of the total distance and 10% of the total distance (Jurcak et al., 2007). As referred in the exposed definition of the EEG, each electrode signal records the difference between the electric potentials from the respective location and a reference electrode. Post re-referencing can be done to re-reference our data to a common average, other electrodes, or other solutions, depending on the implemented protocol (Lei & Liao, 2017).

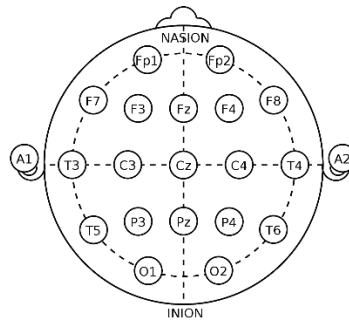


Figure 1.2- 10/20 Electrode Placement System. Adapted from (Rojas et al., 2018)

1.3.4 EEG Common Artifacts

When it comes to EEG signals, these are commonly affected by non-electroencephalographic interferences known as artifacts (Schomer & Lopes da Silva, 2017). These artifacts tend to “corrupt” portions of the data leading to misinterpretations. The origin of the artifacts is quite wide, as some reflect physiological functions, whether others are caused by external sources (external to the subject) (Chaumon et al., 2015; Tatum et al., 2011) . Some of the most common artifacts include:

Eye movement artifacts – These are the most common artifacts during conscious EEG recordings and are generated by alterations in the corneoretinal dipole. Alterations/rotations of this dipole generate a potential difference that can be detected on the EEG. In fact, this dipole is the premise for the eye activity measurement through the EOG (Tatum et al., 2011). The signal of eye-related movements has different characteristics depending on if it results from eye blinks or saccades, although in both cases the artifacts will cause an EEG power spectral topology with more prominent values in the frontal electrodes. The blinks will cause interferences, such that in EEG, a high amplitude and low duration signal will appear over the different channels and “corrupt” the delta and theta frequency bands. The saccades, when the signal is decomposed by ICA generates a component that features abrupt step-like variations, with an anterior prominent topology and opposite polarity among hemispheres, and low frequency content (Chaumon et al., 2015).

Myogenic artifacts – These are high frequency (>20 Hz) burst-like artifacts caused by muscular movement and are related to head, facial and neck muscle movements. Particularly, the most commons myogenic artifacts are caused by the temporalis and frontalis muscles, such that sometimes it is recommended to ask the subject to “open their mouth” in order to alleviate temporal muscular artifacts produced by the masseter muscles (Tatum et al., 2011). These have higher prominence on the edge electrodes, and when performing independent component analysis (ICA) the muscular artifacts are characterized as being more focal and not event-related (Chaumon et al., 2015).

Glossokinetic Artifacts – Tongue movements can create EEG artifacts as these produce changes in the tongue dipole, with the tip of the tongue being negative relative to the root. These movements can be, for example, speaking or swallowing, and they generate “intermittent bursts of abnormal slowing or frontal intermittent rhythmic delta activity on the EEG”. Oropharyngeal motions produce artifacts that are diffusely present on frontal and temporal sites (Tatum et al., 2011).

Cardiac artifacts – Interference caused by the cardiac muscles that may mimic certain parts of an EEG signal, with a characteristic frequency and a more distinct amplitude. The presence and prominence of these artifacts differ with the kind of EEG montage and referencing, with referential montages often

accentuating this kind of artifact. Additionally, single channel artifacts may arise from the mechanical force of the heart contraction. The latter also may happen when electrodes are too close to an artery (Tatum et al., 2011).

Other physiological artifacts may be caused by subject's movements, patients sweat, altered skull anatomic, among others (Tatum et al., 2011).

Equipment-related artifacts – These are artifacts related to all the instrumental apparatus necessary to perform the EEG measurement. When these are present, it is necessary to locate the source, when possible, and do the necessary modifications. The artifacts can be inductive, electrostatic, and capacitive, as caused by the electrical wires of the apparatus, radio frequency interferences, among others sources (Tatum et al., 2011).

Environmental artifacts – These are non-physiological artifacts caused by external electric interference from other devices. The most common form of interference is caused by the alternating current present in the power supply of nearby devices. This creates a high frequency noise (+/- 50 Hz in Europe, +/- 60 Hz in the UK) over several channels. Other interferences may arise from the magnetic fields from neighboring devices. With that said, pacemakers, neuro-stimulators, among others have high chances of causing this kind of interferences (Tatum et al., 2011).

Bad Channels – Bad channels are usually related to a poor electrode-scalp contact, which provokes a low frequency and low amplitude activity over a specific electrode. Also, changes in impedance due to movement can cause this kind of artifacts (Chaumon et al., 2015; Tatum et al., 2011).

1.4 Functional Connectivity

1.4.1 Concepts and Basis

Two main frameworks exist that try to explain the mapping of the brain function. The first perspective posits that each specific area in the brain cortex, is specialized in a function. This can be referred as the brain segregation since it is based on the functional segregation over key cortical areas. The second paradigm states that a single function involves several areas of the brain cortex. This can be referred to as the brain integration, since the brain functioning is defined based on the functional integration of several specific areas (Friston, 2011).

In the context of the brain integration paradigm, we tend to analyze the correlation between different areas regarding their neuronal activity. According to Friston (1994), “*functional connectivity is defined as the temporal coincidence of spatially distant neurophysiological events*”. This is a merely correlative concept as it only describes if there is or isn’t a statistical dependency among remote neurophysiological events, and doesn’t consider the origin of the effect, if it is one of the parts that exerts its effect or vice-versa, or even if it is a third regions which exerts its effect on the remaining. To describe in depth the directionality of the effect other concept have been defined, referred to as effective connectivity, and described by the same author as “*the influence that one neural system exerts over another, either at a synaptic or population level*” (Friston, 2011). A third concept of structural connectivity refers to the hard-wired connections, as for example the fiber tracts, between different brain areas; these are the necessary scaffolds for the establishment of a functional connectivity (Eickhoff & Müller, 2015b).

The underlying mechanism of the functional integration is still unclear. One of the most known hypotheses was proposed (Fries, 2005) and revisited (Fries, 2015) by Pascal Fries. This hypothesis is referred as the “*Communication Through Coherence*” and proposes that communication between neural groups is achieved by a rhythmic synchronization on their neural activity. This rhythmic synchronization is accompanied by a modulation of the post-synaptic excitability, with the creation of specific temporal windows of high input gains for synchronous activity, in which the pre-synaptic group fit, with high inhibition of non-synchronous inputs (Fries, 2015). Interestingly, years prior Varela et al. (2001) suggested that “*desynchronization reflects a process of active uncoupling of the underlying neural ensembles that is necessary to proceed from one cognitive state to another*”, serving as clue for the hypothesis that synchronization would be involved in neural integration process.

To measure both effective and functional connectivity, techniques such as fMRI, EEG and MEG can be used (Eickhoff & Müller, 2015b). As the structural connectivity is related to the fiber tracts, the go-to characterization technique is the diffusion tensor imaging (Yeh et al., 2021).

1.4.2 EEG and Functional Connectivity

This subsection will present notions on estimation of FC in EEG data. A description of the principal definitions, and algorithms implemented to estimate FC, will be followed by the description of metrics that can be implemented to perform network analysis over the EEG-derived connectivity matrices. Least but not last, considerations about the main obstacles and limitations of EEG-based FC will be developed, while its main applications will also be mentioned.

1.4.2.1 Algorithms for Functional Connectivity

Through the years, several algorithms have been proposed for the measurement of brain FC in EEG data. In this subsection we will expose and discuss the main implementations. One thing that shall be noticed, is that the focus will be on metrics for scalp chance-based FC estimates, which do not enable to infer in terms of source location analysis (van de Steen et al., 2019). For the source location analysis although, usually, the measurements are also done through non-invasive EEG, there is an intermediate step where an “inverse” transformation is done to detail the source of the activity. When such sources are not estimated and only scalp-based signals are used, no conclusions can be made about the location of underlying neuronal activity. This occurs because scalp channel locations are not an approximation of the anatomical channel sources, because of the volume conduction problem, and spurious connectivity profiles would be reported (van de Steen et al., 2019).

The algorithms used in the context of EEG-based connectivity, can be distinguished according to the approach. The first distinction is between directed and non-directed metrics. While non-directed metrics focus their attention on any sort of interdependence between signals, without any information about the direction of the influence, directed metrics also capture the latter. Another distinction is between model-free/model-based approaches. While model-based approaches make assumptions of linearity on the interactions between the signals, model-free approaches don't make any assumptions concerning the kind of interactions between the signals (Bastos & Schoffelen, 2016). In this report, we will explore mostly the model-based, non-directed approaches. Also, it shall be noticed that most of the FC algorithms are computed in the frequency domain, which usually is represented by $Ae^{i\Phi}$, where A represents the amplitude of the oscillations, and Φ represents the phase of the oscillations.

The first algorithm that we shall refer is the *coherence coefficient*. This is the frequency equivalent to the cross-correlation function, and in terms of the specific frequency, can be interpreted as the amount of variance in one of the signals that can be explained by other signals, or vice-versa. This is mathematically defined as:

$$coh_{xy} = \frac{|\frac{1}{n} \sum_{k=1}^n A_x(f,k) A_y(f,k) e^{i(\Phi_x(f,k) - \Phi_y(f,k))}|}{\sqrt{(\frac{1}{n} \sum_{k=1}^n A_x^2(f,k)) (\frac{1}{n} \sum_{k=1}^n A_y^2(f,k))}} = \frac{|S_{xy}(f)|}{\sqrt{S_{xx}(f) S_{yy}(f)}} \quad (1.5)$$

where f is the frequency, k is a point of the trial (EEG signal), n is the trial duration in data samples and $S(f)$ is a cross spectral correlation operator.

From this equation, we notice that the coherence value is bounded between 0 and 1, with higher values representing higher correlation and higher FC (Bastos & Schoffelen, 2016). If we discard the absolute value operator from the above equation, the computed value is the coherency, C_{xy} and not the coherence. This coherency is a complex value that captures temporal delays in form of phase differences in angles. A downside from both the coherence and coherency metrics is that they consider “zero-phase differences”, which as we will see in later, is associated with several connectivity measurement limitations that are related to the common reference, the volume conduction and the common input problem. Also, sample size bias is commonly reported, and as time-stationarity is not ensured the analysis over several trials can have some bias (Lachaux et al., 2002).

The next algorithm is a refining of the previous one. This was proposed by Lachaux in 1999 (Lachaux et al., 1999), with the premise that coherence confounded phase consistency with phase synchronization, although with no phase synchrony, high amplitude correlations do not imply higher values of coherence, neither low values of amplitude correlation accompanied by high phase synchrony mean low coherence values. Also, as previously referred, the coherence algorithm has the assumption of time stationarity, which limits the analysis of the dynamic connectivity properties. To clear all these limitations, on his algorithm, Lachaux applied the coherence equation to amplitude normalized Fourier Signals (Bastos & Schoffelen, 2016). This algorithm is called *phase locking value* and it has the following mathematical equation, after simplifications:

$$plv(f, k) = \left| \frac{1}{n} \sum_{k=1}^n e^{i(\Phi_x(f, k) - \Phi_x(f, k))} \right| \quad (1.6)$$

This solves the amplitude cofound, as it nullifies its influence on the general calculation, and solves the stationarity problem as, at each instant, is performed a calculation of an instantaneous phase of each signal, by means of Hilbert transform or even Wavelets (le Van Quyen et al., 2001). Notice that the author published two variations of this algorithm, one, here exposed, for the calculation of phase differences within trials (Lachaux et al., 2000), and a second algorithm for the calculation of consistent phase differences over several trials (Lachaux et al., 1999). Recently, Bruña et al. (2018) optimized the implementation of this algorithm in order to ignore zero-phase time lags associated with common reference, volume conduction and common input problem, correcting a big disadvantage of the *phase locking value* algorithm (Bruña et al., 2018) .

Another algorithm is the *Imaginary part of Coherency*. As we exposed above, there are several limitations concerning the measurement of FC, which have as a consequence spurious zero-phase FC values. One example is volume conduction, which under the validity of Maxwell quasi-static approximation (Plonsey & Heppner, 1967), creates zero-phase shift correlations, which under the coherency and coherence algorithms would translate into spurious non-zero functional connections. Nolte et al. (2004) addressed this question when proposing a novel metric for the by only considering the Imaginary part of the Coherency (ImC) equation, as it follows:

$$ImC_{xy}(f, k) = Im \left(C_{xy}(f, k) \right) = \frac{Im(S_{xy}(f, k))}{\sqrt{S_{xx}(f, k)S_{yy}(f, k)}} \quad (1.7)$$

where *Im* corresponds to the “imaginary part” operator.

From the equation we notice that this value is bounded between -1 and 1, with the sign corresponding to the direction of the phase shift. Higher absolute values of *ImC* correspond to higher FC between the two signals. Also, we clearly see that with such equation, zero-phase lag correlations result in a zero *ImC* value. Interestingly, Nolte et al. (2004), opposite to Lachaux et al. (1999), includes the “amplitude component” into its formulation, considering that phase synchrony is not independent of this component.

As one of the main limitations of the *ImC* is the fact that it is biased by the degree of the phase difference, values are maximal for 90-degree phase differences, Stam et al. (2007) proposed a novel algorithm called *Phased Lag index*. This metric evaluates the average phase distribution across observations and addresses the consistency of a positive or negative cross-correlation between signals, with consistent correlations implying a functional relation (Bastos & Schoffelen, 2016). Here the cross-spectrum is calculated with the Hilbert transform or wavelets. This translates to the following mathematical equation:

$$PLI_{xy} = \left| \frac{1}{n} \sum_{k \in n} \text{sgn}(\text{Im}(S_{xy}(f, k))) \right| \quad (1.8)$$

At its original formulation, this algorithm is quite sensitive to perturbations, in the intent that negative signs can easily turn to positive *PLI* and vice-versa, even in the presence of small, signed correlations (Vinck et al., 2011). So, four years later, Vinck et al. (2011) proposed a new *weighted Phase Lag Index* (*wPLI*) which would correct the above question, by normalizing the signs of the phase differences (-1, in negative case, or 1 in positive case), by the weights of the respective phases. This translates to the following mathematical equation:

$$wPLI_{xy} = \frac{|\sum_{k \in n} \text{Im}(S_{xy}(f, k)) \text{sgn}(\text{Im}(S_{xy}(f, k)))|}{\sum_{k \in n} |\text{Im}(S_{xy}(f, k))|} \quad (1.9)$$

With these changes, Vinck et al. (2011) ensured that small perturbations would not have as high influence on the overall data, creating a more stable metric and maintaining the premise of the original formulation. A brief note to the fact that, in the same article, the authors debate over the sample size bias question, specifically, on the fact that both *wPLI* and *PLI* are positively biased in the presence of small sample sizes. In such cases, the authors proposed an alternative formulation that translates into the following mathematical equation:

$$dwPLI_{xy} = \frac{\sum_{j=1}^n \sum_{k \neq j} \text{Im}(S_{xy}(f, j)) \text{Im}(S_{xy}(f, k))}{\sum_{j=1}^n \sum_{k \neq j} |\text{Im}(S_{xy}(f, j)) \text{Im}(S_{xy}(f, k))|} \quad (1.10)$$

An interesting conclusion of this formula is that, in case the sample tends to infinite, this estimator will be consistent with the *wPLI* (Vinck et al., 2011).

Like referred, all the previously described algorithms are model-based and non-directional approaches in the context of the FC measurement. As stated, there are other types of approaches such as directional metrics and model-free metrics. The directional metrics are often used in effective connectivity evaluations, and examples of such algorithms are the *Granger Causality* and the *Phase*

Slope Index. The first, follows the premise that if two signal are asymmetric in their ability of predicting the other signal, the signal that contains more information about the future of the other signal is said to be the driver, while the other is the recipient. This is computed by evaluating the influence of a time-series, by inclusion of its values, on the error in the prediction, by autoregression, of the future values of another time series. If the error is reduced a causal effect between the first and the latter is pointed out (Ding et al., 2006). This metric has quite a lot of problems and the overall performance on real EEG data is very poor (Haufe et al., 2012). The latter, *Phase Slope Index*, was formulated by Nolte et al (2008), and is based on the idea that a flow of information will take some time. Together, with the assumption that information travels at the same speed, a positive slope regarding the positive relation between frequency and phase difference will be generated and studied in this metric. Overall, the signs of the resulting values from this study will inform on the directionality of the relation. Regarding model-free approaches, the main example is the mutual information algorithm, which measures a correlation, which is not assumed as linear, between time signals using principles of the information theory (Kraskov et al., 2004).

1.4.2.2 Network Analysis: Introduction

When the main goal is to analyze FC, and specifically, how certain NF protocols affect the FC outcome, a network-based analysis is usually performed. So, in this subsection we will expose some fundamentals about networks and then, the most common network analysis metrics.

First, we need to introduce some concepts. A network has two main components, the nodes, and the links. In the context of EEG channel-based analysis, the channels can be defined as the nodes and the functional connections as the links, whilst for source-based analysis anatomical connections and even effective connections are represented by the links. These links can be expressed in different forms. They can be represented by weights, which in case of functional/effective connectivity will represent the magnitude of the correlation, case where the weights can be accompanied by a +/- sign that expresses the directionality. Regarding the case of anatomical connectivity, these weights represent the distance between the nodes. Alternatively, these links can be expressed in terms of binary values that denote the presence or absence of relationship. Commonly, when performing a network analysis, the first step is a thresholding of the connectivity values to eliminate spurious/not meaningful connections (Rubinov & Sporns, 2010).

Next, follows the description of some metrics that are usually assessed in this type of analysis. The first is the *degree*, a metric that evaluates the number of links connected to each node, verifying the number of neighbors of that node. This is a metric that tends to reflect the importance of the node on the overall network. One limitation of this metric, mostly in case of weighted inputs, is that FC algorithms often represent the “no correlations” cases as near-zero values instead of zero values. With this said, this near zero correlations are counted in the degree as they still represent a link. So, the *degree* metric is largely dependent on the thresholding of spurious correlations. Other degree-derivative measures are the *degree distribution* and the *density* (mean network degree). With this said, in case of weighted values, there is a more specific metric for the same purpose called *Strength* that is defined as the sum of all weights of neighboring links (Rubinov & Sporns, 2010).

Other commonly used metrics in network analysis aim to evaluate the functional segregation of the brain activity. These metrics report the presence of clusters and their composition. In the case of FC analysis, the presence of clusters supports the existence of specific regions of processing that can be associated with segregated neural processing. The *clustering coefficient* is a metric that measures the

fraction of triangles around a node, hence the fraction of node neighbors that are also neighbors of each other. The *mean clustering coefficient* then reflects the average presence of clustered connectivity in a network. One limitation of this metric is that, since it is normalized over the *degree* metric, there will be a bias caused by this normalization, more specifically in case of low *degree*. Alternatively, there is a metric called *transitivity* which does not suffer from this limitation, despite some similarities with the *mean clustering coefficient*. Other algorithms, like the *modularity*, not only evaluate these clusters, but also return the composition of the different clusters (Rubinov & Sporns, 2010).

There are also metrics and algorithms that can be used to analyze the networks in a functional integration perspective, thus verifying the brain ability to integrate information from different regions. To perform this analysis there is the fundamental concept of *paths*, which will serve as basis for different metrics. *Paths* are sequences of nodes and links that together form routes of information. In the context of anatomical connections, the *length* of these *paths* will be indicative of the integration potential, with shorter paths indicating stronger integration potential. When studying FC and not anatomical connectivity, the interpretation becomes less straightforward (Rubinov & Sporns, 2010). With this said, there are several algorithms that can be used to translate the weighted links into distances, which will make the calculated paths easier to interpret (Floyd, 1962). For the *paths* metric, the *charpath* can be measured, which is defined as the average shortest path length between all pairs of channels, and the *global efficiency (GE)*, which is the inverse of the *charpath*, measures the overall efficiency of the paths. Reduced *charpaths*/ increased *GE* point to a higher integration potential (Rubinov & Sporns, 2010).

We previously referred the *degree* as a metric that can be used to assess the importance of a specific node on the network. Yet, there are other algorithms/metrics that can be used to assess this property. With the premise that central nodes participate in a big fraction of the short paths of the network, working as controls for information flow, there are other two common measures for this purpose, the *closeness centrality* and the *betweenness centrality*. *Closeness centrality* is the inverse of the average short path length between a specific node and the remaining ones, and the *betweenness centrality* measures the fraction of shortest paths that pass by a specific node. Also, we can do more restrictive measures, as for example, given specific clusters, the metric *within-module degree z score* allows to study the degree restricted to the cluster. To assess inter-cluster connection between different nodes we can use the *participation coefficient*. This will not only give feedback about the importance of specific nodes on the network but will also allow to understand the nodes' roles on segregation or integration (Rubinov & Sporns, 2010).

A brief reference to the small world algorithm, as this metrics captures both functional segregation and functional integration (Rubinov & Sporns, 2010).

1.4.2.3 Limitations

Several obstacles can impair the estimates of FC. The first is related with the usage of a common reference channel when performing the EEG measurement. Since each channel's signal results from a difference between the local electric potential and the electric potential at the reference electrode, naturally, changes in the potential of the reference electrode will reflect in the EEG signals from the remaining ones. This will cause a zero-time lag correlation among the different channels which will cause some spurious FC estimates. This can either be solved by using algorithms that ignore zero-time lag correlations, by using bipolar derivations or by separately referencing each channel (Bastos & Schoffelen, 2016; Cohen & Tsuchiya, 2018).

Another concern and limitation of the analysis of FC in EEG-derived data is the previously mentioned volume conduction problem. This is based on the fact that between the source and the scalp, where the signal is measured, there will be a spatial spread of the electromagnetic fields over the surrounding tissues. This will cause the activity generated in a specific source to be detected over multiple channels, even being the channels spatially separated. This will induce spurious FC in the form of instantaneous correlations with 0 phase degree, or 180 phase degree when the sensors are in opposite sides of the dipole (Anzolin et al., 2019; Haufe et al., 2013). This can be solved either by using algorithms that discard the phase differences above, by using source reconstruction, by using a bipolar derivation, or by estimating the current source density by means of a Surface Laplacian, which we will address later (Bastos & Schoffelen, 2016; Tenke & Kayser, 2015).

Another common limitation for EEG-based estimates of FC is the “common input problem”. This is related with the presence of indirect interactions. Imagine, a pair of signals with a so detected FC. This correlation can be due to a direct interaction between both areas or can be caused by the influence of a third source in both areas. In this case, there are two scenarios. The first scenario occurs if a zero-phase lag correlation is detected, case in which algorithms that discard these contributions will be effective. The second one is a worst-case scenario, where a non-zero-phase lag correlation is detected. Such case is more problematic, as it is difficult to deal with, and leads to the detection of spurious correlations. Also, this will be a bigger obstacle in the measurement of effective connections (Bastos & Schoffelen, 2016).

In general, all these problems are related to a more general issue, that is, a reduced signal to noise ratio. The signal to noise ratio is defined as the proportion of power of signal of interest divided by the power of noise in the signal. If, in greater extent, our signal contains a high proportion of noise, some spurious correlations can be detected (Bastos & Schoffelen, 2016).

The last obstacle is the sample size bias. As stated by Bastos et al. (2016) “*measures of connectivity are often biased quantities, where under the null hypothesis of no connectivity the estimates will deviate from zero*”, which greatly depends on sample size. Connectivity measures reflect the magnitude of a vector quantity, which has always a different than zero value, contributing to a tendency of overestimation. Hence, the bias is dependent on the sample size, being larger in smaller sample sizes. This problem can be seen in the very present question “Data Segment length vs. Number of Data Segments” when designing an experiment that aims to measure FC. A consequence of this overestimation is that, even in the absence of true interactions, non-zero FC measurements may arise (Bastos & Schoffelen, 2016). Further in this thesis we will address this limitation.

1.4.2.4 Surface Laplacian

The surface Laplacian (SL) is a commonly used technique to perform spatial filtering on EEG data. This technique is particularly important for attenuating the influence of the volume conduction, which in terms of scalp-based FC estimates could lead to the detection of spurious connections. This technique is based on the Ohms Law (C. Carvalhaes & de Barros, 2015), which establishes the local relationship between “*the SL of scalp potentials and the underlying flow of electric current caused by brain activity*” and it is mathematically defined as the divergence of the gradient of the electric potential:

$$Lap(V) \equiv Div(Grad(V)), \quad (1.1)$$

which, more precisely, will correspond to the second order derivate:

$$Lap_s(V) = \frac{\partial^2 V}{\partial x^2} + \frac{\partial^2 V}{\partial y^2} \quad (1.2)$$

This algorithm generates a reference-free current source density (CSD), accompanied by an improvement in the spatial resolution as it filters low spatial frequencies (Nunez et al., 1997), which consequentially improves the sensitivity of each electrode to a more local tissue beneath the electrode (Bradshaw & Wikswo, 2001; C. Carvalhaes & de Barros, 2015; Srinivasan, 1999). Also, the signal of the CSD estimate reflects the direction of the current flow, with positive values representing current flow from the brain towards the scalp, and negative values representing current flow from the scalp into the brain, yet, it does not provide information about the origin of the neural activity (Kayser & Tenke, 2015b).

In terms of computational implementation of the SL, there are several approaches. One example is the finite difference method, where there is a discretization procedure that allows to perform the SL differential operations more easily. For example, consider the following grid (Figure 1.3):

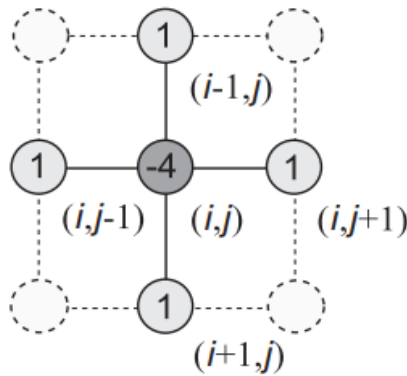


Figure 1.3 - Grid example for the finite difference method—adapted from (Hjorth, 1975).

According to this method, and as done by Hjorth on his approximation (Hjorth, 1975), for each position there is a re-referencing of the data over the average of the 4 nearest neighbors of the node. This translates to the following equation:

$$Lap_s(V)_{(i,j)} \approx \frac{V_{(i-1,j)} + V_{(i+1,j)} + V_{(i,j-1)} + V_{(i,j+1)} - 4V_{(i,j)}}{h^2}, \quad (1.3)$$

where h^2 represents a constant that ensures that the result will be in V/cm^2 .

In the same way, the procedure will be done over all the EEG channels. But clearly, we can notice a problem, as on the EEG channels on the edges, we don't have the "fourth channel". Although, Hjorth proposed a re-referencing with only three channels for this edge channels, it result in a less accurate re-referencing. This is one of the main limitations of this method, whilst other limitations are the strictness in the channels disposition needed for this model to suit, and the fact that, theoretically this only serves to planar scalp model. A last note to the fact that higher orders of re-referencing and denser electrode placement both contribute to a more accurate approximation (C. Carvalhaes & de Barros, 2015).

The second method is the smoothing thin plat SL. In this case, the Laplacian differentiation is performed analytically on a function that can result from interpolation through the data or fitting through the data. This function is a real function in which $f(r_i)=V_i$ in the different positions that minimizes the Residual Sum of Squares (RSS):

$$RSS(f, \lambda) = \frac{1}{N} \sum_i (V_i - f(r_i))^2 + \lambda J_m[f(\mathbf{r})], \quad (1.4)$$

Where r_i is the position of the channel and $r_1 \neq r_2 \neq \dots \neq r_N$, $J_m[f]$ is a measure of roughness, and λ is called the regularization parameter, which regulates the tradeoff between goodness of fit ($\lambda = 0$) and smoothness ($\lambda > 0$).

Again, in general, in this method the denser the array the more accurate are the approximations. Note that all the distances in this method are based on an Euclidean distancing system (C. Carvalhaes & de Barros, 2015).

A big limitation of this method is that it can not be used in case of spherical or ellipsoidal surfaces, where the coordinates are not linearly independent, because during its resolution, a singular matrix raises, and certain parameters do not have a unique solution. To address this, there is another method called smoothing spherical spline lines. This method is quite like the previous one, but the distancing system, instead of being based on the Euclidean distance, is based on the Geodesic distance (C. Carvalhaes & de Barros, 2015). Again, for the smoothing spherical splines, a denser array of electrodes proves to be more accurate (Babiloni et al., 1995).

The advantages of the application of the SL are highly reported on the literature, mainly as a spatial filter (Bradshaw & Wikswo, 2001; Foffani et al., 2004; Kayser & Tenke, 2015b), and consequentially, it proves to be a powerful tool in several areas, like brain computer interfaces (McFarland, 2015; Syam et al., 2017) and much likely, neurofeedback. Another discussed capability of the SL is the removal of muscle artifacts, with Fitzgibbon et al. (2015) describing that the application of a SL before performing ICA is an ideal methodological approach for this reason. Removal of muscle artifacts is achieved since the SL, due to its derivative nature, seems to highlight these more abrupt artifact portions (Fitzgibbon et al., 2015), which in terms of the ICA will result in an easier separation of the muscle artifact component. Interestingly, the application of these methods in the inverse order, hence ICA + SL, is described as the ideal technique for the "deblurring" and for filtering out some volume conduction contamination (C. G. Carvalhaes et al., 2009; Foffani et al., 2004). Although this implementation is quite highlighted as a good practice in EEG preprocessing, with rare studies recalling disadvantages or limitations (Biggins et al., 1991), from the in-depth state-of-the-art review performed in scope of this thesis, only a minority of articles include this technique in their protocol. In fact, this is

one of the main premises of the article “*On the benefits of using surface Laplacian (Current Source Density) methodology in electrophysiology*” by Kayser et al. (2015b). Here the authors discuss potential applications, advantages, and address some of the counterarguments used against the implementations of the SL. The same author had addressed, a year earlier (Kayser & Tenke, 2015a) one of the biggest controversies of the SL, a lower sensitivity of this algorithm to deep generators and preference for superficial generators, which could bias the results. Again, Tenke et al. (2015b), refuted this “limitation” and concluded that the application of SL is advantageous.

1.4.3 Connectivity Context: Diseases and Related Phenomena

To highlight the importance of studying EEG-based FC and more specifically the construction of strategies that can improve the estimates of FC, this sub-section addresses potential clinically-related applications that can benefit from it. Yet, it is relevant to pin-point that FC is not the sole explanation or cause, but that studies do confirm alteration in FC as part of the disease phenotype.

Furthermore, FC studies are related to a multitude of phenomena, beyond disease-related alterations. For example, FC can be used to detect emotions as demonstrated by Gonuguntla et al. (2016). Also, FC studies have been confirming the functional integration hypothesis, as for example in the study by Sorti et al. (2016), where they evaluated arm movement task-related changes in brain activity and functional connectivity, and found significant event-related desynchronization over the alpha and beta bands on the bilateral sensorimotor cortex during the left arm movement, and just in beta band on the contralateral hemisphere during the right arm movement. Also, increases in centrality during task were found for the motor regions.

In the clinical context, which could as well be one of the main future applications for neurofeedback, whether directly by selecting a “functional connectivity” as target metric or even brainwave specific neurofeedback, the first example of a disease with reported abnormalities in the FC that we shall refer is SZ. In a 2014 study, Damaraju et al. (2014b) used resting state with eyes-closed in fMRI of 151 schizophrenia patients, and used both a static and dynamic FC analysis approach, showing dysconnectivity profiles in SZ patients when compared with the healthy controls. In the static analysis, both hyperconnectivity between thalamus and auditory, motor, and visual networks was present, while hypoconnectivity was present between sensory networks. Concerning the dynamic analysis, SZ patients showed less spent time in states typified by large scale connectivity. Also, putamen/sensory networks hypoconnectivity was reported. Through EEG analysis, more specifically, through the network analysis of the theta band connectivity on a P300 ERP task, increased pre-task strengths were found for SZ patients, which were correlated to a worse cognition of the schizophrenia patients (Cea-Cañas et al., 2020).

The Autism Spectrum Disorder has also been associated with altered FC profiles. On their review, Hull et al. (2017) summarized the fMRI major findings, with a consensus that both hypo- and hyper-connectivity profiles have been consistently identified. The most reported hypoconnectivity profile was found in the default-mode network (DMN), with studies linking this hypoconnectivity with the symptom severity. Other regions, like the posterior cingulate cortex, lingual/parahippocampal gyrus, and postcentral gyrus showed hypoconnectivity. On the other hand, hyperconnectivity profiles were found in the striatum, pons and insular cortex, thalamus, basal ganglia, between other areas, with data suggesting an association between the degree of hyperconnectivity, both in thalamus and basal ganglia, and symptoms severity. Through EEG analysis the above-mentioned findings, were also observed, as

reduced DMN, sensorimotor network and dorsal attention network connectivity were reported (Prany et al., 2022).

Baldassare et al. (2016) on their study with BOLD-fMRI data, correlated post-stroke behavioral deficits with the abnormal patterns of resting state FC on both dorsal attention and motor networks. Interestingly, in an older study, Guggisberg et al. (2008) tried to understand how focal lesions affected the FC between that specific lesioned brain area and the healthy ones, using MEG. The primary conclusion was that lesion patients, compared with the healthy controls, had diffuse brain areas with low alpha coherence, whilst showing decreased connectivity estimates for the lesion region in comparison with the intact contralateral region.

In the context of neurodegenerative diseases, abnormal connectivity profiles have been reported. Filippi et al. (2019), in their review, summarized several articles' results concerning this specific topic. Concerning Alzheimer's disease (AD), decreased FC has been shown in the DMN, often accompanied by increased connectivity in the fronto-parietal, attentional, and salience networks, as a compensatory mechanism. Several FC features have been linked with the presence of cognitive impairment in AD. In fact, when using those FC features to feed AI algorithms for the prediction of mild cognitive impairment (MCI) in this disease, accuracies of 88% were reached. Concerning Parkinson's disease, dysconnectivity profiles in the DMN, fronto-parietal, salience and associative networks have been linked with the development of cognitive impairments. Also, in Lewy Body dementia abnormal connectivity profiles were found in the visual, attentional, and executive networks.

In a recent study by Choi et al. (2021), using EEG data, the authors compared side by side how different psychiatric disorders varied in matter of FC parameters over the DMN. Some of the considered diseases were already highlighted before, and they are post-traumatic stress disorders (PTSD), obsessive compulsive disorder (OCD), panic disorders, major depressive disorder (MDD), bipolar disorder, SZ, MCI and AD. For example, considering the clustering coefficients, SZ and AD patients showed hyper-clustering in the theta band while OCD, MCI and AD showed hypo-clustering in the low-alpha band. In fact, disease-specific clustering patterns were found.

Other diseases like epilepsy and dyslexia have also been linked with abnormal FC profiles (Finn et al., 2014; Sargolzaei et al., 2015).

The last disease that we should refer is the ADHD, which has been often linked with FC abnormalities. Cao et al. (2009a) used fMRI data to examine the abnormalities in the FC of medication naïve children with ADHD. Compared with controls, ADHD individuals showed decreases in putamen FC, with the only exception being the connection with the right globus pallidus/thalamus, with which it had increased correlation. Abnormal FC was also reported in the DMN and fronto-striatal circuitry (Cao et al., 2009b) and putamen (Konrad et al., 2006; Lan et al., 2021), through the analysis of fMRI data. Still analyzing fMRI data, the latter also reported abnormalities in the attentional networks (Rubia et al., 2019), ADHD related FC abnormalities in the right inferior frontal cortex and in the DMN. These abnormalities in the DMN and in the attentional networks were also noticed in another by Zhang et al. (2020). Concerning specific connectivity at the level of frequency bands, and using a task-based approach, the authors showed that ADHD patients had increased connectivity in the pre-stimulus theta, alpha and beta band and increased connectivity in the post-stimulus beta band. Another study identified reduced pre-stimulus/post-stimulus change in theta connectivity in ADHD individuals (Micheline et al., 2019).

1.5 Neurofeedback

1.5.1 Concepts

According to Marzbani et al. (2016), NF is a kind of biofeedback, which teaches self-control of brain functions to individuals by measuring brain features and providing a feedback signal to them. The feedback can be given to the user by an auditory, visual, VR, among other possible stimulus modalities. This technique relies on an almost instantaneous loop which enables the user to perceive own brain activity, such that, the individual can adapt and reach the desired performance (Hammond, 2007).

Such training offers a non-pharmacological, non-invasive, non-dependency inducing, and with almost no side effects, way of strengthening the brain circuitry and enhance “brain performance” (Hammond, 2007). The application of this technique has been widely studied, with positive results, for the matter of cognitive enhancement (Loriette et al., 2021), rehabilitation (T. Wang et al., 2018) and even therapy (Niv, 2013). In the next subsection we will refer some of these applications.

1.5.2 Basis

Concerning the neurophysiological mechanisms of the NF learning, these remain quite unclear despite the fact that several mechanisms have been reported to influence the learning process (Niv, 2013). A common point and a big premise of this type of NF training is the operant conditioning principle which relies on associative learning, that sums up the power of the reinforcement and says that a behavior, when rewarded, tends to be promoted and maintained, while when punished, tends to be extinguished (Sherlin et al., 2011). For example, many protocols may adopt a design in which while a subject registers a desired brain pattern, a positive reward reinforcer is displayed as feedback, and in case the objective is not attained a positive punisher reinforcer is displayed as feedback.

In Niv’s review “*Clinical efficacy and potential mechanisms of neurofeedback*” (Niv, 2013), some of the potential neurophysiological mechanisms of NF are referred to, as for example, neuroplasticity, global connectivity, and reinforcement of the DMN, central executive network, and salience network. Neuroplasticity can be understood as the inherent ability the brain has, throughout life, to change, modify itself, and adapt in response to the interactions with environments, as well discussed by Voss et al. (2017). With this said, Niv (2013) suggests that NF may induce neuroplasticity-related changes, more specifically, by enhancing synaptic strength and reorganizing structures by firing repetition and task recurrence. In fact, repetition seems to be a big key for the success of the NF training, as usually, for significant outcomes in studies, at least 8 to 10 sessions are needed, while for clinical applications, it has been consensual that more than 20 sessions are usually required (Gruzelier, 2014; Niv, 2013). According to Ros et al. (2014), through such repetition there will be a promotion of a specific pattern. In this article, the authors also propose a framework for the NF procedure based on this “synaptic strengthening hypothesis” - it states that there is an initial phase where the subjects have an unconditioned pattern of the metric of interest, and that, when the defined reward threshold is reached, point where the positive reinforcement will be done, “reward-modulated signal for synaptic plasticity” is generated. It is suggested this mechanism will promote the integration of and enhancement of such specific brain functioning pattern, as the individual will try to reproduce such state in the posterior phases.

The second mechanism that Niv (2013) refers to is a global connectivity modulation. This means that, overall, NF training increases the effectiveness of the networks in the brain. This is based on the fact that, as will be discussed later, NF has an impact on several connectivity-related syndromes.

The third mechanism that Niv (2013) refers to is related with global connectivity. The premise posits that often the NF protocols target frequencies that are highly related to the DMN, central executive and salience networks. Since all of these are largely involved in the correct functioning of the brain and NF will contribute to their enhancement, this enhancement will also contribute to a better brain functioning (Niv, 2013).

1.5.3 Neurofeedback Loop

The NF training can be seen as a succession of loops, each with 4-steps. The first step is the data acquisition of the brain activity, the second is the data preprocessing and the third is the feature extraction. Depending on the power/value of the metric of interest, more specifically, on how it compares to a threshold, in the fourth step a reinforcement strategy is applied through the feedback. Also, the outcome of the feedback protocol largely depends on the individuals, as there are individuals who are unable to learn self-regulation through this training, the so-called non-learners (Enriquez-Geppert et al., 2017).

In this subsection we will explore in more detail each step of the neurofeedback loop and on the duality learners vs non-learners.

1.5.3.1 Data Acquisition



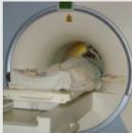

	EEG	MEG	fMRI	fNIRS
				
Underlying Signal	Electrical activity from pyramidal cells perpendicular to the scalp (mainly gyri)	Magnetic fields produced by pyramidal cells perpendicular and tangential to the cortical surface	Blood oxygenation level dependent contrast (which indirectly relates with neuronal activity)	Volume of oxygenated and/or deoxygenated blood (which indirectly relates with neuronal activity)
Typical Feedback Signal Source	One central electrode or a multi-electrode cap	Sensors over sensorimotor cortex	Single brain regions, 3mm × 3mm voxels	Several sensors over sensorimotor cortex
Feedback delay	< 50 ms	< 50 ms	~1.5 s (plus 4-6 s hemodynamic delay)	~0.5 s (plus 4-6 s hemodynamic delay)
Resolution				
temporal	Milliseconds	Milliseconds	Seconds	Seconds
spatial	Centimeters	~10mm	Millimeters	Centimeters
depth	Superficial	Depth constrains interpolation accuracy	Deep (any region)	Superficial (<4 cm)
Portable	Yes	No	No	Yes
Cost (USD)				
Initial set-up	500-50,000	2,000,000	500,000-2,000,000	50,000-300,000
Running costs	No extra fees	~500/hour	~500/hour	No extra fees
Relevant Literature	Plentiful	Emerging	Moderate	Emerging
Main Applications	Pediatric ADHD, epilepsy, various psychological disorders	Brain computer interfaces (Experimental)	Psychological conditions (chronic pain, depression, schizophrenia, etc.) (Experimental)	Brain computer interfaces, stroke rehabilitation (Experimental)

Figure 1.4 - Neurofeedback data acquisition techniques - adapted from (Thibault et al., 2016)

The first step of the neurofeedback loop is the data acquisition, in which the brain activity is captured. For this, several techniques can be used, with the main ones being EEG, MEG, fMRI and fNIRS. EEG is one of the most used techniques in the context of NF, because not only it provides a cheaper, low feedback delay, portable, and safe way to assess the brain activity, but also it has an inherent high temporal resolution in the order of the millisecond. The main pitfalls of the EEG technique are the low spatial resolution and the high susceptibility to artifacts. MEG is also used due to its high inherent millisecond temporal resolution and low feedback delay, yet, it has a high cost and is not portable. Concerning fMRI, this technique provides a high spatial resolution way to assess brain activity, yet, with relatively high associated costs, high feedback delay, and a lower temporal resolution. A cheap and portable alternative way to assess the brain activity is the fNIRS technique, yet it has a high feedback delay and a lower temporal resolution (Lakshmi et al., 2014).

1.5.3.2 Data Preprocessing

This intermediate step is where the data is prepared for the feature extraction. In the case of EEG, the major task in this step is the detection and rejection of artifacts that can pollute all the loop. For example, artifacts in a frequency band that corresponds to the frequency of interest would lead to a biased and incorrect value for the feature of interest, which would lead to a biased and incorrect feedback, resulting in a whole biased feedback loop (Chaumon et al., 2015; Enriquez-Geppert et al., 2017). For the removal of artifacts, several procedures can be applied, from bandpass filtering the data to performing manual and automatic rejection of “artifactful” portions of data, or through detection of the artifacts by interpolation methods in accordance with simultaneous EOG and ECG recordings (Schomer & Lopes da Silva, 2017), there are in fact several strategies to tackle such problem. In the context of manual artifact rejection, several algorithms can be used like ICA method, canonical correlation analysis (CCA), and principal component analysis (PCA) (Kaczorowska et al., 2017; Wim De Clercq et al., 2006). All have in common the fact that they perform a signal decomposition solving a blind source separation problem. Also, other more elegant approaches have been developed in form of automatic rejection, as for example the Adjust pipeline (Mognon et al., 2011) or Prep pipeline (Bigdely-Shamlo et al., 2015), which tend to use ICA or another blind source separation techniques, and find specific properties profiles, like high or low values of skewness, metrics related to the symmetry of the data, kurtosis, which measures the distribution of the data relative to the normal distribution, among others. The automatic evaluation of these profiles will generate a decision over the exclusion of portions of the data.

Unfortunately, during the online procedure, due to the feedback delays that would be generated by the previously referred techniques, most of the methods above are very seldom used. These tend to be used in the post-hoc analysis, together with data re-referencing, time-to-frequency domains transformations, and epoching, for example.

1.5.3.3 Feature Selection and Extraction

The stage of feature selection and extraction is where the specific feature is extracted and computed from the brain activity. The selected feature tends to represent, or have a direct association with the pattern the NF protocols aims to modulate. Usually, the feature is in form of a brainwave specific power on a single channel or even on a set of channels (Enriquez-Geppert et al., 2017; Marzbani et al., 2016), but other features of interest can be used, like the estimated FC in a specific frequency

band (Yamashita et al., 2017), depending on the desired outcome. Also, depending on the intended outcome, the location of the metric of interest may change. For example, Marzbani et al. (2016) report some functional outcomes for specific target areas, such as frontal lobe NF training for cognitive functions like sustained attention and working memory, temporal lobe for improvements in memory, learning and facial recognition, parietal lobe NF training for improvements in problem solving, mathematical processing and spatial recognition, occipital lobe for improvements over visual-related cognitive tasks, and sensorimotor cortex for improvements in skeletal-movement-related functions. Yet, these outcomes depend on the hemisphere.

After the feature “value” is properly extracted the sensory feedback is prepared.

1.5.3.4 Feedback

The feedback will act as a messenger for the NF subject, converting the properties of the feature, such as amplitude or duration, to a sensory stimulus that informs the individual about his state, regarding the targeted brain process, thus, providing an engaging way to self-regulate brain activity (Enriquez-Geppert et al., 2017). This reward threshold will ensure that, for example, a positive reward reinforcement is only present when the intended pattern of brain activity is registered. The definition of the threshold is *per se* limited, having a subjective dimension, as it should be high enough to challenge and engage the subjects, promote the pattern of interest, while low enough to not frustrate and demotivate them, with both these extreme cases harming the training outcome. Unfortunately, there is no established guideline to define the threshold and several approaches have been studied. Whether it is a predefined fixed value, or it is calculated concerning a percentage/average from brain activity at rest, there are several options. Furthermore, no guidelines exist to the matter of how the threshold should be updated on the course of the sessions (Vernon et al., 2009). Concerning the feedback modalities, usually the visual feedback is done via changes on a size, color, and movement over a visual display while the audio feedback is done by changes in sounds pitch, volume, rhythm, timbre, and duration (Jensen et al., 2013). Also, virtual reality NF displays have been studied, with reported advantages over 2-dimensional screen-based visual feedback displays (B.-H. Cho et al., 2004). It is to note that the success of the NF protocol also depends on subjects’ states, such as mood (Subramaniam and Vinogradov, 2013) and motivation (Pérez-Elvira et al., 2021). Hence, the choice of the feedback stimulus has an additional component as, ideally, it should fulfill the subjectivity of the subjects’ preferences, which in turn could lead to better outcomes.

1.5.3.5 Learners

Although the NF training has proven successful in increasing several features of interest, with possible implications on treatment and rehabilitation in the clinical context, about one third of the subjects are unable to succeed in the self-regulation task associated with the NF training (Alkoby et al., 2018), even after repeated training sessions (Wan et al., 2014). These subjects also show no significant differences in behavioral outcomes (Hanslmayr et al., 2005a). These individuals can be described as non-learners and, unfortunately, a consensual definition on how to define and distinguish this group on the context of EEG NF data analysis remains to be settled (Vernon et al., 2009).

1.5.4 Independence of the NF-training

Just a brief note to the fact that, although the NF training tends to select a specific feature of brain activity for self-regulation, there are cases in which collateral alterations of non-targeted features may happen. A primary example of such case is in brain waves band-oriented NF-training. In fact, as referred in (Huster et al., 2014) the neighboring bands can be affected, and according to Egner et al. (2004), changes on the spectral topology that arise from NF-training are not restricted to the targeted bands. With this said, this must be taken into account in our analysis.

1.6 Applications

Alpha and UA NF training protocols have a wide range of applications, which will be briefly described in this section. Also, a revision is performed on NF studies in the context of FC, including those with a more clinical scope. To end this section, the influence of the feedback stimulus modality on the outcome of the NF training will be reviewed.

1.6.1 Alpha and Upper-Alpha Neurofeedback

Throughout the years, several studies highlighted the role of alpha-band NF in the enhancement of cognitive performance. Yeh et al. (2021) performed a meta-analysis over 16 studies that implemented alpha NF training and working memory outcome evaluation. The sample would be composed by 427 subjects, split into a control group of 217 subjects that does not undergo the NF training, and into an alpha NF training group with 210 healthy subjects. The objective of this meta-analysis was to explore the effects of alpha NF training on working memory, which the authors confirmed as being related to an increase on such working memory. Hsueh et al. (2016) also reported that EEG alpha NF training contributed to improvements over the episodic memory. Another study by Cho and colleagues (2008), still in the context of EEG alpha NF training, reported that since between the NF training sessions it was usual to have a bounce back on the alpha activity levels, a higher number of training sessions would diminish the extent to which the activity bounces-back between sessions, serving as clue to the conclusion that alpha NF training contributes to the maintenance of alpha activity. Concerning the specific time course of an EEG alpha NF training, Dekker et al. (2014) investigated the time course of both LA and UA over 15 eye-open alpha NF training sessions, on 18 subjects, with each session split into 3 periods of 8-min NF training with intercalated cognitive assessment. The authors reported an increase of the total alpha power until the tenth session, point at which a plateau was reached for the LA power (8-10 Hz) whereas the UA power (10-12 Hz) started to decrease. Also, the authors noticed that in the first two periods of each session the total alpha power increased, but that it decreased in the third period as a consequence of UA power reduction. The authors discuss that attention and motivation can justify these decreases and suggest different trainability timelines for lower and upper-alpha bands (Dekker et al., 2014).

Concerning specific EEG-based NF training in the UA band, studies have also reported that self-regulation of the UA seems to be related with cognitive outcomes, as for example, increases in the performance over a mental rotation task (Hanslmayr et al., 2005b). Escolano et al. (2011) reported an increase on children working memory effectiveness, after an EEG-based UA NF training with 18 sessions. Interestingly, in another study by the same author (Escolano et al., 2014), while 18 sessions seemed to be enough to register significant changes on working memory function, a 1-day long training,

also registered increases in working memory and mental rotation effectiveness, yet non-significant when compared to a control group—these results suggest that to achieve long-lasting changes in neurophysiology and brain function, so as to enhance behavioral outcomes, a higher number of training sessions seems necessary. Interestingly, for the mental rotation task, significant increases in a NF training group that underwent UA up-regulation were found after 5 sessions across 7 days, in a study by Zoefel et al. (2011). Moreover, among the possible clinical applications of EEG-based UA NF training, one can mention major depressive disorder, as Escolano et al. (2013) on an uncontrolled preliminary study reported that such protocol was effective in increasing diversity of cognitive functions such as working memory, attention and executive function, in the referred context. In the context of ADHD, the same author applied the same training protocol on 20 children diagnosed with ADHD, composed by 18 sessions, along which the training aimed at an increment in the UA. After the training, the parents rated a clinical improvement in the children concerning the inattention and hyperactivity/impulsivity, further confirmed by neuropsychological assessments, which reported improvements in the working memory, concentration, and impulsivity. These results support the hypothesis that EEG-based UA NF training is effective in improving certain domains of cognitive performance in ADHD (Escolano, Navarro-Gil, Garcia-Campayo, Congedo, et al., 2014). In the context of stroke survivors, Kober et al. (2017) studied two chronic stroke patients with memory deficits, patient A with a bilateral subarachnoid hemorrhage, and patient B with an ischemic stroke in the left arteria cerebri media, which were compared with an healthy elderly control group composed by 24 subjects that were enrolled in a 10-session length UA EEG-based NF training. Both patients showed improvements in memory functions, and a “normalization” over topographical distribution of certain brainwave frequencies, where previously abnormal. This result may underline the potential use of NF training as neurological rehabilitation tool, yet it needs to be replicated in a bigger group of stroke survivors, and properly controlled for NF training, for definite conclusions on the topic.

1.6.2 Neurofeedback and Functional Connectivity

Regarding the effects of different NF protocols on the connectivity patterns and brain networks of study subjects, the work by Shtark and colleagues (2018), called “*Neuroimaging Study of Alpha and Beta EEG Biofeedback Effects on Neural Networks*”, enrolled 23 healthy men in 20 sessions of Alpha upregulation with EEG-based NF training, and 12 healthy men in 20 sessions of Beta upregulation with EEG-based NF training, so as to study the differences in NF outcome when training upregulation of distinct frequency bands. Additionally, simultaneous EEG-fMRI data acquisition sessions would be performed in the beginning, in the middle, and at the end of the 20-sessions long NF training protocol. For those subjects that succeeded in the alpha up-regulation task, these showed a weakening of some functional connections among cerebellum, visuospatial network, right executive control network and cuneus, and the formation the complex containing the precuneus, cuneus, the visuospatial network accompanied by a strengthening of the connection between the anterior salience network (ASN) and the precuneus. Concerning the beta training group, a weakening of the interactions between the precuneus and the DMN, and cuneus with primary visual network were noted. Compared to the beta training, alpha training showed a more pronounced interaction between the cerebellum and the precuneus/right execute network, and decreased interaction between the primary visual network and high visual network. Such trends accentuated over the course of the training sessions (Kober, Schweiger, et al., 2017).

Concerning alpha-to-theta ratio NF training, Imperatori et al. (2017) studied the influence of this NF protocol on source reconstructed brain networks, using 10 sessions of 27-min length each, and comparing the outcomes between a NF training group and a control group, each with 22 subjects;

mentalization questionnaires were also applied to assess mentalization. The results showed that, compared with control subjects, the NF group had significant increases in the mentalization questionnaire scores. Also, several DMN-related brain areas showed increases in FC. Also, a study that applied a sensorimotor rhythm (20-30 Hz) enhancing NF protocol, also reported reorganization of the sensorimotor connectivity patterns (Terrasa et al., 2019).

Finally, and concerning specifically the UA NF protocol, the one that mainly interests us, two studies should be pointed, both with researchers from the LaSEEB group, ISR-Lisboa Institute. A Master Thesis by Cristiano Berhanu, with the title “*Connectivity-based EEG-neurofeedback in VR*”, implemented 2 protocols of VR EEG-based NF training, with a time design like ours (our experiment also contains data from his thesis). In the first protocol, the target for upregulation was the alpha weighted-node-degree (WND) ImC at the Cz channel, while in the second protocol, the target for upregulation was the relative amplitude of the UA (RAUA) at the Cz. For each of the protocols, an increase in the metric of interest was observed, with negligible effects on neighboring frequency bands. An interesting observation was the fact that, while the FC NF training group showed almost no changes in terms of RAUA, the RAUA training group, showed an increase on the alpha WND-ImC at Cz channel, which was higher than the increase caused by the FC training. Yet, the sample size is too small to draw robust conclusions, whereas it may serve as clue to the influence of the UA NF protocol on the brain FC (Berhanu, 2019). In the second study, Wang et al. (2021) performed a 2-day long protocol, with 5-blocks of NF training per day, and 28 healthy subjects, aiming at alpha downregulation at the Oz channel, in a EEG-based NF protocol. The authors used the PLV metric to infer on alpha FC changes, whilst network analysis included the *clustering coefficient*, the *charpath* and the *GE* algorithms. The protocol was well succeeded in terms of reducing the individual alpha band (IAB) power, as a constant decrease was verified over the training blocks in both days. Also, during the first day and the first blocks of the second day, increases on the overall parietal and occipital channels functional connections were registered. In the last 2 block of the second day, decreases on the connectivity of the same regions were seen. The authors suggest this could be a clue for a “breakthrough point” in which the subjects NF task-efficiency stagnated and even decreased. Interestingly, the network analysis led to similar conclusions, as both *clustering coefficient* and *GE*, after increasing through all the earlier stages, started to decrease when reaching the 8th block, while the *charpath* had an opposite behavior. The emphasis on this article relates to the current work, keeping in mind that we might expect a similar behavior during the analysis of our data, despite the differences in protocols.

The previously referred articles support what was exposed when discussing the global connectivity theory that underlies the NF learning outcome. As in fact, it seems that even in cases in which the NF training protocol targets up- or down-regulation of a specific frequency band, the brain reorganizes, and changes occur in the associated functional paths. In line with this thought, Li et al. (Li et al., 2019) demonstrated the possibility of targeting a FC-related feature in NF training, through self-regulation of the theta coherence among multiple regions simultaneously, which resulted in behavioral changes translated into improvement of working memory outcomes.

Now, getting back to the topic of FC-related clinical application through NF training, for ADHD, for example, Rubia et al. (2019) demonstrated, using an fMRI-based NF protocol with 11 trials of 8.5 min, strengthening of FC within fronto-cingulo-striatal networks and decreases in FC with the posterior DMN regions, which was considered by the authors as an improvement in the clinical outcome (Rubia et al., 2019). More recently, Wang et al. (2021) using theta-to-beta ratio as target metric, performed an EEG-based NF training of 60 sessions on 22 ADHD children. The overall progression of the children’s effective connectivity was analyzed and compared with a control group composed by 15 subjects. Also, topological properties of the networks and flow gain, and the metric for the intensity of

information transmission, were analyzed for delta, theta, alpha and beta bands. Before the training, ADHD children, compared with the controls, revealed higher clustering coefficient in the delta band as well as a lower *charpath*, and weakened anterior-to-posterior flow gain, while for the alpha band a strengthened posterior-to-anterior flow gain was observed, and the beta band revealed a strengthened anterior-to-posterior flow gain. Interestingly, after the training the topological properties and flow gain of ADHD children were close to those of healthy controls, and, according to the parents, with significant improvements in the ADHD symptoms. The authors state this to be the first-ever evidence that differences in phase-based effective connectivity in ADHD children, compared with healthy children, could be reduced with the application of a targeted NF training protocol. In the case of dementia and MCI, both EEG-based and fMRI-based NF training techniques have demonstrated to produce improvements in the patients' cognitive scores (Trambaiolli et al., 2021). In the case of PTSD, a study by Nicholson et al. (2016) showed that 30-min long alpha desynchronization EEG-based NF training produced a shift in amygdala complex connectivity from areas implicated in defensive, emotional, and fear processing/memory retrieval to prefrontal areas implicated in emotion regulation/modulation. These results were negatively correlated to PTSD symptom severity and were suggested as promising for the treatment of such condition. In the scope of stroke patients, Mottaz et al. (2018) showed in a study with 10 chronic stroke survivors that through modulation of the alpha frequency band WND of the ipsilesional primary motor cortex using visual feedback assistance, improvements in motor functions could be achieved. Another group (Giulia et al., 2021) tried to assess, in chronic stroke patients, the effects of alternated protocol with periods of bimodal EEG-fMRI NF and periods of EEG-only NF training, on the effective connectivity, which was analyzed through dynamic causal modelling, and targeted both left and right hemisphere motor cortices activation over the frequency interval of 8 to 30 Hz. The authors reported that NF upregulation of the target area not only reshaped the activation patterns but also decreased inter-hemispheric FC between the primary and pre-motor regions, and reduced ipsilesional self-inhibitory functional connections, underlying an increase in activation of such area. Both these studies are useful to perceive the underlying pathophysiology of chronic stroke and open up space for the design of new NF strategies for the purpose of stroke rehabilitation. A brief note to a recent study by Albarrán-Cárdenas and colleagues (2021) that revealed, through a 30-session long theta-to-alpha ratio EEG-based NF training, in the context of children with reading disorders, that not only NF training contributed to EEG power normalization and cognitive-behavioral improvement, but that it also lead to changes in FC, with interhemispheric coherence being reduced in the beta, theta and delta bands, mainly on Fp regions, and intrahemispheric coherence increase in the alpha band and decreases in the beta, theta and delta bands. The authors found, among all the significant changes, that the highest association with reading outcomes and scores occurred with the reduction in the theta band coherence, paving the way for NF treatments in the context of reading disorders (Albarrán-Cárdenas et al., 2021).

1.6.3 Neurofeedback Sensory Modalities and Functional Connectivity

In the matter of how different feedback sensory modalities affect the outcome of the NF procedure, which is one of the more understudied areas in NF, as verified during an in-depth literature review, guidelines on the choice of the feedback sensory modality are lacking. There are scarce articles directly comparing the different modalities, which is also reported by both Enriquez-Geppert et al. (2017), and Huster et al. (2014).

The main articles that directly perform this comparison are “*Neurofeedback in Learning Disabled Children: Visual versus Auditory Reinforcement*”, by Fernández et al. (2016), and Bucho et al. (2019) article “*Comparison of Visual and Auditory Modalities for Upper-Alpha EEG-*

Neurofeedback”, as far as identified. In the first, Fernández et al (2016) performed a theta-to-alpha ratio downregulation with an EEG-based NF protocol that enrolled over 20 children with learning disabilities. The authors compared both the implementation with visual feedback (a white square) and with auditory feedback (tone of a 500 Hz sound). Only the auditory group showed behavioral/cognitive improvements, which might be related to attention processing. In the second study, upregulation of RAUA at the Cz channel was the target in a EEG-based NF protocol, applied to 16 subjects split into two groups, an auditory and a visual feedback modality group, respectively, while simultaneously assessing outcomes in working memory—this experiment was performed at LaSEEB, and the recorded data are used in this Master Thesis project. The results of this study demonstrated that both groups had increases in the RAUA feature on the course of the 4-day training sessions, despite not accompanied by significant improvements regarding the working memory scores, with the authors concluding that none of the sensory modalities seemed to outperform the other for this specific protocol. A limitation in this study, similarly to what is found generally in NF literature, is the small sample size, which impairs the capacity to generalize results to the population level.

In the context of VR-based NF protocols, the researchers usually compare the immersive visual feedback (VR) with two-dimensional screen displays, with results suggesting the potential superiority of the former for power-regulation based trainings (Berger et al., 2022; B.-H. Cho et al., 2004; Kober, Reichert, et al., 2017).

Concerning how different feedback sensory modalities in NF training may affect the brain FC profile, there are currently no studies that explore this topic specifically, as far as we could identify. The “scarce articles” mentioned above, usually tend to analyze spectral evolution and cognitive outcomes, but FC analysis is usually not done.

1.7 Objectives

As seen in the section 1.4.3, the field of FC and modulation of brain’s integrated activity may represent a possible landscape for the implementation of NF training, specifically as there is a wide range of diseases that can benefit from the FC and brain’s integrated activity modulation that such technique provides. Thus, this still seems to be reserved to the future as, at the moment, too many topics remain underexplored and not clearly characterized in the scope of NF training methodology, for this to be fully ready to be used in clinical context. Indeed, one of the main unclarities resorts with the choice of the NF-training sensory feedback modality. There are just a few studies which explore how these can affect the fate of the training, and none of them analyzed possible “integrated activity modulation effects” in terms of functional connectivity. With this said, this thesis aims to go further on such topic and answer the following question:

“How is the individual’s brain functional connectivity affected by the use of different sensory modalities in EEG-based Neurofeedback training protocols that target the upper alpha band?”

In other words, we will analyze how the usage of different sensory modalities in EEG-based Neurofeedback training protocols targeting the upper alpha band, will affect and modulate the brains integrated activity, analyzed by means of functional connectivity and network analyzes.

Hopefully, the results achieved in this work may provide a step further on understanding what are the underlying mechanisms of NF training and, to pave the way to improve the overall quality of the design of NF-protocols, as indeed these will benefit of knowing, in dept, how different feedback sensory

modalities will, or will not, have influence on the fate of the NF-training, on the reorganization of the brain networks, among others... Such that, in the future this technique can be more explored, at its full potential, in clinical context, more specifically in the field of the previously reported connectivity-related diseases.

Last but not least, since there is not a clear consolidation of the implementation of the SL method as a spatial filtering technique in EEG, and more specifically in the context of FC analysis in EEG data, this study has the secondary purpose of analyzing further this topic, by comparing the implementation of SL re-referenced data, with common average re-referenced data, over the different analyses.

2 Methods

In this section we will explore the applied methodology. By the following order, we will detail the subjects' characteristics, the neurofeedback protocol design, the equipment setup and signal acquisition settings, the data preprocessing pipeline, and the assessment of the training effects. Note that in scope of this project the data that are analyzed had been acquired in two previous experiments at LaSEEB, ISR-Lisboa. The first study was Teresa Bucho's master thesis, "*Comparison of auditory and visual modalities for EEG-neurofeedback*" (Bucho et al., 2019), and the second was Cristiano Berhanu's master thesis, "*Connectivity-based EEG-neurofeedback in VR pipeline development and experimental validation*" (Berhanu, 2019). Teresa's master thesis experiment (from now on Experiment 1) contains data from EEG-based UA Neurofeedback using visual and auditory feedback modalities, while Cristiano's master thesis (from now on Experiment 2) contains data from EEG-Based UA Neurofeedback using a visually immersive VR feedback modality.

2.1 Subjects

For this research, the data of 20 healthy subjects, from the previously referred experiments, were considered. In both experiments, the subjects were mostly students and researchers from Instituto Superior Técnico, Universidade de Lisboa, and participation was voluntary, without any monetary compensation. Also, in both cases, exclusion criteria would rule out individuals with serious health problems, for example ophthalmic or auditory disease, , psychiatric or psychological disorders, and with historic of drug abuse/dependence or under medical prescription of psychoactive substances. In Experiment 1, the age of subjects ranged between 18 to 30 years old, while in Experiment 2 subjects age ranged between 18 to 50 years old. All the subjects signed an informed consent after duly informed about the respective experimental procedures, objectives, possible side effects and exclusion criteria. Hence, in this project, 3 groups of subjects are considered: i) the visual NF-training group, containing 8 subjects (4 males and 4 females, with ages in the range 22.5 ± 2.73), ii) the auditory NF-training group, containing 8 subjects (3 males and 5 females, with ages in the range 22.88 ± 1.25), and iii) the VR NF-training group, containing 4 subjects, (2 males, 2 females, with ages in the range 34 ± 12 years old). All groups were randomly assembled in the respective experiments.

2.2 Neurofeedback Protocol

2.2.1 Protocol Design

Concerning the time design for the NF protocol, both experiments used the same temporal organization. Each session would start with a 4-minute calibration period, consisting of alternated 1-minute periods of eyes open and eyes closes, in which the subjects would be in a passive state. The calibration was used to extract a baseline for UA activity, to build an appropriate threshold for the feedback parameter of the NF procedure, but also to extract the IAB. After this period, the NF training period started, which was divided into five sets, with each set composed by three blocks, and each block was composed by two 1-minute trials. In between trials there was a 10 second interval, and in between blocks there was a 15 seconds interval and, if necessary, in between sets the interval could be more than 15 seconds long. All of this would make a total duration of approximately 37 minutes. In the end of the NF training, another calibration would be done to obtain a post-training baseline and IAB, and the

subjects would be asked to fill-in some questionnaires. All the subjects recorded four sessions, on consecutive days, at approximately the same time of the day.

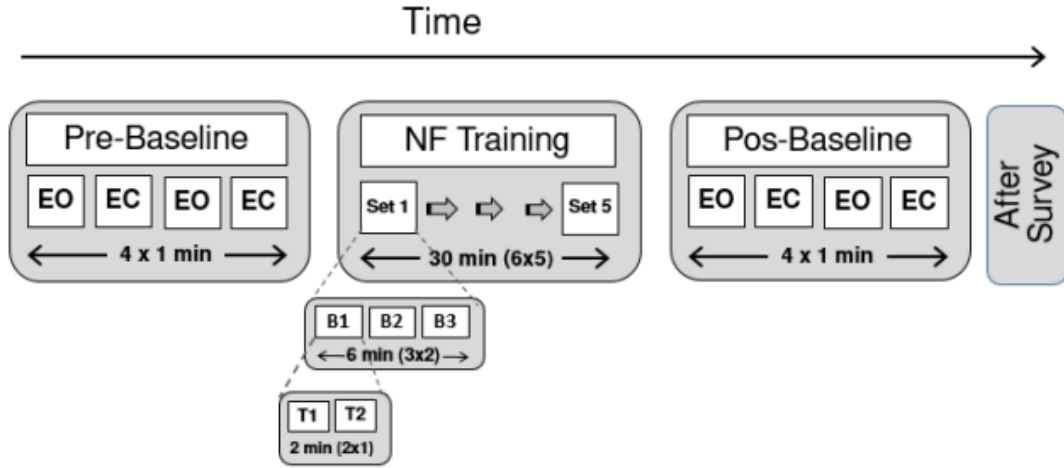


Figure 2.1 - Time design of a NF training session

2.2.2 Feedback

In both experiments, the individual UA band was the target of the NF protocol, specifically the RAUA at the Cz channel, defined by Wan et al. (Wan et al., 2014) with the following equation:

$$RAUA = \frac{\sum_{k=IAF/\Delta f}^{HTF/\Delta f} X(k)}{HTF - IAF} / \frac{\sum_{k=4/\Delta f}^{30/\Delta f} X(k)}{30 - 4} \quad (2.1)$$

where $X(k)$ is the frequency amplitude spectrum at frequency k , calculated by means of a sliding window FFT, Δf the frequency resolution, IAF is the individual alpha frequency and HTF is the higher transition frequency

To present the desired feedback to the subjects, 3 sensory modalities were used. The individuals from the visual group received the feedback in form of visual stimuli, which consisted in a sphere set over a horizon background, with the sphere size reflecting the RAUA on the Cz electrode. Also, the color of the sphere would change accordingly to whether the RAUA was above or below the specified threshold, between white and red, respectively. The main goal of the subjects was to keep the sphere as large as possible and to keep it white as big as possible.

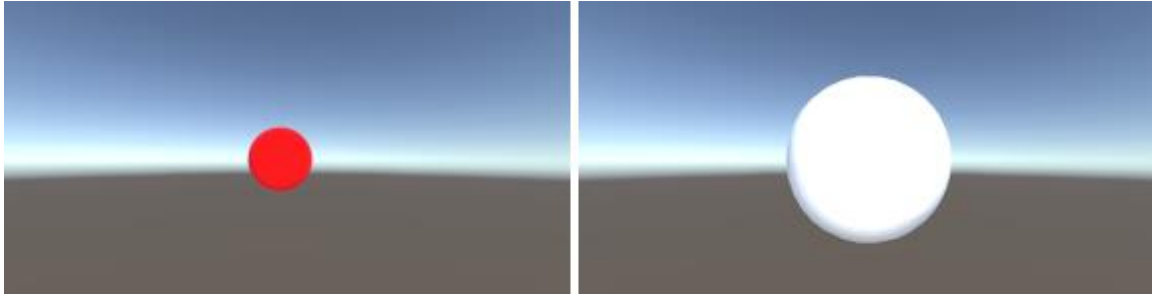


Figure 2.2 - Visual feedback presented to the subjects. (Left) When the Cz-RAUA is below the threshold, the sphere color is red and the radius is smaller. (Right) When the Cz-RAUA is above the threshold, the sphere color is white and the radius is bigger. Adapted from (Bucho et al., 2019).

The individuals from the auditory group received the feedback in form of an auditory stimulus, which consisted in a sound with the volume exponentially modulated by the RAUA. In this modality, the individuals would remain with their eyes open while visualizing the same horizon background presented in the visual feedback. When the feedback parameter was below the specified threshold, a white noise was heard with a volume that would grow in amplitude when the RAUA was farther from the threshold. When the RAUA at Cz was above the specified threshold, a 30-second piano loop would appear, with a volume that grew for higher values of RAUA.

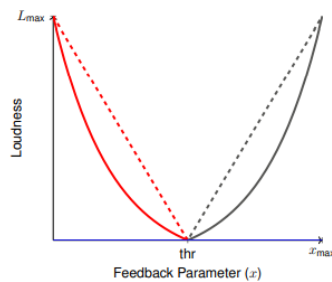


Figure 2.3 - Auditory feedback modulation. thr = threshold. Red curves: the dashed represents the perceived and the solid represents the actual noise volume. Gray curves: the dashed represents the perceived and the solid represents the actual music volume. Adapted from (Bucho et al., 2019).

The individuals from the VR group received feedback in form of a VR stimulus, displayed through the Oculus Rift hardware, which consisted of a planet in background with a rotating sphere of particles. To avoid repetitiveness, and provide a sense of progress to the subjects, three specific feedback tasks could be instructed. The task could consist in i) increasing the size of the rotating sphere, ii) increasing the rotation speed of the sphere of particles, or iii) reducing the distance, perceived by the subject, to the sphere of particles, and if possible, reach out the center of the particle system. When the latter happened, the subject would return to the initial position/perspective and would be instructed to, again, reduce the perceived distance. The goal would be to reach the center of particles as many times as possible. In the first session, the “size” feedback task was used, while in the second session the “rotation speed” task was used. In the third session the “distance” task was used. In the fourth session, each set would have a specific task. In the first and fourth set the “size” task was performed, in the second set the “rotation speed” task was used, and, finally, in the third and fifth set, the “distance” task was performed. Again, the feedback electrode was the electrode at position Cz.

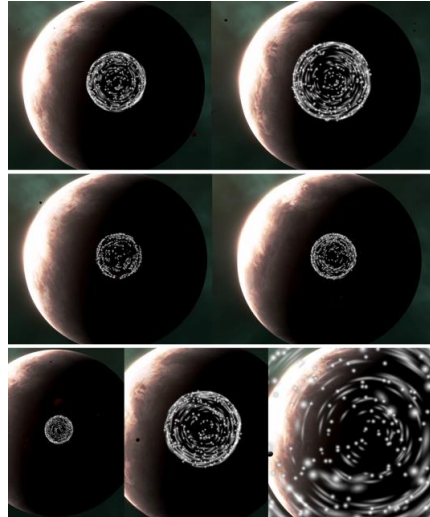


Figure 2.4 - VR feedback presented to the Subjects. Top row: particle system changes size, middle row: particle system changes rotation speed, bottom row: camera approaches particle system with changing speed. Adapted from (Berhanu, 2019)

2.2.3 Surveys

While enrolled in the experiment, the subjects were asked to answer some questionnaires to assess specific states and features.

In Experiment 1, at the end of each session the subjects were asked to fill-in a mental state questionnaire. Also, specifically, in the first session, before the NF training protocol, the subjects would be asked to fill health-related questionnaires, including the 36-Item Short Form Survey (SF-36) and Hospital Anxiety And Depression Scale (HADS) and some memory tests like the Digit Span and N-back. In the fourth session, the subjects were asked to perform the memory tests another time.

In Experiment 2, at the end of each session, the subjects were asked to perform a simulator sickness questionnaire, to assess the any negative sensation caused by the VR experiment, and a self-perceived load questionnaire. Similarly to Experiment 1, memory tests would be performed both before the first session and after the last session. In the last session, the subjects were asked to fill a sense of presence questionnaire to assess the quality of the immersion in the VR experiment.

2.3 Signal Acquisition and Equipment Setup

The data for both Experiment 1 and Experiment 2 were collected in the NeuroLab room of the Evolutionary Systems and Biomedical Engineering Lab, a research lab of the Institute for Systems and Robotics (ISR) at Instituto Superior Técnico. The room provides both light and sound isolation, appropriate for the acquisition of EEG data. On the course of the experiments, the subjects would sit, comfortably, on a swivel chair with no wheels, placed approximately 1 meter from the monitor. Also, the subject would wear headphones and a researcher would supervise all the procedure in a separate partition. To record the EEG signals, the EEG amplifier LiveAmp (Brain Products GmbH, Germany) interface was used, connected to the OpenVibe (Inria Rennes, France) software. The ActiCap's headset system of 32 channels, based on the extended 10-10 system was used, and data was collected with a sampling frequency of 500Hz. The following electrodes were active: Fp1, Fz, F3, F7, FT9, FC5, FC1,

C3, T7, FCz, CP5, CP1, Pz, P3, P7, O1, Oz, O2, P4, P8, TP10, CP6, CP2, Cz, C4, T8, FT10, FC6, FC2, F4, F8 and Fp2. The ground electrode was located at the forehead while the reference was located on the left mastoid, on the TP9 electrode. The electrodes are connected in a splitter box, connected to the LiveAmp interface. In Experiment 1, circuit impedance was kept below 10 k Ω for all electrodes, by scrubbing the respective scalp position with an alcohol-soaked Q-tip and then injecting gel (SuperVisc, EasyCap, Germany) on the electrode aperture using a blunt needle, before placing the electrode. Using the same method, the impedances were kept below 25 k Ω in Experiment 2.

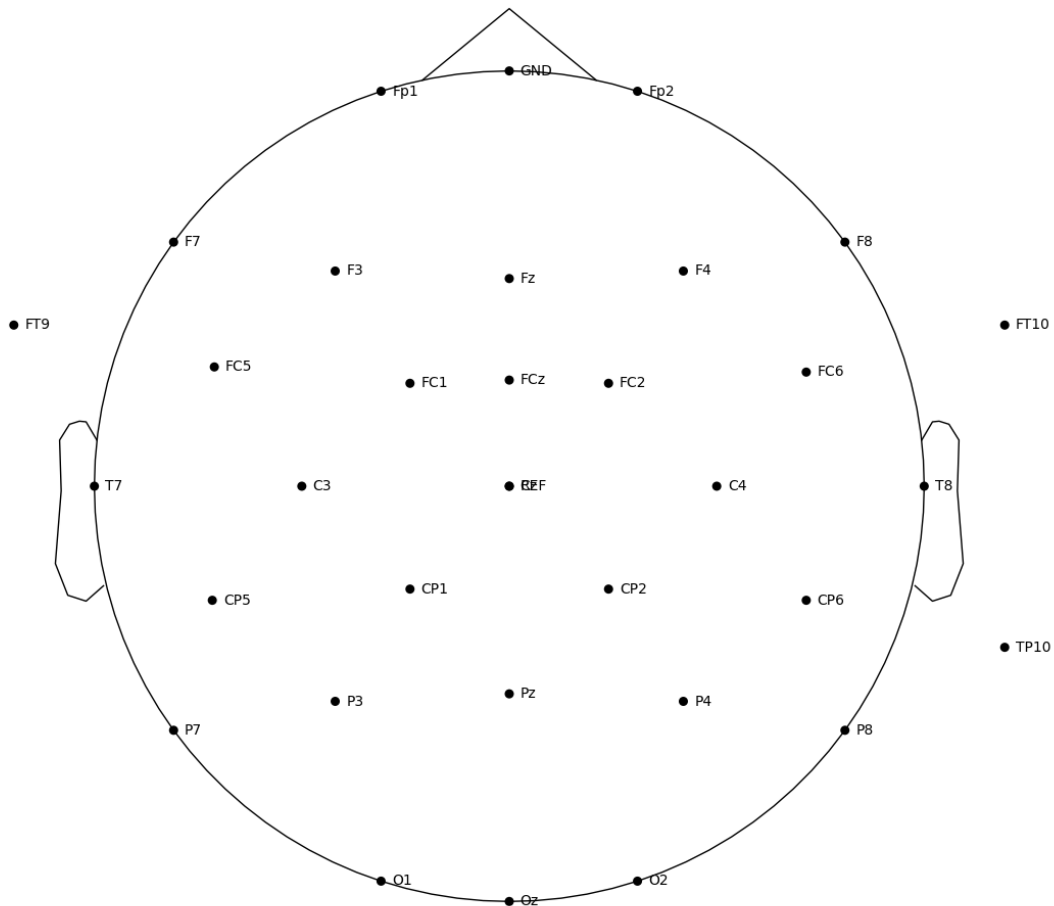


Figure 2.5 - Electrode positioning system used for the experiment

2.4 Data Preprocessing

As we were dealing with raw EEG data containing artifacts, we needed to perform a preprocessing pipeline that ensured that in posterior analyses we wouldn't have erroneous results, and in consequence, erroneous conclusions.

Firstly, raw data and the correspondent power spectral density plots were visually inspected to verify whether there were bad channels. If present, they would be marked and omitted from the following steps. Then, the raw data were band-pass filtered from 1 Hz, to remove slow drifts, until 45 Hz, to remove the power line noise and narrow the frequency content to the range of interest (de Cheveigné & Nelken, 2019). Notice that in order to exclude possible time distortions caused by the filtering process (de Cheveigné & Nelken, 2019; Yael et al., 2018), we used the MNE default FIR zero-delay filter. The following step was the data epoching, splitting each session into epochs, with each

epoch consisting in one NF trial that contained 60 seconds of data. However, in some sessions, movement-related artifact could not be corrected for at the end of beginning of the trials, and in these specific cases the duration of the epochs was reduced to exclude the noisy time-intervals. For instance, in some sessions, the artifacts would be focused on the first and last 5 seconds of each trial. In this case, the epochs for that session corresponded to the interval from 5 seconds to 55 seconds of each trial. After this, two ICAs were applied. The first, would mainly serve to remove ocular artifacts like blinks, horizontal eye movements and well-defined muscular artifacts (Lakshmi et al., 2014). The second ICA, tried to remove remaining muscular artifacts as it was fitted by a high passed epoch (cut frequency=15 Hz). This was based on the conclusion of Frolach et al. (Frølich & Dowding, 2018), which reported that adequate high pass filtering was more important for muscular artifact detection than the type of ICA algorithm. On both ICA's we considered the recommendations made by Chaumons et al.(2015). Then, the channels marked as bad were interpolated and the data were re-referenced to the common average (avgREF), a referencing technique with well-known advantages (Lakshmi et al., 2014). Since the volume conduction problem is one of the main causes of error in FC measurements (Anzolin et al., 2019; Bastos & Schoffelen, 2016) and the benefits of using SL, especially with an ICA, are highlighted in recent literature, as exposed in the sections above (Foffani et al., 2004; Kayser & Tenke, 2015b), we performed two different configurations of spline lines SL on the re-referenced data. The first one (SL4) with the default parameters of stiffness (=4) and regularization(=1e-5) and the second (SL3) with stiffness=3 and regularization=0.000156, chosen according to the optimal parameters defined in the tutorial review by Kayser & Tenke (2015a). Ideally, we evaluated using the SL transformation before the ICA, as it would help on the deblurring task while aiding on the task of removing muscle activity (C. G. Carvalhaes et al., 2009; Fitzgibbon et al., 2015). However, that was not possible because the ICA function in MNE Python doesn't supports *.csd* type of data, that is, MNE-python only supports ICA followed by SL. Finally, both avgREF data, SL3 data, and SL4 data were exported. A brief note to the fact that one subject from the auditory NF group was ruled out from the following analysis due to large portion of artifacts, which could not be dealt with the pre-processing steps previously described.

2.5 Assessment of the training effects

2.5.1 Spectral Analysis

In this analysis we aimed to assess the effect of the NF training on the RAUA. To calculate the specific spectral density, we first translated our data to the frequency domain. Although the multitaper method has been defined as the “go to method” because of the highly reported advantages on literature (Babadi & Brown, 2014; van Vugt et al., 2007), its high computational cost, led us to choose to use the Welch method, with an overlap of 50 points.

Using the Welch method, we estimated the per-block RAUA for every subject and each of the respective NF training sessions. As we wanted to separate subjects which were learners, from the subjects who weren't, we fitted, for each subject and each session, the previously calculated block RAUA into a linear regression. Then for each subject, a mean slope, IntraS, would be obtained from the 4 sessions' linear regressions. If the mean linear regression slope was negative, then the subject would be classified as a non-learner. The previously described IntraS is translated to the following equation:

$$IntraS = \frac{m_1 + m_2 + m_3 + m_4}{4} \quad (2.2)$$

Note that this was only calculated for the avgREF data, as this is the re-referencing method that was used on the online protocol, and we didn't want to bias our results by analyzing other re-referencing method.

Once the non-learners were identified, further data analysis was performed only with the data from the Learners. First, we analyzed intra-session variations in RAUA in a per-set analysis over the visual, auditory and VR NF-training groups, by plotting, for each group, the median Per-Set RAUA at the Cz channel. Recalling that each NF training session is composed of 5 sets per session, in a total of 4 session, for every session, we performed an Intra-Session Spearman correlation between a "cloud" containing the set mean Cz-RAUA, normalized with respect to the first set of the respective session, and a list containing the respective numbers of the sets. We also performed a within-session correlation over the groups median set Cz-RAUA and the set number. Then, we established a new metric that would synthetize the within-session variations of Cz-RAUA for all the sessions, per-each subject. This was defined as the IntraA1, and was calculated through the following equation:

$$IntraA1 = \frac{\sum_1^{n_{session}} \sum_2^{n_{sets}} (set_i - set_1)_{session}}{n_{session} * (n_{set} - 1)} \quad (2.3)$$

Considering this, we performed a Wilcoxon Signed Rank test, over the list of the IntraA1 values of the learners for each modality. The Wilcoxon test was be used to find out whether the median of each RAUA list was greater than zero, which would correspond to a modality persistent significant within-session increase of the Cz-RAUA.

To end the analysis of the spectral changes caused by the neurofeedback training, we addressed for each group, the learners RAUA median topological distribution across the sets of the first session and the median topological distribution of the first session vs the fourth session. A similar topological analysis was performed for the relative amplitude of the theta (4 to IAF-2 Hz), lower-alpha (IAF-2 to IAF Hz), Alpha (IAF-2, IAF+2), lower-beta (IAF+2 to 20 Hz), upper-beta (20 Hz to 30 Hz) and beta band (IAF+2 to 30 Hz). This would also be used to analyze the independence of the other bands regarding the context of UA EEG-based NF training.

2.5.2 Functional Connectivity Analysis

This section contains three different subsections. The first part exposes a preliminary analysis that aimed to point out the best approach for the FC calculus. More precisely, we aimed to select the most appropriate algorithm from a set or pre-selected options, and we aimed to avoid the sample size bias problem, thus ensuring that the chosen algorithm would be stable. The second part explains how the effect of NF EEG-based NF training on brain FC was evaluated. This will be done in two parts, the first in which we explain the evaluation of the evolution of FC patterns over the course of the training, and the second where we expose our Network analysis, in particular the network metrics that were used.

2.5.2.1 Choice of Metric and Time Design for Functional Connectivity Analysis

As previously exposed, in EEG there are several algorithms and metrics used to estimate FC. Also, a frequent limitation in the FC measurement is the sample size bias. Too few epochs or even

epochs with small lengths tend to bias the FC results (Bastos & Schoffelen, 2016; Miljevic et al., 2022). To answer and explore in depth both issues, we performed an intermediate analysis where the *ImC* and *wPLI* were considered. Notice that we only used these metrics because they have quite known advantages, like the removal of instantaneous interactions (commonly caused by the common input or volume conduction problem) (Bastos & Schoffelen, 2016). We split a specific session trial, block, and set in windows of 1, 2, 4 and 6 seconds. For example, in the block splitting, we would have a list containing the N-s windows of the correspondent merged two trials, this means that if a trial contains 60 seconds, our “block list”, with the window of 1s, would contain 120 epochs/windows of one second. The same applies to the set but in such case, it contains 6 trials merged. Using both metrics, *ImC* and *wPLI*, we performed the FC analysis of the UA band over the different time profiles, and with the guidance of heatmaps and violin plots we verified which was the most stable and suited design of FC analysis. Our results came in agreement to those exposed by Fraschini et al. (2016), as the *wPLI* barely became stable in the specified time designs. This can be linked with the described 12 seconds windows duration, which is reported as the ideal for the FC measuring with this algorithm. The *ImC* turned out to be more stable with shorter epoch duration, with splittings of 4-s and 6-s proofing to be enough to enable a stable output. Also, as the per-set analysis is the temporal profile that reports less variations we agreed to perform a per-set analysis.

In summary, a per-set computation of the *ImC* was performed over windows of 4-s, for the UA band. This would return several channel connectivity matrices. The results for this preliminary analysis experiment are in the Appendix 7.1.

2.5.2.2 Functional Connectivity Evolution

With the data resulting from the previous computation, we would perform a FC evolution analysis, more specifically, we would verify the intra-session evolution of the FC for every recorded session. This intra-session evolution was assessed for the learners per-channel-pair, comparing the values of FC between set 5 and set 1, and using the Wilcoxon Signed Rank 2-tailed Test, with Benjamin/Hochberg false discovery rate multiple comparison correction, to analyze if these sets were significantly differences. Significance level was reached when the p-value was less than 0.05. This analysis was performed across all the learners of all modalities, across learners of the visual NF-training group, across learners of the auditory NF-training group, and across learner of the VR NF-training group.

2.5.2.3 Network Analysis

The next step aimed at a network analysis in order to obtain more information on functional organization. For this analysis, a preliminary thresholding step was performed to remove spurious correlations. This threshold would be equal to the quantile 0.20 of the mean connectivity matrix for the corresponding NF training session. FC estimates from interpolated channels were considered below threshold.

Then, using the brain-connectivity Python toolbox *bctpy* - <https://pypi.org/project/bctpy/> we performed a per-set computation of the *strength*, *betweenness centrality*, *transitivity*, *charpath* and *GE*. For the latter two, we performed an intermediate step to obtain the weight corresponding distance, based on Floyd’s proposed transform (Floyd, 1962). Each metric was computed on the median set connectivity matrix of each groups’ learners and for each session. For the *transitivity*, the *charpath* and *GE* we

performed within-session Spearman correlations between the cloud containing each learner normalized values, normalized with respect to the first set of the same session, and set number, and correlation between the learner's normalized median set value, again normalized with respect to the first set of the same session of the referred metric and the number of the set. For both *transitivity* and *GE*, the Spearman correlations aimed to test if there was a positive correlation between the metric of interest and the set number, thus the test being a 1-tailed test for positive correlation values with significance threshold being reached when p-value is <0.05 , meaning that the metric's value would increase with the set number. On the other hand, for the *charpath* computation, the Spearman correlation aimed at evaluating if there was a negative correlation among the *charpath* per-set values and the number of the set, thus the test being a 1-tailed test for negative correlation values with significance threshold being reached when p-value is < 0.05 , meaning that if the set number increases, the *charpath* decreases. Also, for the *transitivity*, *charpath* and *GE*, set 1 vs set 5 differences were assessed across the learners of the different groups, for each session, using a Wilcoxon Signed Rank 1-tailed with significance threshold reached when p-value <0.05 . We aimed to evaluate if the metrics *transitivity* and *GE* would be greater in set 5 than in set 1, whilst for the *charpath* we evaluated if the metric values were greater in the set 1 than in the set 5.

With both *strength* and *betweenness centrality* we tried to verify whether there was a significant reinforcement of specific nodes, whereas with the *transitivity* metric we tried to verify whether there was a significant reinforcement of functional segregation. Finally, with the *charpath* and *GE* we tried to analyze whether there was a reinforcement of the functional integration.

A brief note to the fact, that we also considered implementing the *modularity* algorithms as we considered interesting to disentangle the clusters' composition. Unfortunately, due to lack of information about the cluster assignment and some randomness associated with the algorithm, we excluded *modularity* from the analysis. Also, the *strength* and *betweenness centrality* results are exposed in the appendix as they didn't produce a specific interpretable pattern.

Note:

Before we move to the next session, we shall refer that according to the guidelines exposed in the review by Miljevic et al. (2022) "*Electroencephalographic Connectivity: A Fundamental Guide and Checklist for Optimal Study Design and Evaluation*" our study is classified as having a moderate-quality assessment of FC with a total score of 4.5 out of 7, as we fulfill, by order, the following: "Laplacian Re-referencing", "4-6s epoch duration", "50-100s epochs", "All types of artefacts addressed", "Lag, weighted, source or Laplacian", both "valid post hoc control" for non-network analysis", and "model-data driven: threshold or weighted" for network analysis, and our sample size had "no considerations".

3 Results

3.1 Spectral Analysis: Results

3.1.1 Learner vs non-Learner

The results from the identification of learners and non-learners are displayed in Tables 3.1, 3.2, and 3.3, for each group of subjects, with the respective IntraA1 metric value and the learner status. In the visual NF-training group one non-learner was identified (subject V2), whereas for the auditory NF-training group two non-learners were found (subject AUD2 and Aud3). The VR NF-training group did not have non-learners.

Table 3.1 - Learners vs Non-Learners for the Visual NF-training Group

Visual NF-Training Group		
Subject	IntraS	Learner Status
1	1.13×10^{-2}	Learner
2	-6.52×10^{-3}	Non-Learner
3	7.46×10^{-4}	Learner
4	7.29×10^{-4}	Learner
5	1.97×10^{-3}	Learner
6	1.71×10^{-2}	Learner
7	4.90×10^{-2}	Learner
8	7.25×10^{-2}	Learner

Table 3.2 - Learners vs Non-Learners for the VR NF-training Group

VR NF-Training Group		
Subject	IntraS	Learner Status
1	1.02×10^{-2}	Learner
2	1.94×10^{-2}	Learner
3	3.70×10^{-2}	Learner
4	6.77×10^{-3}	Learner

Table 3.3 - Learners vs Non-Learners for the Auditory NF-training Group

Auditory NF-Training Group		
Subject	IntraS	Learner Status
1	3.06×10^{-2}	Learner
2	-3.93×10^{-2}	Non-Learner
3	-2.57×10^{-2}	Non-Learner
4	4.28×10^{-2}	Learner
5	1.23×10^{-3}	Learner
6	7.94×10^{-2}	Learner
7	1.23×10^{-3}	Learner

3.1.2 Per-Set Cz Channel RAUA Evolution

Figure 3.1 depicts the median per-set RAUA in the Cz channel, for each NF-training group and for each re-referencing method. Analyzing such figure, for the visual NF-training group, we noticed an initial increase of the median per-set Cz RAUA corresponding to the first session, independently of the applied re-referencing technique, while for session 2 an increase over such metric is reported only when data was re-referenced to the average. For the remaining sessions, increases on the per-set Cz RAUA were visually noticeable, independently of the applied re-referencing technique. For the VR NF-training group, an increase of the median per-set Cz RAUA was observed in every session when applying an avgREF re-referentiatio, whereas when applying a SL re-referentiatio a similar pattern was observed with the exception of session 3 where a decreasing tendency was observed. Finally, for the auditory NF-training group, an increase in median per-set Cz RAUA was observed for all the sessions when using the avgREF re-referentiatio, but when applying SL transformation only the first two sessions maintained the pattern while session 3 and session 4 show a stable and a decreasing pattern, respectively. Indeed, these results were confirmed by the correlation coefficients presented on the table 3.4.

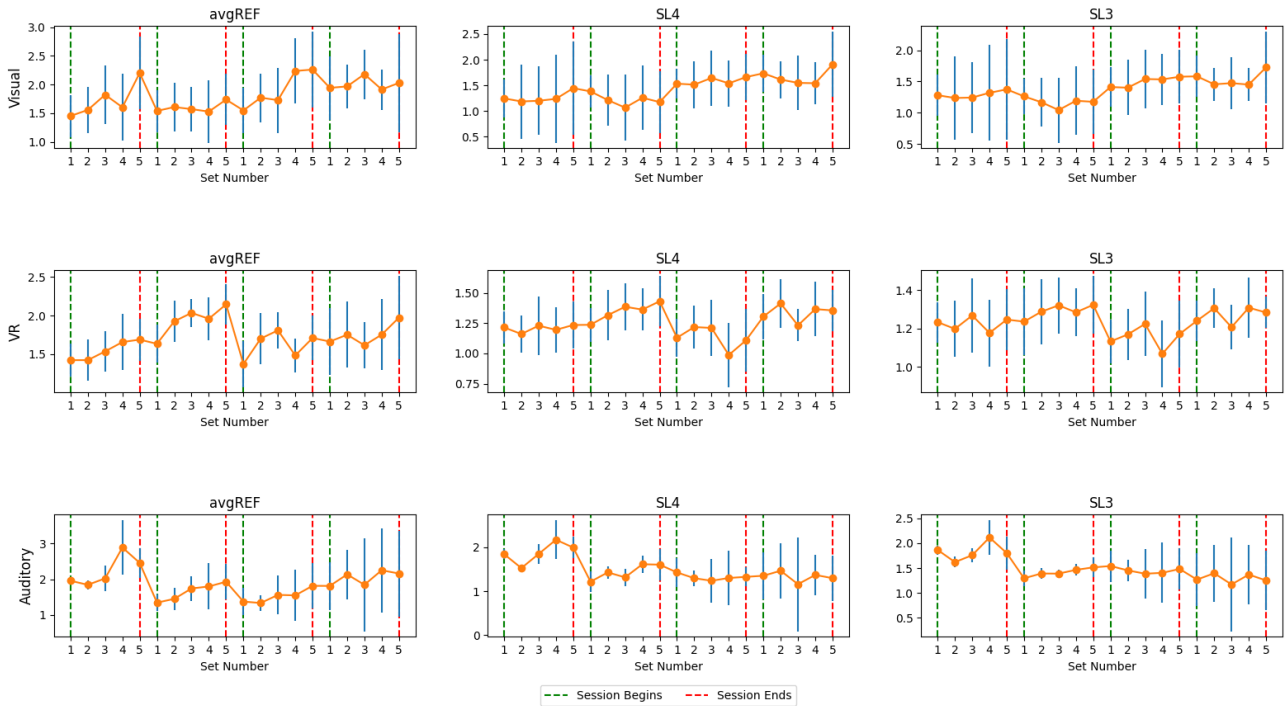


Figure 3.1 - Median Per-Set RAUA for the Cz Channel for each sensory modality (rows) and for each re-referencing method (columns). Error bars represent the inter-quartile interval.

In Table 3.4, spearman's correlation coefficients and p-values are reported for the analysis between the Cz RAUA per-set values and the set number, using both all the values for each subject and the median values per-set. The results are presented for each NF-training group and re-referentiatio method. When the avgREF was applied, significant positive correlations were identified for the visual NF-training group between the median RAUA per-set and set number for sessions 1 and 3, and in session 2 for all Cz RAUA per-set values and Set Number. When the SL was applied, independently of its configuration, significant positive correlations were noticed in the session 2 between all Cz RAUA per-set values and Set Number. Regarding the VR NF-training group, when the avgREF was applied significant positive correlations were identified between all Cz RAUA per-set values and set number, in

the session 1 and 4, and between the median Cz RAUA values and the set number, in the session 1 and 2. When the SL4 is applied significant positive correlations are identified between all Cz RAUA per-set values and set number, in the session 1, and between the median Cz RAUA values and the set number, in the session 2. When the SL3 is applied, no significant positive correlations are reported. Finally, for the auditory group, significant positive correlations are identified between all Cz RAUA per-set values and set number, in the session 1, independently of its configuration, and between the median Cz RAUA values and the set number, in the session 2 for both avgREF and SL3 configurations.

Table 3.4 - Spearman Correlation between RAUA per-set and Set Number, for the Cz channel. H_0 : Correlation coefficient is positive (Significance threshold reached for p -value < 0.05 & no correction for multiple comparisons)

			Visual NF-training Group			VR NF-training Group			Auditory NF-training Group		
			avgREF	SL4	SL3	avgREF	SL4	SL3	avgREF	SL4	SL3
Session 1	All Values	Corr coef	0.279	0.102	0.064	0.794	0.430	0.178	0.377	0.381	0.370
		P-value	0.052	0.279	0.357	1.464e-5	0.029	0.225	0.031	0.030	0.034
	Median	Corr coef	0.900	0.400	0.700	0.999	0.500	0.100	0.800	0.800	0.200
		P-value	0.019	0.252	0.094	7.021e-25	0.195	0.436	0.052	0.052	0.373
Session 2	All Values	Corr coef	0.335	0.315	0.327	0.024	0.030	0.068	0.118	0.295	0.260
		P-value	0.024	0.032	0.027	0.458	0.448	0.388	0.286	0.076	0.105
	Median	Corr coef	0.300	-0.499	-0.199	0.900	0.900	0.700	0.999	0.800	0.900
		P-value	0.311	0.804	0.626	0.019	0.018	0.094	7.021e-25	0.052	0.018
Session 3	All Values	Corr coef	0.223	0.070	0.072	0.102	-0.347	-0.243	0.078	-0.008	0.074
		P-value	0.100	0.344	0.339	0.335	0.933	0.849	0.354	0.515	0.361
	Median	Corr coef	0.900	0.800	0.800	0.500	-0.6	0.200	0.800	-0.100	-0.300
		P-value	0.018	0.052	0.052	0.196	0.857	0.373	0.052	0.564	0.688
Session 4	All Values	Corr coef	0.249	0.232	0.127	0.443	0.339	0.172	0.185	0.031	0.059
		P-value	0.075	0.089	0.234	0.025	0.072	0.233	0.187	0.440	0.390
	Median	Corr coef	0.200	0	0.100	0.700	0.100	0.300	0.800	-0.300	-0.300
		P-value	0.187	0.500	0.436	0.094	0.436	0.311	0.052	0.688	0.688

Finally, Table 3.5 shows the results for the IntraA1 analysis, for each of the NF-training groups and for each re-referentiation method. With Wilcoxon Signed Rank test we tested the hypothesis H_0 : The median of the IntraA1 list is greater than 0, which only reached statistical significance ($p < 0.05$) for the Auditory NF-Training Group when SL4 was applied.

Table 3.5 - Wilcoxon Signed Rank test - H_0 : The median of the IntraA1 list is greater than 0. (Significance threshold reached for p -value < 0.05 & no correction for multiple comparisons)

	Visual NF-training Group			VR NF-training Group			Auditory NF-training Group		
	avgREF	SL4	SL3	avgREF	SL4	SL3	avgREF	SL4	SL3
P-value	0.054	0.148	0.109	0.062	0.437	0.437	0.062	0.031	0.062

3.1.3 Topological Changes

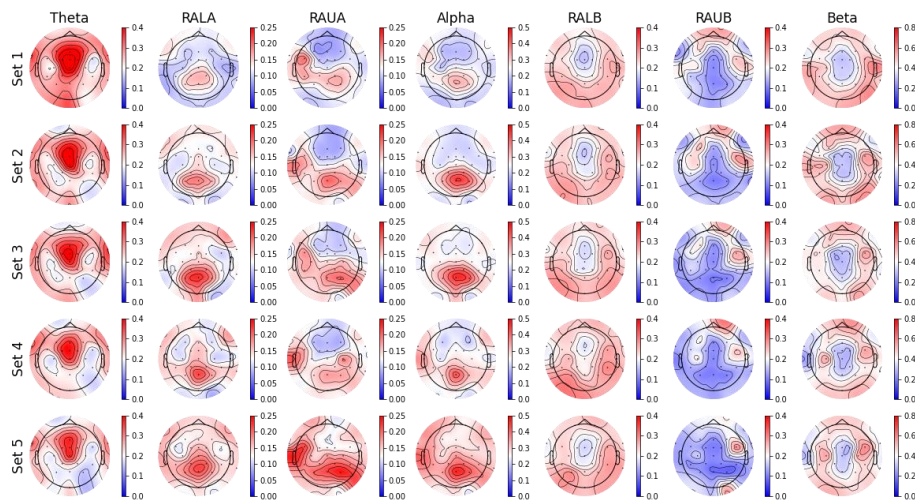


Figure 3.2 – Median relative power spectral density values across the Sets for the Session 1 for the Visual NF-training group and avgREF.

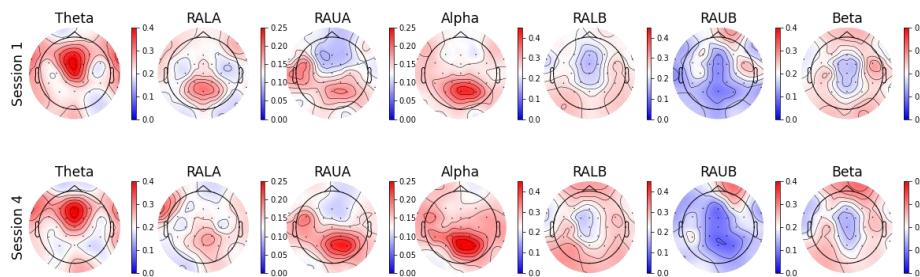


Figure 3.3 – Median Values of the Session 1 vs Session 4 for the Visual NF-training group and avgREF

The topological representation of the median relative power spectral density is displayed in Figure 3.3 for the visual group and avgREF data. We verified that across the sets of the session 1, an upper-alpha relative power increment happened over the right parietal area and the left temporal area, with the same tendency being noticed, when comparing the visual NF-training group session 1 mean upper-alpha band topology with their mean upper-alpha band topology on the session 4. Regarding the theta band power topology, we verified a narrowing of the high theta activity areas accompanied by an overall reduction of such activity on peripheral areas. This peripheral reduction tendency is also noticed when comparing session 1 mean theta band power topology with their mean theta band power topology on the session 4. The lower-alpha band registers an increment on midline parietal activity and consequentially, and the alpha band reports an overall increment over the left temporal and central parietal alpha activity. Concerning the beta band, this wasn't largely affected by the procedure. On the same analysis over SL re-referenced data, presented on the supplemental figures 7.13, 7.14, 7.19 and 7.20, both SL configurations, maintained the above tendencies yet more focal activity was detected and non-focal activity was attenuated, in every frequency band. Left temporal activity on the upper-alpha band was attenuated. Reducing the stiffness of the SL spline lines produced smother “isopotential” lines.

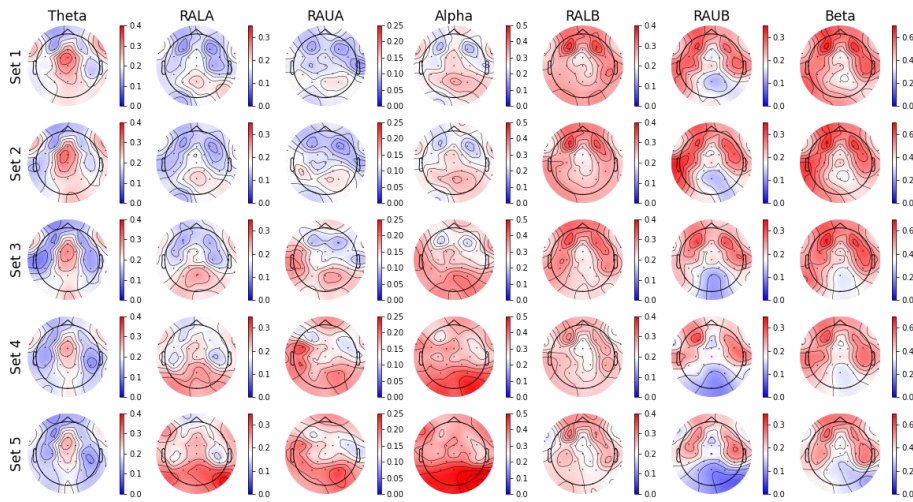


Figure 3.4 - Median values across the Sets for the Session 1 for the VR NF-training group and avgREF.

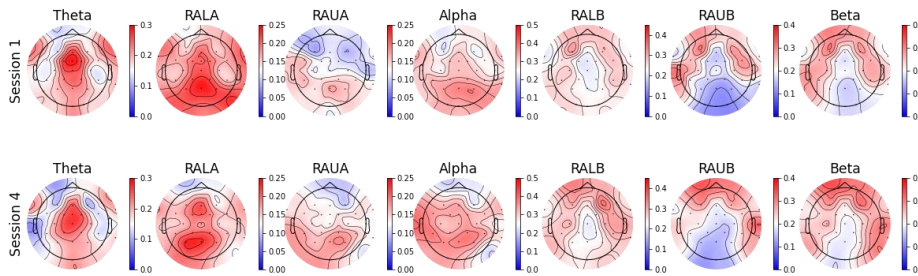


Figure 3.5 - Median Values of the Session 1 vs Session 4 for the VR NF-training group and avgREF.

Concerning VR NF-training group, for the avgREF data, we verified that across the session 1, there were increments on the power of the upper alpha band for the left temporal and mainly for the occipital areas. Also, theta and beta non-focal activity registered a reduction, and an increment in the occipital lower-alpha activity. When comparing session 1 mean upper-alpha band topology of the learners of the VR NF-training group with their mean topology on the session 4, a more left temporal profile of upper-alpha activity was noted on the session 4, and the theta non-focal activity is reduced. Concerning the same results for the SL re-referenced data, presented on the supplemental figures 7.15, 7.16, 7.21 and 7.22 the above referred tendencies are maintained, while more focal activity profiles are verified. The application of the SL4 configuration revealed a more prominent right occipital upper-alpha activity, while attenuated the left temporal activity. The application of the SL3 configuration, attenuated even more the left temporal upper-alpha activity, highlighting the occipital activity, and again, produced smoother isopotential lines due to the reduced stiffness.

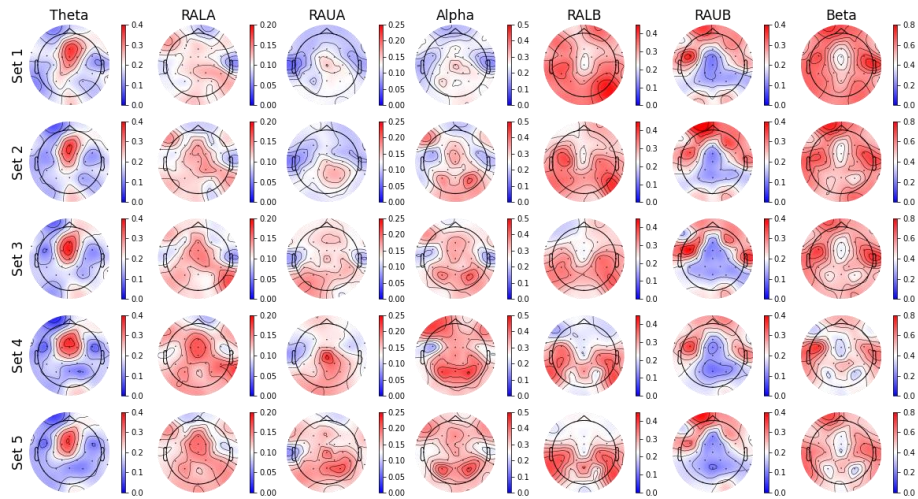


Figure 3.6 - Median values across the Sets for the Session 1 for the Auditory NF-training group and avgREF.

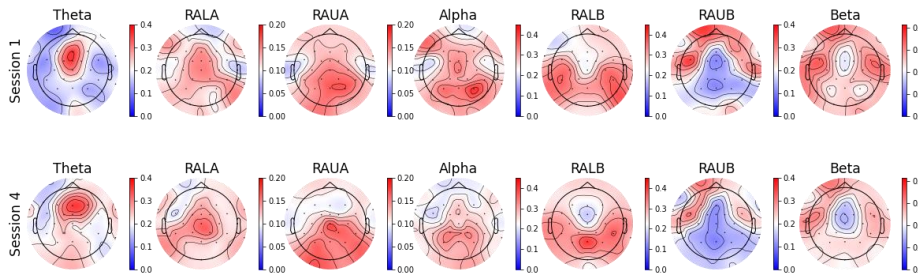


Figure 3.7 - Median Values of the Session 1 vs Session 4 for the Auditory NF-training group and avgREF.

For the auditory NF-training group, for the avgREF data, we noticed that, across sets, the evolution of upper-alpha focal activity didn't follow a specific tendency. Across the sets, the theta-band activity diminished in peripheral areas while maintaining the fronto-central midline tendency, as lower-beta band denoted a high-reduction in the frontal and occipital activity. Concerning the lower-alpha sub-band it was noted an establishment of such activity on the central areas. When comparing session 1 mean upper-alpha band topology of the learners of the auditory NF-training group, with their mean topology on the session 4, the occipital profile of the upper-alpha activity was accentuated. The application of different configurations of SL, presented on the supplemental results figures 7.17, 7.18, 7.23 and 7.24, highlighted a clearer right central-parietal activity. Also, both implementations resulted in a reduction on the non-focal activity, across the different frequency bands. Again, reducing the stiffness of the SL spline lines produced smoother isopotential lines.

3.2 Functional Connectivity Analysis: Results

3.2.1 Functional Connectivity Evolution

Regarding the results, for the visual NF-training group and more specifically considering avgREF data, figure 3.8, on the session 1, a “significant” increase over the right parietal (CP6, TP10, P8, P4) and occipital channels (O2) functional connections was noted. The FC1 channel significantly increased its correlation with Occipital channels and Pz channel. Also, the Pz channel presented a notable “significant” increase of functional connectivity with right parietal (P8, P4), temporal-parietal (TP10), central-parietal (CP6) areas and with some left frontal and central areas. A few significant decreases in the functional connectivity among the fronto-central inter-hemispheric groups were verified. Concerning the second session of the same group, a few significant decreases in the connectivity between contralateral frontal and central channels were verified (F4-F7, FC6, F8, FC2-FT9). In the left hemisphere it occurred a significant increase of the functional connectivity between Fz, F3, F7, and FT9. The left parietal area (P3) registered a significant increase in the functional connectivity with some specific frontal (F7), temporal (T7, FT9), and central parietal (CP1) areas. Finally, the midline occipital area and right occipital area, registered a significant increase in the functional connectivity with some right frontal, frontal-central, central, central-parietal, and parietal areas, thus, pointing out to a strengthening of the previously referred occipital/parietal complex. On the third session no significant differences over the channel-pairwise FC, between the set 1 and set 5, are detected. On the fourth session it was noted a significant increase of the functional connectivity of left and midline frontal/frontal-temporal/frontal-central areas and some specific central/central-parietal/parietal areas. Regarding more posterior areas, mixed effects appeared over the parietal-to-occipital connections, as for example, the Pz significantly increased his connectivity with both O1 and Oz, the P4 significantly decreased its correlation with Oz and O2, and CP2 significantly decreased its correlation with Pz, O1, Oz and O2. This can represent a desegregation or rearrangement of the previously referred complex. When this analysis was performed over the SL4 data, figure 3.9, overall changes in the heatmaps were verified. In the session 1 some specific parietal/central-parietal channels, like the CP6, P4, P8, significantly increased their functional connections with both right parietal areas, right temporal and right temporal-parietal areas. Still in the same session, the FC6 channel significantly increased his functional connections with left parietal/central-parietal areas while significantly decreasing its functional connectivity with left frontal areas. For the session 2, the FC5 significantly reduced its correlation with the right temporal areas while increasing with right occipital, O2, right parietal, P4, and right central-parietal-area. T7 channel significantly decreased its correlation with contralateral frontal area, F8. More significant connection changes were reported, with no adjacent pattern. Also, on the third session, no pattern of evolution was noticed, although some changes were highlighted. On the fourth session, the CP1 significantly increased his functional connectivity with both parietal areas, as the P3 and P8, and frontal central area, FC1. Interestingly, both Pz and P4 revealed significant increases in the functional connections with the frontal-central area. A desegregation pattern was verified over the parieto-occipital connections. Similar heatmaps resulted from such analysis on SL4 and SL3 data, figure 3.10.

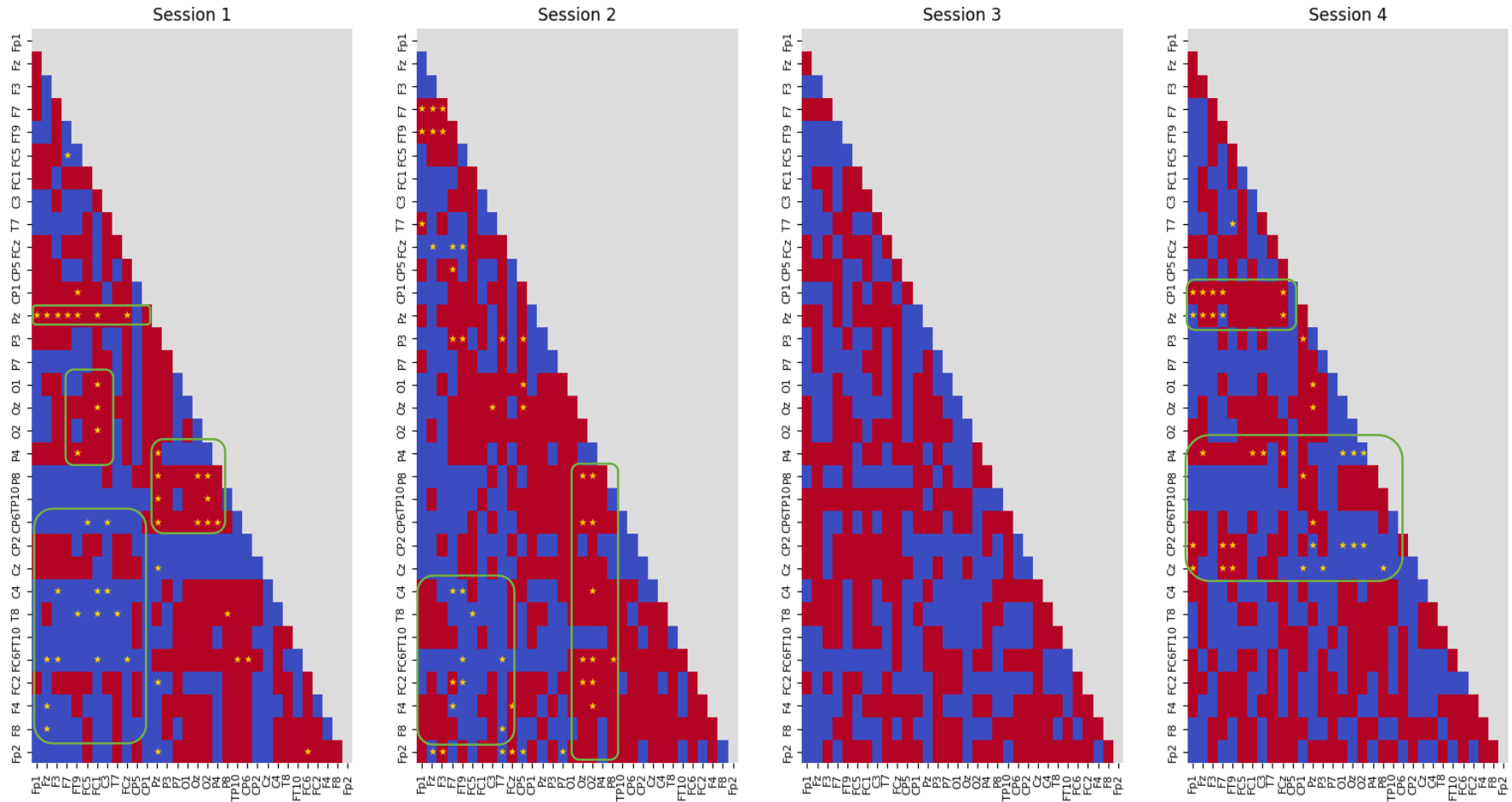


Figure 3.8 - Changes in Functional Connectivity within session. Results are shown for the Visual NF-training group with avgREF, when comparing changes in ImC between Set 1 and Set 5, in each NF-training session. Red: increases; Blue: decreases; *: $p < 0.05$ (corrected for multiple comparisons). The green boxes highlight specific patterns of connectivity changes.

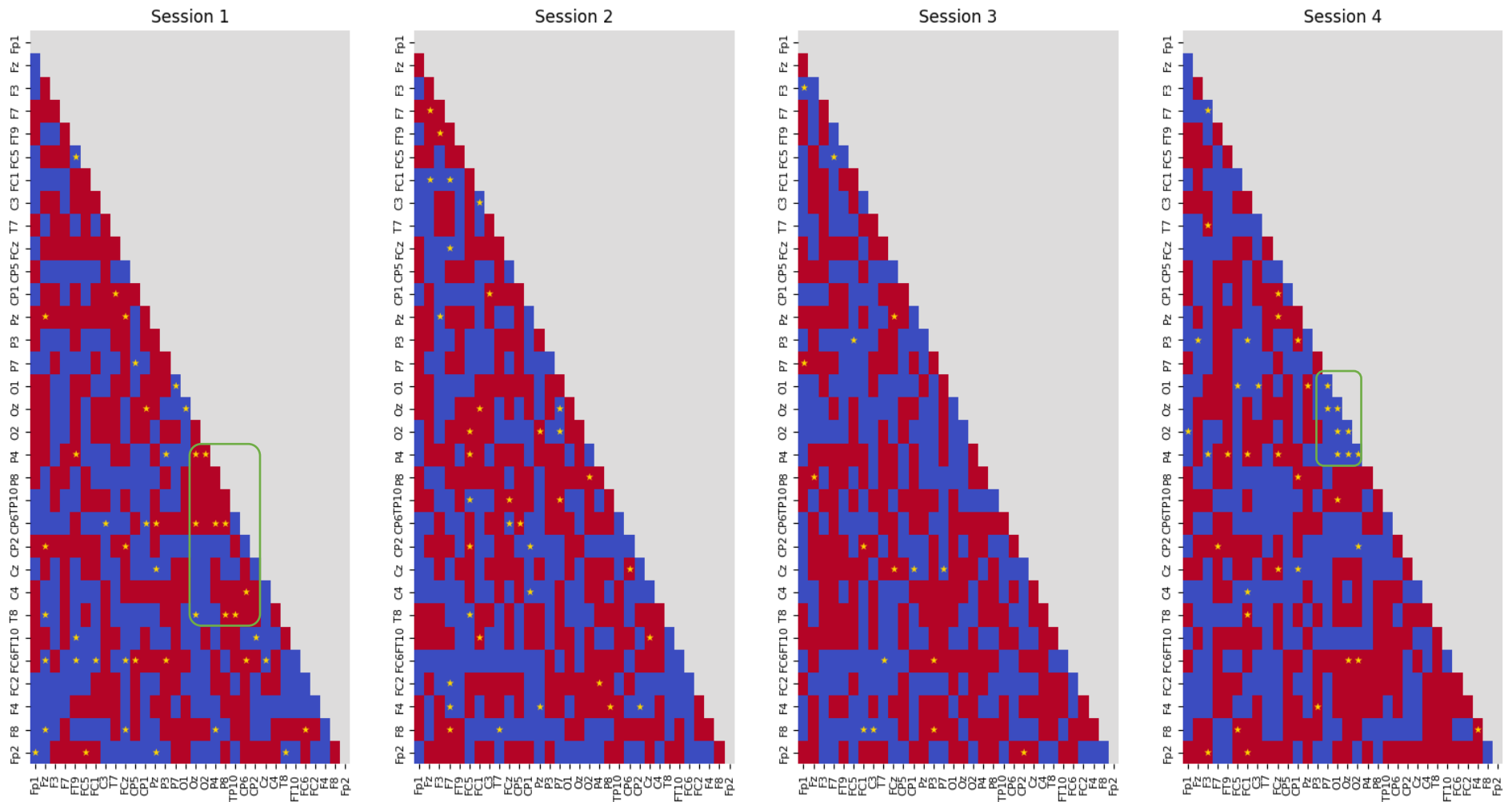


Figure 3.9 - Changes in Functional Connectivity within session. Results are shown for the Visual NF-training group with SL4, when comparing changes in ImC between Set 1 and Set 5, in each NF-training session. Red: increases; Blue: decreases; *: $p < 0.05$ (corrected for multiple comparisons) The green boxes highlight specific patterns of connectivity changes.

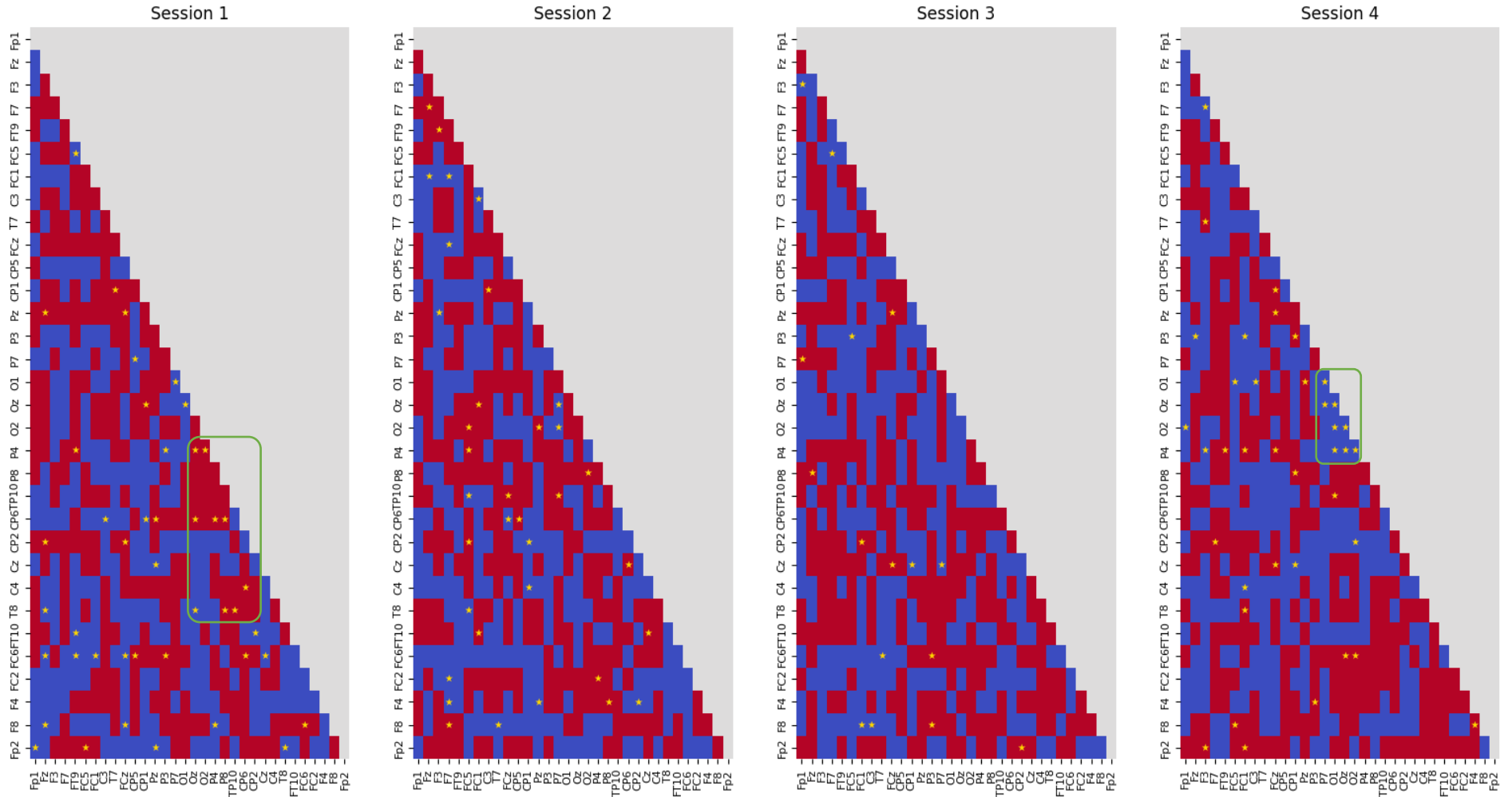


Figure 3.10 - Changes in the Functional Connectivity within session. Results are shown for the Visual NF-training group with SL3, when comparing ImC values between Set 1 and Set 5. Red: increases; Blue: decreases, *: $p < 0.05$ (corrected for multiple comparisons). The green boxes highlight specific patterns of connectivity changes.

Now referring to the group that merges all the learners from the different NF-training modalities, for the session 1 and avgREF, figure 3.11, the Pz increased its functional connectivity with left frontal, frontal-temporal and frontal central channels, while also increasing its correlation with right and left parietal areas, right temporal-parietal areas, right central parietal areas and occipital areas. CP6, C4 and FC6 channels revealed significant increases in their functional connectivity with right parietal, right temporal-parietal, and occipital channels, while decreasing their connectivity with left frontal, temporal and central areas. Temporal-parietal area, TP10, significantly increased its FC with the temporal area T8. Significant decreases over some contralateral frontal, frontal-central and central areas were verified. P8 and CP6 increased their correlation with right frontal areas. Concerning the second session, it was mainly verified the establishment of functional connections between the channels Oz, O2 and P4 with both right and left frontal and central areas. Also in this session, significant decreases were verified among some specific contralateral connections between frontal and frontal-central areas. In the third session, some significant decreases were verified among parietal connections, more specifically, the P7 and P3 channel, P7 and CP1 channel, and P8 and CP1 channel. On the fourth session, pontal connectivity changes were verified. When the same group was considered, but the same analysis was performed over the SL4 data, figure 3.12, for the session 1, the Pz both established correlations with left frontal, left frontal-central, midline frontal-central areas, right parietal areas and occipital areas. Also, the CP1 and P4 significantly increased its correlations with occipital areas, while the CP6 and C4 significantly increased, their correlation with right parietal channels. Both right temporal area, and CP2 verified a significant decrease on their correlation with the occipital area. Also, now instead of directly increasing its correlation with right parietal areas, the right temporal areas significantly increased their connectivity with some contralateral central/parietal electrodes. The P3 channel also revealed increasing correlations with contra-lateral frontal/frontal-central areas. Although this may underlie the establishment of the previously referred parietal complex, this points out to a different configuration of such “complex”. Concerning the second session, reduction of the correlations between contralateral frontal areas, frontal-central areas, and temporal areas were noticed. Also, both left medial central-parietal area (CP1) increased its correlation with contralateral frontal areas (F4, FC2), while left parietal(P3) and left occipital (O1) increased their functional connectivity with the right frontal-central area. Regarding the third session, some left Parietal/central-parietal/occipital areas revealed a significant reduction on their connection with left and medial frontal/frontal central areas, while contralateral areas statistically increased such functional connections, as for example the P8 and CP2 areas. The Cz channel increased its functional connectivity with both Oz and O2 channel. Again, a significant increment of the FC between left and medial parietal area, CP1 and Pz, and the right frontal-central area, more specifically, FC6, was verified. On the fourth session, we verified that certain right parietal and occipital to frontal/frontal-central functional connections significantly diminished, as it was verified for the channels in the CP6, P4, P8 and TP10 and O1. For the case of the P4 channel, it significantly increased its connection with the midline frontal-central area. Just a final mention to both Cz channel, which significantly increased its connectivity with the Fz, F3, FC5, FCz and O2 channels, while decreasing its correlation with the CP1, Pz, P3, P8 and CP6 channels, and C4 channel which significantly decreased its connectivity with the Fz, F3 and FC1 channel, while significantly increasing with the P4, P8 and CP6 channel. Again, both heatmaps and significant differences resultant from this analysis on the SL4 data returned similar values to the ones from this analysis on the SL3 data, figure 3.13

Regarding both VR NF-training group and the auditory NF-training group, these are presented on the appendix, figure 7.25 to 7.30, since no significant-differences are verified over the learners’ channel-pairwise set 1 vs set 5 functional connectivity comparison, independently of the application, or not, of the SL. This seems to be highly related with the low sample size of the learners of both

groups. The Wilcoxon Ranked Sum test is largely dependent on the sample size, and for low sample sizes the algorithm is quite more restricted when considering if differences are significant.

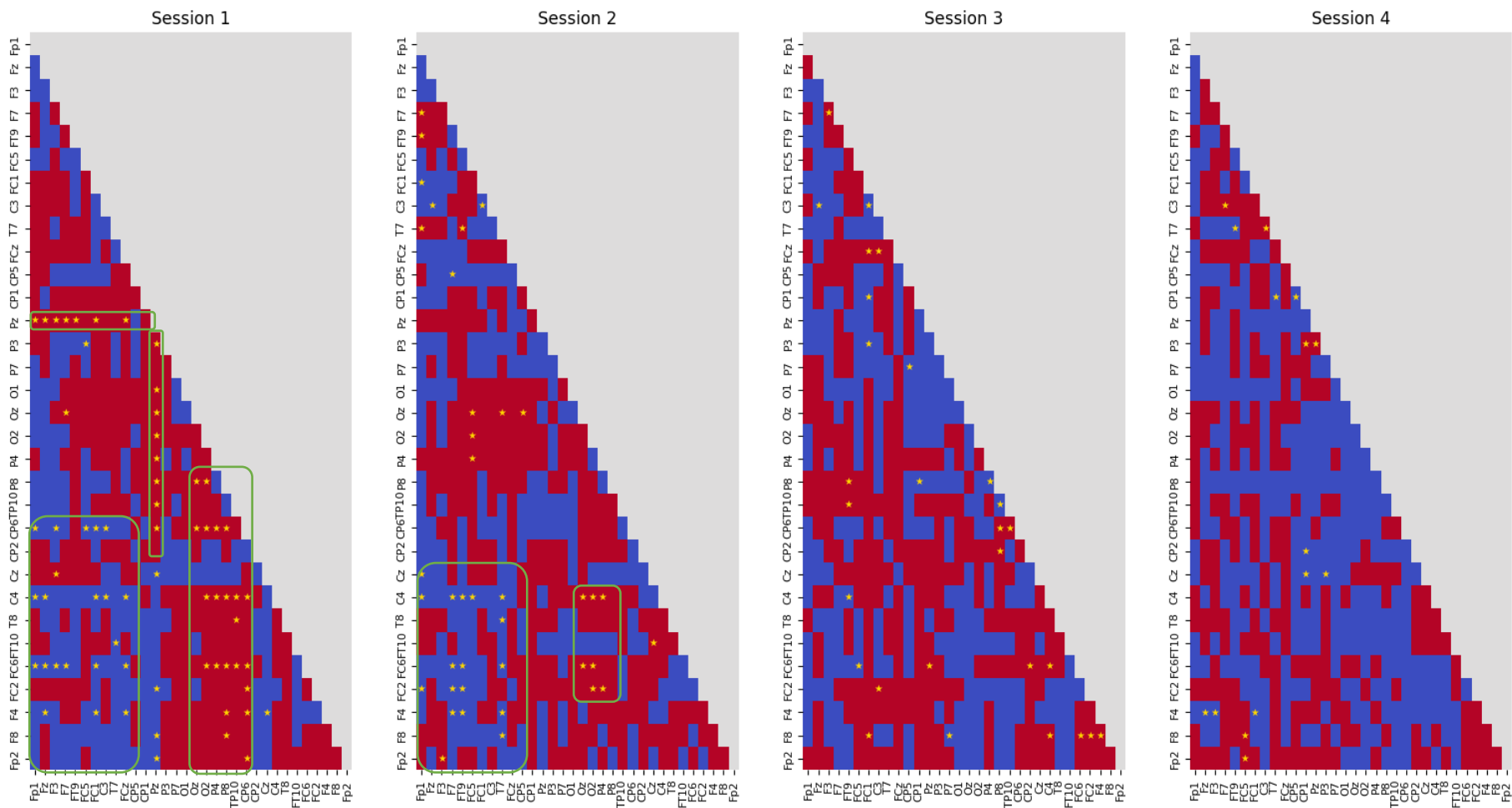


Figure 3.11 - Changes in the Functional Connectivity within session for the Learners of all the NF-training groups (visual, auditory, and VR). Results are shown for the avgREF, when comparing ImC values between Set 1 and Set 5. Red: increases; Blue: decreases, *: $p < 0.05$ (corrected for multiple comparisons). The green boxes highlight specific patterns of connectivity changes.

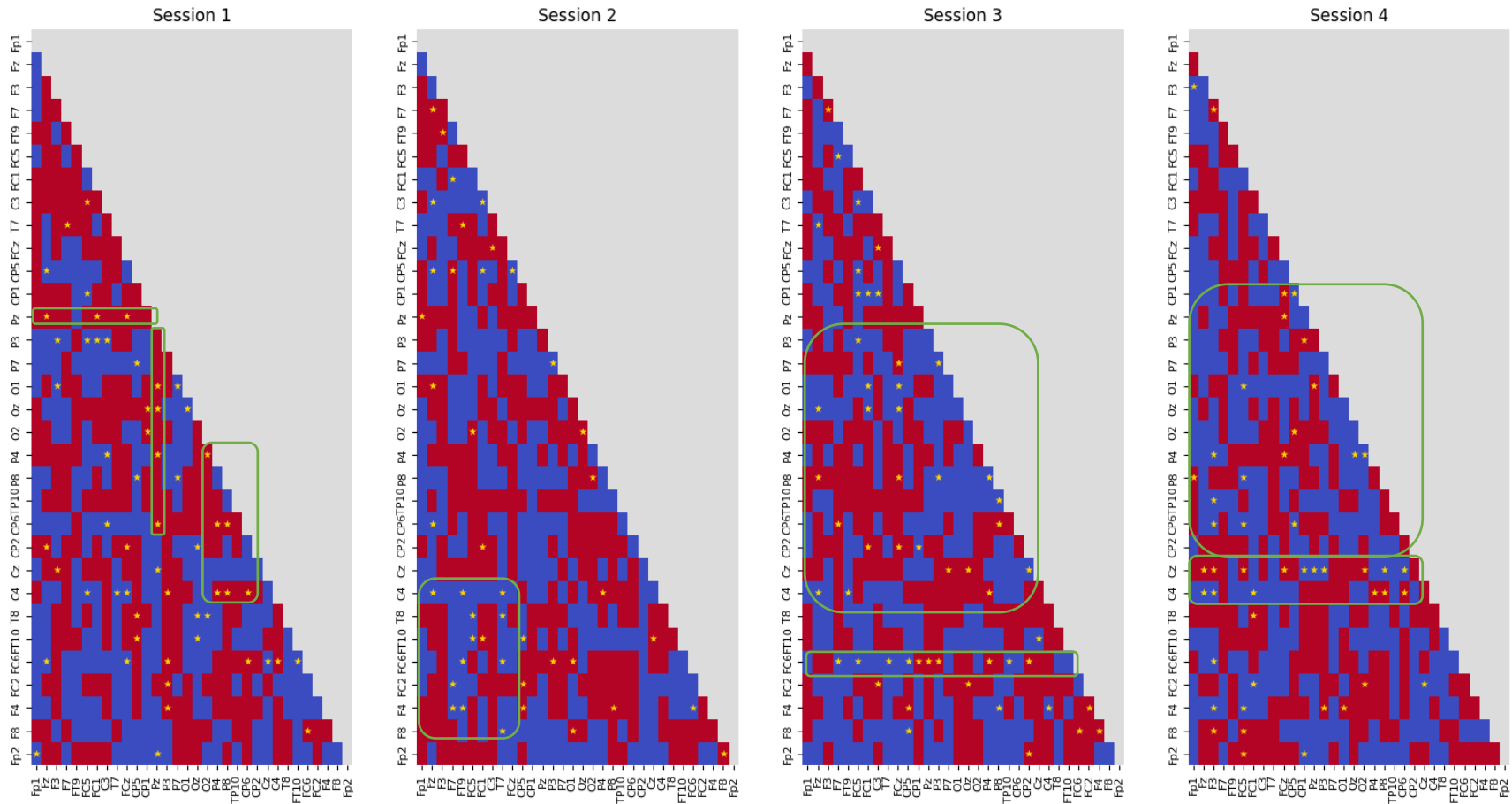


Figure 3.12 - Changes in the Functional Connectivity within session for the Learners of all the NF-training groups (visual, auditory, and VR). Results are shown for the SLA, when comparing ImC values between Set 1 and Set 5. Red: increases;, Blue: decreases, *: $p < 0.05$ (corrected for multiple comparisons). The green boxes highlight specific patterns of connectivity changes.

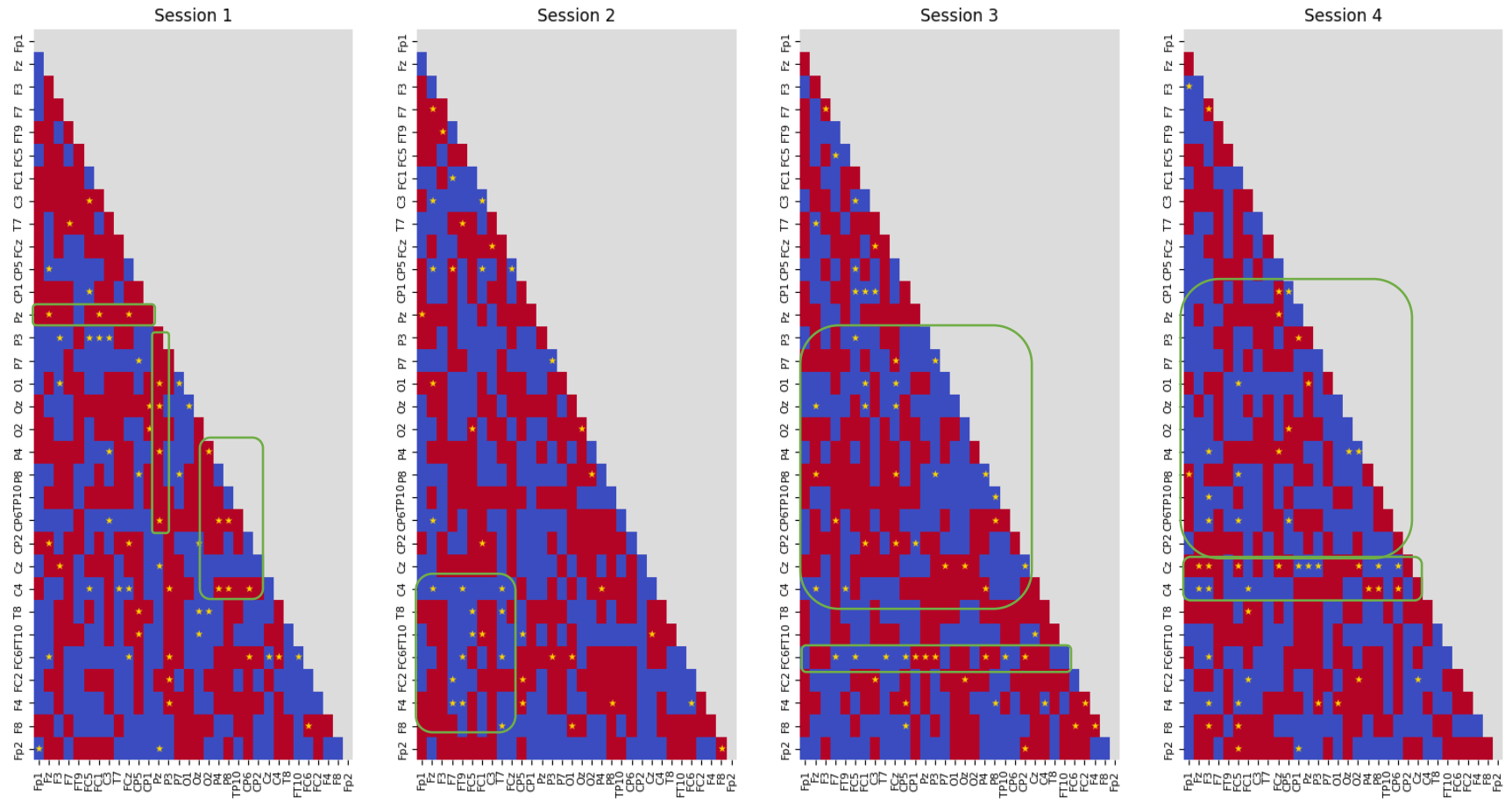


Figure 3.13 - Changes in the Functional Connectivity within session for the Learners of all the NF-training groups (visual, auditory, and VR). Results are shown for the SL3, when comparing ImC values between Set 1 and Set 5. Red: increases; Blue: decreases, *: $p < 0.05$ (corrected for multiple comparisons). The green boxes highlight specific patterns of connectivity changes.

3.2.2 Network Analysis

3.2.2.1 Transitivity

Figure 3.14 depicts the evolution of the median *transitivity* along each NF-training session, representing graphically results per sensory modality and method of data re-referentiation. For the visual NF-training group and avgREF, we verified that in the first 4 sets from the session 1 the median *transitivity* didn't change as much, yet it increased for the fifth set. On the second session, the last two sets, had greater median *transitivity* values when compared with the first three sets. On the third session the median *transitivity* oscillated among sets without having a specific increment or reduction. On the fourth session a clear decreasing tendency was noted on the last four sets. When the SL was applied, independently of its configuration, an increasing tendency was verified on the median *transitivity* for the first three sessions, while in the last, is not as present. Regarding the VR NF-training group, for the avgREF, on the session 1, we verified that the last three sets had higher median *transitivity* values than the first set of the session. On the second and third session, an increasing tendency was noted. For the last session the median *transitivity* oscillated among sets without having a specific increment or reduction. When the SL was applied, independently of its configuration, increasing tendencies are verified in every session. Regarding the auditory group, independently of the re-referencing method an increasing tendency was verified across all the sessions.

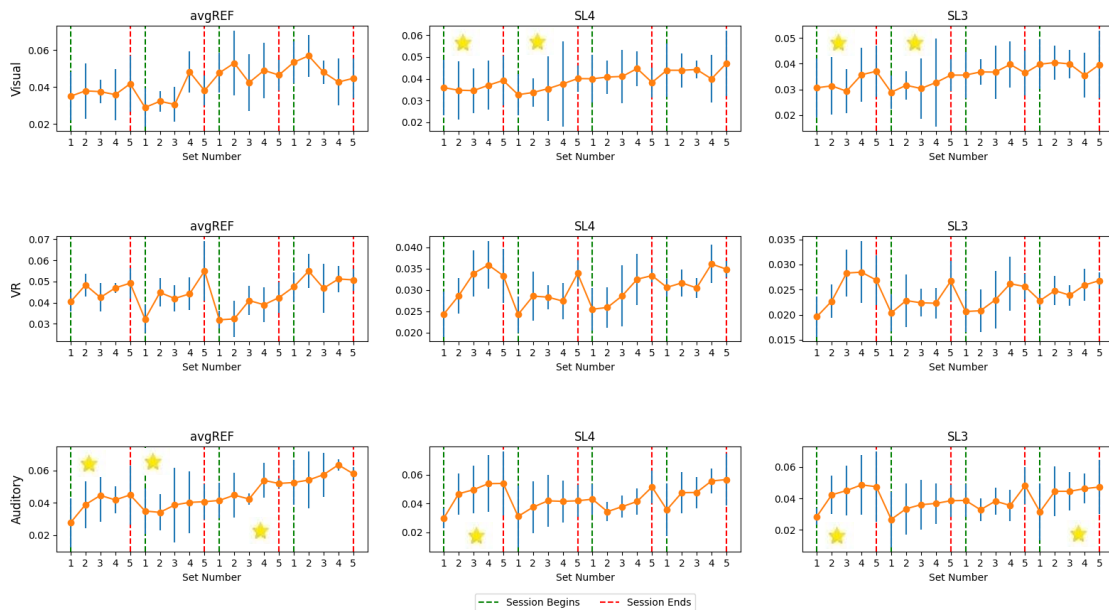


Figure 3.14 - Median transitivity (orange dots) and interquartile range (blue bars), per-set across the four NF-training sessions. Rows: NF-training modality. Columns: data re-referentiation method. Yellow stars mark sessions where the Wilcoxon Rank Sum Test with H_0 denotes that the median Transitivity is greater in set 5 than in the set 1. (Significance threshold reached for p -value < 0.05 & no correction for multiple comparisons)

Spearman's correlation coefficients between the median group *transitivity* values/ all group *transitivity* values, and the set number are shown in Table 3.6. For the Visual NF-training group, we verify that in the first session, although both "median *transitivity* correlation" and "all *transitivity* values correlation" only registered positive correlation coefficients, statistical significance was only reached when all the *transitivity* values were considered and the SL was applied, independently of its configuration. The same happened for the second session, where both in "all *transitivity* values correlation" and "median *transitivity* correlation", although only positive correlation coefficients were

presented, only significant values were reported in the cases where SL was applied. Indeed, both in Session 1 and Session 2, concerning the SL4 and SL3 data, the Wilcoxon test (H_0 : The median *transitivity* is greater in Set 5 than in the set 1) reached a significant value (p -value <0.05) highlighting a *transitivity* increase from the first set to the fifth; Wilcoxon test results are presented in Table 3.7. For the remaining sessions no significant correlations were reported, with negative correlation coefficients appearing in certain cases, and no significant within-session *transitivity* differences are highlighted on the Wilcoxon test.

For the VR NF-training group, regarding the table 3.6, in the first session, only positive correlations were verified both for the “median *transitivity* correlation” and the “all *transitivity* values correlation”, but only in the latter, for the SL4 and SL3 data, the significance level was reached (p -value <0.05). For the second session, while the “median correlations” only returned positive correlation coefficients with no significance, the “all *transitivity* values correlation”, independently of being avgREF, SL4 or SL3 data, returned only significant positive correlation coefficients. In the third session, significant positive coefficients were found for the “median *transitivity* correlation” and the “all *transitivity* values correlation”, independently of being analyzed SL4, SL3 or avgREF data. Concerning the last session although, for both “median *transitivity* and all *transitivity* values correlation” only positive correlation coefficients are reported, these only reached significance in the “median correlation” for the SL3 data, and in the “all-valued correlation” for both SL3 and SL4 data. Regarding the Wilcoxon Rank Sum Test results, presented at the table 3.7, although the significance level ($p<0.05$) was almost reached, no significant differences were found.

Finally, for the auditory NF-training group, regarding the table 3.6, we verified that both in the first and second session, the “median correlation” and “all *transitivity* values correlation” only registered significant positive correlation coefficients. Also, in both sessions, significant differences were revealed by Wilcoxon Rank Sum test, table 3.7, although on the second session this is only verified over the avgREF data, even that for the SL4 and SL3 data significance level was almost reached. Considering the third session, only positive correlation coefficients were verified whether on the “median correlation” and the “all-valued correlation”, table 3.6. With this said, only the correlation coefficients returned from the “all-valued correlation” were presented as significant, and again, the Wilcoxon Rank test, table 3.7 over the avgREF data highlighted a significant *transitivity* increase from the first to the last set. Regarding the last session, only positive correlation coefficients were returned for both the “median” and “all-valued” correlations, table 3.6. In fact, all the “median correlation” coefficients, were highlighted as significant, independently of the application, or not, of the SL, while for the “all-valued correlation”, only when it’s computed over SL4 resulting data it is non-significant. Wilcoxon Rank test, presented in the table 3.7, over the SL4 and SL3 data, highlighted a significant ($p<0.05$) increase in the *transitivity* values, from the set 1 to the set 5.

Table 3.6 – Spearman’s Correlation Between Set Transitivity and Set Number - H_0 : Correlation coefficient is positive. (Significance threshold reached for p -value < 0.05 & no correction for multiple comparisons)

			Visual NF-training Group			VR NF-training Group			Auditory NF-training Group		
			avgREF	SL4	SL3	avgREF	SL4	SL3	avgREF	SL4	SL3
Session 1	All Values	Corr coef	0.247	0.315	0.456	0.357	0.683	0.745	0.547	0.701	0.689
		P-value	0.076	0.032	0.003	0.061	0.0005	8.280e-05	0.002	4.766e-05	6.969e-05
	Median	Corr coef	0.600	0.600	0.700	0.700	0.700	0.700	0.900	0.999	0.900
		P-value	0.142	0.142	0.090	0.094	0.094	0.094	0.019	7.021e-25	0.019
Session 2	All Values	Corr coef	0.223	0.353	0.416	0.702	0.523	0.425	0.441	0.382	0.437
		P-value	0.099	0.018	0.007	0.0002	0.009	0.031	0.013	0.030	0.014
	Median	Corr coef	0.800	0.999	0.900	0.700	0.600	0.600	0.900	0.900	0.999
		P-value	0.052	7.021e-25	0.019	0.094	0.142	0.142	0.019	0.019	0.019
Session 3	All Values	Corr coef	0.197	-0.030	0.048	0.526	0.440	0.471	0.539	0.394	0.465
		P-value	0.129	0.568	0.392	0.009	0.026	0.018	0.003	0.026	0.009
	Median	Corr coef	-0.300	0.000	0.300	0.900	0.999	0.900	0.800	0.400	0.300
		P-value	0.688	0.500	0.312	0.019	7.021e-25	0.019	0.052	0.252	0.311
Session 4	All Values	Corr coef	-0.014	-0.235	-0.062	0.123	0.548	0.615	0.386	0.256	0.449
		P-value	0.532	0.912	0.639	0.302	0.006	0.002	0.028	0.108	0.012
	Median	Corr coef	-0.800	0.300	-0.600	0.100	0.600	0.900	0.900	0.999	0.900
		P-value	0.948	0.311	0.858	0.436	0.142	0.019	0.019	7.021e-25	0.019

Table 3.7 Wilcoxon Rank Sum Test P-values - H_0 : The median transitivity is greater in Set 5 than in the set 1. (Significance threshold reached for p -value < 0.05 & no correction for multiple comparisons)

	Visual NF-training Group			VR NF-training Group			Auditory NF-training Group		
	avgREF	SL4	SL3	avgREF	SL4	SL3	avgREF	SL4	SL3
Session 1	0.109	0.023	0.015	0.063	0.063	0.063	0.031	0.031	0.031
Session 2	0.234	0.023	0.023	0.063	0.063	0.063	0.031	0.094	0.094
Session 3	0.188	0.756	0.594	0.125	0.188	0.188	0.031	0.094	0.063
Session 4	0.531	0.756	0.756	0.188	0.063	0.0625	0.094	0.156	0.031

3.2.2.2 Charpath and GE

The evolution of the median *GE* and *charpath* are depicted in Figure 3.15 and Figure 3.16, respectively, along each NF-training session, representing graphically results per sensory modality and method of data re-referentiation. For the visual NF-training group and avgREF, we verified that in the session 1 the median *GE* and *charpath* oscillates and no specific increment or reduction was noted. On the second session, the last two sets, had greater median *GE* values, lower *charpath* values, when compared with the first three sets. On the third session, both median *charpath* and *GE* oscillated among sets without having a specific increment or reduction. On the fourth session a clear decreasing tendency was noted, for the *GE*, and increasing tendency was noted for the *charpath*, on the last four sets. When the SL was applied, independently of its configuration, an increasing/reduction tendency was verified on the median *GE/charpath* for the first three sessions, while in the last, is not as present. Regarding the VR NF-training group, for the avgREF, on the session 1, we verified that the last three sets had higher median *GE* values, lower median *charpath* values, than the first set of the session. On the second, third and fourth session, an increasing tendency was noted for the *GE*, and a decreasing tendency was noted for the *charpath*. When the SL was applied, independently of its configuration, increasing *GE/* decreasing *charpath* tendencies were verified in every session. Regarding the auditory group, independently of the re-referencing method an increasing *GE/* decreasing *charpath* tendency was verified across all the sessions.

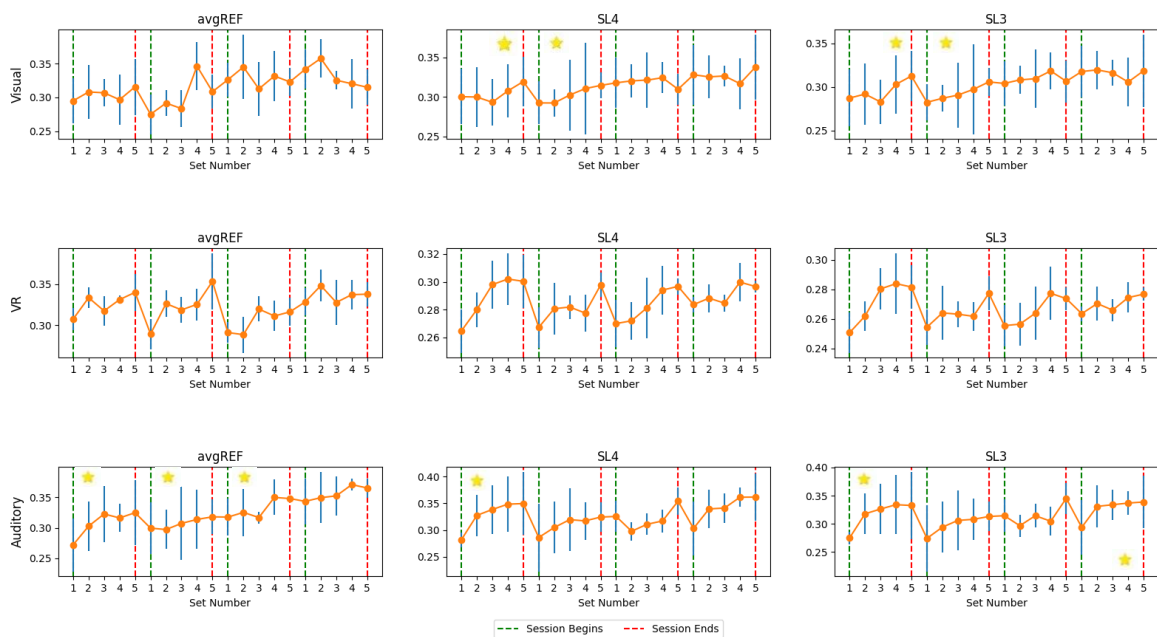


Figure 3.15 - Median *GE* (orange dots) and interquartile range (blue bars), per-set across the four NF-training sessions. Yellow stars mark sessions where the Wilcoxon Rank Sum Test with H_0 denotes that the median *GE* is greater in set 5 than in the set 1. (Significance threshold reached for p -value < 0.05 & no correction for multiple comparisons)

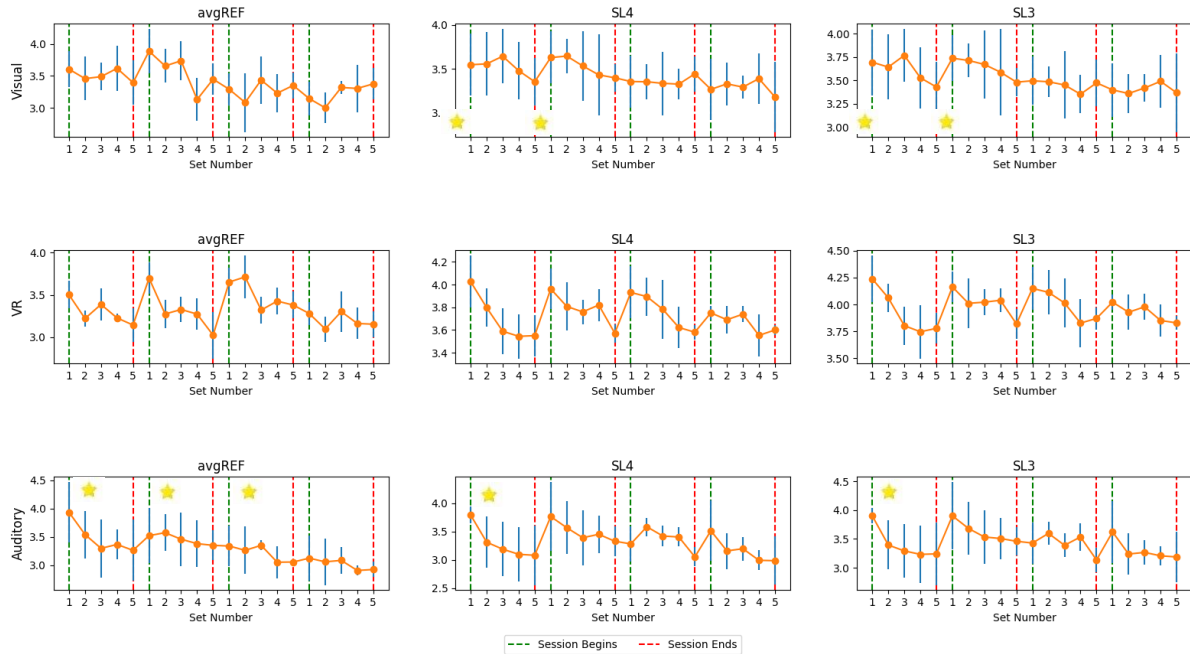


Figure 3.16 - Median Charpath (orange dots) and interquartile range (blue bars), per-set across the four NF-training sessions. Yellow stars mark sessions where the Wilcoxon Rank Sum Test with H_0 denotes that the median charpath is lower in set 5 than in the set 1. (Significance threshold reached for p -value < 0.05 & no correction for multiple comparisons)

Spearman’s correlation coefficients between the median group *charpath* values/ all group *charpath* values, and the set number are shown in Table 3.8. Spearman’s correlation coefficients between the median group *GE* values/ all group *GE* values, and the set number are shown in Table 3.10.

Regarding the visual NF-training group, on the table 3.8 and 3.10, we verified that significant positive correlation between the *GE* and set number, accompanied by significant negative correlations between the *charpath* and the set number, were obtained for the session one, on the “cloud correlation” computation over the SL4 and the SL3 data, and for the second session, on both “median correlation” and cloud computation over the SL4 and SL3 data. Also, for the referred session, Wilcoxon test on the SL4 and SL3 data, on the table 3.9 and 3.11, revealed a significant increase over the *GE* from the first to the last set, while a significant reduction occurred over the *charpath*. In the sub-sequential sessions no significant correlations and differences were reported. In fact, on both third and fourth session, positive *charpath* correlation coefficients, and negative *GE* correlation coefficients were noted.

Considering such results, for the learners of the VR NF-training group, we verified that significant positive correlation between the *GE* and set number, accompanied by significant negative correlations between the *charpath* and the set number, occurred for all the “all-valued correlations”, among the session 1, 2 and 3, while on the fourth session, only the “all-valued correlations” computed across the SL4 and SL3 data are significant. Concerning the “median correlations”, significant positive correlations of the *GE*, accompanied by significant negative correlations of the *charpath*, appeared only on the session 1 and 3, for the SL4 and SL3 data, and 4, for the SL3 data. The “median correlation”, for the session 2, computed on the avgREF data, returned a significant per-set negative correlation coefficient of the *charpath* that was not accompanied by a significant per-set positive correlation coefficient of the *GE*. Concerning the Wilcoxon Rank Sum Test results, presented in both tables 3.9 and 3.11, although for the session 1 and 2 significance level is almost reached, no significant differences were found.

Regarding the results for the learners of the auditory NF-training group, presented in both table 3.8 and 3.10, we verified that significant positive correlation between the *GE* and set number,

accompanied by significant negative correlations between the *charpath* and the set number, occurred for all the “all-valued correlations”, among the session 1, 2 and 3, while on the fourth session only the correlation computed on the SL3 data, was significant. Concerning the “median correlations”, we verified that significant positive correlation between the *GE* and set number, accompanied by significant negative correlations between the *charpath* and the set number, occurred for all avgREF, SL3 and SL4 data, in the session 1, 2 and 4. Regarding the results of the Wilcoxon Rank Sum test over this group, both presented at the table 3.9 and 3.11, significant increases on the *GE* from the set 1 to set 5, and significant decreases on the *charpath* from the set 1 to set 5, were found on the session 1, for both avgREF, SL4 and SL3 data, and on the session 2 and 3, for the avgREF data. Also, *GE* significantly increased on the fourth session for the SL3 data.

Table 3.8-Spearmans Correlation Between Set Charpath and Set Number - H0: Correlation coefficient is negative. (Significance threshold reached for p-value < 0.05 & no correction for multiple comparisons)

			Visual NF-training Group			VR NF-training Group			Auditory NF-training Group		
			avgREF	SL4	SL3	avgREF	SL4	SL3	avgREF	SL4	SL3
Session 1	All Values	Corr coef	-0.232	-0.416	-0.530	-0.499	-0.677	-0.788	-0.614	-0.689	-0.693
		P-value	0.089	0.007	0.001	0.012	0.0005	1.862e-05	0.0005	6.969e-05	6.152e-05
	Median	Corr coef	-0.300	-0.600	-0.700	-0.700	-0.900	-0.900	-0.900	-0.999	-0.900
		P-value	0.312	0.142	0.094	0.094	0.019	0.019	0.019	7.021e-25	0.019
Session 2	All Values	Corr coef	-0.265	-0.341	-0.386	-0.739	-0.542	-0.492	-0.532	-0.390	-0.476
		P-value	0.062	0.022	0.011	0.0001	0.006	0.013	0.003	0.027	0.008
	Median	Corr coef	-0.800	-0.900	-0.999	-0.900	-0.700	-0.600	-0.900	-0.900	-0.999
		P-value	0.052	0.019	7.021e-25	0.019	0.094	0.142	0.019	0.019	7.021e-25
Session 3	All Values	Corr coef	-0.181	0.042	-0.022	-0.440	-0.440	-0.545	-0.512	-0.343	-0.460
		P-value	0.150	0.595	0.450	0.026	0.026	0.006	0.004	0.047	0.010
	Median	Corr coef	0.300	0.000	-0.700	-0.600	-0.999	-0.900	-0.600	-0.400	-0.500
		P-value	0.688	0.500	0.094	0.142	7.021e-25	0.019	0.142	0.252	0.196
Session 4	All Values	Corr coef	0.028	0.171	0.100	-0.185	-0.492	-0.579	-0.256	-0.319	-0.362
		P-value	0.564	0.837	0.717	0.218	0.013	0.004	0.108	0.060	0.038
	Median	Corr coef	0.800	-0.100	0.200	-0.200	-0.800	-0.900	-0.800	-0.900	-0.900
		P-value	0.948	0.436	0.626	0.374	0.052	0.019	0.052	0.019	0.019

Table 3.9 - Wilcoxon Rank Sum Test P-values - H0: The median Charpath is greater in set 1 than in the set 5. (Significance threshold reached for p-value < 0.05 & no correction for multiple comparisons)

	Visual NF-training Group			VR NF-training Group			Auditory NF-training Group		
	avgREF	SL4	SL3	avgREF	SL4	SL3	avgREF	SL4	SL3
Session 1	0.055	0.023	0.023	0.063	0.063	0.063	0.031	0.031	0.031
Session 2	0.234	0.023	0.016	0.063	0.063	0.063	0.031	0.063	0.063
Session 3	0.188	0.813	0.656	0.125	0.125	0.063	0.031	0.094	0.063
Session 4	0.531	0.711	0.766	0.188	0.063	0.063	0.156	0.156	0.063

Table 3.10 - Spearman's Correlation Between Set GE and Set Number - H0: Correlation coefficient is positive. (Significance threshold reached for p-value < 0.05 & no correction for multiple comparisons)

			Visual NF-training Group			VR NF-training Group			Auditory NF-training Group		
			avgREF	SL4	SL3	avgREF	SL4	SL3	avgREF	SL4	SL3
Session 1	All Values	Corr coef	0.267	0.426	0.530	0.499	0.720	0.775	0.618	0.661	0.685
		P-value	0.060	0.005	0.001	0.013	0.0002	2.947e-05	0.0004	0.0002	7.880e-05
	Median	Corr coef	0.600	0.600	0.700	0.700	0.900	0.900	0.900	0.999	0.900
		P-value	0.142	0.142	0.094	0.094	0.019	0.019	0.019	7.021e-25	0.019
Session 2	All Values	Corr coef	0.239	0.353	0.372	0.757	0.499	0.468	0.567	0.398	0.457
		P-value	0.083	0.019	0.013	5.577e-05	0.013	0.019	0.002	0.024	0.010
	Median	Corr coef	0.800	0.900	0.999	0.700	0.700	0.600	0.900	0.900	0.999
		P-value	0.052	0.019	7.021e-25	0.094	0.094	0.142	0.019	0.019	7.021e-25
Session 3	All Values	Corr coef	0.185	-0.022	0.034	0.440	0.453	0.446	0.488	0.394	0.429
		P-value	0.144	0.550	0.423	0.026	0.023	0.024	0.007	0.026	0.016
	Median	Corr coef	-0.300	0.000	0.400	0.600	0.999	0.900	0.600	0.400	0.300
		P-value	0.688	0.500	0.252	0.142	7.021e-25	0.019	0.142	0.252	0.312
Session 4	All Values	Corr coef	-0.024	-0.188	-0.186	0.166	0.492	0.566	0.307	0.323	0.488
		P-value	0.555	0.861	0.859	0.241	0.014	0.005	0.067	0.058	0.007
	Median	Corr coef	-0.900	0.100	-0.200	0.200	0.800	0.900	0.900	0.999	0.999
		P-value	0.981	0.436	0.626	0.374	0.052	0.019	0.019	7.021e-25	7.021e-25

Table 3.11 - Wilcoxon Rank Sum Test P-values - H0: The median GE is greater in set 5 than in the set 1. (Significance threshold reached for p-value < 0.05 & no correction for multiple comparisons)

	Visual NF-training Group			VR NF-training Group			Auditory NF-training Group		
	avgREF	SL4	SL3	avgREF	SL4	SL3	avgREF	SL4	SL3
Session 1	0.110	0.016	0.016	0.063	0.063	0.063	0.031	0.031	0.031
Session 2	0.234	0.023	0.023	0.063	0.063	0.063	0.031	0.094	0.094
Session 3	0.148	0.766	0.594	0.125	0.125	0.125	0.031	0.094	0.094
Session 4	0.656	0.711	0.852	0.188	0.063	0.063	0.219	0.156	0.031

4 Discussion

4.1 Spectral Analysis

4.1.1 Learners vs Non-Learners

The results for this analysis are exposed in the section 3.1.1, with supplemental results exposed in the appendix section 7.2.1. Starting by the supplemental results, just a brief remark to the fact that as we verified among the several plots, the per-block computation of the RAUA returned highly variable values, among the different blocks. With this said, although this provided a greater number of values where a linear model can be fitted, sometimes the fit was not as efficient and informative. Yet, if we performed a per-set linear model fitting, although we could had more “fitted” model, this would be computed just over 5 values, which indeed could cause a sample size bias.

Concerning the exposed results on the previous section, we verified that the subject V2 from the visual NF-training group, and both subject AUD2 and AUD3 from the auditory NF-training group were considered non-learners as they have a negative mean average slope across the four NF-training sessions. The VR sample only had subjects classified as learners. It is important to mention that, as can be observed Table 3.1, that subjects V3 and V4 had an almost negligible positive mean slope, yet they were considered learners according to our metric. When observing the effects of NF-training on the levels of RAUA, as depicted in the supplementary Figure 7.10, both subjects showed a quite negligible effect of the NF-training, that is, an increasing trend for the RAUA is not clearly observed. If using other metrics to classify learners from non-learners it might be possible that these individuals be considered non-learners, which would obviously change overall group-level analyses. For example, Escolano et al.(2011) considered non learners, those whose the UA power on the last trial of the last session, wasn't significantly higher than the same band power on the “pre-active” assessment block. Weber et al. (2011), performed a study to attempt to predict the performance of an SMR training protocol concerning the spectral changes on such frequency range. On such study, the authors defined learners as being the ones whose, 1) mean percentage increase in EEG amplitude during training (compared to baseline) for the last 5 training days exceeded 8% and 2) the EEG amplitudes of the subjects should tend to increase across all training sessions. Maybe these could represent better methods to implement and adapt to our experiment, as they are stricter, as the method by Escolano et al. (2011) only consider learners those who registered significant increments, and as the method by Weber et Al. (2011) ensures that an increasing tendency is maintained across all the sessions, what indeed lacks in our experiment, as some sessions register negative slopes. At the bottom line, all of this reinforces the necessity of establishing an exact guideline when performing such differentiation.

4.1.2 Per-Set Cz Channel RAUA Evolution

First, we shall recall the main findings from such According to the Table 3.4, where spearman's correlation coefficients and p-values are reported for the analysis between the Cz RAUA per-set values and the set number, using both all the values for each subject and the median values per-set. When the avgREF was applied, significant positive correlations were identified for the visual NF-training group between the median RAUA per-set and set number for sessions 1 and 3, and in session 2 for all Cz RAUA per-set values and Set Number. When the SL was applied, independently of its configuration, significant positive correlations exist in session 2 between all Cz RAUA per-set values and Set Number. For the VR NF-training group, when the avgREF was applied, significant positive correlations were

identified between all Cz RAUA per-set values and set number, in the session 1 and 4, and between the median Cz RAUA values and the set number, in the session 1 and 2. When the SL4 was applied, significant positive correlations were identified between all Cz RAUA per-set values and set number, in the session 1, and between the median Cz RAUA values and the set number, in the session 2. When the SL3 was applied, no significant positive correlations were reported. For the auditory group, significant positive correlations were identified between all Cz RAUA per-set values and set number, in the session 1, independently of its configuration, and between the median Cz RAUA values and the set number, in the session 2 for both avgREF and SL3 configurations. Regarding the results for Wilcoxon Signed Rank test for the IntraA1 analysis, table 3.5, only reached statistical significance ($p < 0.05$) for the Auditory NF-Training Group when SL4 is applied.

Excluding the visual NF-training group, both the VR and the auditory NF-training groups, on the correlation analysis presented at the table 3.4, seem to point out an initial statistically significant per-set increase of the Cz-RAUA over their learners in the first sessions of NF-training. In posterior stages of the NF-training, all the modalities revealed non-significant positive correlations and, in fact, when the SL is applied, some negative trends may appear on later stage correlations. Concerning the effects of the NF-training on the Cz-RAUA upregulation, evaluated in terms of the IntraA1 metric, we verify that, although almost significant results are pointed out, inclusively in the auditory NF-training group for the SL4 data a significant difference is detected, we can't conclude that the NF-training significantly improved the Cz-RAUA. This comes in agreement with what was expected, as only 4 sessions of training were performed and 8 sessions, are defined as the minimum number of sessions for effective improvements in investigation context (Gruzelier, 2014). Also, as the sample of each modality group, is quite small, the previously results can be largely biased.

4.1.3 Topological Changes

Regarding the results above exposed for the UA NF-training, independently of the feedback modality, it seemed to promote a more parietal and occipital profile over such band activity pattern. This is interesting, as this are the main areas that are related to the alpha band activity on a relaxed state according to Groppe et al. (Groppe et al., 2013). Unfortunately, due to the low sample size, we can't generalize such results, yet these can reflect expected alterations of the functional connectivity profiles, that we are going to verify below.

In matter of the independence of the brainwaves, we noticed that upper-alpha NF-training didn't only produced alterations on the "upper-alpha topology" but also in the near bands, most evident ones being theta band and lower-alpha band. This comes in agreement to what Egner et al. reported that usually a training protocol didn't strictly alter the target band topography, but also alter the near frequency bands topography (Egner et al., 2004). Interestingly, the lower-alpha bands seemed to accompany the increasing tendency and topographic evolution of the upper-alpha band, the overall theta band power seemed to diminish, while maintaining a specific frontal-central activity. This "obeys" to the reported results of Klimesch et al., where such brainwave bands show an opposite behavior (Klimesch, 1999).

Concerning the results of the implementation of the SL, when compared to the avgREF ones, as we expected a deblurring tendency was verified as more focal activity was highlighted and overall non-focal activity was highly reduced in every frequency band. In fact, a quite evident case was auditory NF-training group session 1 per-set mean upper-alpha topographic distribution, that when computed over the avgREF data didn't reveal any specific pattern, due to the widespread distribution of less

“powerful activity”, but when computed over SL reveal a more focal and well-defined “hot” activity areas. This seems to reinforce that is advantageous the re-referencing procedure of the SL as a spatial filtering and “deblurring” technique, as Kayser et al. support (Kayser & Tenke, 2015b). Also as expected by reducing the stiffness parameter of the spline lines used for the computation of the laplacian, smoother, more well-defined and focal isopotential lines arise (Kayser & Tenke, 2015a).

4.2 Functional Connectivity Analysis

4.2.1 Functional Connectivity Evolution

Recalling the results of the the pair-wise analysis of the FC within-session, exposed on subsection 3.2.1, for the visual NF-training group with avgREF, figure 3.8, on the session 1, a “significant” increase over the right parietal (CP6, TP10, P8, P4) and occipital channels (O2) functional connections was noted. The FC1 channel significantly increased its correlation with Occipital channels and Pz channel. Also, the Pz channel presented a notable “significant” increase of functional connectivity with right parietal (P8, P4), temporal-parietal (TP10), central-parietal (CP6) areas and with some left frontal and central areas. A few significant decreases in the functional connectivity among the fronto-central inter-hemispheric groups were verified. The latter also happened on the second session. Also in the second session, the left parietal area (P3) registered a significant increase in the functional connectivity with some specific frontal (F7), temporal (T7, FT9), and central parietal (CP1) areas. Finally, the midline occipital area and right occipital area, registered a significant increase in the functional connectivity with some right frontal, frontal-central, central, central-parietal, and parietal areas. On the third session no significant differences over the channel-pairwise FC, between the set 1 and set 5, are detected. On the fourth session it was noticed a significant increase of the functional connectivity of left and midline frontal/frontal-temporal/frontal-central areas and some specific central/central-parietal/parietal areas. Regarding more posterior areas, mixed effects appeared over the parietal-to-occipital connections, as for example, the Pz significantly increased his connectivity with both O1 and Oz, the P4 significantly decreased its correlation with Oz and O2, and CP2 significantly decreased its correlation with Pz, O1, Oz and O2. When this analysis was performed over the SL4 and SL3 data, figure 3.9, overall changes in the heatmaps were verified. In the session 1 some specific parietal/central-parietal channels, like the CP6, P4, P8, significantly increased their functional connections with both right parietal areas, right temporal and right temporal-parietal areas. Still in the same session, the FC6 channel significantly increased his functional connections with left parietal/central-parietal areas while significantly decreasing its functional connectivity with left frontal areas. For the session 2, the FC5 significantly reduced its correlation with the right temporal areas while increasing with right occipital, O2, right parietal, P4, and right central-parietal-area. On the third session, no pattern of evolution is noticed, although some changes were noticed. On the fourth session, the CP1 significantly increased his functional connectivity with both parietal areas, as the P3 and P8, and frontal central area, FC1, and both Pz and P4 revealed significant increases in the functional connections with the frontal-central area. A desegregation pattern was verified over the parieto-occipital connections.

Regarding the group that merges all the learners from training, for the session 1 and avgREF, figure 3.11, again, the Pz increased its functional connectivity with left frontal, frontal-temporal and frontal central channels, while also increasing its correlation with right and left parietal areas, right temporal-parietal areas, right central parietal areas and occipital areas. CP6, C4 and FC6 channels revealed significant increases in their functional connectivity with right parietal, right temporal-parietal, and occipital channels, while decreasing their connectivity with left frontal, temporal and central areas. Temporal-parietal area, TP10, significantly increased its FC with the temporal area T8. P8 and CP6 increased their correlation with right frontal areas. Concerning the second session, it was mainly verified the establishment of functional connections between the channels Oz, O2 and P4 with both right and

left frontal and central areas, and significant decreases were verified among some specific contralateral connections between frontal and frontal-central areas. In the third session, some significant decreases were verified among parietal connections, more specifically, the P7 and P3 channel, P7 and CP1 channel, and P8 and CP1 channel. On the fourth session, pontual connectivity changes were verified. When the same group was considered, but the same analysis was performed over the SL4 and SL3 data, figure 3.12, for the session 1, the Pz both established correlations with left frontal, left frontal-central, midline frontal-central areas, right parietal areas and occipital areas. Also, the CP1 and P4 significantly increased its correlations with occipital areas, while the CP6 and C4 significantly increased, their correlation with right parietal channels. Both right temporal area, and CP2 verified a significant decrease on their correlation with the occipital area. Also, now instead of directly increasing its correlation with right parietal areas, the right temporal areas significantly increased their connectivity with some contralateral central/parietal electrodes. The P3 channel also revealed increasing correlations with contra-lateral frontal/frontal-central areas. Concerning the second session, both left medial central-parietal area (CP1) increased its correlation with contralateral frontal areas (F4, FC2), while left parietal (P3) and left occipital (O1) increased their functional connectivity with the right frontal-central area. Regarding the third session, some left Parietal/central-parietal/occipital areas revealed a significant reduction on their connection with left and medial frontal/frontal central areas, while contralateral areas statistically increased such functional connections, as for example the P8 and CP2 areas. The Cz channel increased its functional connectivity with both Oz and O2 channel. Again, a significant increment of the FC between left and medial parietal area, CP1 and Pz, and the right frontal-central area, more specifically, FC6, was verified. On the fourth session, we verified that certain right parietal and occipital to frontal/frontal-central functional connections significantly diminished, as it was verified for the channels in the CP6, P4, P8 and TP10 and O1. For the case of the P4 channel, it significantly increased its connection with the midline frontal-central area. Just a final mention to both Cz channel, which significantly increased its connectivity with the Fz, F3, FC5, FCz and O2 channels, while decreasing its correlation with the CP1, Pz, P3, P8 and CP6 channels, and C4 channel which significantly decreased its connectivity with the Fz, F3 and FC1 channel, while significantly increasing with the P4, P8 and CP6 channel.

Regarding both VR NF-training group and the auditory NF-training group no significant within session variations were noticed.

Considering the avgREF data results for the learners of the visual NF-training group and for the “merged learners’ group”, we verified that, for early training stages, both point out to the formation of a right parietal complex (CP6, TP10, P8, P4), which relates with other central areas, temporal areas, and occipital areas. For the “merged learners’ group” such complex was more pronounced. Furthermore, this may underlie the existence of a specific upper-alpha neurofeedback training functional connectivity pattern of evolution, which might be shared in the training with different feedback modalities. Interestingly both analyses highlighted an initial increase over functional connectivity of the Pz channel, with widespread areas, thus, this channel may work as enabler for the establishment of the FC-improvements-related pathways. In fact, recalling the results for the upper-alpha topographic analysis, all the different groups reveal a tendency of increasing the upper-alpha activity the parietal areas that we previously referred as a “complex”, thus indicating that the upregulation of the upper-alpha in such channels, was accompanied by the establishment of new functional connections with such specific areas. Also, for both groups, after the session 2, there weren’t as many “significant” differences over the Functional connectivity values, with only specific pairs of channels reporting statistically significant changes on their functional connectivity and no clear pattern being evident. This result leads us to believe that it exists a breakthrough point, like the one in Wang et al. (2021) article, where the connectivity “improvements” started to be less accentuated and even some connectivity “reductions” were noticed. Unfortunately, due to the reduced number of learners in both VR NF-training group and auditory NF-training group, no statistically meaningful differences were reported, thus, no conclusions can be made in such cases, and we can’t enrich the analysis concerning the modality comparison.

Regarding the implementation of the SL, it alters the connectivity profiles showed in this analysis, The complex previously denoted is less pronounced, yet statistically significant increments over the functional connections of some central parietal, left and right parietal and temporal parietal areas were noticed. Also, interestingly, for the visual NF-training group on the fourth session it became evident a certain rearrangement of the referred complex. Apart from that, specific pairwise connection changes were revealed, as for example some statistically significant hotspots disappeared. Likely, this is a manifestation of the effect of the SL in the removal of spurious connections related to volume conduction.

4.2.2 Network Analysis

4.2.2.1 *Betweenness Centrality*

Concerning the *betweenness centrality* analysis whose results are exposed in the supplemental results exposed on the appendix section 7.3.2.1, no specific reinforcement profiles were noticed, due to the high variability of values per channel across the sets of each NF-training sessions. With this said we can't highlight a particular node on such analysis, which may result from the low sample size for each group of learners. Another contribution may come from the misclassification of subjects into learners and non-learners, which might possibly bias the group analysis for specific features that have lower effect-sizes. A brief note to the fact that as expected, the implementation of the SL alters the between centrality profiles.

4.2.2.2 *Strength*

Regarding the *strength* analysis, with results are exposed in the supplemental results in the appendix section 7.3.2.2, no specific reinforcement profiles were observed, due to the high variability of values presented by each channel across the sets within each of the NF-training sessions. With this said we can't highlight a particular node/channel on such analysis, which might result from the low sample size for each the NF-training groups. Hence, statistical power will not be sufficient to identify potential patterns, if existing. Also, the previously referred non-clear definition of learners vs non-learners, might contribute to a misclassification of an individual as learner or non-learner, and possibly corrupt the analysis of group specific features. A brief note to the fact that as expected, the implementation of the SL creates different *strength* values for each channel, set, and session.

4.2.2.3 *Transitivity*

The results for this analysis are exposed in the results section 3.2.2.1, with supplementary results exposed in the appendix section 7.3.2.3. As we previously referred the *transitivity* is a metric/algorithm that measures the clustered activity of the network.

Concerning the results for the analysis of the *transitivity*, presented in the section 3.2.2.3, over the Visual NF-training group, these suggests an increase on the RAUA clustered activity during the first two sessions of such training protocol. For the remaining sessions, as no within-session *transitivity* significant differences were identified, and no significant positive correlations were reported, we cannot conclude that a reinforcement of the UA clustered activity is present. In fact, during the third and fourth sessions the *transitivity* sometimes decreases. This is interesting as the third session was the

breakthrough point for the FC evolution, for the learners of the visual NF-training group. Thus, a similar tendency was previously observed in the study by Wang et al. (2021) , in which a decrease was shown to be significant for the *clustering coefficient* analysis after such breakthrough point—when FC ceased to increase, network metrics started to decrease. The results for the VR NF-training group are in sharp contrast to those observed in the visual NF-training group, with longer lasting significant positive correlations between both the median *transitivity* and all-*transitivity* values vs set number, even for the fourth NF-training session. This might point out to the possibility that the UA upregulation in NF-training with VR feedback promotes clustered UA activity during a greater amount of time, but we these results can not be generalized since the sample is composed of only four subjects. In addition, for the Wilcoxon test that compares if median *transitivity* is greater in Set 5 than in the set 1, presented in the table 3.7, no significant differences were reported, although some results were close to such significance level. Finally, for the auditory NF-training group, similarly to the VR NF-training group, longer lasting significant positive correlations were reported between the group median *transitivity* and Set Number and all *transitivity* values group learners' and Set Number. Regarding the Wilcoxon test results, that compared if median *transitivity* was greater in Set 5 than in the set 1, presented in the table 3.7, we verified that the application of the SL largely affected the results, as for the avgREF the first three sessions significant increases of the upper-alpha band *transitivity* from the set 1 to the set 5 were reported, and when the SL was applied, independently of the configuration, significant increases in *transitivity* for the UA up-regulation were noticed in session 1 and in session 4. Overall, we may conclude that auditory NF-training promotes clustered UA activity.

4.2.2.4 Charpath and GE

The results for these analyses are both in sections 3.2.2.2 and 3.2.2.3. Supplemental results are exposed in the appendix sections 7.3.2.4 and 7.3.2.5. As we previously referred, both *charpath* and *GE* are metrics that measure the integrated activity of a network.

A primary comment to the fact that, just by observing the results shown in Tables 3.8 to 3.11 that synthetize the results for both the *Charpath* and the *GE* analyses, we verify that for the correlation Tables 3.8 and 3.10, the coefficients that reached statistical significance occur in similar conditions, this means, same re-referencing configurations, reinforcing the fact that these two metrics are intimately connected. A more surprising appointment can be made when comparing the above referred tables, and the table that synthetizes the results for the *transitivity* analysis. Again, and although with some exceptions, the majority of the “significant correlation coefficient” occurred in similar conditions. These same appointments can also be done regarding the tables 3.9 and 3.11 that synthesize the results from the Wilcoxon Rank Sum Test, that verified if the median *charpath* was less in set 5 than in the set 1, and if the median *GE* was greater in set 5 than in the set 1, respectively, as only for the Session 4 of the auditory NF-training group there aren't consistent “marked statistically significances”. Thus, this might support the conclusion that the NF-training reorganizes the brain clustered activity, associated with the functional segregation, while also reorganizing the brain “integrated” activity, associated with the functional integration.

Furtermore, regarding the Tables 3.8 and 3.10 that contain the results for *charpath* and *GE* analyses, respectively, and as expected, the correlation coefficients have opposite signs throughout the results. For example, in session 1 of the visual NF-training group, both the median *charpath* values, and all *charpath* values, correlation with set number returned only negative coefficients. This occurs independently of the re-referencing method, avgREF, SL3 or SL4. In contrast, for the GE analysis with

the same group, on the *GE* analysis, only positive coefficients were returned (although they aren't necessarily significant). This in fact, translates the inverse relation that these metrics have, and is also seen through the results for the remaining sessions, and groups. Greater *GE* will be associated with smaller paths for the information transmission such that the *characteristic path* will consequentially diminish.

Regarding the results for the learners of the visual NF-training group, during the first two session, significant positive spearman's correlation and statistically significant increments within-session were detected, but only for the data with SL applied. This may suggest the optimization of the "network" paths during such sessions. Interestingly, as we referred to, this only was reported for the SL re-referenced data, thus leading us to suggest that the process of spatial filtering and the removal of volume conduction interferences affected the detection of such dispersed connected activity that was previously overshadowed by the blurring effect. In the following sessions 3 and 4 no significant correlations and no significant differences were reported, even if noting that positive *charpath* correlation coefficients and negative *GE* correlation coefficients are reported, respectively. Thus, these may represent a possible degrading over the functional integration-related paths. Again, for the visual NF-training group, the third session seems to be a breakthrough point where the training stops to induce improvements, or changes, on such network metrics. On the other hand, for the VR NF-training group, longer lasting paths optimization was reported, as significant correlations were detected in all the sessions for both *charpath* and *GE*. Again, concerning the Wilcoxon Rank Sum Test results, presented on the tables 3.9 and 3.11, that verified if the median *charpath* was lower in set 5 than in the set 1, and if the median *GE* was greater in set 5 than in the set 1, respectively, no significant differences were found due to the low sample. These results suggest the possibility that UA upregulation during NF-training with VR feedback may actively contribute to the promotion of integrated UA activity. However, since no significant differences were found within the different sessions, mainly due to the low sample, these findings cannot be generalized. Finally, considering the results of both *charpath* and *GE* network analyses for the learners of the auditory NF-training group, similarly to what was observed in VR NF-training group, longer lasting paths optimization was reported, since these significant associations/correlations were detected in all the four sessions. Regarding the results of the Wilcoxon Rank Sum test over this group, presented on the tables 3.9 and 3.11, that verified if the median *charpath* was less in set 5 than in the set 1, and if the median *GE* was greater in set 5 than in the set 1, respectively, significant within-session increases on the *GE*/decreases on the *charpath* were found on the session 1, 2 and 3 for the avgREF data, while for the SL data, significance was only reached in the first session. These results point out that the UA upregulation NF-training with auditory feedback actively contributes to the promotion of integrated UA activity, yet mainly on early stages of the training.

4.2.2.5 Modality Comparison

First, we shall recall the main question that we want to answer with this thesis:

"How is the individual's brain functional connectivity affected by the use of different sensory modalities in EEG-based Neurofeedback training protocols that target the upper alpha band?"

Regarding such question, some comments can be made. First, from the results of the FC analysis, specifically when considering all the learners together, from the three groups / sensory modalities, significant changes between set 1 and set 5 FC values are identified in channels over right parietal (P4,P8, CP6, TP10) and central parietal areas (Pz) in sessions 1 and 2.. This suggests a shared parietal connectivity profile across the learners of the UA EEG-based Neurofeedback training,

independently of the feedback modality. In fact, recalling the results from the topological analysis, we notice that such parietal and occipital areas tend to be reinforced, in terms of relative UA band power, within-session and from the first to the last session. This formation of a complex, in the initial stages of training, is also evident when we narrow our scope to the visual NF-training group. Unfortunately, due to the reduced sample neither for VR NF-training group, neither for the auditory NF-training group, we can extract conclusion regarding such matter. Although for later stages of training both “merged learners group” and Visual NF-training group seem to have less within-session connectivity variations, becoming more stable, in the Visual NF-training group a desegregation of the parietal complex can be noticed. This might be linked with the existence of a breakthrough point for the Visual NF-training, where not only the “learning” stabilized, but also the functional connectivity for such parietal complex starts to decrease. In the matter of the Network analyzes, no conclusions can be extracted from both *betweenness centrality* and *strength* analyzes. Concerning the *transitivity* analysis, we notice that while Visual NF-training has a short-term effect on promoting the clustered/segregated upper-alpha band activity, mainly on the first two sessions, while after the third session it stabilizes or even decreases, the VR and auditory NF-training seem to have a longer lasting reinforcement effect over the upper alpha segregated activity. With this said, further studies with greater samples are required to confirm such results. Regarding the *GE* and *charpath* analyzes, similar conclusions can be made, as a short-term effect of reinforcement in the integrated upper-alpha activity happens on the Visual NF-training. Again, after the third session it stabilizes and in some case the *GE* decreases. In opposite way, both VR and Auditory NF-training point to a longer lasting integrated upper-alpha activity reinforcement. Again, further studies with greater samples are required to confirm such results.

4.2.2.6 Surface Laplacian Application

Regarding whether the implementation of the SL re-referencing technique was advantageous for our protocol, and how different configurations of such technique affected our data, we shall first recall the topological analysis results. There, both SL3 and SL4 contributed as a spatial filter, by narrowing our focal activity and decreasing the non-focal one, which might be associated with low spatial frequencies, as expected. So, indeed it accomplished its spatial filtering purpose. For the FC analyzes, on the heatmaps, we noticed that consistently for the avgREF more “cold zones” and “hot zones” were reported, while on the SL re-referenced data less of such “zones” were present. This indeed can be a manifestation of the filtering power, more specifically, with the reduction of volume conduction on FC estimates. Regarding the *transitivity*, *GE* and *Charpath*, the implementation of the SL, significantly alters each metric profile when compared to the results from the same analysis on the avgREF data. A final remark to the fact that, while for the spectral analysis, the implementation of the SL3 created different results from the same analysis over SL4 data, whether by narrowing and smoothing the focal activity of each frequency band in the topological analysis due to the less rigidity of the spline lines, whether by changing the behavior of the per-set median RAUA activity on the Cz channel, for the FC connectivity analysis and network analysis almost no different statistically significant results are reported. Unfortunately, although the spatial filtering advantage of using the SL is verified in the topological analysis, and from our FC analysis and Networks analysis, indeed different results are produced when such technique is deployed, no clear conclusion can be made in terms of a possible causal-effect advantageous relationship of the application of the SL. Possibly, the best method to perform this analysis, is with simulated signals, as in such case we control the time-series, and indeed know what to expect after performing such filtering technique. On our case, as we only access a time-series that almost surely is biased, we can't clearly state that after performing such technique, our data

won't have for example volume conduction problems, as we don't have a control group where the volume conduction problem was already solved, to compare with.

5 Conclusion

In this thesis, data, from Cz-RAUA EEG-based NF-training with different feedback sensory modalities, was analyzed to verify if, by varying the feedback modality, different training outcomes would be reported in terms of FC. The data were preprocessed and evaluated in terms of the RAUA band upregulation at the Cz channel, theta, LA, UA, alpha, LB, UB and beta bands relative amplitude topological distribution across sets and sessions, in terms of per-set variations of FC in the UA band, among every possible channel pair, and in terms of a UA network analysis that would be used to assess node importance, clustered activity, and integrated activity of the brain networks, as assessed at the sensor level. Also, as there is a great discussion on the literature about the benefits of the application of the SL on the EEG data as a “deblurring method”, we performed the above analysis on preprocessed data re-referenced to a common average reference, and re-referenced through spline lines SL, through a stiffer interpolation and a smoother interpolation.

The results suggest a tendency for the increase of Cz-RAUA increases within each session, for all the NF-training groups, although no significant differences are registered when comparing values between sets at the beginning and at the end of the session. Regarding the topological changes, an increase in RAUA was observed in all the NF-training groups for channel in parieto-central, parietal, and parieto-occipital areas. Interestingly, the application of the different configurations of the spline lines SL contributed to highlight more focal activity, while negatively shifting the non-focal one, which may underlie the deblurring effect of such technique. Regarding the pair-wise analysis of the FC within-session, no significant variations are obtained for both the VR and auditory NF-training group, which might be related to the low number of learners that were considered for such modalities. The visual NF-training reported significant variations with an early increment over the medial and right parietal connections to widespread locations, but also, with the strengthening of the connections within such areas, pointing the existence of a specific cluster in such area. Also, some connections are established between the midline parietal and left frontal, frontal-temporal and frontal central areas. Then, a strengthening of such right parietal cluster happens, with the reinforcement of right parietal-to-right occipital areas, and right occipital-to-right frontal and frontal central areas. Also, on such stage of the training some left-temporal to left-parietal and left-occipital are reinforced. After, on the third session of training, no significant within-session differences are verified, and on the last a desegregation of the right parietal- to right-occipital connections happens. Thus, the third session may underlie a breakthrough point for such group. The same analysis over the SL re-referenced data, highlights previous results, and for early stages also notes the establishment of some left-parietal to medial and right-frontal/frontal central/temporal correlations. The same analysis over all the learners of the experiment, also highlights these same features, although in the last session no significant desegregation is noted, leading us to believe that such parietal reinforcement is an upper-alpha training inherent outcome and not a feedback modality specific outcome. On the network analysis, for the *betweenness centrality* and *strengths* analyzes, no specific patterns were found. Regarding the *transitivity*, although positive significant correlations with the set number were verified for all the groups, only for the visual and the auditory NF-training groups significant within-session increases were verified. Thus, neurofeedback with both auditory and visual feedback modalities seem to promote clustered upper-alpha band activity, while for the VR modality, although the results also suggest the same conclusion, no significant differences are found within the session. Recall that these results might be biased by the low sample that each group has. Interestingly, for the learners of the visual training group, the third session is also a breakthrough point for the increment of the *transitivity*, where no more significant increases are verified. Now considering the *GE* and the *charpath*, significant negative *charpath* per-set correlations accompanied by significant positive per-set *GE* correlations are found for all the feedback modalities,

but only for the visual and auditory NF-training groups, significant within-session variations are reported. Thus, neurofeedback with both auditory and visual feedback modalities seem to promote integrated upper-alpha band activity, while for the VR modality although the results also suggest the same conclusion, no significant differences are found within the session. Again, these results might be biased by the low sample that each group contains.

The results here presented, suggest that the upper-alpha NF-training establishes higher connections over specific parietal areas, independently of the feedback modality. Also, all the modalities seem to promote both clustered and integrated brain activity, although for the VR-group due to the low sample, no significant differences can be verified. Interestingly, while for the visual NF-training group the third session seems to be a breakthrough point, for the auditory NF-training group longer lasting “increases” are reported. With this said, for such low number of subjects, no significant differences between functional connectivity outcomes of the training can be linked with the different feedback modalities that are used. Further investigation, with a larger sample, is needed to confirm such results. Also, guidelines for the distinction of learners from non-learners are needed such that only real learners are selected, as with the procedure that we used we can't clearly ensure that some of the classified learners were indeed real learners, what can also bias the results. No clear conclusion can be made in terms of a possible causal-effect advantageous relationship of the application of the SL.

A final remark to the fact that, for future publication, we predict that we are going to replace the Spearman correlation models, here presented, by generalized mixed linear effect models which capture better the randomness associated with the individuals, and that mainly corrupts the cloud correlations. This might help us to extract new and more precise conclusion.

6 References

- Abhang, P. A., Gawali, B. W., & Mehrotra, S. C. (2016). Technological Basics of EEG Recording and Operation of Apparatus. In *Introduction to EEG- and Speech-Based Emotion Recognition* (pp. 19–50). Elsevier. <https://doi.org/10.1016/B978-0-12-804490-2.00002-6>
- Albarrán-Cárdenas, L., "Sylva-Pereyra, J., "Martínez-Briones, B., "Bosch-Bayard, J., & "Fernández, T. (2021). Neurofeedback Effects on EEG Connectivity in Children with Reading Disorder: I. Coherence. *Preprints*.
- Alkoby, O., Abu-Rmileh, A., Shriki, O., & Todder, D. (2018). Can We Predict Who Will Respond to Neurofeedback? A Review of the Inefficacy Problem and Existing Predictors for Successful EEG Neurofeedback Learning. *Neuroscience*, 378, 155–164. <https://doi.org/10.1016/j.neuroscience.2016.12.050>
- Anzolin, A., Presti, P., van de Steen, F., Astolfi, L., Haufe, S., & Marinazzo, D. (2019). Quantifying the Effect of Demixing Approaches on Directed Connectivity Estimated Between Reconstructed EEG Sources. *Brain Topography*, 32(4), 655–674. <https://doi.org/10.1007/s10548-019-00705-z>
- Arns, M., Conners, C. K., & Kraemer, H. C. (2013). A Decade of EEG Theta/Beta Ratio Research in ADHD. *Journal of Attention Disorders*, 17(5), 374–383. <https://doi.org/10.1177/1087054712460087>
- Babadi, B., & Brown, E. N. (2014). A Review of Multitaper Spectral Analysis. *IEEE Transactions on Biomedical Engineering*, 61(5), 1555–1564. <https://doi.org/10.1109/TBME.2014.2311996>
- Babiloni, F., Babiloni, C., Fattorini, L., Carducci, F., Onorati, P., & Urbano, A. (1995). Performances of surface Laplacian estimators: A study of simulated and real scalp potential distributions. *Brain Topography*, 8(1), 35–45. <https://doi.org/10.1007/BF01187668>
- Baldassarre, A., Ramsey, L., Rengachary, J., Zinn, K., Siegel, J. S., Metcalf, N. v., Strube, M. J., Snyder, A. Z., Corbetta, M., & Shulman, G. L. (2016). Dissociated functional connectivity profiles for motor and attention deficits in acute right-hemisphere stroke. *Brain*, 139(7), 2024–2038. <https://doi.org/10.1093/brain/aww107>
- Barry, R. J., Clarke, A. R., Johnstone, S. J., Magee, C. A., & Rushby, J. A. (2007). EEG differences between eyes-closed and eyes-open resting conditions. *Clinical Neurophysiology*, 118(12), 2765–2773. <https://doi.org/10.1016/j.clinph.2007.07.028>
- Bastos, A. M., & Schoffelen, J.-M. (2016). A Tutorial Review of Functional Connectivity Analysis Methods and Their Interpretational Pitfalls. *Frontiers in Systems Neuroscience*, 9. <https://doi.org/10.3389/fnsys.2015.00175>
- Bauer, C. C. C., Okano, K., Ghosh, S. S., Lee, Y. J., Melero, H., Angeles, C. de los, Nestor, P. G., del Re, E. C., Northoff, G., Niznikiewicz, M. A., & Whitfield-Gabrieli, S. (2020). Real-time fMRI neurofeedback reduces auditory hallucinations and modulates resting state connectivity of involved brain regions: Part 2: Default mode network -preliminary evidence. *Psychiatry Research*, 284, 112770. <https://doi.org/10.1016/j.psychres.2020.112770>
- Berhanu, C. (2019). *Connectivity-based EEG-neurofeedback in VR: pipeline development and experimental validation*. Instituto Superior Técnico.

- Bigdely-Shamlo, N., Mullen, T., Kothe, C., Su, K.-M., & Robbins, K. A. (2015). The PREP pipeline: standardized preprocessing for large-scale EEG analysis. *Frontiers in Neuroinformatics*, 9. <https://doi.org/10.3389/fninf.2015.00016>
- Biggins, C. A., Fein, G., Raz, J., & Amir, A. (1991). Artificially high coherences result from using spherical spline computation of scalp current density. *Electroencephalography and Clinical Neurophysiology*, 79(5), 413–419. [https://doi.org/10.1016/0013-4694\(91\)90206-J](https://doi.org/10.1016/0013-4694(91)90206-J)
- Bradshaw, L. A., & Wikswo, J. P. (2001). Spatial filter approach for evaluation of the surface laplacian of the electroencephalogram and magnetoencephalogram. *Annals of Biomedical Engineering*, 29(3), 202–213. <https://doi.org/10.1114/1.1352642>
- Bruña, R., Maestú, F., & Pereda, E. (2018). Phase locking value revisited: teaching new tricks to an old dog. *Journal of Neural Engineering*, 15(5), 056011. <https://doi.org/10.1088/1741-2552/aacfe4>
- Bucho, T., Caetano, G., Vourvopoulos, A., Accoto, F., Esteves, I., i Badia, S. B., Rosa, A., & Figueiredo, P. (2019). Comparison of Visual and Auditory Modalities for Upper-Alpha EEG-Neurofeedback. *2019 41st Annual International Conference of the IEEE Engineering in Medicine and Biology Society (EMBC)*, 5960–5966. <https://doi.org/10.1109/EMBC.2019.8856671>
- Cao, X., Cao, Q., Long, X., Sun, L., Sui, M., Zhu, C., Zuo, X., Zang, Y., & Wang, Y. (2009a). Abnormal resting-state functional connectivity patterns of the putamen in medication-naïve children with attention deficit hyperactivity disorder. *Brain Research*, 1303, 195–206. <https://doi.org/10.1016/j.brainres.2009.08.029>
- Cao, X., Cao, Q., Long, X., Sun, L., Sui, M., Zhu, C., Zuo, X., Zang, Y., & Wang, Y. (2009b). Abnormal resting-state functional connectivity patterns of the putamen in medication-naïve children with attention deficit hyperactivity disorder. *Brain Research*, 1303, 195–206. <https://doi.org/10.1016/j.brainres.2009.08.029>
- Carvalhoes, C., & de Barros, J. A. (2015). The surface Laplacian technique in EEG: Theory and methods. *International Journal of Psychophysiology*, 97(3), 174–188. <https://doi.org/10.1016/j.ijpsycho.2015.04.023>
- Carvalhoes, C. G., Perreau-Guimaraes, M., Grosenick, L., & Suppes, P. (2009). EEG classification by ICA source selection of Laplacian-filtered data. *2009 IEEE International Symposium on Biomedical Imaging: From Nano to Macro*, 1003–1006. <https://doi.org/10.1109/ISBI.2009.5193224>
- Cea-Cañas, B., Gomez-Pilar, J., Núñez, P., Rodríguez-Vázquez, E., de Uribe, N., Díez, Á., Pérez-Escudero, A., & Molina, V. (2020). Connectivity strength of the EEG functional network in schizophrenia and bipolar disorder. *Progress in Neuro-Psychopharmacology and Biological Psychiatry*, 98, 109801. <https://doi.org/10.1016/j.pnpbp.2019.109801>
- Chaumon, M., Bishop, D. V. M., & Busch, N. A. (2015). A practical guide to the selection of independent components of the electroencephalogram for artifact correction. *Journal of Neuroscience Methods*, 250, 47–63. <https://doi.org/10.1016/j.jneumeth.2015.02.025>
- Cho, B.-H., Kim, S., Shin, D. I., Lee, J. H., Min Lee, S., Young Kim, I., & Kim, S. I. (2004). Neurofeedback Training with Virtual Reality for Inattention and Impulsiveness. *CyberPsychology & Behavior*, 7(5), 519–526. <https://doi.org/10.1089/cpb.2004.7.519>

- Cho, M. K., Jang, H. S., Jeong, S.-H., Jang, I.-S., Choi, B.-J., & Lee, M.-G. T. (2008). Alpha neurofeedback improves the maintaining ability of alpha activity. *NeuroReport*, *19*(3), 315–317. <https://doi.org/10.1097/WNR.0b013e3282f4f022>
- Choi, K.-M., Kim, J.-Y., Kim, Y.-W., Han, J.-W., Im, C.-H., & Lee, S.-H. (2021). Comparative analysis of default mode networks in major psychiatric disorders using resting-state EEG. *Scientific Reports*, *11*(1), 22007. <https://doi.org/10.1038/s41598-021-00975-3>
- Cohen, D., & Tsuchiya, N. (2018). The Effect of Common Signals on Power, Coherence and Granger Causality: Theoretical Review, Simulations, and Empirical Analysis of Fruit Fly LFPs Data. *Frontiers in Systems Neuroscience*, *12*. <https://doi.org/10.3389/fnsys.2018.00030>
- Damaraju, E., Allen, E. A., Belger, A., Ford, J. M., McEwen, S., Mathalon, D. H., Mueller, B. A., Pearlson, G. D., Potkin, S. G., Preda, A., Turner, J. A., Vaidya, J. G., van Erp, T. G., & Calhoun, V. D. (2014a). Dynamic functional connectivity analysis reveals transient states of dysconnectivity in schizophrenia. *NeuroImage: Clinical*, *5*, 298–308. <https://doi.org/10.1016/j.nicl.2014.07.003>
- Damaraju, E., Allen, E. A., Belger, A., Ford, J. M., McEwen, S., Mathalon, D. H., Mueller, B. A., Pearlson, G. D., Potkin, S. G., Preda, A., Turner, J. A., Vaidya, J. G., van Erp, T. G., & Calhoun, V. D. (2014b). Dynamic functional connectivity analysis reveals transient states of dysconnectivity in schizophrenia. *NeuroImage: Clinical*, *5*, 298–308. <https://doi.org/10.1016/j.nicl.2014.07.003>
- de Cheveigné, A., & Nelken, I. (2019). Filters: When, Why, and How (Not) to Use Them. *Neuron*, *102*(2), 280–293. <https://doi.org/10.1016/j.neuron.2019.02.039>
- Dekker, M. K. J., Sitskoorn, M. M., Denissen, A. J. M., & van Boxtel, G. J. M. (2014). The time-course of alpha neurofeedback training effects in healthy participants. *Biological Psychology*, *95*, 70–73. <https://doi.org/10.1016/j.biopsycho.2013.11.014>
- Ding, M., Chen, Y., & Bressler, S. L. (2006). Granger Causality: Basic Theory and Application to Neuroscience. In *Handbook of Time Series Analysis* (pp. 437–460). Wiley-VCH Verlag GmbH & Co. KGaA. <https://doi.org/10.1002/9783527609970.ch17>
- Egner, T., Zech, T. F., & Gruzelier, J. H. (2004). The effects of neurofeedback training on the spectral topography of the electroencephalogram. *Clinical Neurophysiology*, *115*(11), 2452–2460. <https://doi.org/10.1016/j.clinph.2004.05.033>
- Eickhoff, S. B., & Müller, V. I. (2015a). Functional Connectivity. In *Brain Mapping* (pp. 187–201). Elsevier. <https://doi.org/10.1016/B978-0-12-397025-1.00212-8>
- Eickhoff, S. B., & Müller, V. I. (2015b). Functional Connectivity. In *Brain Mapping* (pp. 187–201). Elsevier. <https://doi.org/10.1016/B978-0-12-397025-1.00212-8>
- Enriquez-Geppert, S., Huster, R. J., & Herrmann, C. S. (2017). EEG-Neurofeedback as a Tool to Modulate Cognition and Behavior: A Review Tutorial. *Frontiers in Human Neuroscience*, *11*. <https://doi.org/10.3389/fnhum.2017.00051>
- Escolano, C., Aguilar, M., & Minguez, J. (2011). EEG-based upper alpha neurofeedback training improves working memory performance. *2011 Annual International Conference of the IEEE Engineering in Medicine and Biology Society*, 2327–2330. <https://doi.org/10.1109/IEMBS.2011.6090651>

- Escolano, C., Navarro-Gil, M., Garcia-Campayo, J., Congedo, M., & Minguez, J. (2014). The Effects of Individual Upper Alpha Neurofeedback in ADHD: An Open-Label Pilot Study. *Applied Psychophysiology and Biofeedback*, 39(3–4), 193–202. <https://doi.org/10.1007/s10484-014-9257-6>
- Escolano, C., Navarro-Gil, M., Garcia-Campayo, J., & Minguez, J. (2013). EEG-based upper-alpha neurofeedback for cognitive enhancement in major depressive disorder: A preliminary, uncontrolled study. *2013 35th Annual International Conference of the IEEE Engineering in Medicine and Biology Society (EMBC)*, 6293–6296. <https://doi.org/10.1109/EMBC.2013.6610992>
- Escolano, C., Navarro-Gil, M., Garcia-Campayo, J., & Minguez, J. (2014). The Effects of a Single Session of Upper Alpha Neurofeedback for Cognitive Enhancement: A Sham-Controlled Study. *Applied Psychophysiology and Biofeedback*, 39(3–4), 227–236. <https://doi.org/10.1007/s10484-014-9262-9>
- Fernández, T., Bosch-Bayard, J., Harmony, T., Caballero, M. I., Díaz-Comas, L., Galán, L., Ricardo-Garcell, J., Aubert, E., & Otero-Ojeda, G. (2016). Neurofeedback in Learning Disabled Children: Visual versus Auditory Reinforcement. *Applied Psychophysiology and Biofeedback*, 41(1), 27–37. <https://doi.org/10.1007/s10484-015-9309-6>
- Filippi, M., Spinelli, E. G., Cividini, C., & Agosta, F. (2019). Resting State Dynamic Functional Connectivity in Neurodegenerative Conditions: A Review of Magnetic Resonance Imaging Findings. *Frontiers in Neuroscience*, 13. <https://doi.org/10.3389/fnins.2019.00657>
- Finn, E. S., Shen, X., Holahan, J. M., Scheinost, D., Lacadie, C., Papademetris, X., Shaywitz, S. E., Shaywitz, B. A., & Constable, R. T. (2014). Disruption of Functional Networks in Dyslexia: A Whole-Brain, Data-Driven Analysis of Connectivity. *Biological Psychiatry*, 76(5), 397–404. <https://doi.org/10.1016/j.biopsych.2013.08.031>
- Fitzgibbon, S. P., DeLosAngeles, D., Lewis, T. W., Powers, D. M. W., Whitham, E. M., Willoughby, J. O., & Pope, K. J. (2015). Surface Laplacian of scalp electrical signals and independent component analysis resolve EMG contamination of electroencephalogram. *International Journal of Psychophysiology*, 97(3), 277–284. <https://doi.org/10.1016/j.ijpsycho.2014.10.006>
- Floyd, R. W. (1962). Algorithm 97: Shortest path. *Communications of the ACM*, 5(6), 345. <https://doi.org/10.1145/367766.368168>
- Foffani, G., Bianchi, A. M., Cincotti, F., Babiloni, C., Carducci, F., Babiloni, F., Rossini, P. M., & Cerutti, S. (2004). Independent Component Analysis Compared to Laplacian Filtering as "Deblurring" Techniques for Event Related Desynchronization/ Synchronization. *Methods of Information in Medicine*, 43(01), 74–78. <https://doi.org/10.1055/s-0038-1633839>
- Fraschini, M., Demuru, M., Crobe, A., Marrosu, F., Stam, C. J., & Hillebrand, A. (2016). The effect of epoch length on estimated EEG functional connectivity and brain network organisation. *Journal of Neural Engineering*, 13(3), 036015. <https://doi.org/10.1088/1741-2560/13/3/036015>
- Fries, P. (2005). A mechanism for cognitive dynamics: neuronal communication through neuronal coherence. *Trends in Cognitive Sciences*, 9(10), 474–480. <https://doi.org/10.1016/j.tics.2005.08.011>
- Fries, P. (2015). Rhythms for Cognition: Communication through Coherence. *Neuron*, 88(1), 220–235. <https://doi.org/10.1016/j.neuron.2015.09.034>
- Friston, K. J. (1994). Functional and effective connectivity in neuroimaging: A synthesis. *Human Brain Mapping*, 2(1–2), 56–78. <https://doi.org/10.1002/hbm.460020107>

- Friston, K. J. (2011). Functional and Effective Connectivity: A Review. *Brain Connectivity*, *1*(1), 13–36. <https://doi.org/10.1089/brain.2011.0008>
- Frølich, L., & Dowding, I. (2018). Removal of muscular artifacts in EEG signals: a comparison of linear decomposition methods. *Brain Informatics*, *5*(1), 13–22. <https://doi.org/10.1007/s40708-017-0074-6>
- Giulia, L., Adolfo, V., Julie, C., Quentin, D., Simon, B., Fleury, M., Leveque-Le Bars, E., Bannier, E., Lécuyer, A., Barillot, C., & Bonan, I. (2021). The impact of neurofeedback on effective connectivity networks in chronic stroke patients: an exploratory study. *Journal of Neural Engineering*, *18*(5), 056052. <https://doi.org/10.1088/1741-2552/ac291e>
- Gómez-Ramírez, J., Freedman, S., Mateos, D., Pérez Velázquez, J. L., & Valiante, T. A. (2017). Exploring the alpha desynchronization hypothesis in resting state networks with intracranial electroencephalography and wiring cost estimates. *Scientific Reports*, *7*(1), 15670. <https://doi.org/10.1038/s41598-017-15659-0>
- Gonuguntla, V., Mallipeddi, R., & Veluvolu, K. C. (2016). Identification of emotion associated brain functional network with phase locking value. *2016 38th Annual International Conference of the IEEE Engineering in Medicine and Biology Society (EMBC)*, 4515–4518. <https://doi.org/10.1109/EMBC.2016.7591731>
- Groppe, D. M., Bickel, S., Keller, C. J., Jain, S. K., Hwang, S. T., Harden, C., & Mehta, A. D. (2013). Dominant frequencies of resting human brain activity as measured by the electrocorticogram. *NeuroImage*, *79*, 223–233. <https://doi.org/10.1016/j.neuroimage.2013.04.044>
- Gruzelier, J. H. (2014). EEG-neurofeedback for optimising performance. III: A review of methodological and theoretical considerations. *Neuroscience & Biobehavioral Reviews*, *44*, 159–182. <https://doi.org/10.1016/j.neubiorev.2014.03.015>
- Guggisberg, A. G., Honma, S. M., Findlay, A. M., Dalal, S. S., Kirsch, H. E., Berger, M. S., & Nagarajan, S. S. (2008). Mapping functional connectivity in patients with brain lesions. *Annals of Neurology*, *63*(2), 193–203. <https://doi.org/10.1002/ana.21224>
- Hämäläinen, M., Hari, R., Ilmoniemi, R. J., Knuutila, J., & Lounasmaa, O. v. (1993). Magnetoencephalography—theory, instrumentation, and applications to noninvasive studies of the working human brain. *Reviews of Modern Physics*, *65*(2), 413–497. <https://doi.org/10.1103/RevModPhys.65.413>
- Hammond, D. C. (2007). What Is Neurofeedback? *Journal of Neurotherapy*, *10*(4), 25–36. https://doi.org/10.1300/J184v10n04_04
- Hanslmayr, S., Sauseng, P., Doppelmayr, M., Schabus, M., & Klimesch, W. (2005a). Increasing Individual Upper Alpha Power by Neurofeedback Improves Cognitive Performance in Human Subjects. *Applied Psychophysiology and Biofeedback*, *30*(1), 1–10. <https://doi.org/10.1007/s10484-005-2169-8>
- Hanslmayr, S., Sauseng, P., Doppelmayr, M., Schabus, M., & Klimesch, W. (2005b). Increasing Individual Upper Alpha Power by Neurofeedback Improves Cognitive Performance in Human Subjects. *Applied Psychophysiology and Biofeedback*, *30*(1), 1–10. <https://doi.org/10.1007/s10484-005-2169-8>
- Haufe, S., Nikulin, V. v., Müller, K.-R., & Nolte, G. (2013). A critical assessment of connectivity measures for EEG data: A simulation study. *NeuroImage*, *64*, 120–133. <https://doi.org/10.1016/j.neuroimage.2012.09.036>

- Haufe, S., Nikulin, V. v., & Nolte, G. (2012). *Alleviating the Influence of Weak Data Asymmetries on Granger-Causal Analyses* (pp. 25–33). https://doi.org/10.1007/978-3-642-28551-6_4
- He, B., & 'Lin, D. (2013). Electrophysiological mapping and neuroimaging. In *Neural Engineering: Second Edition* (pp. 499–553).
- Herweg, N. A., Solomon, E. A., & Kahana, M. J. (2020). Theta Oscillations in Human Memory. *Trends in Cognitive Sciences*, 24(3), 208–227. <https://doi.org/10.1016/j.tics.2019.12.006>
- Hjorth, B. (1975). An on-line transformation of EEG scalp potentials into orthogonal source derivations. *Electroencephalography and Clinical Neurophysiology*, 39(5), 526–530. [https://doi.org/10.1016/0013-4694\(75\)90056-5](https://doi.org/10.1016/0013-4694(75)90056-5)
- Hsueh, J.-J., Chen, T.-S., Chen, J.-J., & Shaw, F.-Z. (2016). Neurofeedback training of EEG alpha rhythm enhances episodic and working memory. *Human Brain Mapping*, 37(7), 2662–2675. <https://doi.org/10.1002/hbm.23201>
- Hull, J. v., Dokovna, L. B., Jacokes, Z. J., Torgerson, C. M., Irimia, A., & van Horn, J. D. (2017). Resting-State Functional Connectivity in Autism Spectrum Disorders: A Review. *Frontiers in Psychiatry*, 7. <https://doi.org/10.3389/fpsy.2016.00205>
- Huster, R. J., Mokom, Z. N., Enriquez-Geppert, S., & Herrmann, C. S. (2014). Brain–computer interfaces for EEG neurofeedback: Peculiarities and solutions. *International Journal of Psychophysiology*, 91(1), 36–45. <https://doi.org/10.1016/j.ijpsycho.2013.08.011>
- Imperatori, C., della Marca, G., Amoroso, N., Maestoso, G., Valenti, E. M., Massullo, C., Carbone, G. A., Contardi, A., & Farina, B. (2017). Alpha/Theta Neurofeedback Increases Mentalization and Default Mode Network Connectivity in a Non-Clinical Sample. *Brain Topography*, 30(6), 822–831. <https://doi.org/10.1007/s10548-017-0593-8>
- Jensen, C. B. F., Petersen, M. K., Larsen, J. E., Stopczynski, A., Stahlhut, C., Ivanova, M. G., Andersen, T., & Hansen, L. K. (2013). Spatio temporal media components for neurofeedback. *2013 IEEE International Conference on Multimedia and Expo Workshops (ICMEW)*, 1–6. <https://doi.org/10.1109/ICMEW.2013.6618362>
- Jurcak, V., Tsuzuki, D., & Dan, I. (2007). 10/20, 10/10, and 10/5 systems revisited: Their validity as relative head-surface-based positioning systems. *NeuroImage*, 34(4), 1600–1611. <https://doi.org/10.1016/j.neuroimage.2006.09.024>
- Kaczorowska, M., Plechawska-Wojcik, M., Tokovarov, M., & Dmytruk, R. (2017). Comparison of the ICA and PCA methods in correction of EEG signal artefacts. *2017 10th International Symposium on Advanced Topics in Electrical Engineering (ATEE)*, 262–267. <https://doi.org/10.1109/ATEE.2017.7905095>
- Kayser, J., & Tenke, C. E. (2015a). Issues and considerations for using the scalp surface Laplacian in EEG/ERP research: A tutorial review. *International Journal of Psychophysiology*, 97(3), 189–209. <https://doi.org/10.1016/j.ijpsycho.2015.04.012>
- Kayser, J., & Tenke, C. E. (2015b). On the benefits of using surface Laplacian (current source density) methodology in electrophysiology. *International Journal of Psychophysiology*, 97(3), 171–173. <https://doi.org/10.1016/j.ijpsycho.2015.06.001>

- Kirschstein, T., & Köhling, R. (2009). What is the Source of the EEG? *Clinical EEG and Neuroscience*, 40(3), 146–149. <https://doi.org/10.1177/155005940904000305>
- Klimesch, W. (1999). EEG alpha and theta oscillations reflect cognitive and memory performance: a review and analysis. *Brain Research Reviews*, 29(2–3), 169–195. [https://doi.org/10.1016/S0165-0173\(98\)00056-3](https://doi.org/10.1016/S0165-0173(98)00056-3)
- Klimesch, W., Schimke, H., & Pfurtscheller, G. (1993). Alpha frequency, cognitive load and memory performance. *Brain Topography*, 5(3), 241–251. <https://doi.org/10.1007/BF01128991>
- Kober, S. E., Reichert, J. L., Schweiger, D., Neuper, C., & Wood, G. (2017). Does Feedback Design Matter? A Neurofeedback Study Comparing Immersive Virtual Reality and Traditional Training Screens in Elderly. *International Journal of Serious Games*, 4(3). <https://doi.org/10.17083/ijsg.v4i3.167>
- Kober, S. E., Schweiger, D., Reichert, J. L., Neuper, C., & Wood, G. (2017). Upper Alpha Based Neurofeedback Training in Chronic Stroke: Brain Plasticity Processes and Cognitive Effects. *Applied Psychophysiology and Biofeedback*, 42(1), 69–83. <https://doi.org/10.1007/s10484-017-9353-5>
- Konrad, K., Neufang, S., Hanisch, C., Fink, G. R., & Herpertz-Dahlmann, B. (2006). Dysfunctional Attentional Networks in Children with Attention Deficit/Hyperactivity Disorder: Evidence from an Event-Related Functional Magnetic Resonance Imaging Study. *Biological Psychiatry*, 59(7), 643–651. <https://doi.org/10.1016/j.biopsych.2005.08.013>
- Kragel, J. E., VanHaerents, S., Templer, J. W., Schuele, S., Rosenow, J. M., Nilakantan, A. S., & Bridge, D. J. (2020). Hippocampal theta coordinates memory processing during visual exploration. *eLife*, 9. <https://doi.org/10.7554/eLife.52108>
- Kraskov, A., Stögbauer, H., & Grassberger, P. (2004). Estimating mutual information. *Physical Review E*, 69(6), 066138. <https://doi.org/10.1103/PhysRevE.69.066138>
- Lachaux, J.-P., Lutz, A., Rudrauf, D., Cosmelli, D., le Van Quyen, M., Martinerie, J., & Varela, F. (2002). Estimating the time-course of coherence between single-trial brain signals: an introduction to wavelet coherence. *Neurophysiologie Clinique/Clinical Neurophysiology*, 32(3), 157–174. [https://doi.org/10.1016/S0987-7053\(02\)00301-5](https://doi.org/10.1016/S0987-7053(02)00301-5)
- LACHAUX, J.-P., RODRIGUEZ, E., le VAN QUYEN, M., LUTZ, A., MARTINERIE, J., & VARELA, F. J. (2000). STUDYING SINGLE-TRIALS OF PHASE SYNCHRONOUS ACTIVITY IN THE BRAIN. *International Journal of Bifurcation and Chaos*, 10(10), 2429–2439. <https://doi.org/10.1142/S0218127400001560>
- Lachaux, J.-P., Rodriguez, E., Martinerie, J., & Varela, F. J. (1999). Measuring phase synchrony in brain signals. *Human Brain Mapping*, 8(4), 194–208. [https://doi.org/10.1002/\(SICI\)1097-0193\(1999\)8:4<194::AID-HBM4>3.0.CO;2-C](https://doi.org/10.1002/(SICI)1097-0193(1999)8:4<194::AID-HBM4>3.0.CO;2-C)
- Lakshmi, M. R., Prasad, T. v., & Chandra Prakash, V. (2014). Survey on EEG Signal Processing Methods. In *International Journal of Advanced Research in Computer Science and Software Engineering* (Vol. 4, Issue 1). <https://www.researchgate.net/publication/328419840>
- Lan, Z., Sun, Y., Zhao, L., Xiao, Y., Kuai, C., & Xue, S.-W. (2021). Aberrant Effective Connectivity of the Ventral Putamen in Boys With Attention-Deficit/Hyperactivity Disorder. *Psychiatry Investigation*, 18(8), 763–769. <https://doi.org/10.30773/pi.2020.0422>

- le Van Quyen, M. (2011). The brainweb of cross-scale interactions. *New Ideas in Psychology*, 29(2), 57–63. <https://doi.org/10.1016/j.newideapsych.2010.11.001>
- le Van Quyen, M., Foucher, J., Lachaux, J.-P., Rodriguez, E., Lutz, A., Martinerie, J., & Varela, F. J. (2001). Comparison of Hilbert transform and wavelet methods for the analysis of neuronal synchrony. *Journal of Neuroscience Methods*, 111(2), 83–98. [https://doi.org/10.1016/S0165-0270\(01\)00372-7](https://doi.org/10.1016/S0165-0270(01)00372-7)
- Lei, X., & Liao, K. (2017). Understanding the Influences of EEG Reference: A Large-Scale Brain Network Perspective. *Frontiers in Neuroscience*, 11. <https://doi.org/10.3389/fnins.2017.00205>
- Li, Z., Wang, H., Wu, X., Xu, X., Wei, S., & Yao, L. (2019). Working Memory Training Using EEG Neurofeedback Based on Theta Coherence of Brain Regions. *2019 7th International Winter Conference on Brain-Computer Interface (BCI)*, 1–6. <https://doi.org/10.1109/IWW-BCI.2019.8737262>
- Loriette, C., Ziane, C., & ben Hamed, S. (2021). Neurofeedback for cognitive enhancement and intervention and brain plasticity. *Revue Neurologique*, 177(9), 1133–1144. <https://doi.org/10.1016/j.neurol.2021.08.004>
- Malik, A. S., & Amin, H. U. (2017). Chapter 1 - Designing an EEG Experiment. In A. S. Malik & H. U. Amin (Eds.), *Designing EEG Experiments for Studying the Brain* (pp. 1–30). Academic Press. <https://doi.org/https://doi.org/10.1016/B978-0-12-811140-6.00001-1>
- Marzbani, H., Marateb, H., & Mansourian, M. (2016). Methodological Note: Neurofeedback: A Comprehensive Review on System Design, Methodology and Clinical Applications. *Basic and Clinical Neuroscience Journal*, 7(2). <https://doi.org/10.15412/J.BCN.03070208>
- McFarland, D. J. (2015). The advantages of the surface Laplacian in brain–computer interface research. *International Journal of Psychophysiology*, 97(3), 271–276. <https://doi.org/10.1016/j.ijpsycho.2014.07.009>
- Mecarelli, O. (2019). Electrode Placement Systems and Montages. In *Clinical Electroencephalography* (pp. 35–52). Springer International Publishing. https://doi.org/10.1007/978-3-030-04573-9_4
- Michelini, G., Jurgiel, J., Bakolis, I., Cheung, C. H. M., Asherson, P., Loo, S. K., Kuntsi, J., & Mohammad-Rezazadeh, I. (2019). Atypical functional connectivity in adolescents and adults with persistent and remitted ADHD during a cognitive control task. *Translational Psychiatry*, 9(1), 137. <https://doi.org/10.1038/s41398-019-0469-7>
- Miljevic, A., Bailey, N. W., Vila-Rodriguez, F., Herring, S. E., & Fitzgerald, P. B. (2022). Electroencephalographic Connectivity: A Fundamental Guide and Checklist for Optimal Study Design and Evaluation. *Biological Psychiatry: Cognitive Neuroscience and Neuroimaging*, 7(6), 546–554. <https://doi.org/10.1016/j.bpsc.2021.10.017>
- Mognon, A., Jovicich, J., Bruzzone, L., & Buiatti, M. (2011). ADJUST: An automatic EEG artifact detector based on the joint use of spatial and temporal features. *Psychophysiology*, 48(2), 229–240. <https://doi.org/10.1111/j.1469-8986.2010.01061.x>
- Mottaz, A., Corbet, T., Doganci, N., Magnin, C., Nicolo, P., Schnider, A., & Guggisberg, A. G. (2018). Modulating functional connectivity after stroke with neurofeedback: Effect on motor deficits in a controlled cross-over study. *NeuroImage: Clinical*, 20, 336–346. <https://doi.org/10.1016/j.nicl.2018.07.029>

- Nicholson, A. A., Ros, T., Frewen, P. A., Densmore, M., Théberge, J., Kluetsch, R. C., Jetly, R., & Lanius, R. A. (2016). Alpha oscillation neurofeedback modulates amygdala complex connectivity and arousal in posttraumatic stress disorder. *NeuroImage: Clinical*, *12*, 506–516. <https://doi.org/10.1016/j.nicl.2016.07.006>
- Niv, S. (2013). Clinical efficacy and potential mechanisms of neurofeedback. *Personality and Individual Differences*, *54*(6), 676–686. <https://doi.org/10.1016/j.paid.2012.11.037>
- Nolte, G., Bai, O., Wheaton, L., Mari, Z., Vorbach, S., & Hallett, M. (2004). Identifying true brain interaction from EEG data using the imaginary part of coherency. *Clinical Neurophysiology*, *115*(10), 2292–2307. <https://doi.org/10.1016/j.clinph.2004.04.029>
- Nolte, G., Ziehe, A., Nikulin, V. v., Schlögl, A., Krämer, N., Brismar, T., & Müller, K.-R. (2008). Robustly Estimating the Flow Direction of Information in Complex Physical Systems. *Physical Review Letters*, *100*(23), 234101. <https://doi.org/10.1103/PhysRevLett.100.234101>
- Nunez, P. L., Silberstein, R. B., Cadusch, P. J., Wijesinghe, R. S., Westdorp, A. F., & Srinivasan, R. (1994). A theoretical and experimental study of high resolution EEG based on surface Laplacians and cortical imaging. *Electroencephalography and Clinical Neurophysiology*, *90*(1), 40–57. [https://doi.org/10.1016/0013-4694\(94\)90112-0](https://doi.org/10.1016/0013-4694(94)90112-0)
- Nunez, P. L., Srinivasan, R., Westdorp, A. F., Wijesinghe, R. S., Tucker, D. M., Silberstein, R. B., & Cadusch, P. J. (1997). EEG coherency. *Electroencephalography and Clinical Neurophysiology*, *103*(5), 499–515. [https://doi.org/10.1016/S0013-4694\(97\)00066-7](https://doi.org/10.1016/S0013-4694(97)00066-7)
- Olejniczak, P. (2006). Neurophysiologic Basis of EEG. *Journal of Clinical Neurophysiology*, *23*(3), 186–189. <https://doi.org/10.1097/01.wnp.0000220079.61973.6c>
- Pérez-Elvira, R., Oltra-Cucarella, J., Carrobbles, J. A., Moltó, J., Flórez, M., Parra, S., Agudo, M., Saez, C., Guarino, S., Costea, R. M., & Neamtu, B. (2021). Enhancing the Effects of Neurofeedback Training: The Motivational Value of the Reinforcers. *Brain Sciences*, *11*(4), 457. <https://doi.org/10.3390/brainsci11040457>
- Plonsey, R., & Heppner, D. B. (1967). Considerations of quasi-stationarity in electrophysiological systems. *The Bulletin of Mathematical Biophysics*, *29*(4), 657–664. <https://doi.org/10.1007/BF02476917>
- Prany, W., Patrice, C., Franck, D., Fabrice, W., Mahdi, M., Pierre, D., Christian, M., Jean-Marc, G., Fabian, G., Francis, E., Jean-Marc, B., & Bérengère, G.-G. (2022). EEG resting-state functional connectivity: evidence for an imbalance of external/internal information integration in autism. *Journal of Neurodevelopmental Disorders*, *14*(1), 47. <https://doi.org/10.1186/s11689-022-09456-8>
- Purves, D., Augustine, G., Fitzpatrick, D., Katz, L., LaMantia, A., McNamara, J., & Williams, M. (2001). Stages of Sleep. In *Neuroscience* (2nd ed.).
- Rojas, G. M., Alvarez, C., Montoya, C. E., de la Iglesia-Vayá, M., Cisternas, J. E., & Gálvez, M. (2018). Study of Resting-State Functional Connectivity Networks Using EEG Electrodes Position As Seed. *Frontiers in Neuroscience*, *12*. <https://doi.org/10.3389/fnins.2018.00235>
- Ros, T., J. Baars, B., Lanius, R. A., & Vuilleumier, P. (2014). Tuning pathological brain oscillations with neurofeedback: a systems neuroscience framework. *Frontiers in Human Neuroscience*, *8*. <https://doi.org/10.3389/fnhum.2014.01008>

- Rubia, K., Criaud, M., Wulff, M., Alegria, A., Brinson, H., Barker, G., Stahl, D., & Giampietro, V. (2019). Functional connectivity changes associated with fMRI neurofeedback of right inferior frontal cortex in adolescents with ADHD. *NeuroImage*, *188*, 43–58. <https://doi.org/10.1016/j.neuroimage.2018.11.055>
- Rubinov, M., & Sporns, O. (2010). Complex network measures of brain connectivity: Uses and interpretations. *NeuroImage*, *52*(3), 1059–1069. <https://doi.org/10.1016/j.neuroimage.2009.10.003>
- Rutkove, S. B. (2007). Introduction to Volume Conduction. In A. S. Blum & S. B. Rutkove (Eds.), *The Clinical Neurophysiology Primer* (pp. 43–53). Humana Press. https://doi.org/10.1007/978-1-59745-271-7_4
- Sargolzaei, S., Cabrerizo, M., Goryawala, M., Eddin, A. S., & Adjouadi, M. (2015). Scalp EEG brain functional connectivity networks in pediatric epilepsy. *Computers in Biology and Medicine*, *56*, 158–166. <https://doi.org/10.1016/j.combiomed.2014.10.018>
- Sazgar, M., & Young, M. G. (2019). Overview of EEG, Electrode Placement, and Montages. In *Absolute Epilepsy and EEG Rotation Review* (pp. 117–125). Springer International Publishing. https://doi.org/10.1007/978-3-030-03511-2_5
- Schacter, D. L. (1977). EEG theta waves and psychological phenomena: A review and analysis. *Biological Psychology*, *5*(1), 47–82. [https://doi.org/10.1016/0301-0511\(77\)90028-X](https://doi.org/10.1016/0301-0511(77)90028-X)
- Schomer, D. L., & Lopes da Silva, F. (2012). *Niedermeyer's electroencephalography: Basic principles, clinical applications, and related fields: Sixth edition*.
- Schomer, D. L., & Lopes da Silva, F. H. (Eds.). (2017). *Niedermeyer's Electroencephalography* (Vol. 1). Oxford University Press. <https://doi.org/10.1093/med/9780190228484.001.0001>
- Shaw, J. C. (1996). Intention as a component of the alpha-rhythm response to mental activity. *International Journal of Psychophysiology*, *24*(1–2), 7–23. [https://doi.org/10.1016/S0167-8760\(96\)00052-9](https://doi.org/10.1016/S0167-8760(96)00052-9)
- Sherlin, L. H., Arns, M., Lubar, J., Heinrich, H., Kerson, C., Strehl, U., & Serman, M. B. (2011). Neurofeedback and Basic Learning Theory: Implications for Research and Practice. *Journal of Neurotherapy*, *15*(4), 292–304. <https://doi.org/10.1080/10874208.2011.623089>
- Shtark, M. B., Kozlova, L. I., Bezmaternykh, D. D., Mel'nikov, M. Ye., Savelov, A. A., & Sokhadze, E. M. (2018). Neuroimaging Study of Alpha and Beta EEG Biofeedback Effects on Neural Networks. *Applied Psychophysiology and Biofeedback*, *43*(2), 169–178. <https://doi.org/10.1007/s10484-018-9396-2>
- Sitaram, R., Ros, T., Stoeckel, L., Haller, S., Scharnowski, F., Lewis-Peacock, J., Weiskopf, N., Blefari, M. L., Rana, M., Oblak, E., Birbaumer, N., & Sulzer, J. (2017). Closed-loop brain training: the science of neurofeedback. *Nature Reviews Neuroscience*, *18*(2), 86–100. <https://doi.org/10.1038/nrn.2016.164>
- Srinivasan, R. (1999). *Methods to Improve the Spatial Resolution of EEG* (Vol. 1, Issue 1).
- Louis, E., Frey, L., Britton, J., Hopp, J., Korb, P., Koubeissi, M., Lievens, W., & Pestana-Knight, E. (2016). *Electroencephalography (EEG): An Introductory Text and Atlas of Normal and Abnormal Findings in Adults, Children, and Infants*. American Epilepsy Society. <https://doi.org/10.5698/978-0-9979756-0-4>

- Stam, C. J., Nolte, G., & Daffertshofer, A. (2007). Phase lag index: Assessment of functional connectivity from multi channel EEG and MEG with diminished bias from common sources. *Human Brain Mapping, 28*(11), 1178–1193. <https://doi.org/10.1002/hbm.20346>
- Storti, S. F., Formaggio, E., Manganotti, P., & Menegaz, G. (2016). Brain Network Connectivity and Topological Analysis During Voluntary Arm Movements. *Clinical EEG and Neuroscience, 47*(4), 276–290. <https://doi.org/10.1177/1550059415598905>
- Syam, S. H.-F., Lakany, H., Ahmad, R. B., & Conway, B. A. (2017). Comparing Common Average Referencing to Laplacian Referencing in Detecting Imagination and Intention of Movement for Brain Computer Interface. *MATEC Web of Conferences, 140*, 01028. <https://doi.org/10.1051/matecconf/201714001028>
- Tatum, W. O., Dworetzky, B. A., & Schomer, D. L. (2011). Artifact and Recording Concepts in EEG. *Journal of Clinical Neurophysiology, 28*(3), 252–263. <https://doi.org/10.1097/WNP.0b013e31821c3c93>
- Tenke, C. E., & Kayser, J. (2015). Surface Laplacians (SL) and phase properties of EEG rhythms: Simulated generators in a volume-conduction model. *International Journal of Psychophysiology, 97*(3), 285–298. <https://doi.org/10.1016/j.ijpsycho.2015.05.008>
- Thakor, N. v., & Sherman, D. L. (2013). EEG Signal Processing: Theory and Applications. In *Neural Engineering* (pp. 259–303). Springer US. https://doi.org/10.1007/978-1-4614-5227-0_5
- Thibault, R. T., Lifshitz, M., & Raz, A. (2016). The self-regulating brain and neurofeedback: Experimental science and clinical promise. In *Cortex* (Vol. 74, pp. 247–261). Masson SpA. <https://doi.org/10.1016/j.cortex.2015.10.024>
- Trambaiolli, L. R., Cassani, R., Mehler, D. M. A., & Falk, T. H. (2021). Neurofeedback and the Aging Brain: A Systematic Review of Training Protocols for Dementia and Mild Cognitive Impairment. *Frontiers in Aging Neuroscience, 13*. <https://doi.org/10.3389/fnagi.2021.682683>
- van de Steen, F., Faes, L., Karahan, E., Songsiri, J., Valdes-Sosa, P. A., & Marinazzo, D. (2019). Critical Comments on EEG Sensor Space Dynamical Connectivity Analysis. *Brain Topography, 32*(4), 643–654. <https://doi.org/10.1007/s10548-016-0538-7>
- van Vugt, M. K., Sederberg, P. B., & Kahana, M. J. (2007). Comparison of spectral analysis methods for characterizing brain oscillations. *Journal of Neuroscience Methods, 162*(1–2), 49–63. <https://doi.org/10.1016/j.jneumeth.2006.12.004>
- Varela, F., Lachaux, J.-P., Rodriguez, E., & Martinerie, J. (2001). The brainweb: Phase synchronization and large-scale integration. *Nature Reviews Neuroscience, 2*(4), 229–239. <https://doi.org/10.1038/35067550>
- Vernon, D., Dempster, T., Bazanova, O., Rutterford, N., Pasqualini, M., & Andersen, S. (2009). Alpha Neurofeedback Training for Performance Enhancement: Reviewing the Methodology. *Journal of Neurotherapy, 13*(4), 214–227. <https://doi.org/10.1080/10874200903334397>
- Vinck, M., Oostenveld, R., van Wingerden, M., Battaglia, F., & Pennartz, C. M. A. (2011). An improved index of phase-synchronization for electrophysiological data in the presence of volume-conduction, noise and sample-size bias. *NeuroImage, 55*(4), 1548–1565. <https://doi.org/10.1016/j.neuroimage.2011.01.055>

- Voss, P., Thomas, M. E., Cisneros-Franco, J. M., & de Villers-Sidani, É. (2017). Dynamic Brains and the Changing Rules of Neuroplasticity: Implications for Learning and Recovery. *Frontiers in Psychology*, 8. <https://doi.org/10.3389/fpsyg.2017.01657>
- Wan, F., Nan, W., Vai, M. I., & Rosa, A. (2014). Resting alpha activity predicts learning ability in alpha neurofeedback. *Frontiers in Human Neuroscience*, 8. <https://doi.org/10.3389/fnhum.2014.00500>
- Wang, S., Zhang, D., Fang, B., Liu, X., Yan, G., Sui, G., Huang, Q., Sun, L., & Wang, S. (2021). A Study on Resting EEG Effective Connectivity Difference before and after Neurofeedback for Children with ADHD. *Neuroscience*, 457, 103–113. <https://doi.org/10.1016/j.neuroscience.2020.12.038>
- Wang, T., Mantini, D., & Gillebert, C. R. (2018). The potential of real-time fMRI neurofeedback for stroke rehabilitation: A systematic review. *Cortex*, 107, 148–165. <https://doi.org/10.1016/j.cortex.2017.09.006>
- Wang, Z., Wong, C. M., Nan, W., Tang, Q., Rosa, A. C., Xu, P., & Wan, F. (2021). Learning curve of a short time neurofeedback training: Reflection of brain network dynamics based on phase locking value. *IEEE Transactions on Cognitive and Developmental Systems*, 1–1. <https://doi.org/10.1109/tcds.2021.3125948>
- Weber, E., Köberl, A., Frank, S., & Doppelmayr, M. (2011). Predicting Successful Learning of SMR Neurofeedback in Healthy Participants: Methodological Considerations. *Applied Psychophysiology and Biofeedback*, 36(1), 37–45. <https://doi.org/10.1007/s10484-010-9142-x>
- Wim De Clercq, Vergult, A., Vanrumste, B., van Paesschen, W., & van Huffel, S. (2006). Canonical Correlation Analysis Applied to Remove Muscle Artifacts From the Electroencephalogram. *IEEE Transactions on Biomedical Engineering*, 53(12), 2583–2587. <https://doi.org/10.1109/TBME.2006.879459>
- Yael, D., Vecht, J. J., & Bar-Gad, I. (2018). Filter-Based Phase Shifts Distort Neuronal Timing Information. *Eneuro*, 5(2), ENEURO.0261-17.2018. <https://doi.org/10.1523/ENEURO.0261-17.2018>
- Yamashita, A., Hayasaka, S., Kawato, M., & Imamizu, H. (2017). Connectivity Neurofeedback Training Can Differentially Change Functional Connectivity and Cognitive Performance. *Cerebral Cortex*, 27(10), 4960–4970. <https://doi.org/10.1093/cercor/bhx177>
- Yeh, C., Jones, D. K., Liang, X., Descoteaux, M., & Connelly, A. (2021). Mapping Structural Connectivity Using Diffusion $\langle \text{scp} \rangle \text{MRI} \langle / \text{scp} \rangle$: Challenges and Opportunities. *Journal of Magnetic Resonance Imaging*, 53(6), 1666–1682. <https://doi.org/10.1002/jmri.27188>
- Yeh, W.-H., Hsueh, J.-J., & Shaw, F.-Z. (2021). Neurofeedback of Alpha Activity on Memory in Healthy Participants: A Systematic Review and Meta-Analysis. *Frontiers in Human Neuroscience*, 14. <https://doi.org/10.3389/fnhum.2020.562360>
- Zhang, H., & Jacobs, J. (2015). Traveling Theta Waves in the Human Hippocampus. *Journal of Neuroscience*, 35(36), 12477–12487. <https://doi.org/10.1523/JNEUROSCI.5102-14.2015>
- Zhang, H., Zhao, Y., Cao, W., Cui, D., Jiao, Q., Lu, W., Li, H., & Qiu, J. (2020). Aberrant functional connectivity in resting state networks of ADHD patients revealed by independent component analysis. *BMC Neuroscience*, 21(1), 39. <https://doi.org/10.1186/s12868-020-00589-x>

Zoefel, B., Huster, R. J., & Herrmann, C. S. (2011). Neurofeedback training of the upper alpha frequency band in EEG improves cognitive performance. *NeuroImage*, 54(2), 1427–1431.
<https://doi.org/10.1016/j.neuroimage.2010.08.078>

7 Appendix

7.1 Preliminary Study: Choice of FC metric and time

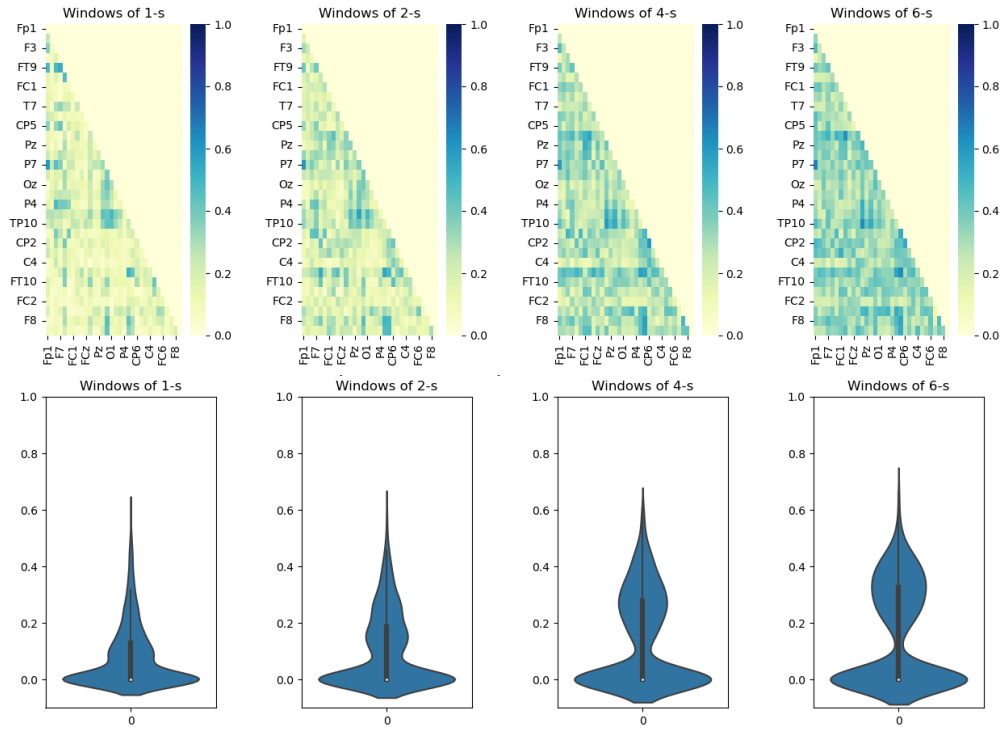


Figure 7.1 - Per-Epoch wPLI computation

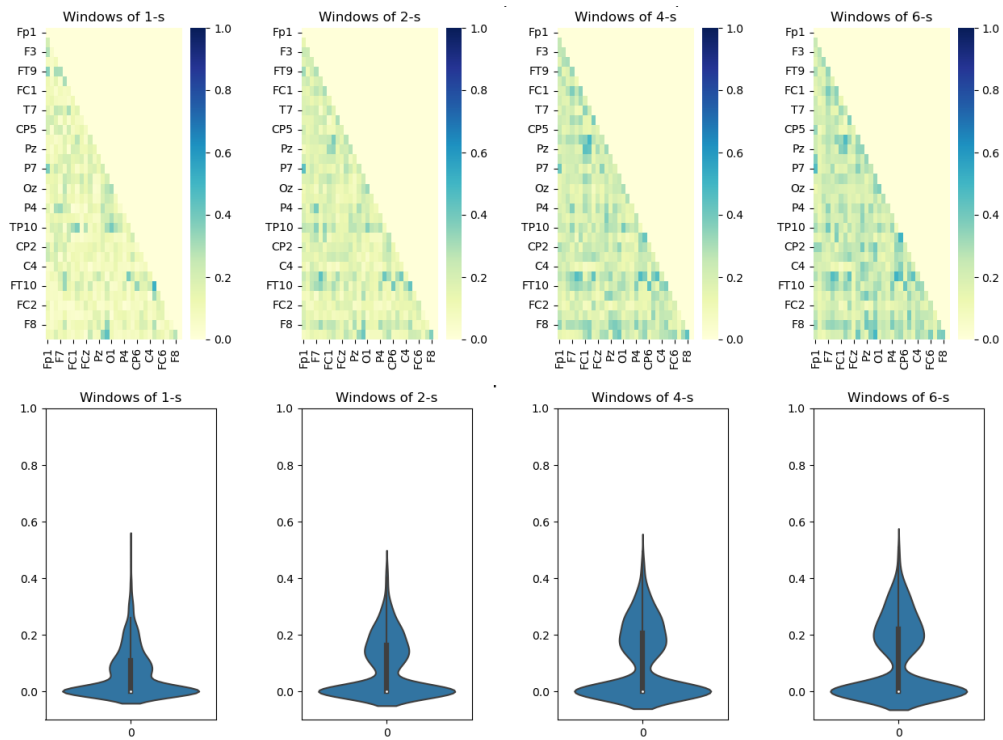


Figure 7.2 - Per-Block wPLI computation

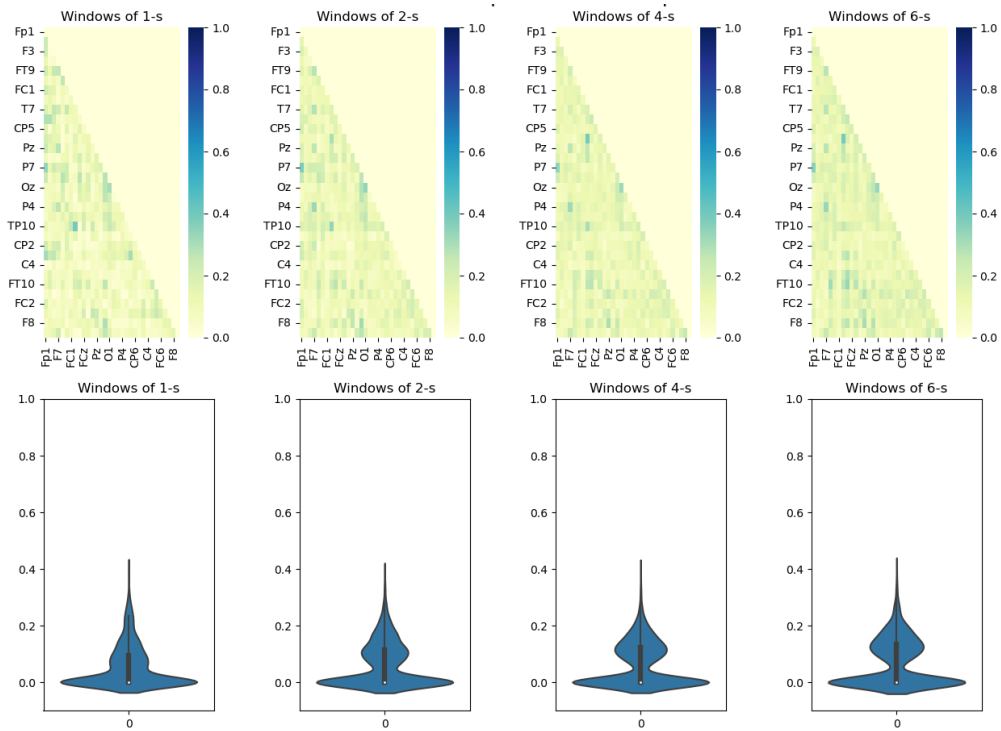


Figure 7.3 - Per-Set wPLI computation

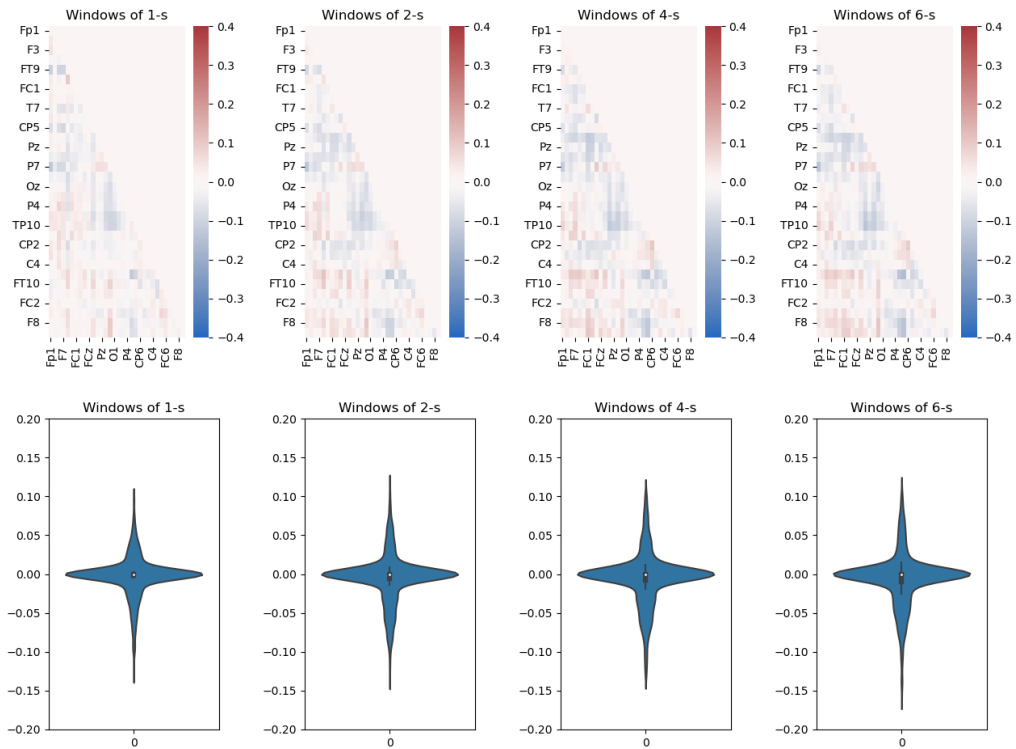


Figure 7.4 - Per-Epoch ImC computation

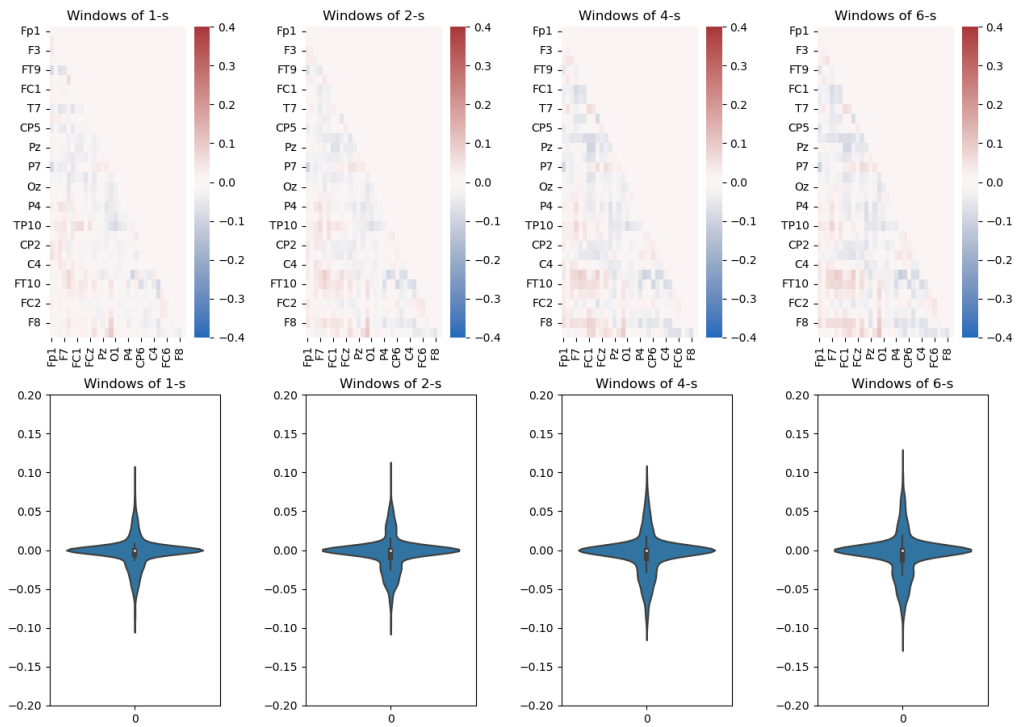


Figure 7.5 - Per-Block ImC computation

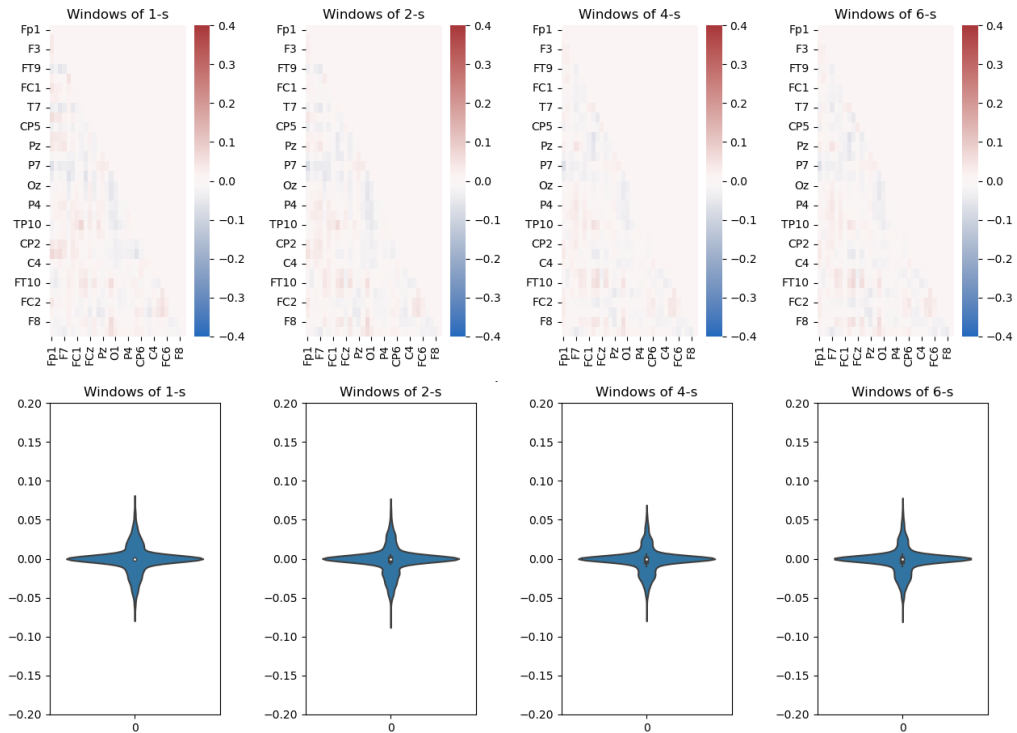


Figure 7.6 - Per-Set ImC computation

7.2 Spectral Analysis

7.2.1 Learners vs Non-Learners

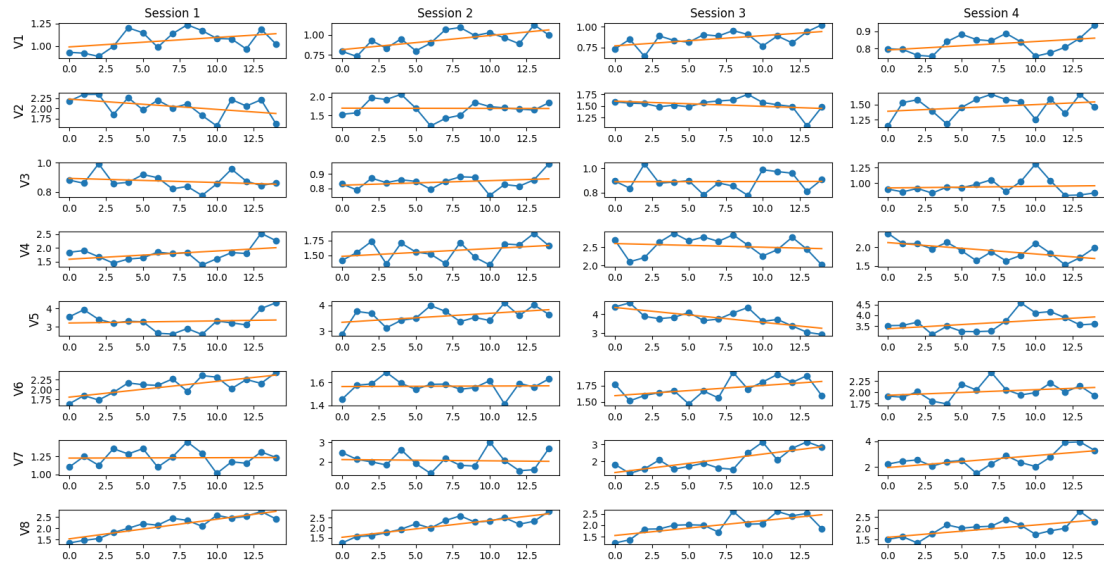


Figure 7.7 - Per-Block RAUA at Cz channel for Visual NF-training group

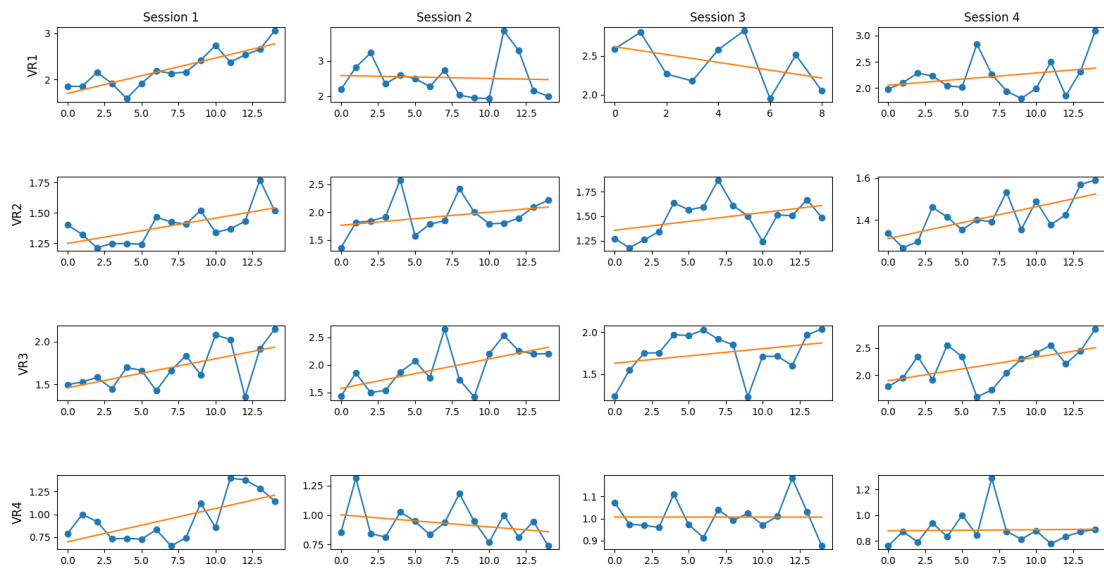


Figure 7.8 - Per-Block RAUA at Cz channel for VR NF-training group

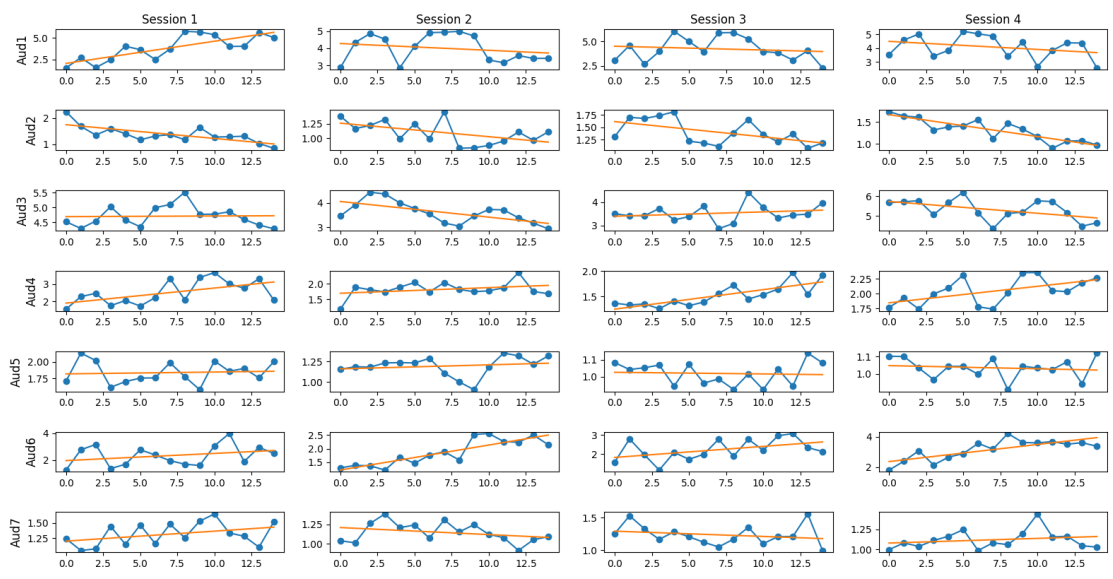


Figure 7.9 – Per-Block RAUA at Cz channel for Auditory NF-Training group

7.2.2 Per-Set Cz Channel RAUA Evolution

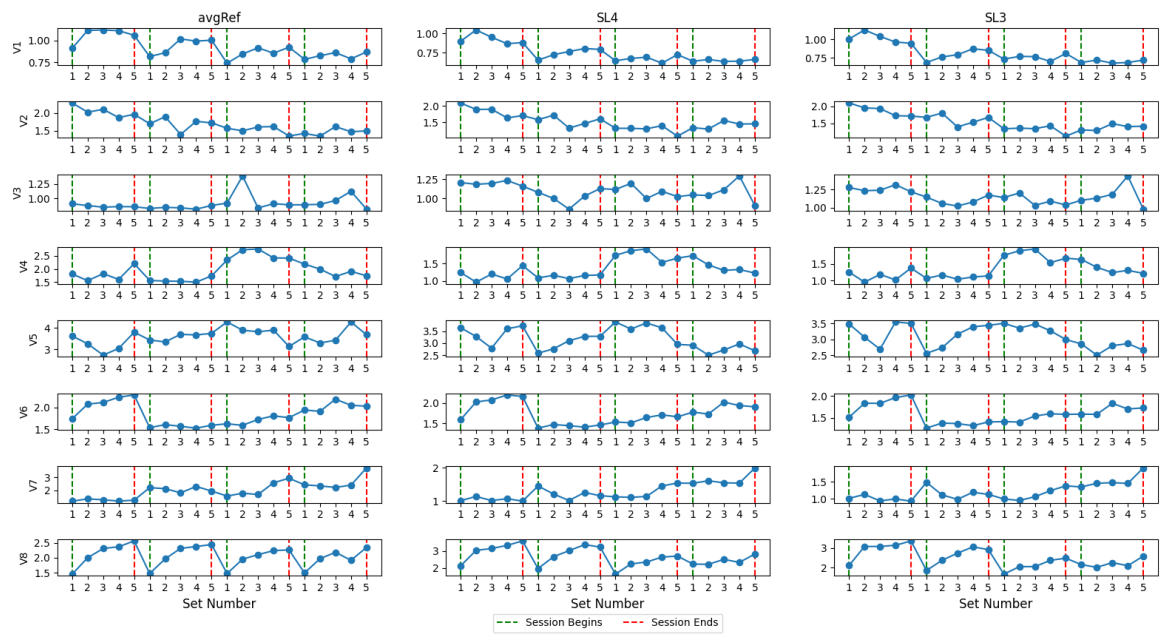


Figure 7.10 - Per-Set RAUA at Cz channel for the Visual NF-training group

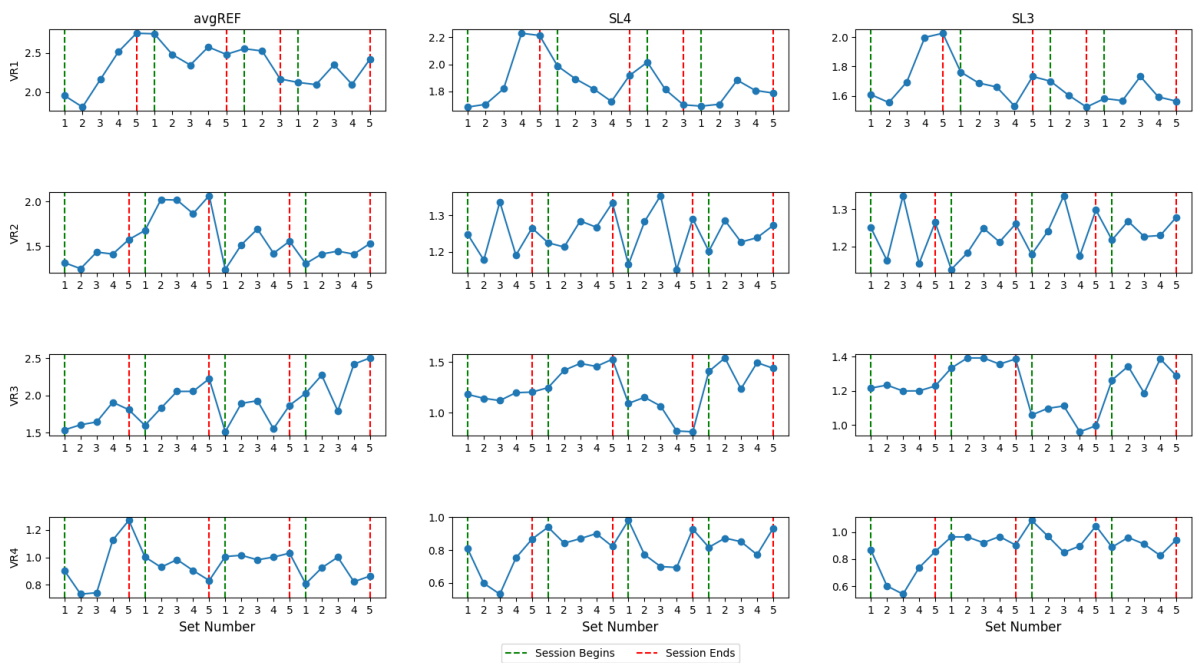


Figure 7.11 - Per-Set RAUA at Cz channel for the VR NF-training group

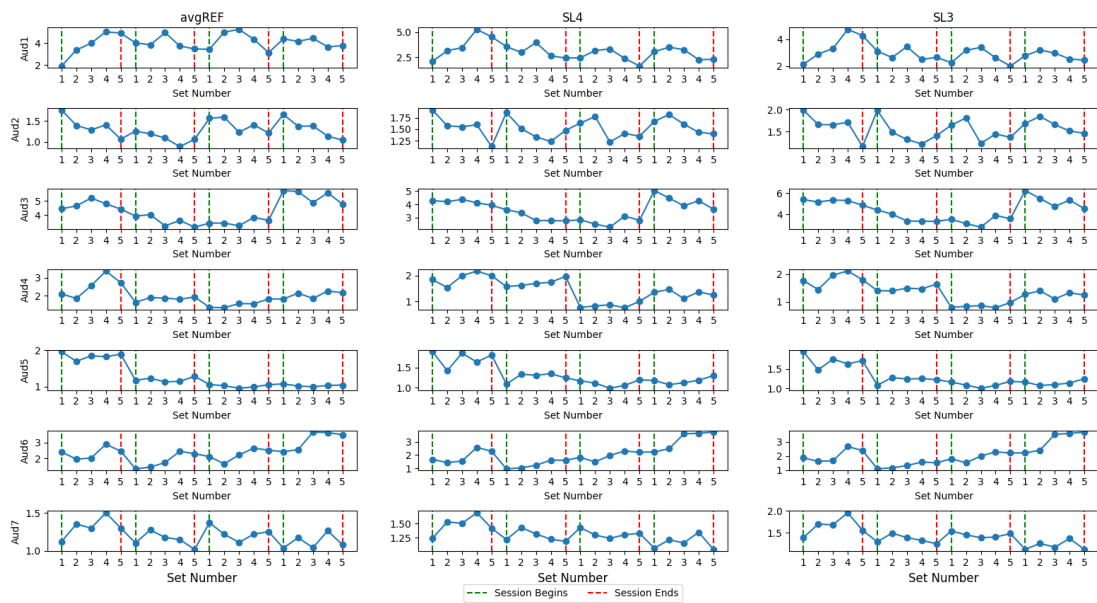


Figure 7.12 - Per-Set RAUA at Cz channel for the Auditory NF-training group

7.2.3 Topological Changes

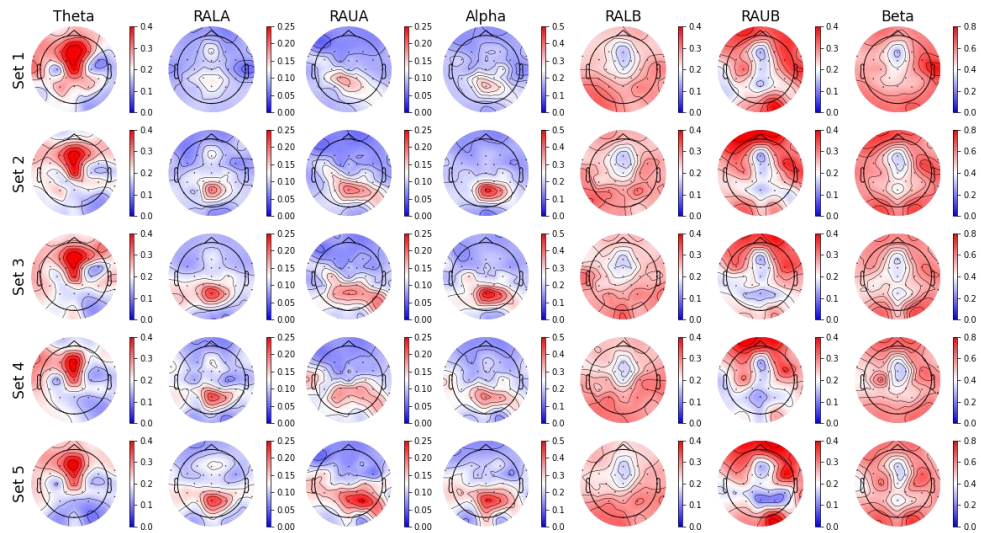


Figure 7.13 - Median values across the Sets for the Session 1. Learners of the Visual NF-training group with SL4

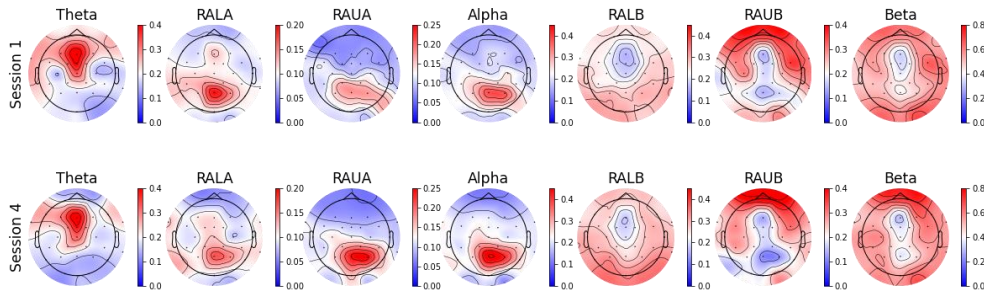


Figure 7.14 - Median Values of the Session 1 vs Session 4. Learners of the Visual NF-training group with SL4

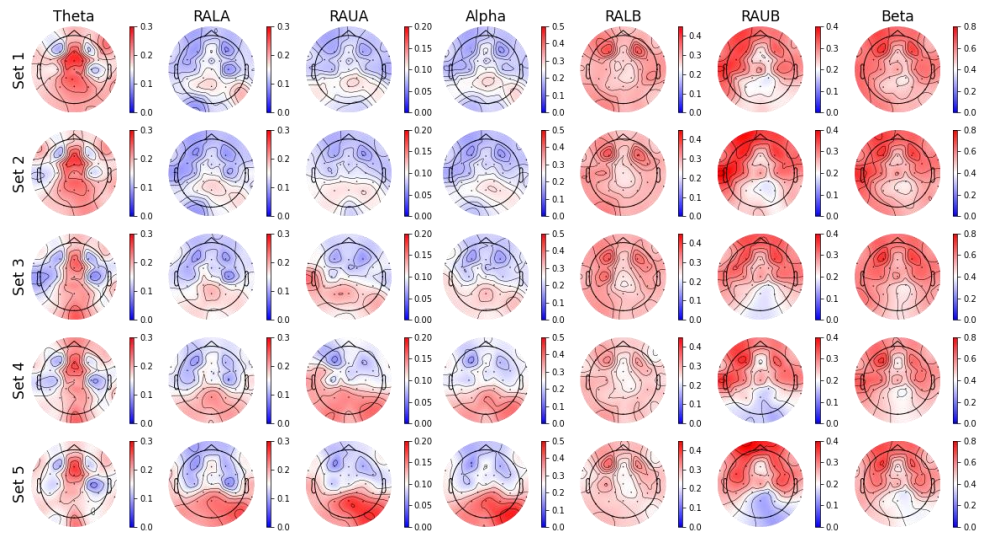


Figure 7.15 - Median values across the Sets for the Session 1. Learners of the VR NF-training group and SL4

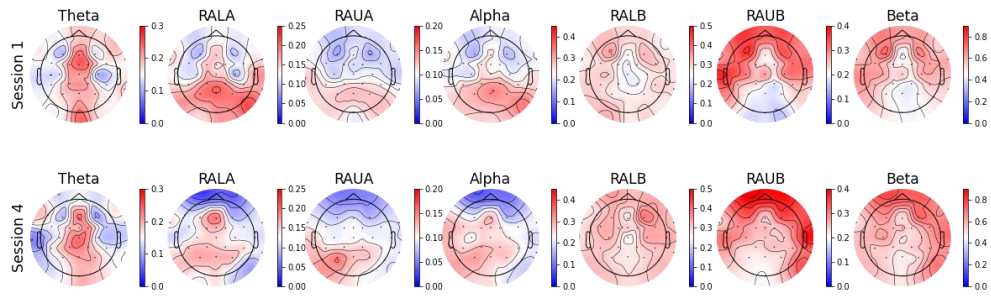


Figure 7.16 - Median Values of the Session 1 vs Session 4. Learners of the VR NF-training group and SL4

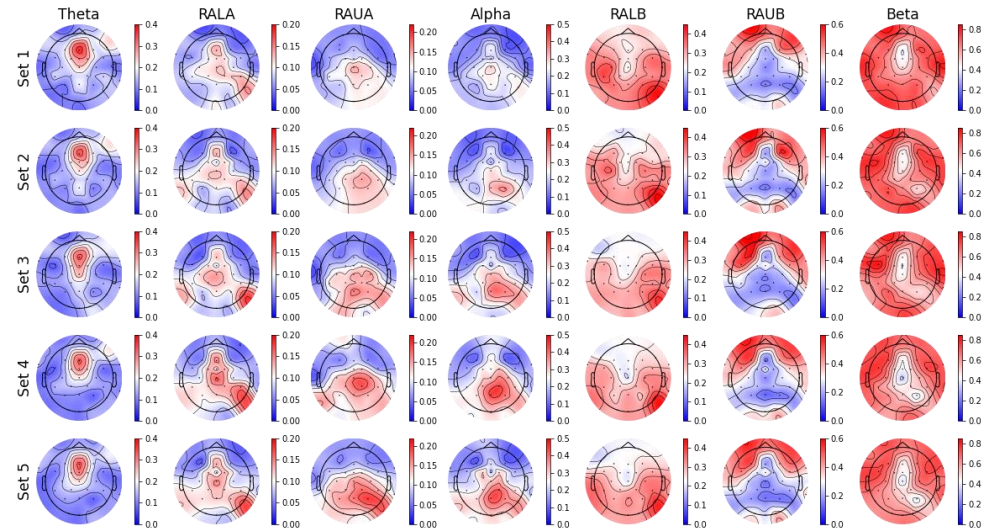


Figure 7.17 - Median values across the Sets for the Session 1. Learners of the Auditory NF-training group and SL4

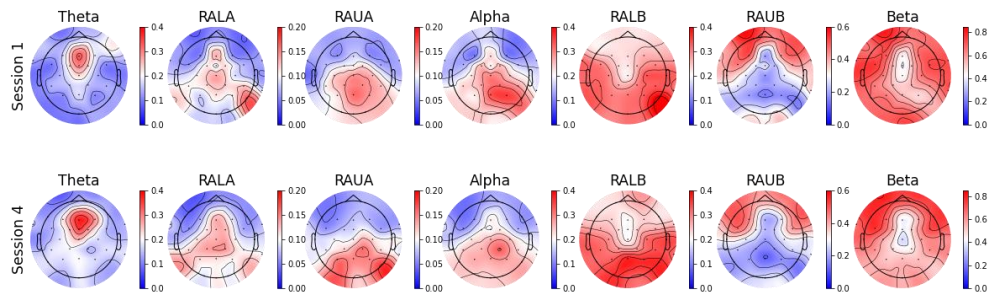


Figure 7.18 - Median Values of the Session 1 vs Session 4. Learners of the Auditory NF-training group and SL4

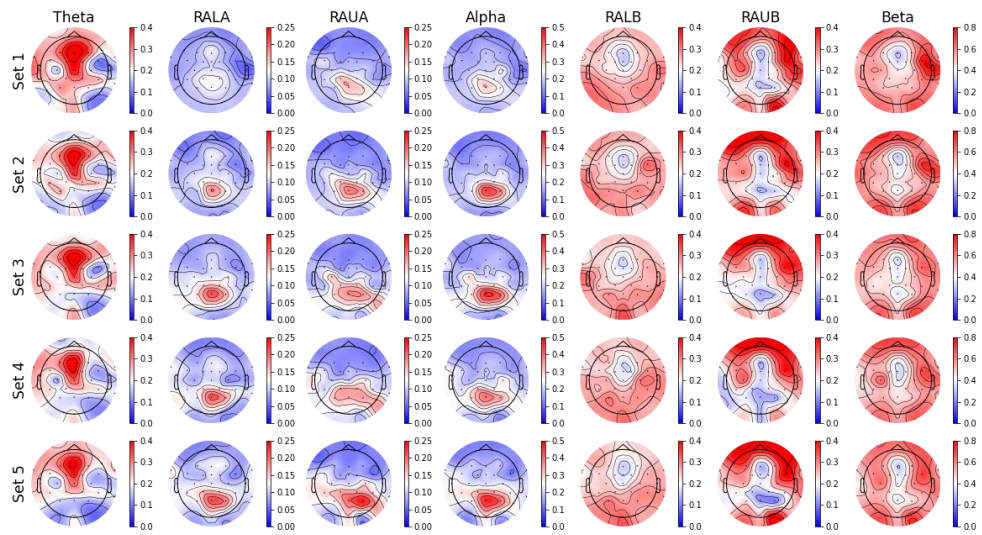


Figure 7.19 - Median values across the Sets for the Session 1. Learners of Visual NF-training group and SL3

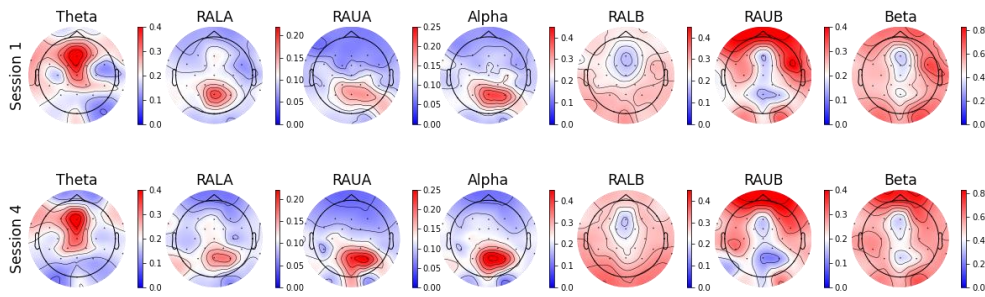


Figure 7.20 - Median Values of the Session 1 vs Session 4. Learners of Visual NF-training group and SL3

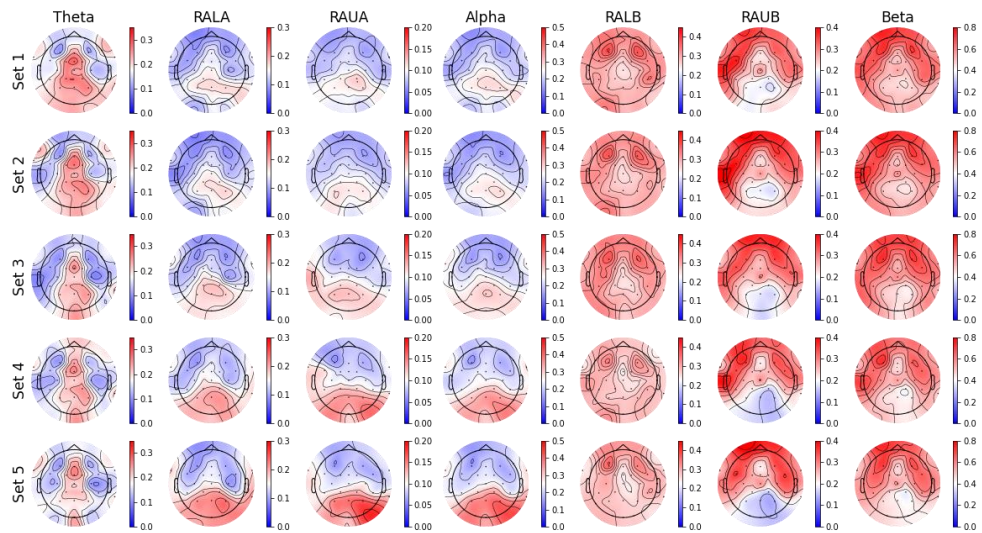


Figure 7.21 - Median values across the Sets for the Session 1. Learners of the VR NF-training group and SL3

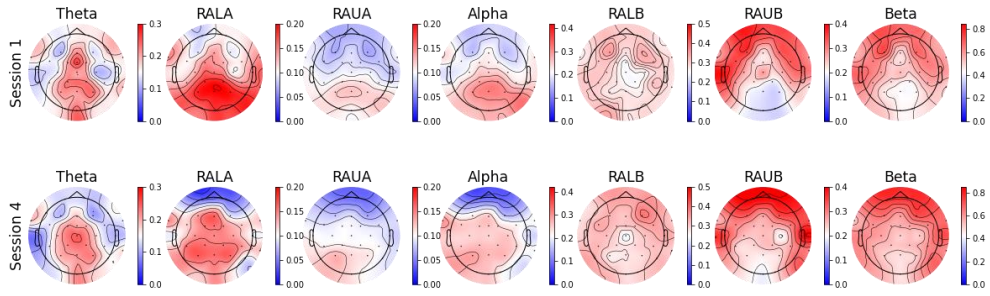


Figure 7.22 - Median Values of the Session 1 vs Session 4. Learners of the VR NF-training group and SL3

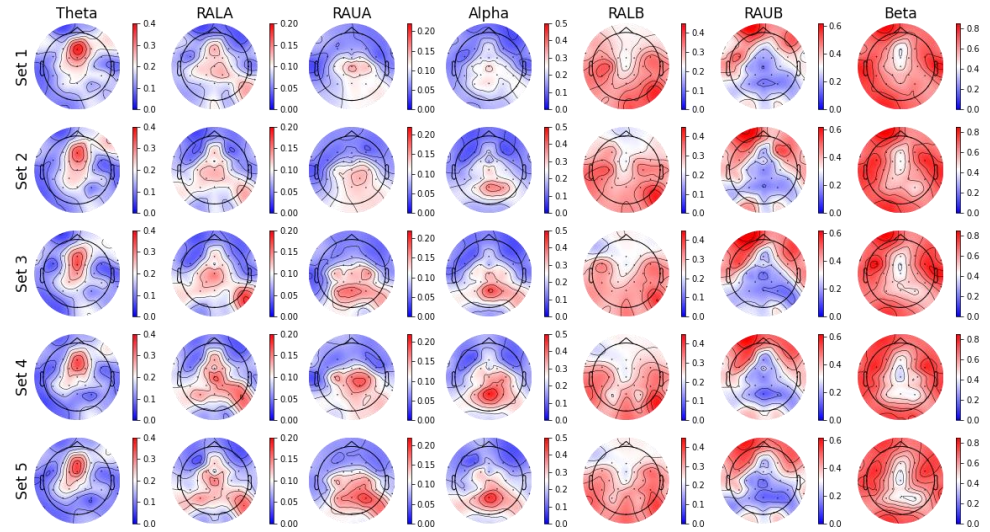


Figure 7.23 - Median values across the Sets for the Session 1. Learners of the Auditory NF-training group and SL3

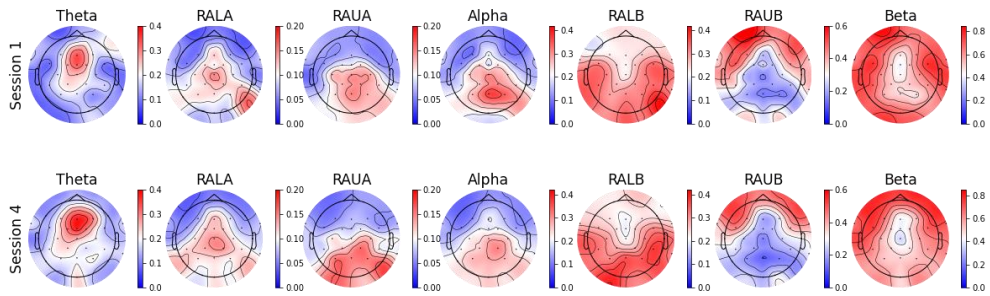


Figure 7.24 - Median Values of the Session 1 vs Session 4. Learners of the Auditory NF-training group and SL3

7.3 Functional Connectivity Analysis

7.3.1 Functional Connectivity Evolution

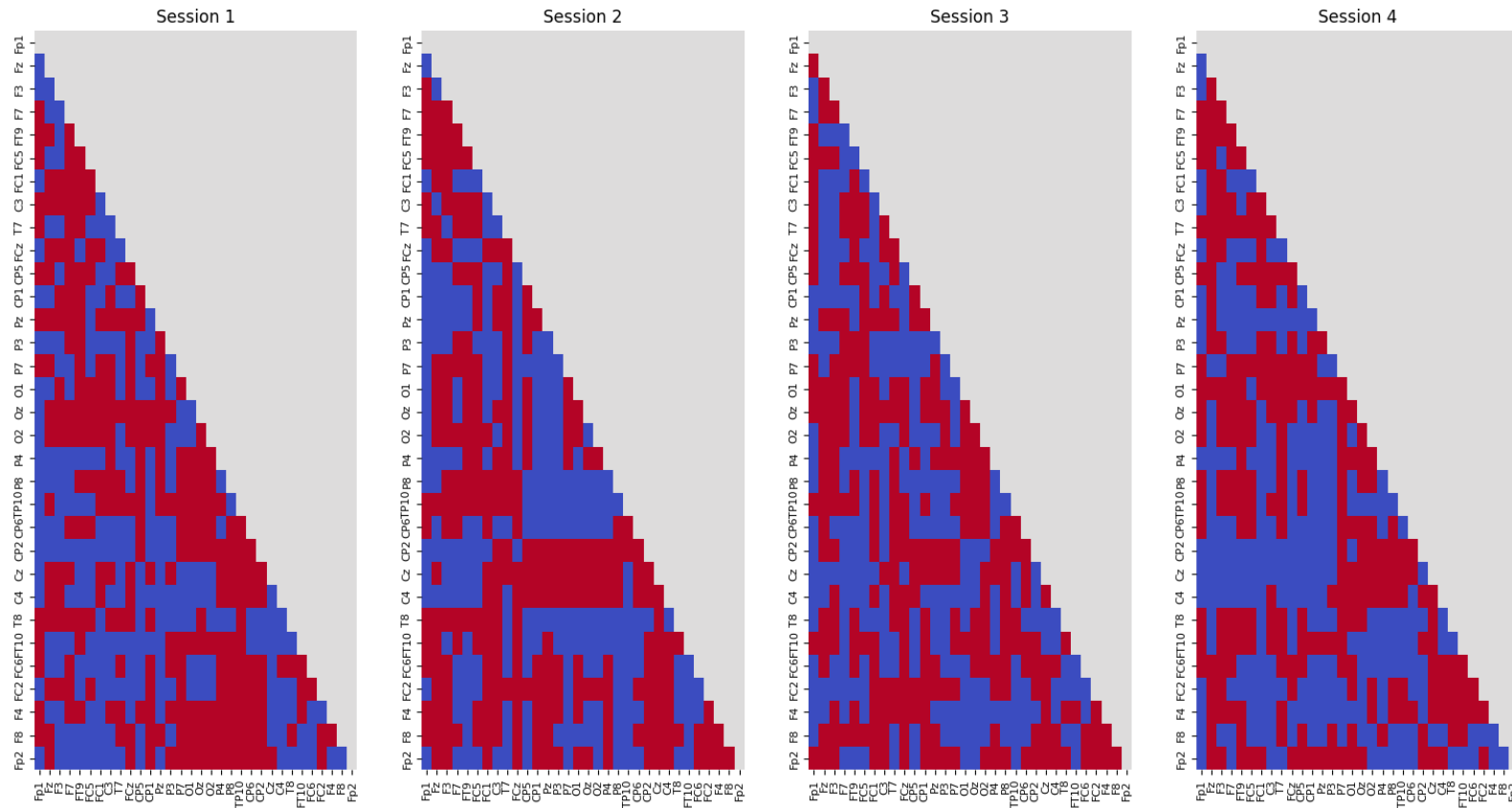


Figure 7.25 - Changes in Functional Connectivity within session. Results are shown for the VR NF-training group with avgREF, when comparing changes in ImC between Set 1 and Set 5, in each NF-training session. Red: increases; Blue: decreases; *: $p < 0.05$ (corrected for multiple comparisons)

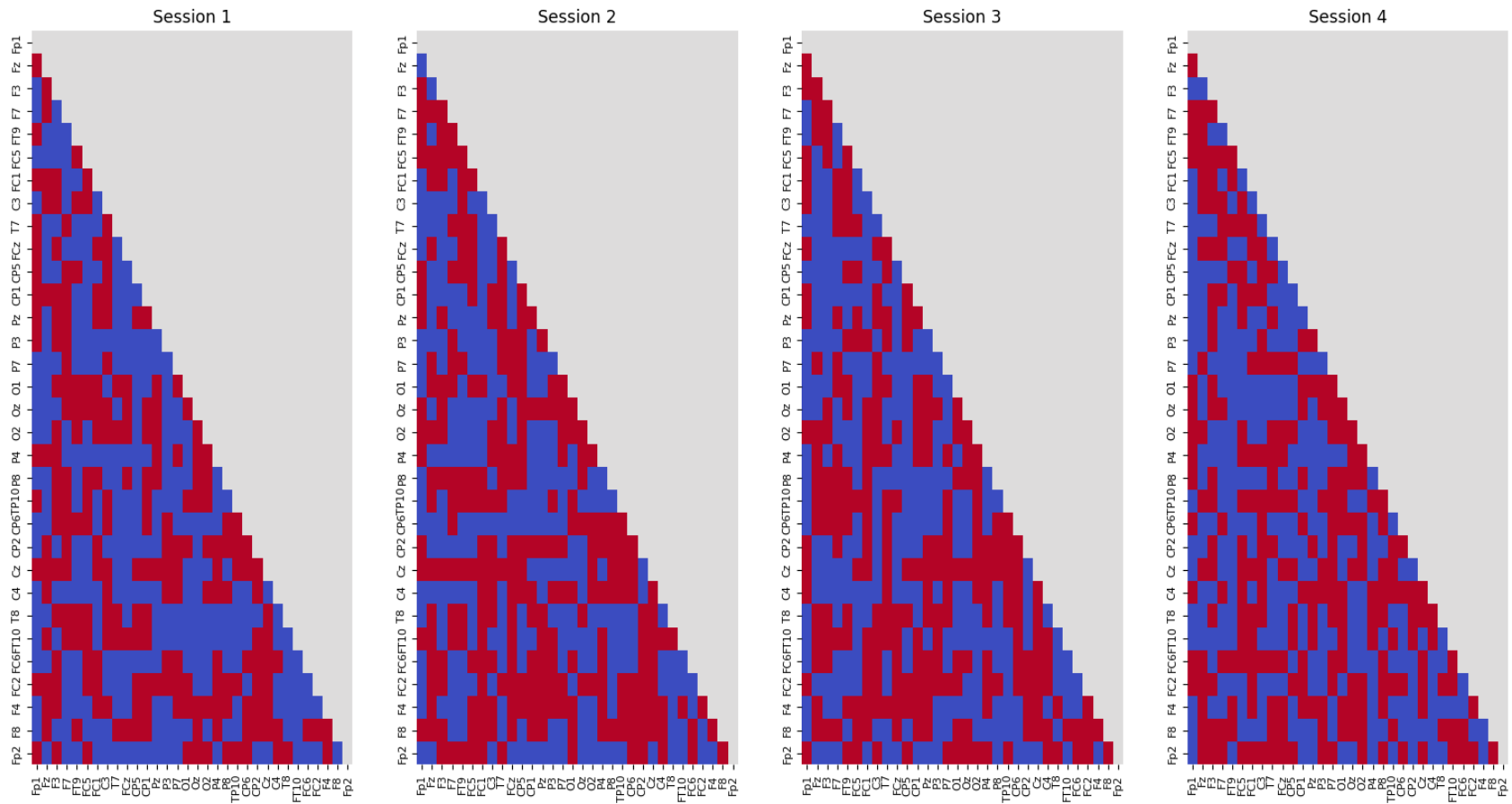


Figure 7.26 - Changes in Functional Connectivity within session. Results are shown for the VR NF-training group with SLA, when comparing changes in ImC between Set 1 and Set 5, in each NF-training session. Red: increases; Blue: decreases; *: $p < 0.05$ (corrected for multiple comparisons)

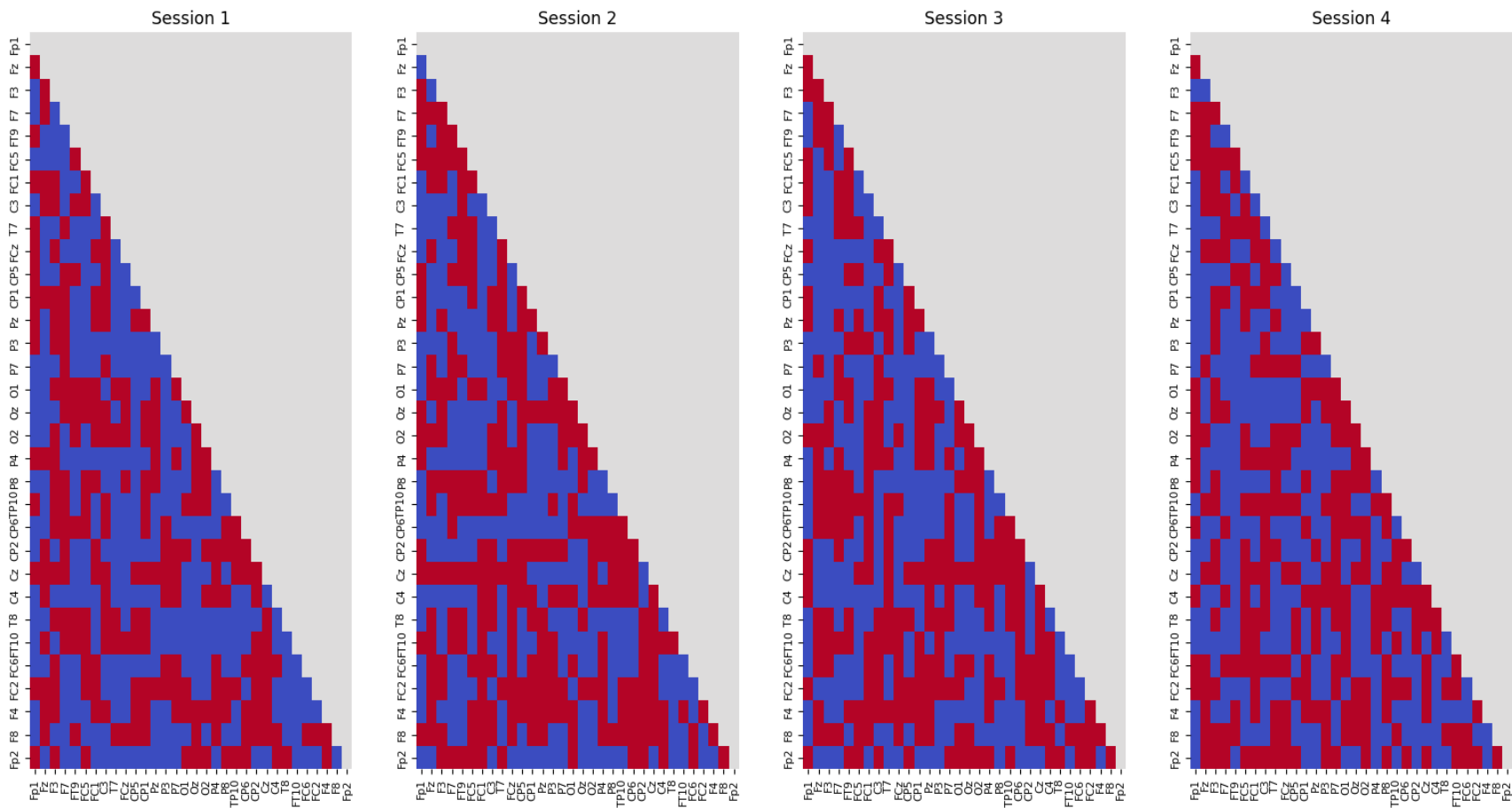


Figure 7.27 - Changes in Functional Connectivity within session. Results are shown for the VR NF-training group with SL3, when comparing changes in ImC between Set 1 and Set 5, in each NF-training session. Red: increases; Blue: decreases; *: $p < 0.05$ (corrected for multiple comparisons)

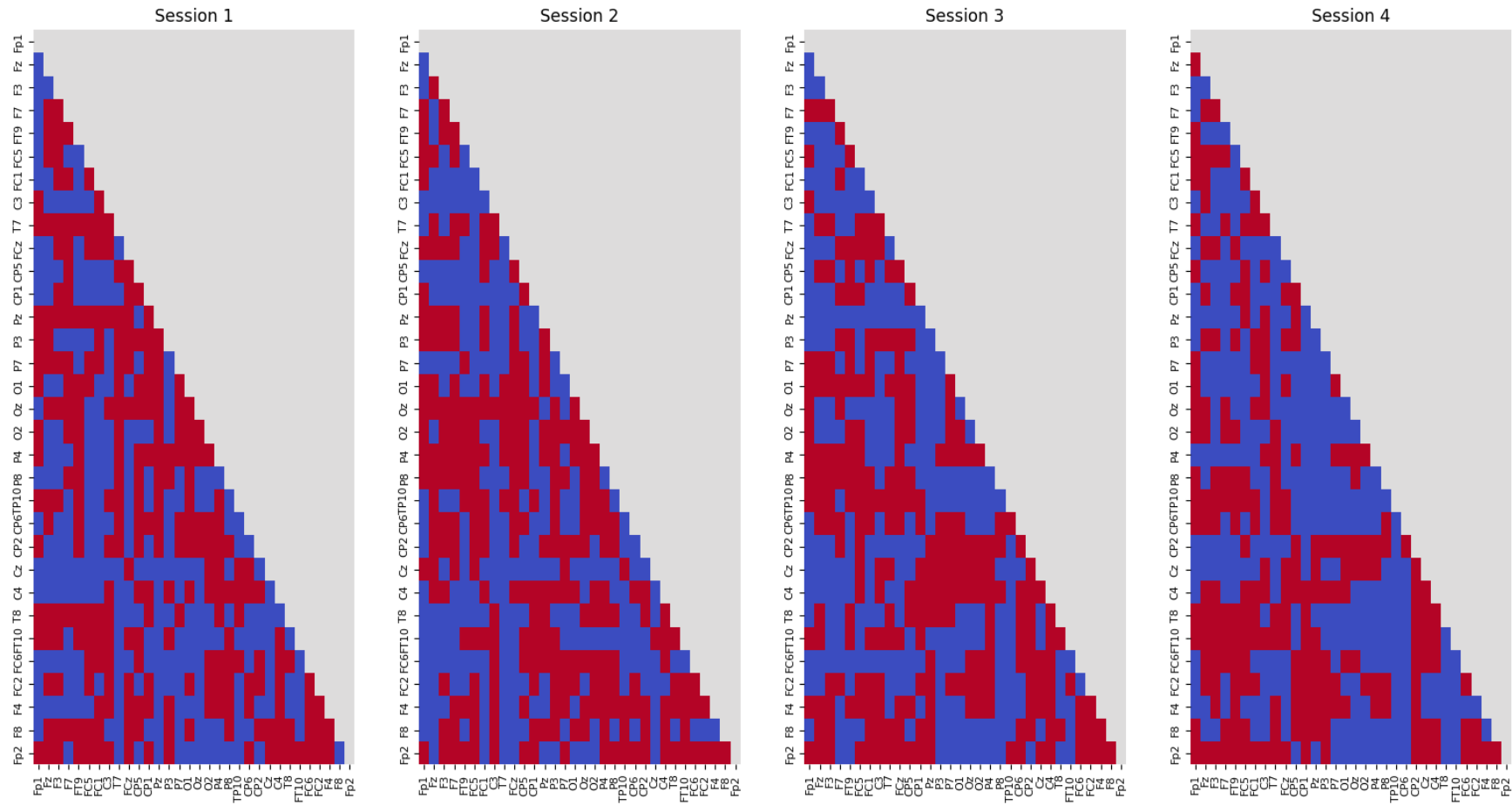


Figure 7.28 - Changes in Functional Connectivity within session. Results are shown for the Auditory NF-training group with avgREF, when comparing changes in ImC between Set 1 and Set 5, in each NF-training session. Red: increases; Blue: decreases; *: $p < 0.05$ (corrected for multiple comparisons)

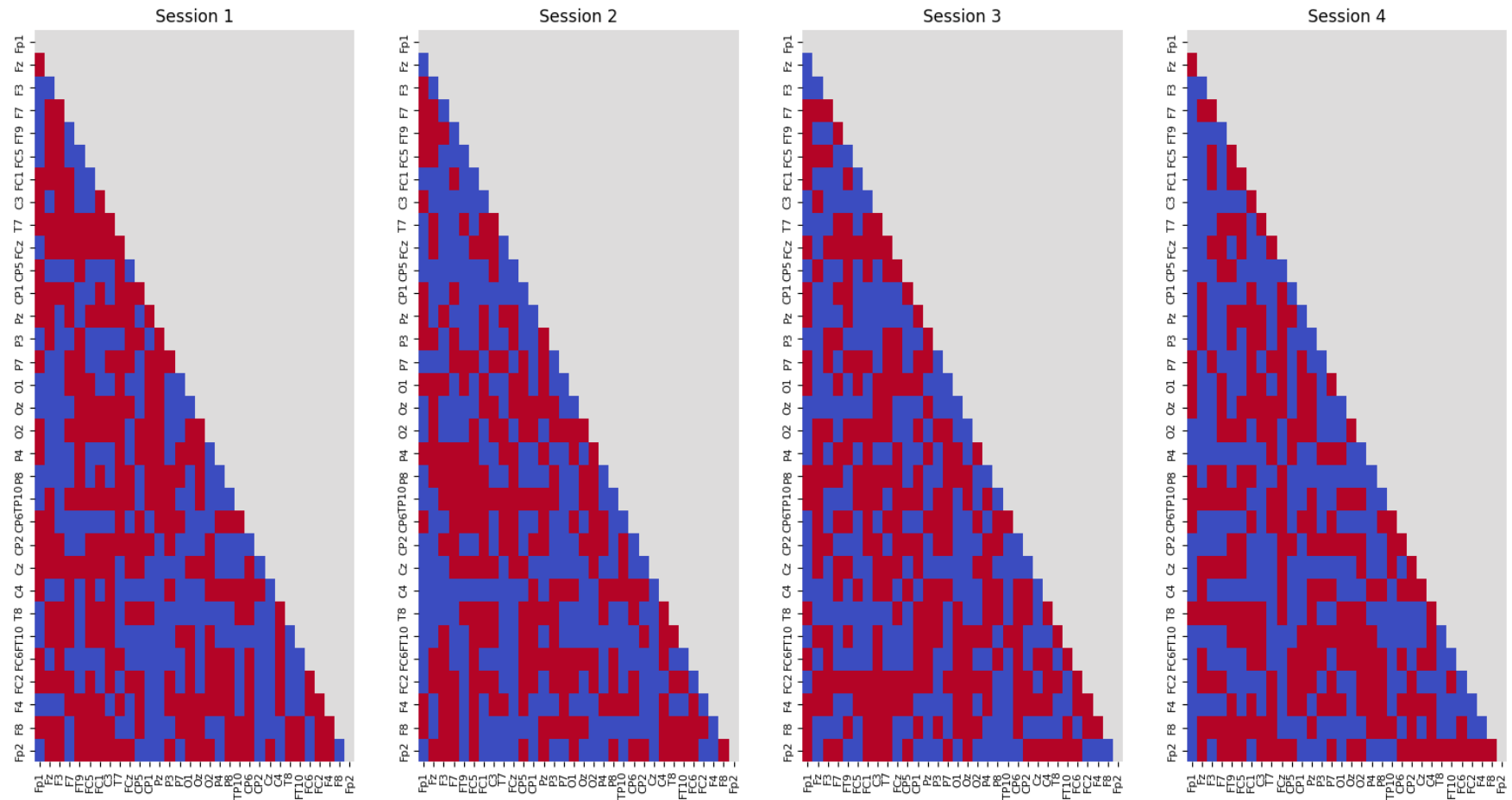


Figure 7.29 - Changes in Functional Connectivity within session. Results are shown for the Auditory NF-training group with SL4, when comparing changes in ImC between Set 1 and Set 5, in each NF-training session. Red: increases; Blue: decreases; *: $p < 0.05$ (corrected for multiple comparisons)

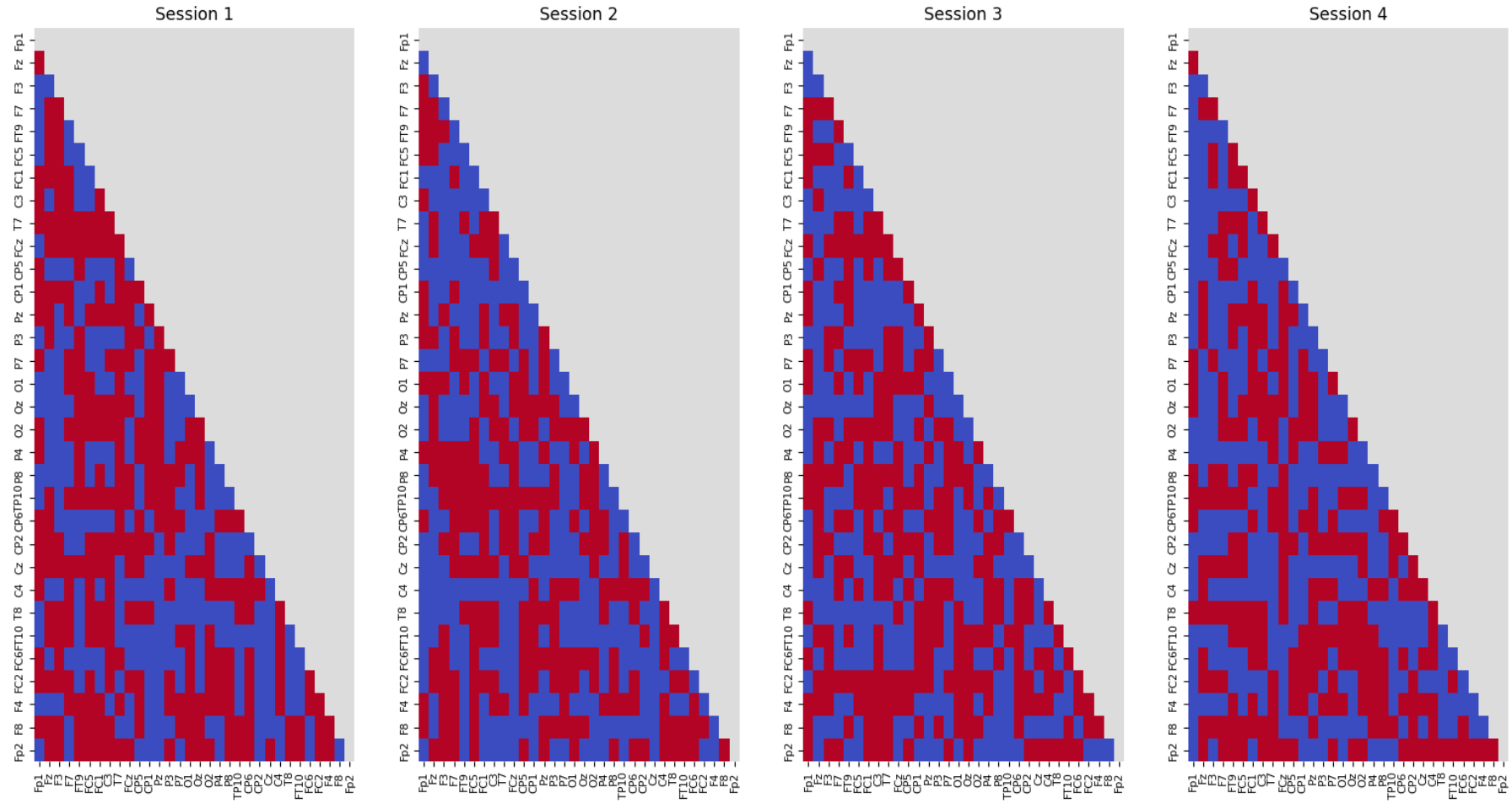


Figure 7.30 - Changes in Functional Connectivity within session. Results are shown for the Auditory NF-training group with SL3, when comparing changes in ImC between Set 1 and Set 5, in each NF-training session. Red: increases; Blue: decreases; *: $p < 0.05$ (corrected for multiple comparisons)

7.3.2 Network Analysis

7.3.2.1 Betweenness Centrality

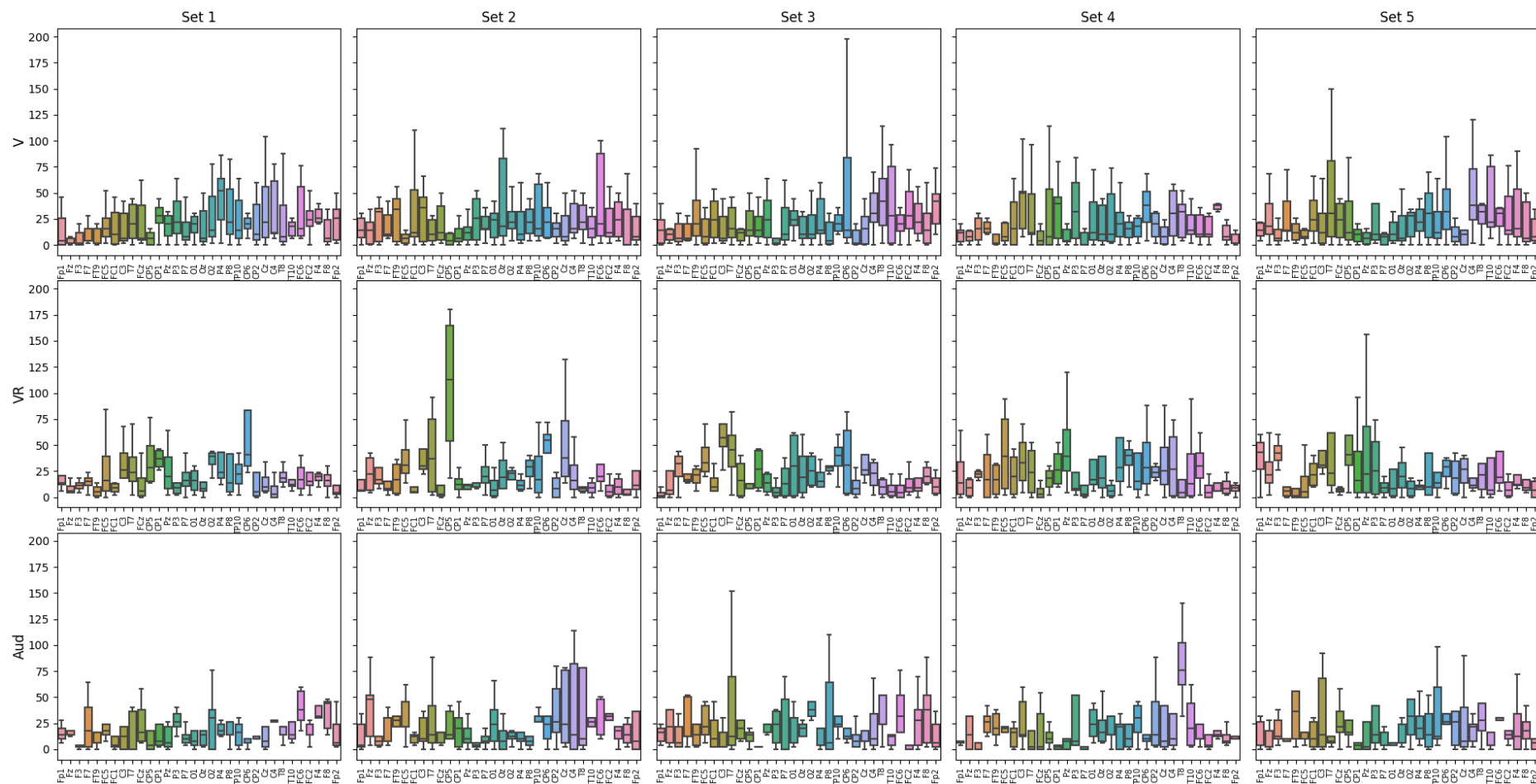


Figure 7.31- Betweenness Centrality per Set for the Session 1, with avgREF data.

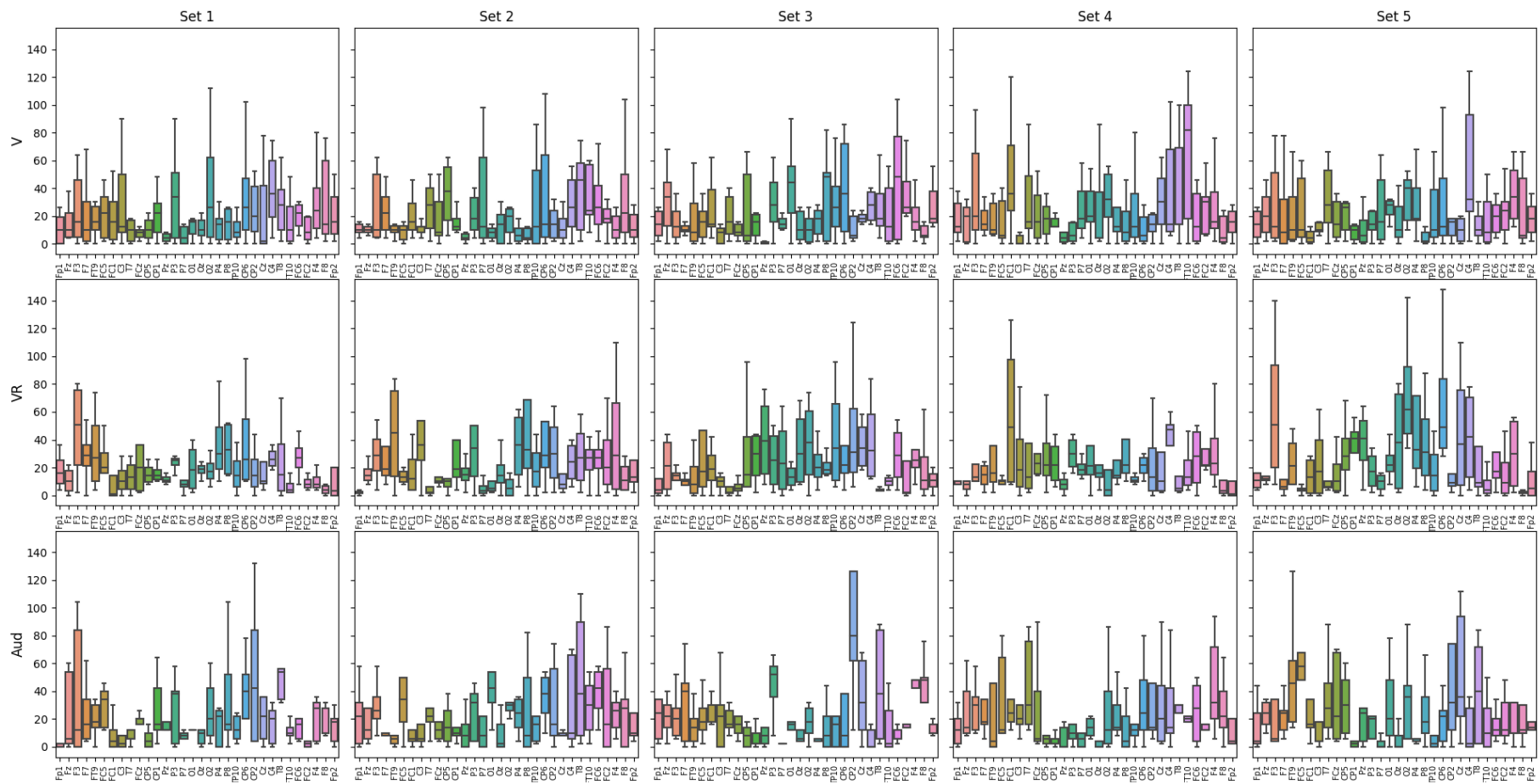


Figure 7.32 - Betweenness Centrality per Set for the Session 2 – avgREF

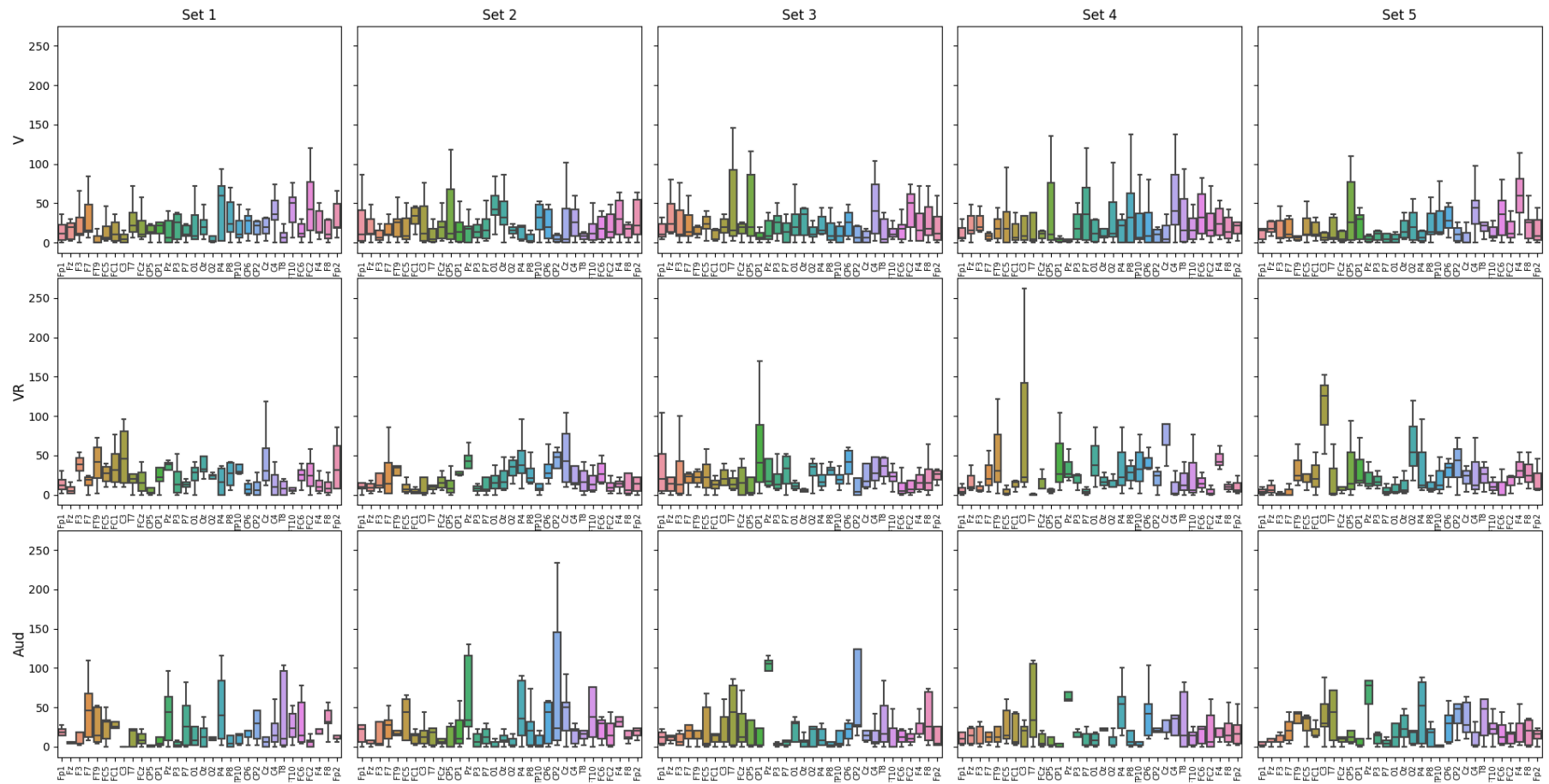


Figure 7.33 - Betweenness Centrality per Set for the Session 3 – avgREF

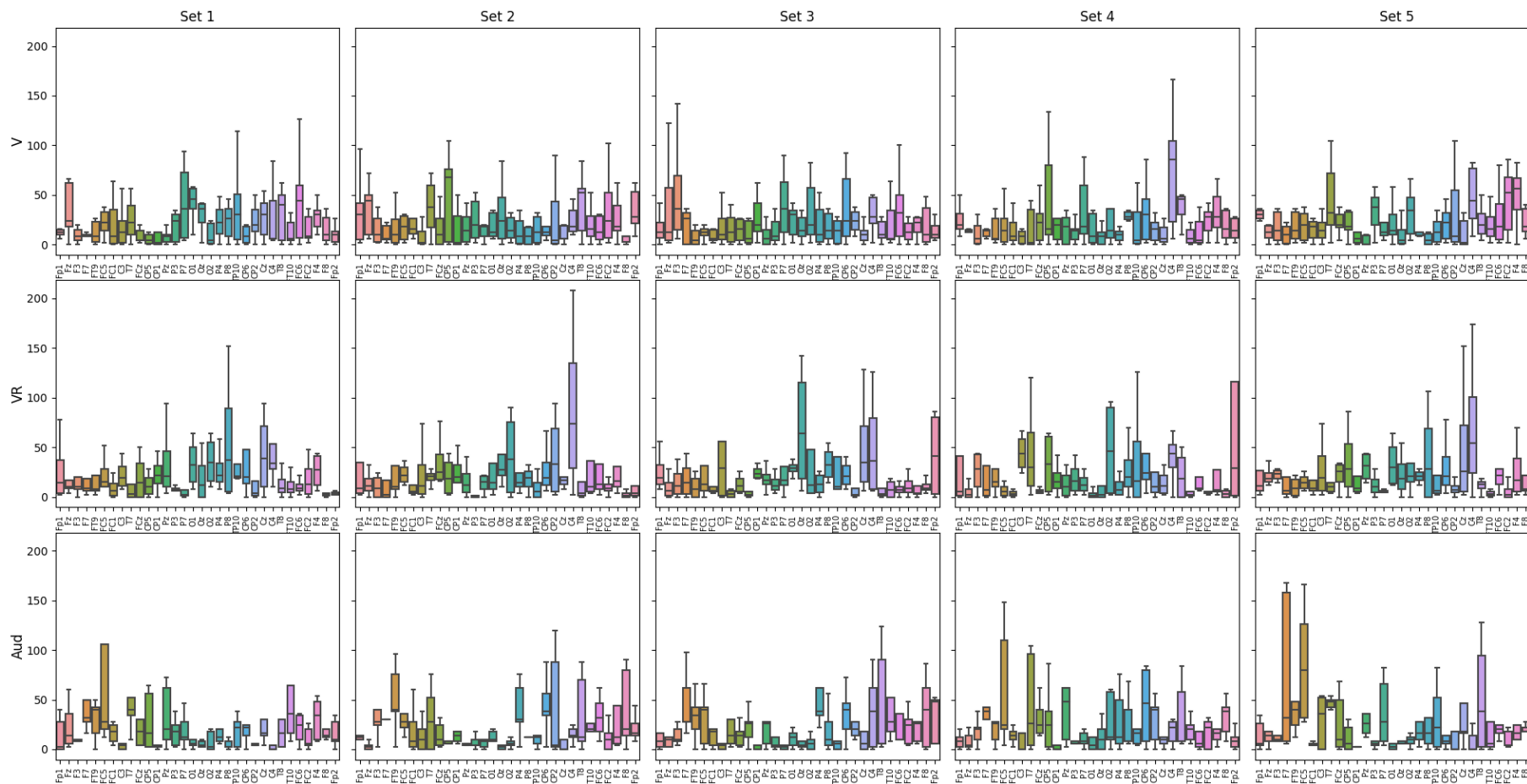


Figure 7.34 - Betweenness Centrality per Set for the Session 4 – avgREF

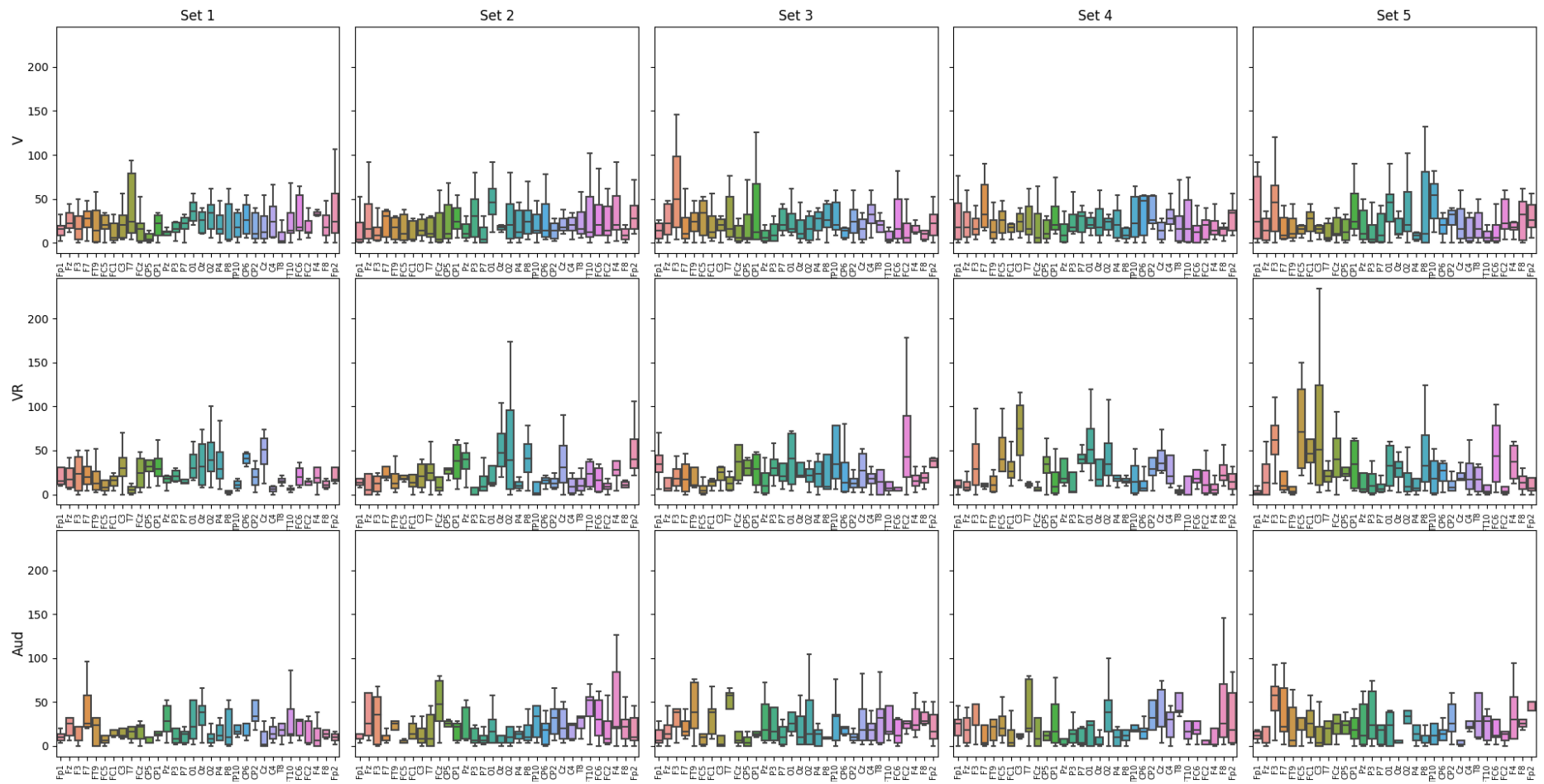


Figure 7.35 - Betweenness Centrality per Set for the Session 1 – SL4 data

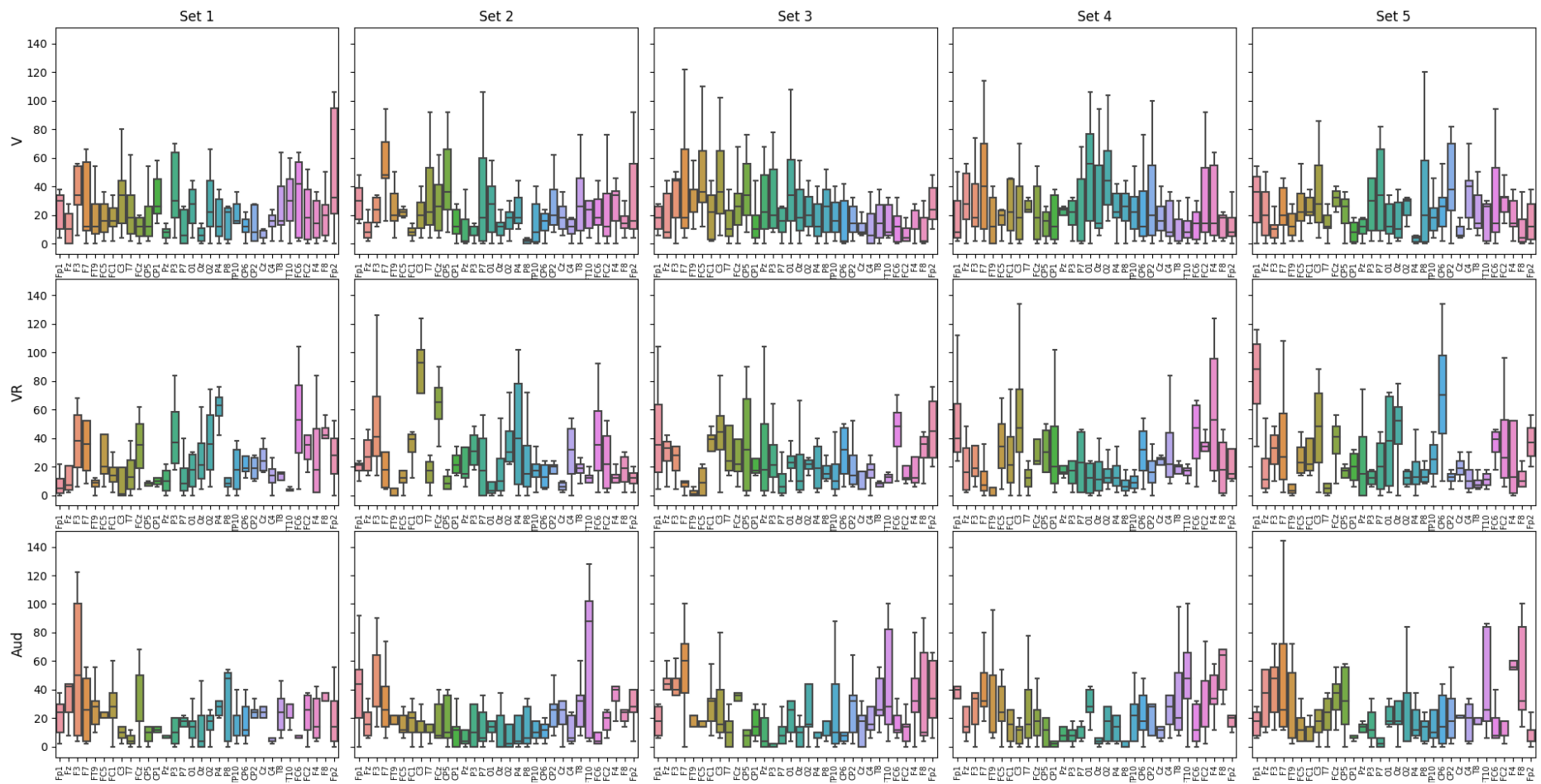


Figure 7.36 - Betweenness Centrality per Set for the Session 2 – SL4 data

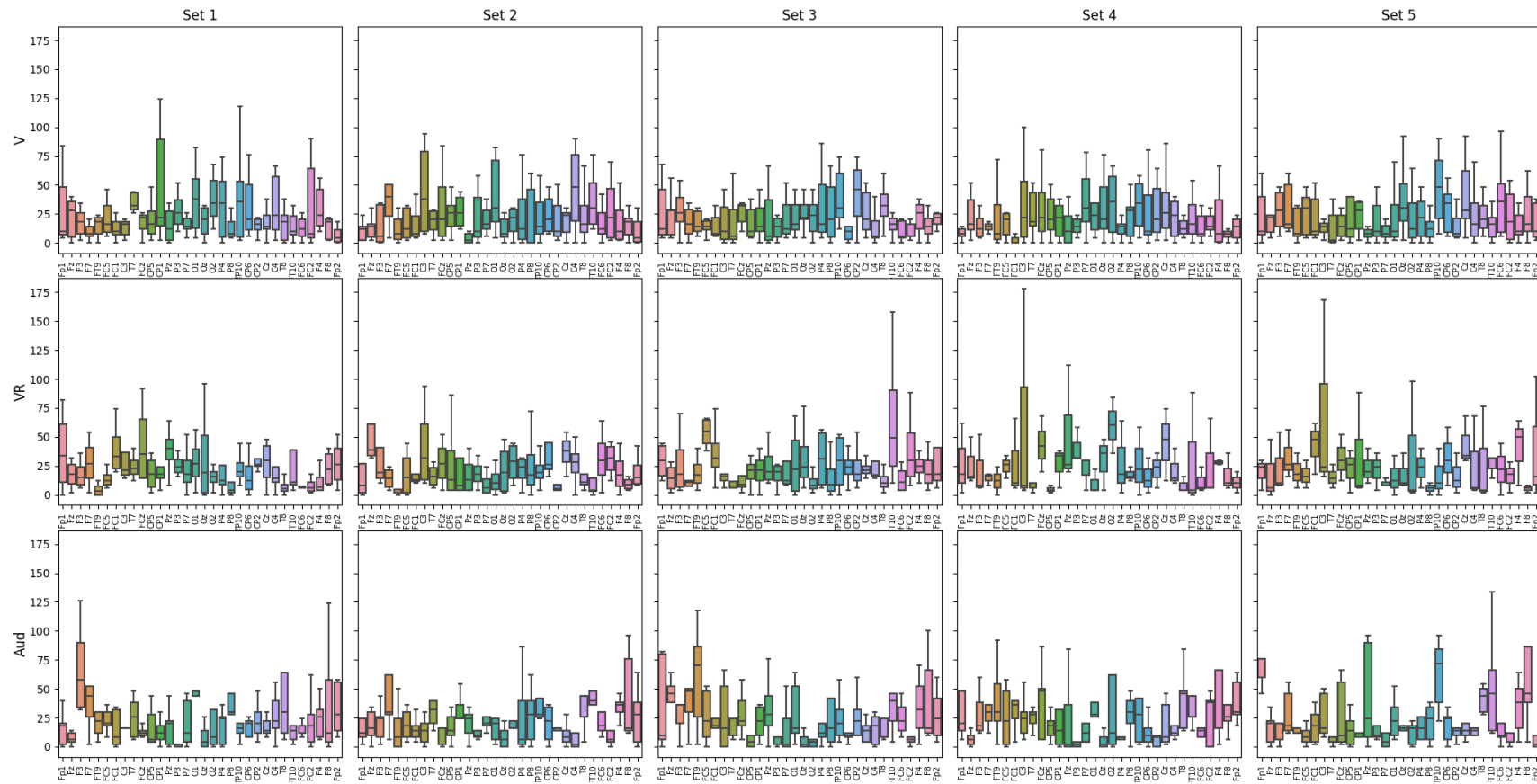


Figure 7.37 - Betweenness Centrality per Set for the Session 3 – SL4 data

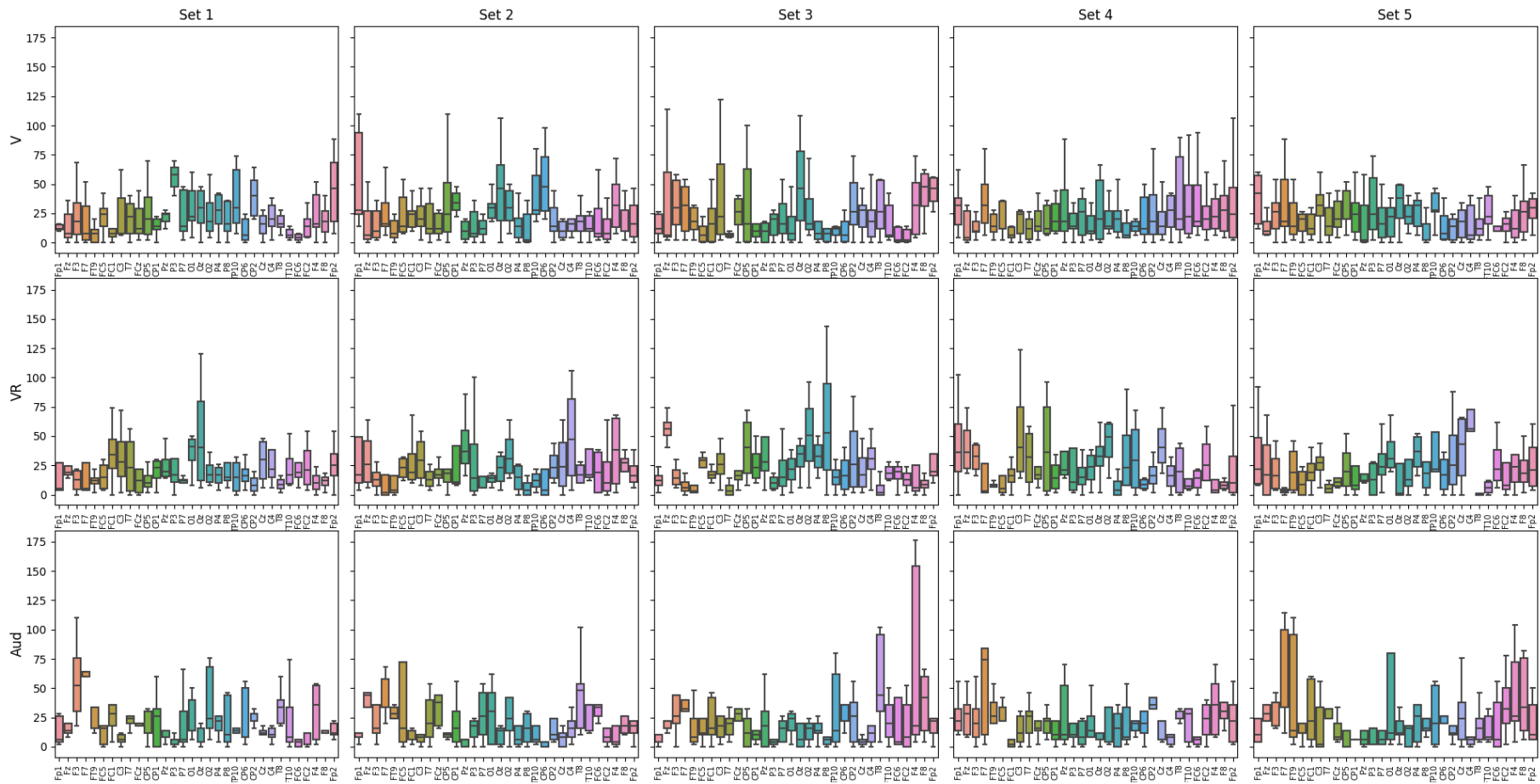


Figure 7.38 - Betweenness Centrality per Set for the Session 4 – SL4 data

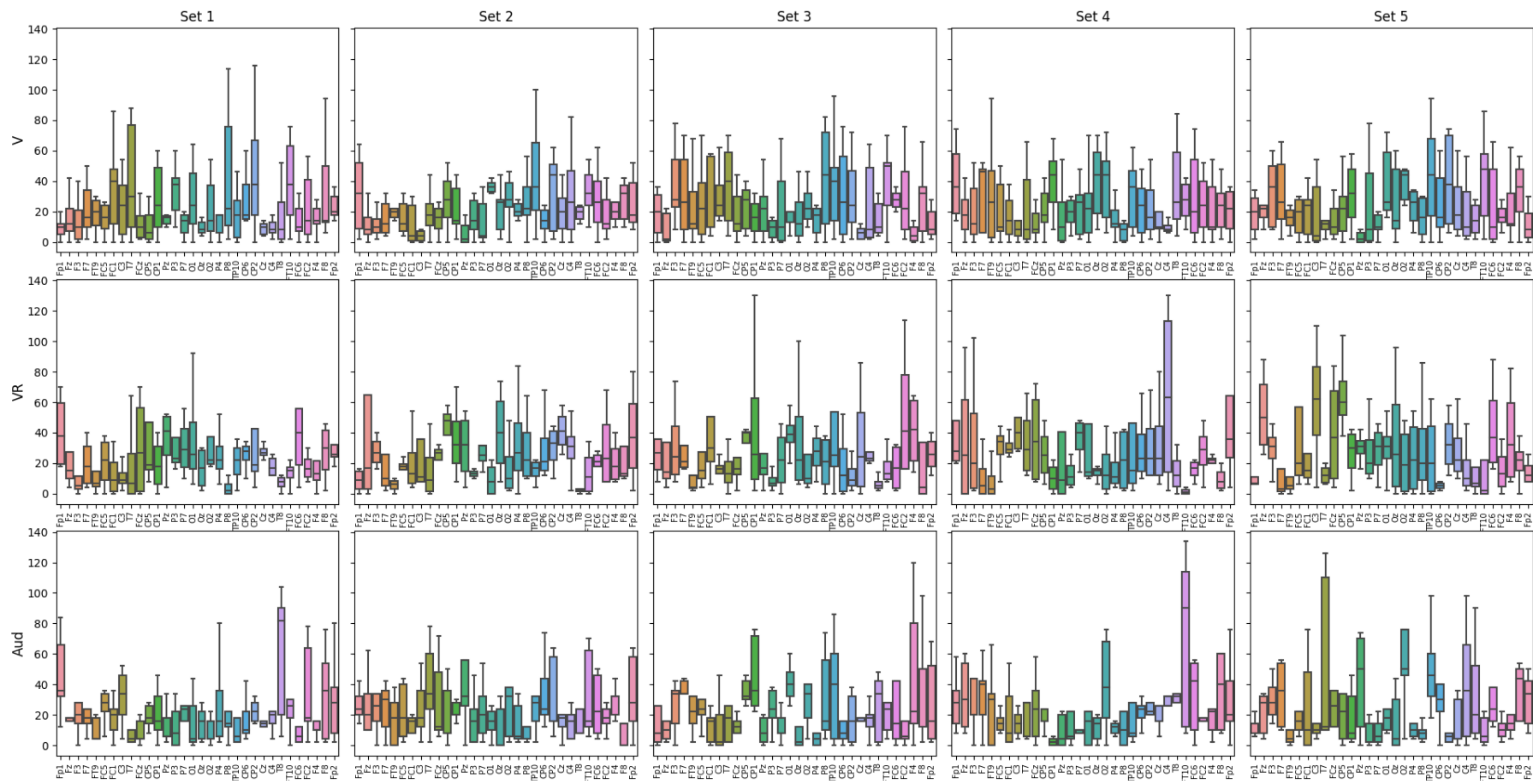


Figure 7.39 - Betweenness Centrality per Set for the Session 1 – SL3 data

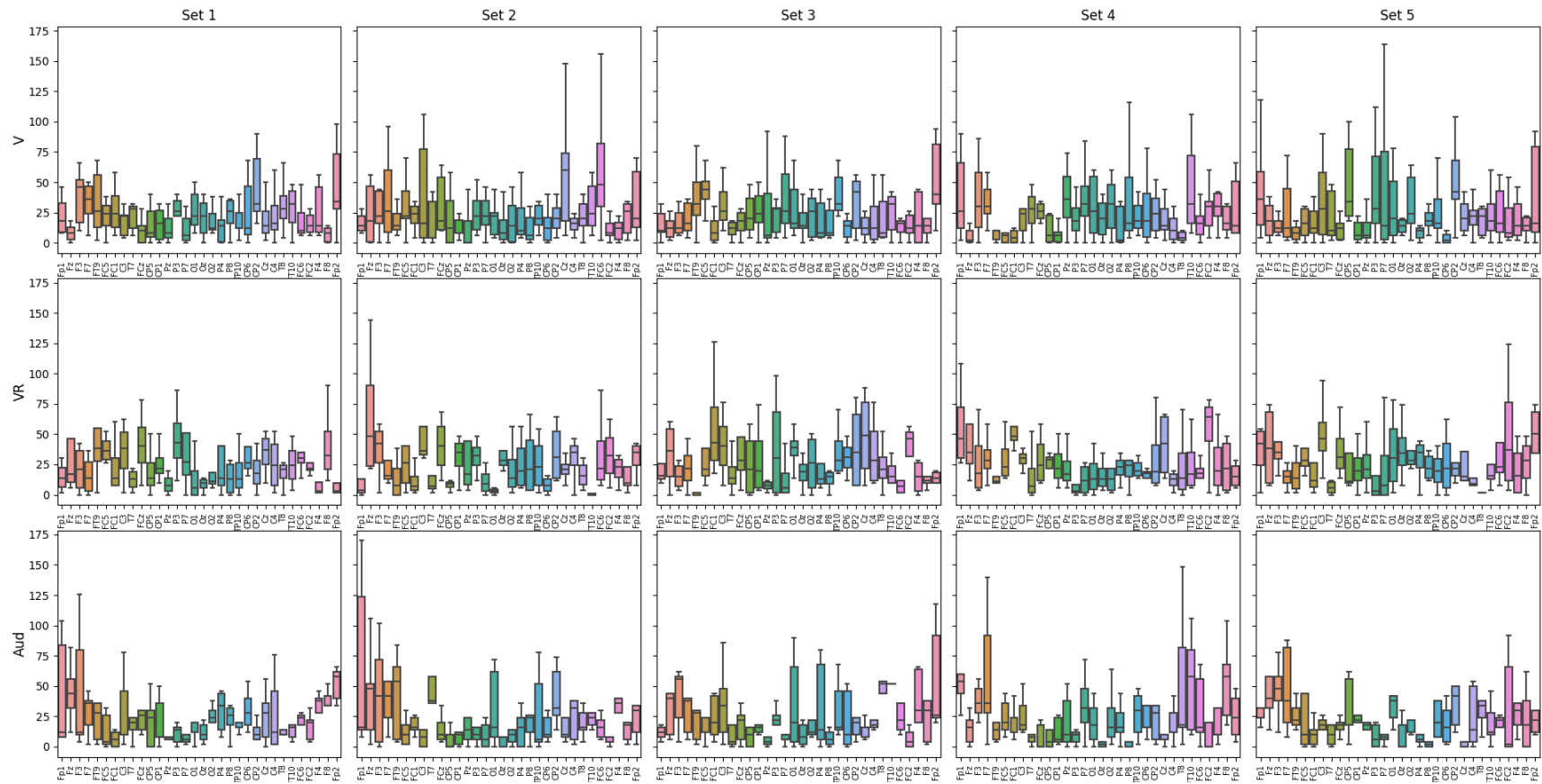


Figure 7.40 - Betweenness Centrality per Set for the Session 2 – SL3 data

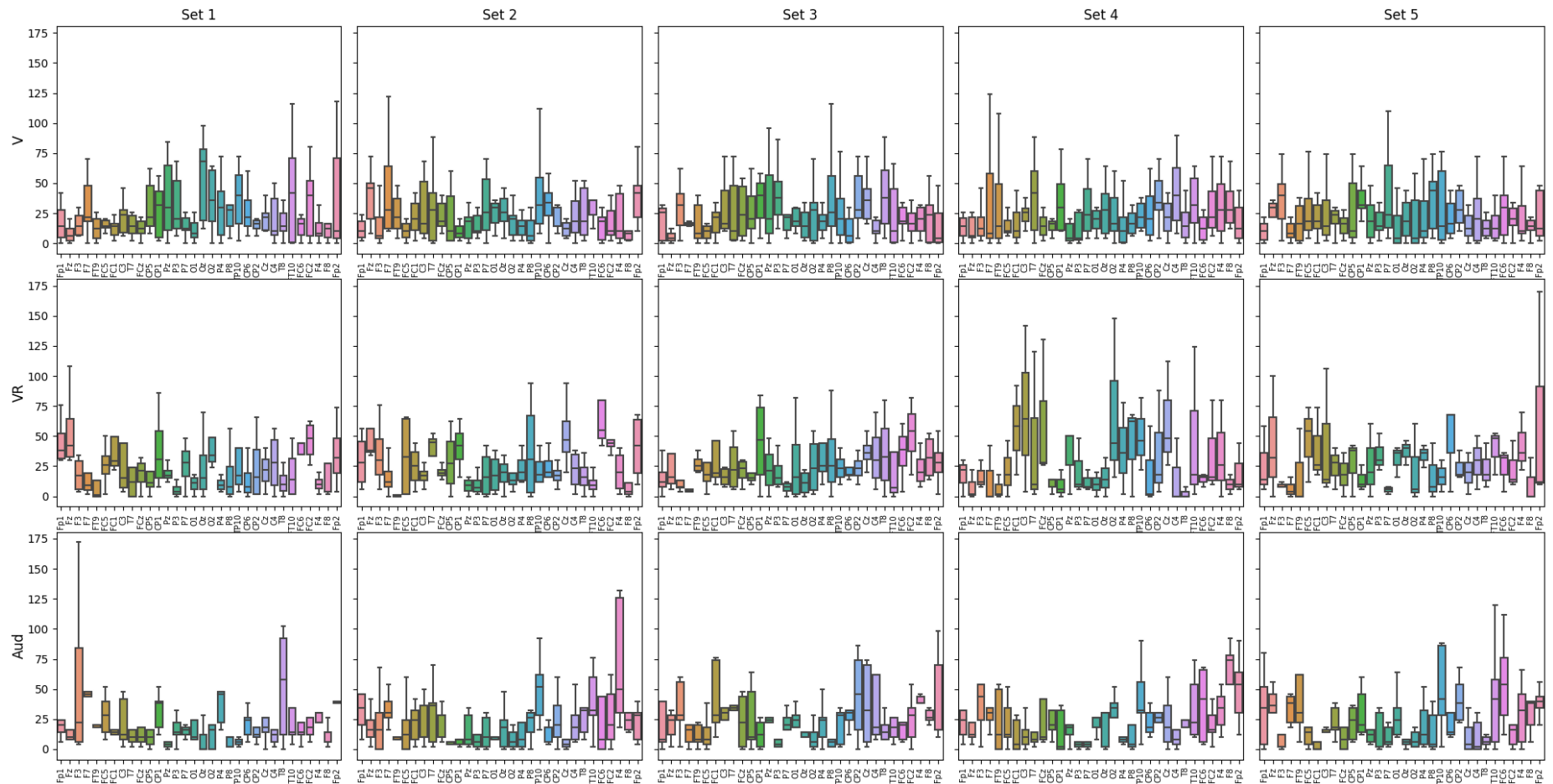


Figure 7.41 - Betweenness Centrality per Set for the Session 3 – SL3 data

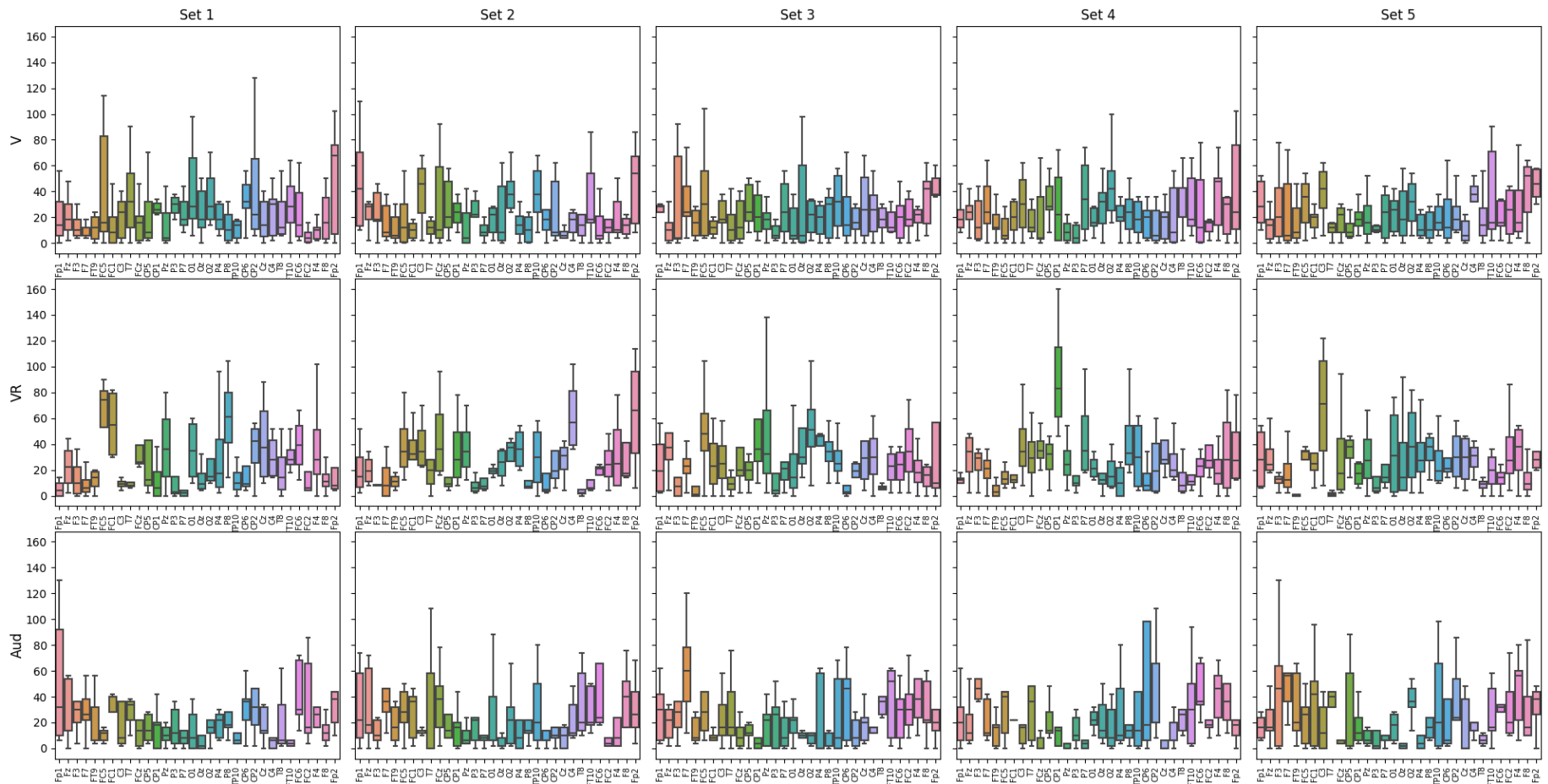


Figure 7.42 - Betweenness Centrality per Set for the Session 4 – SL3 data

7.3.2.2 Strength

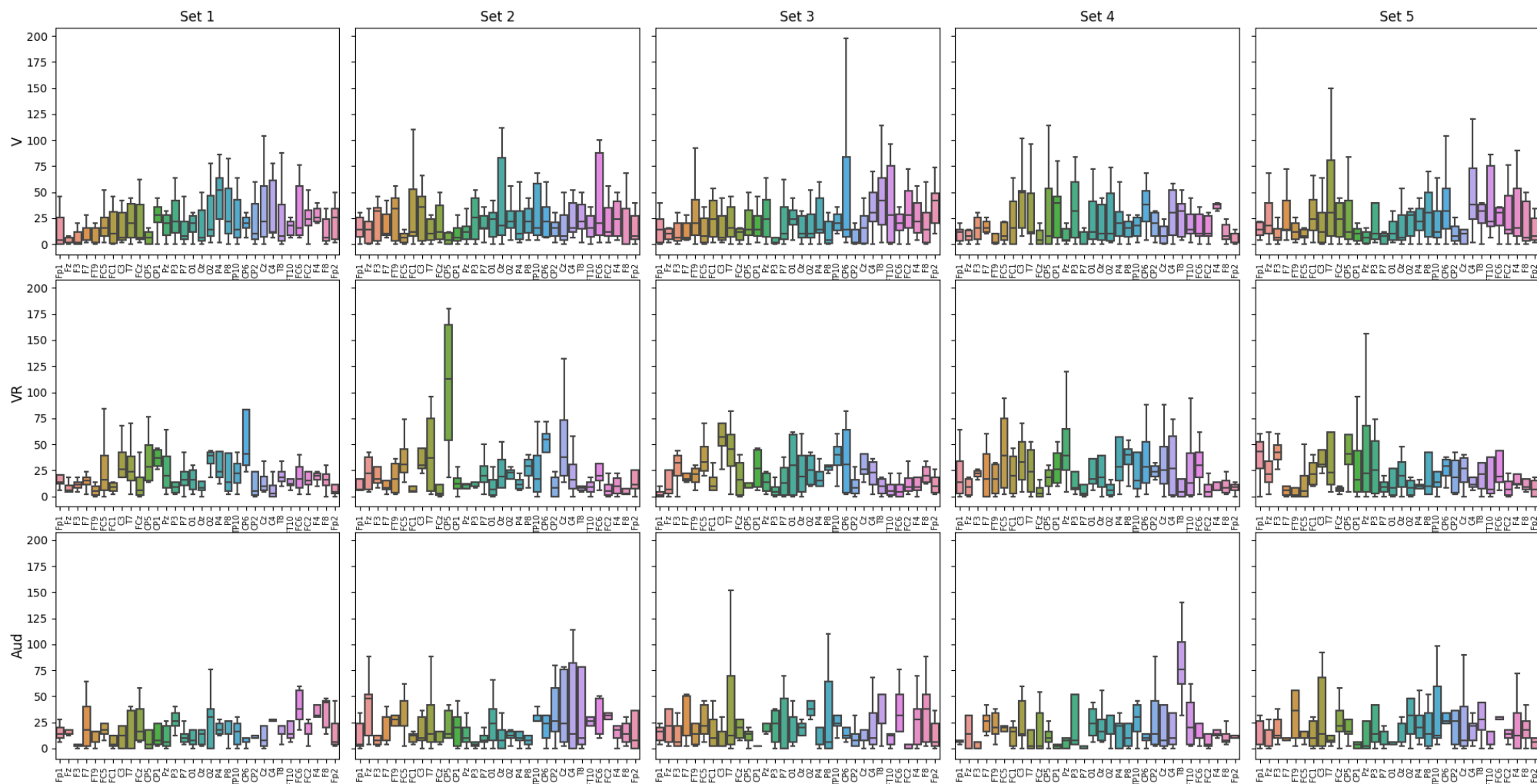


Figure 7.43 - Strength per Set for the Session 1, with avgREF data.

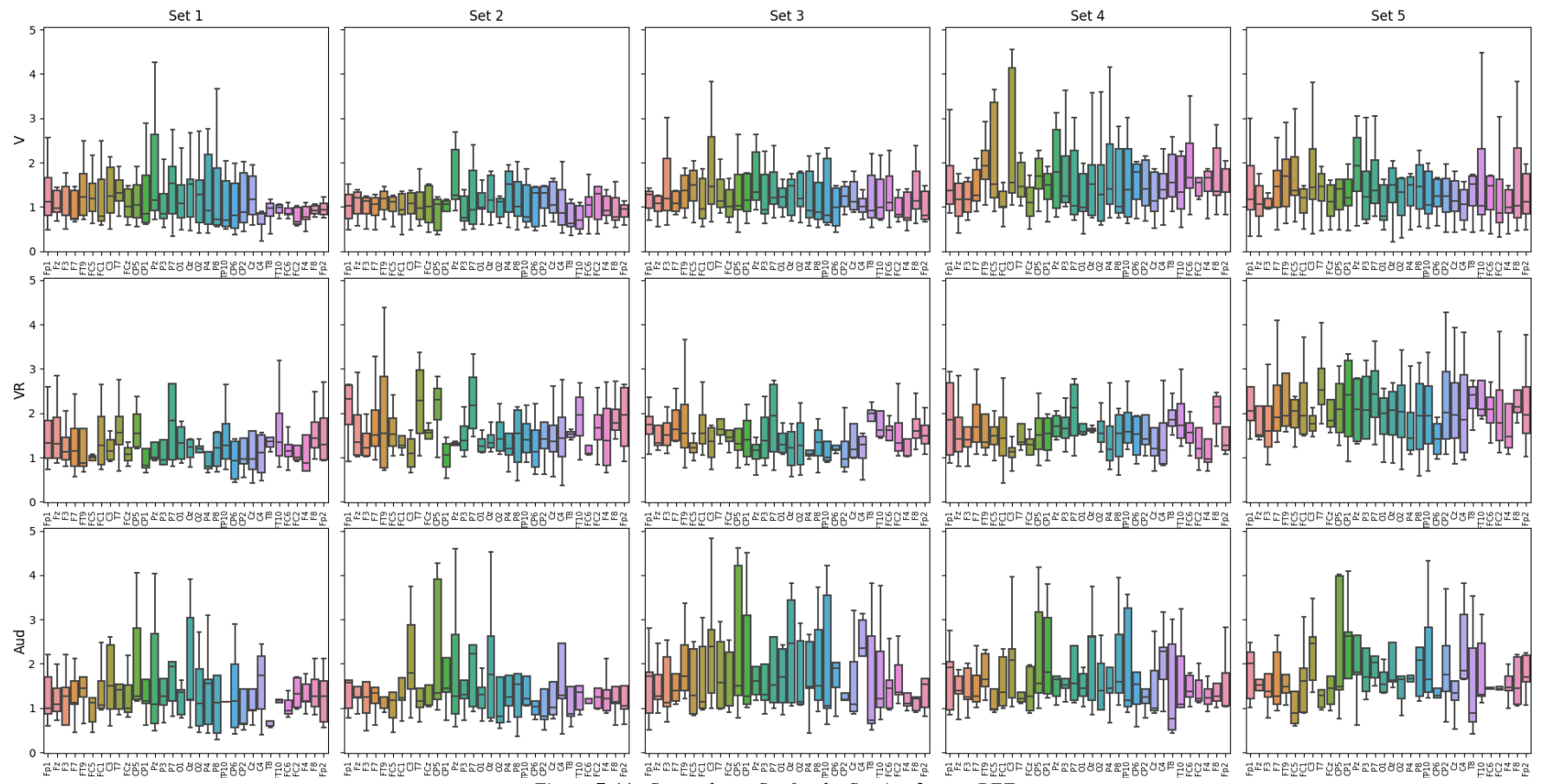


Figure 7.44 - Strength per Set for the Session 2 – avgREF

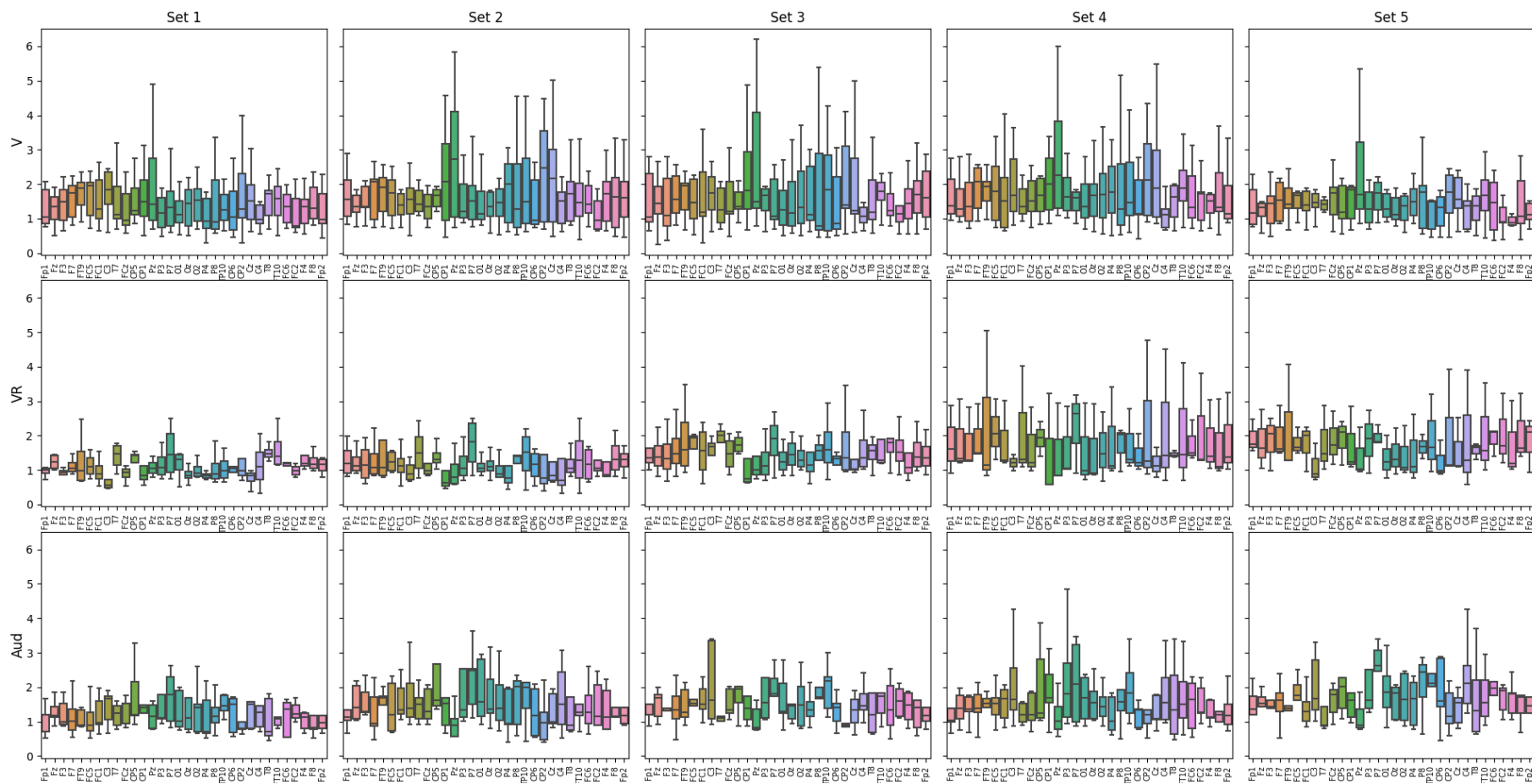


Figure 7.45 - Strength per Set for the Session 3 – avgREF

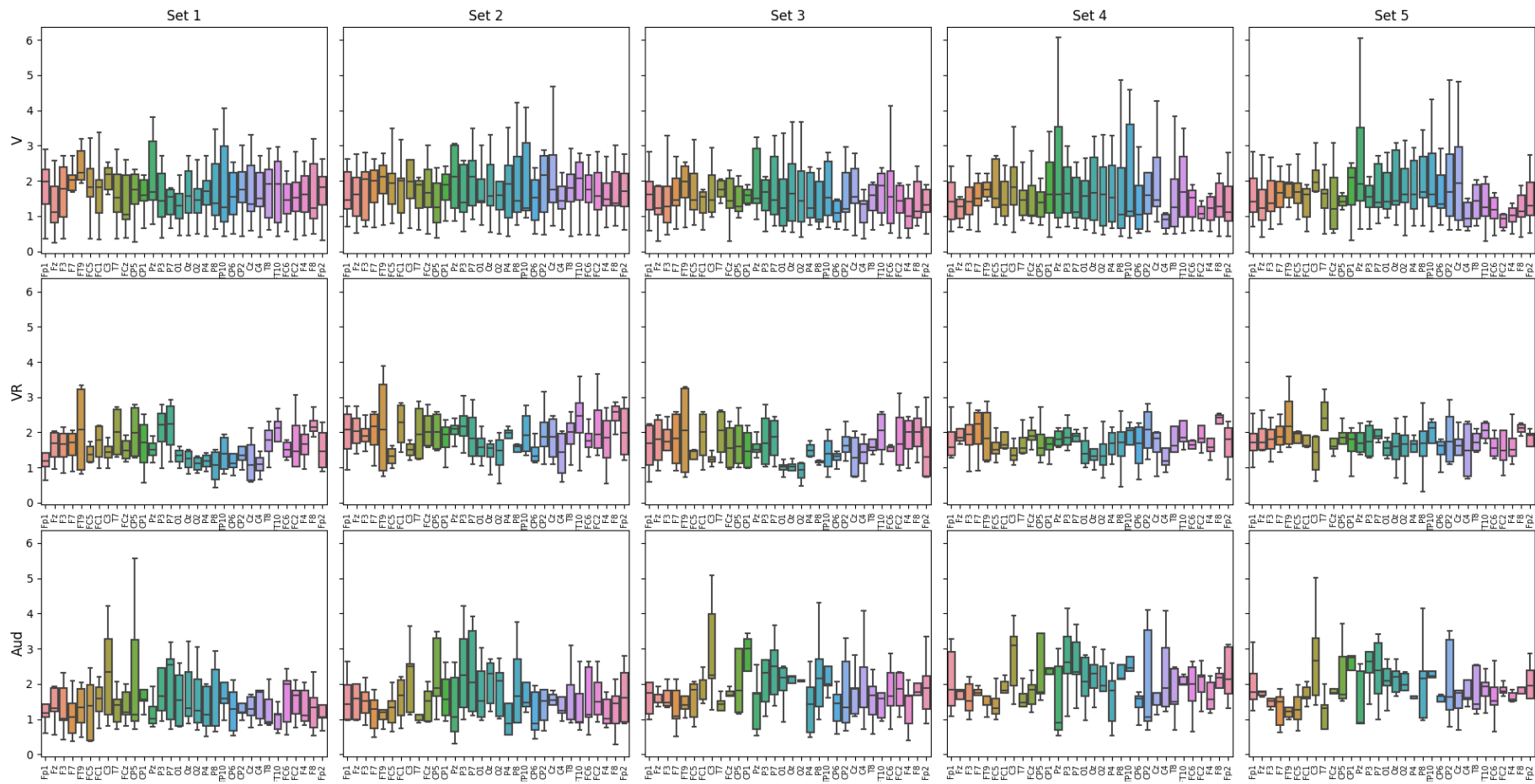


Figure 7.46 - Strength per Set for the Session 4 – avgREF

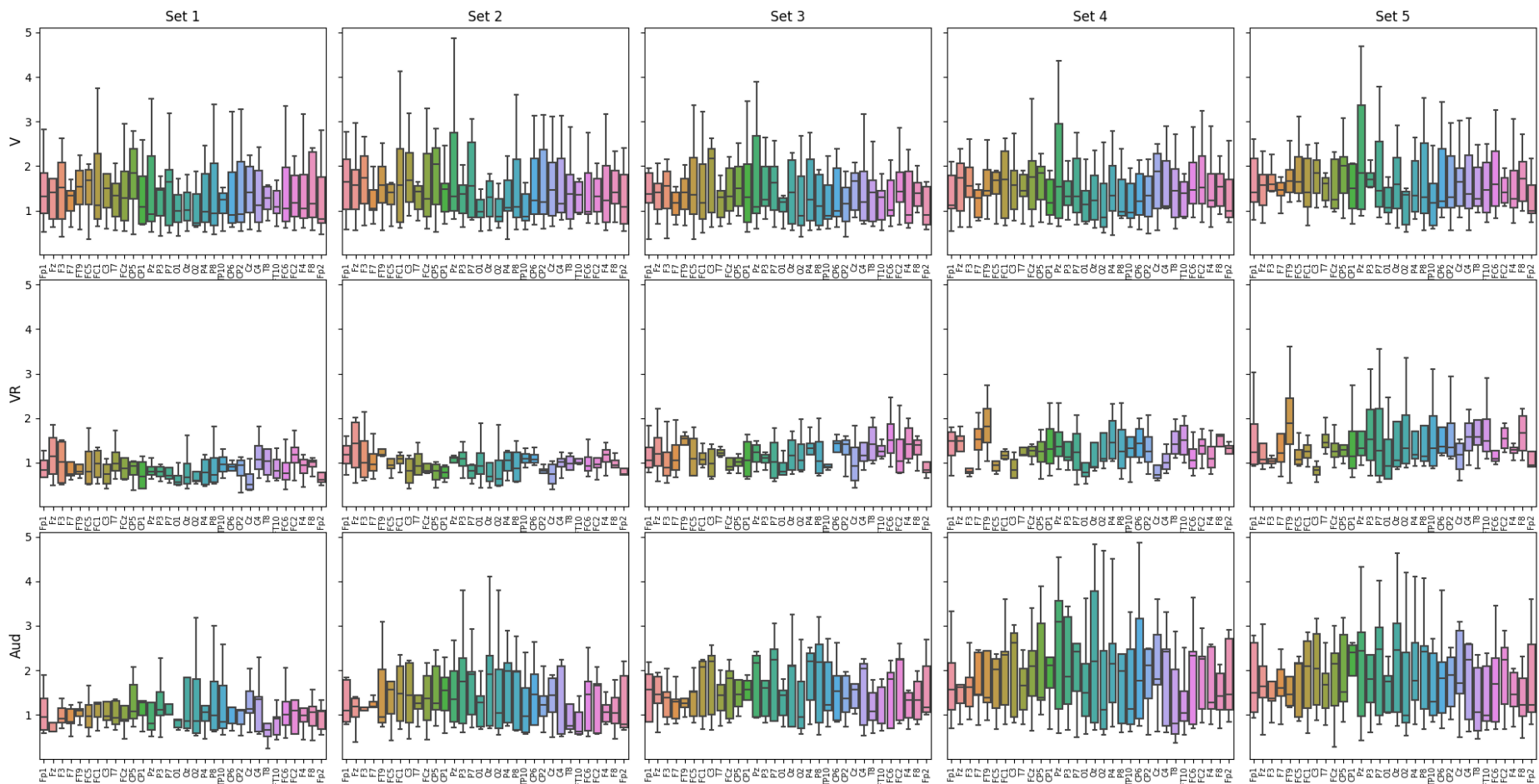


Figure 7.47 - Strength per Set for the Se7ssion 1 – SLA data

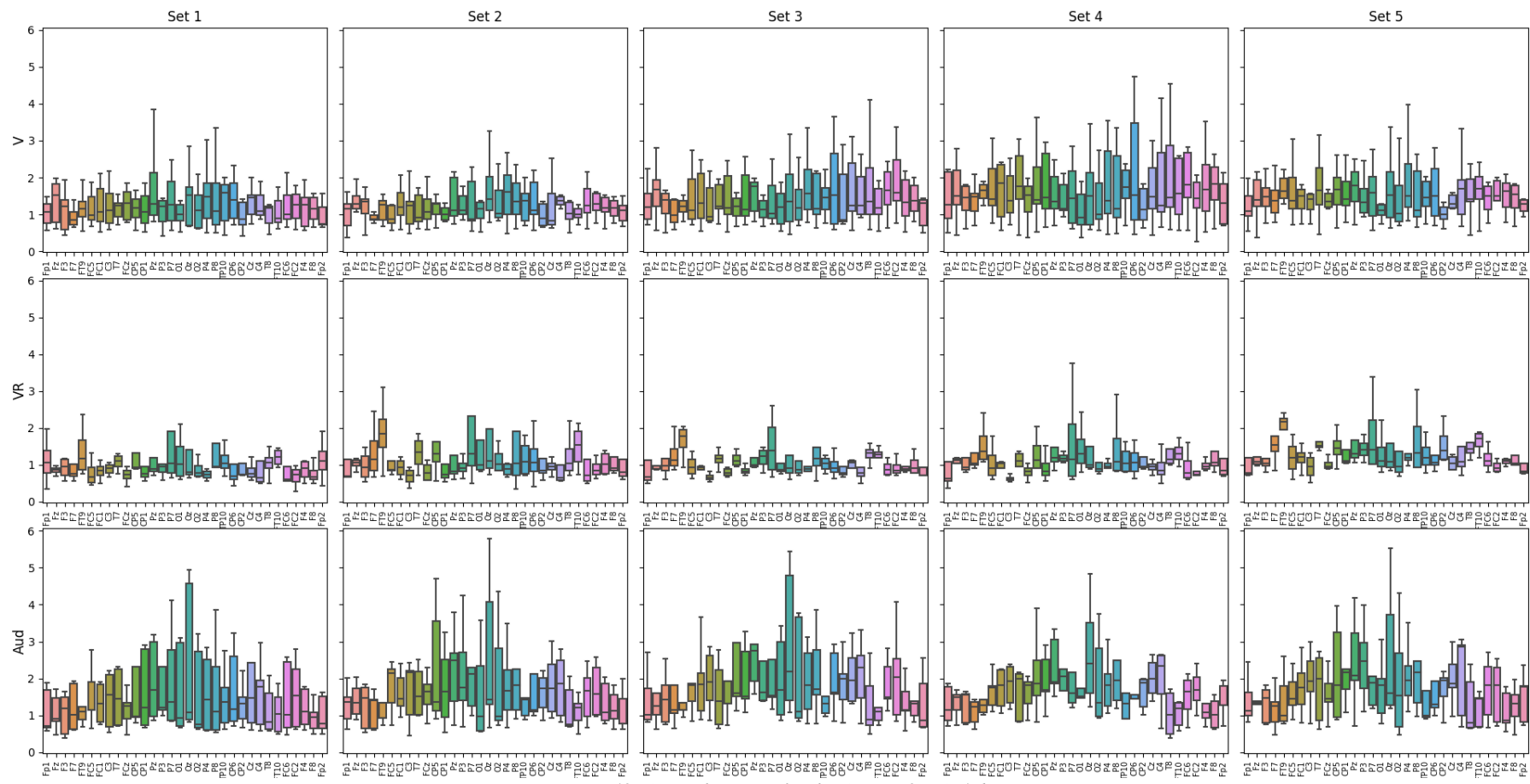


Figure 7.48 -Strength per Set for the Session 2 – SL4 data

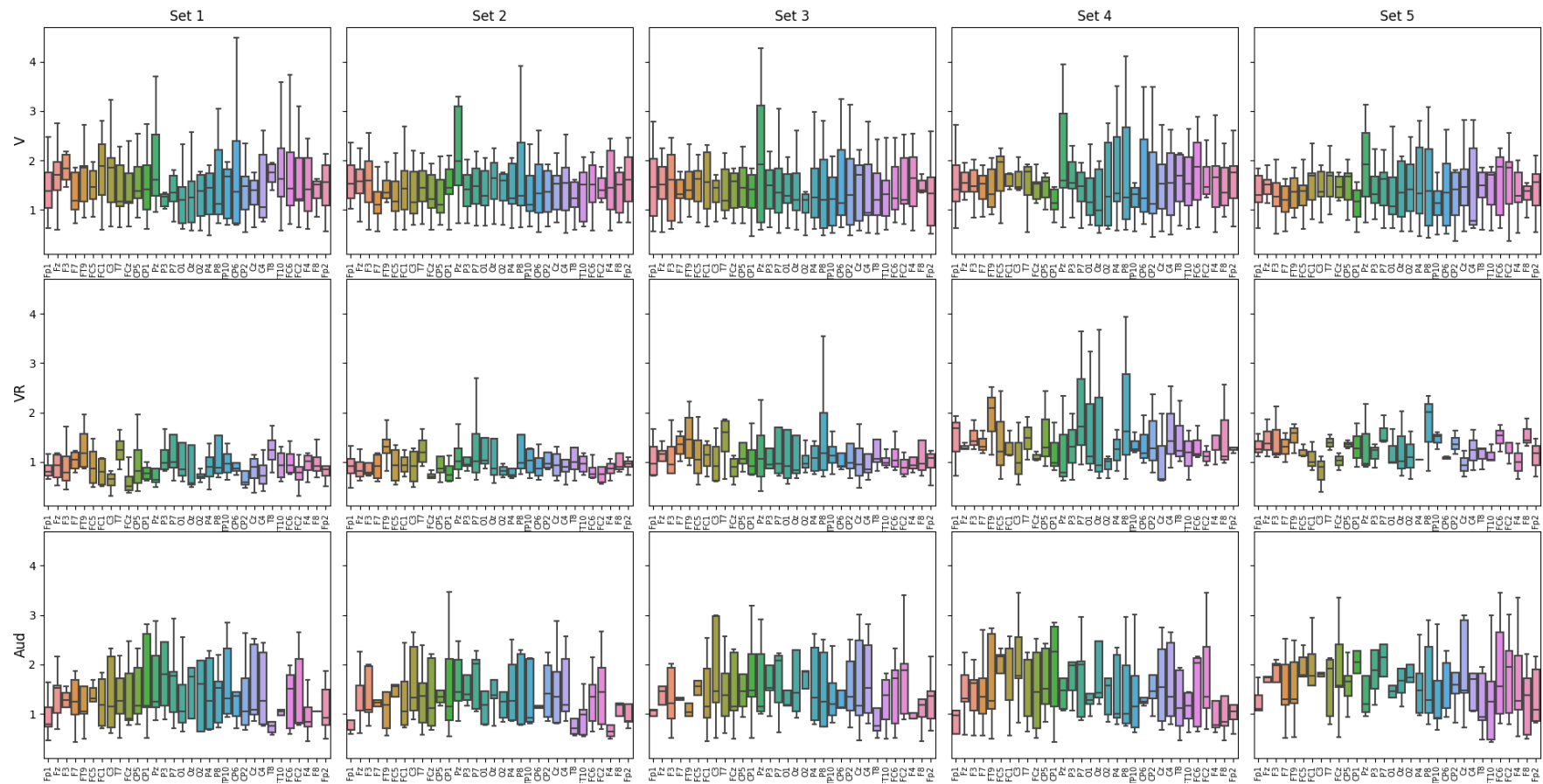


Figure 7.49 - Strength per Set for the Session 3 – SL4 data

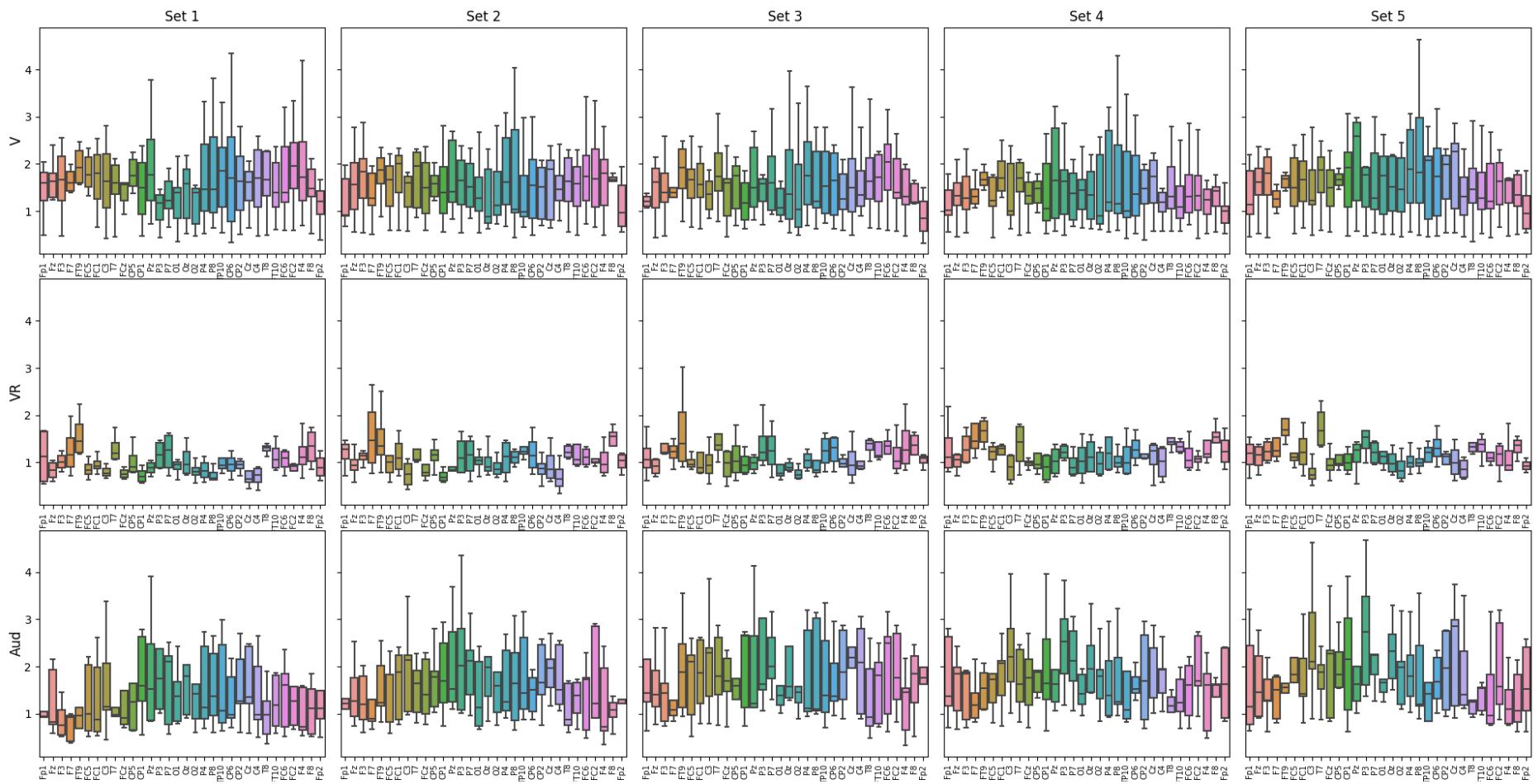


Figure 7.50 - Strength per Set for the Session 4 – SLA data

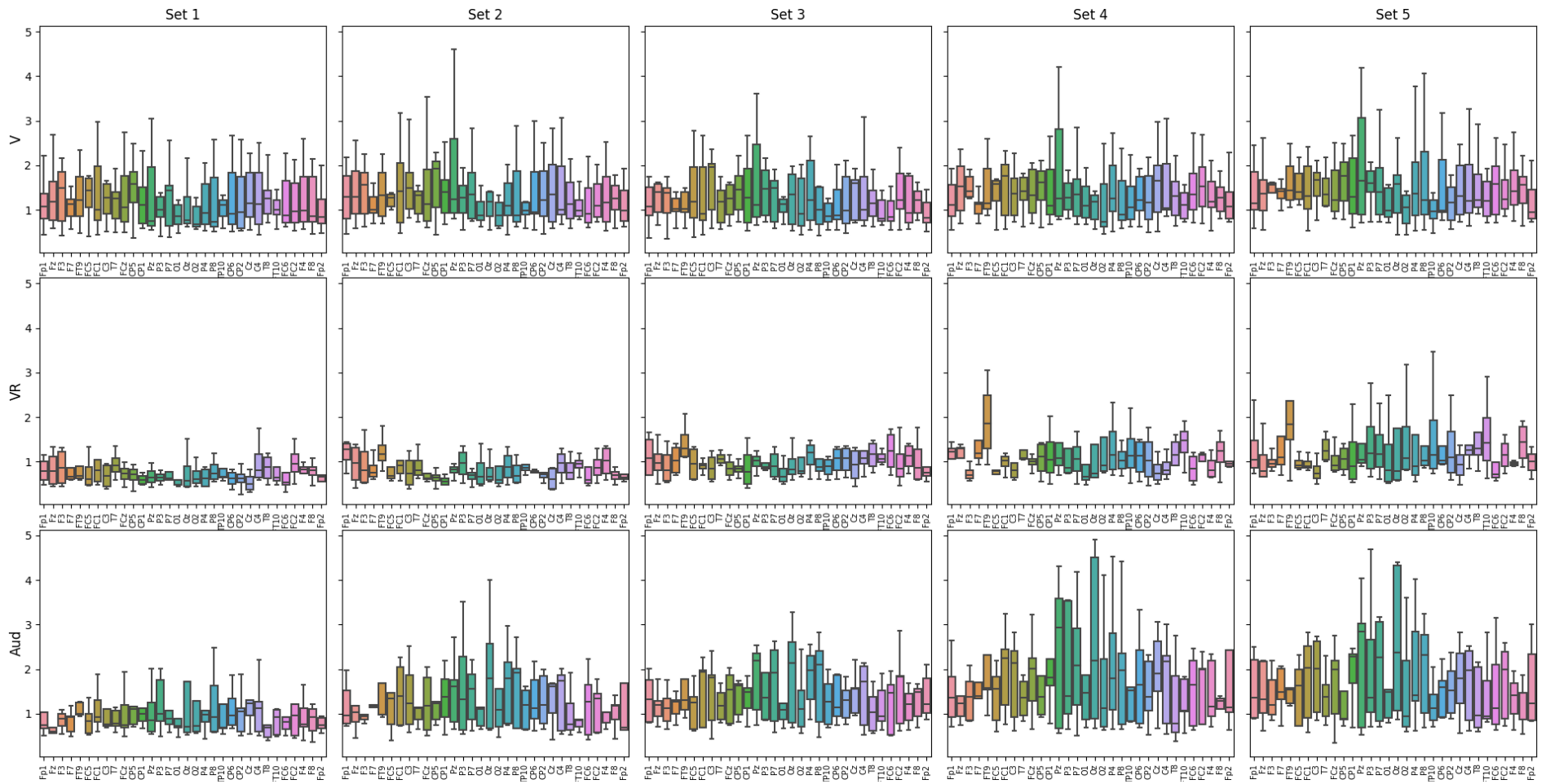


Figure 7.51 - Strength per Set for the Session 1 – SL3 data

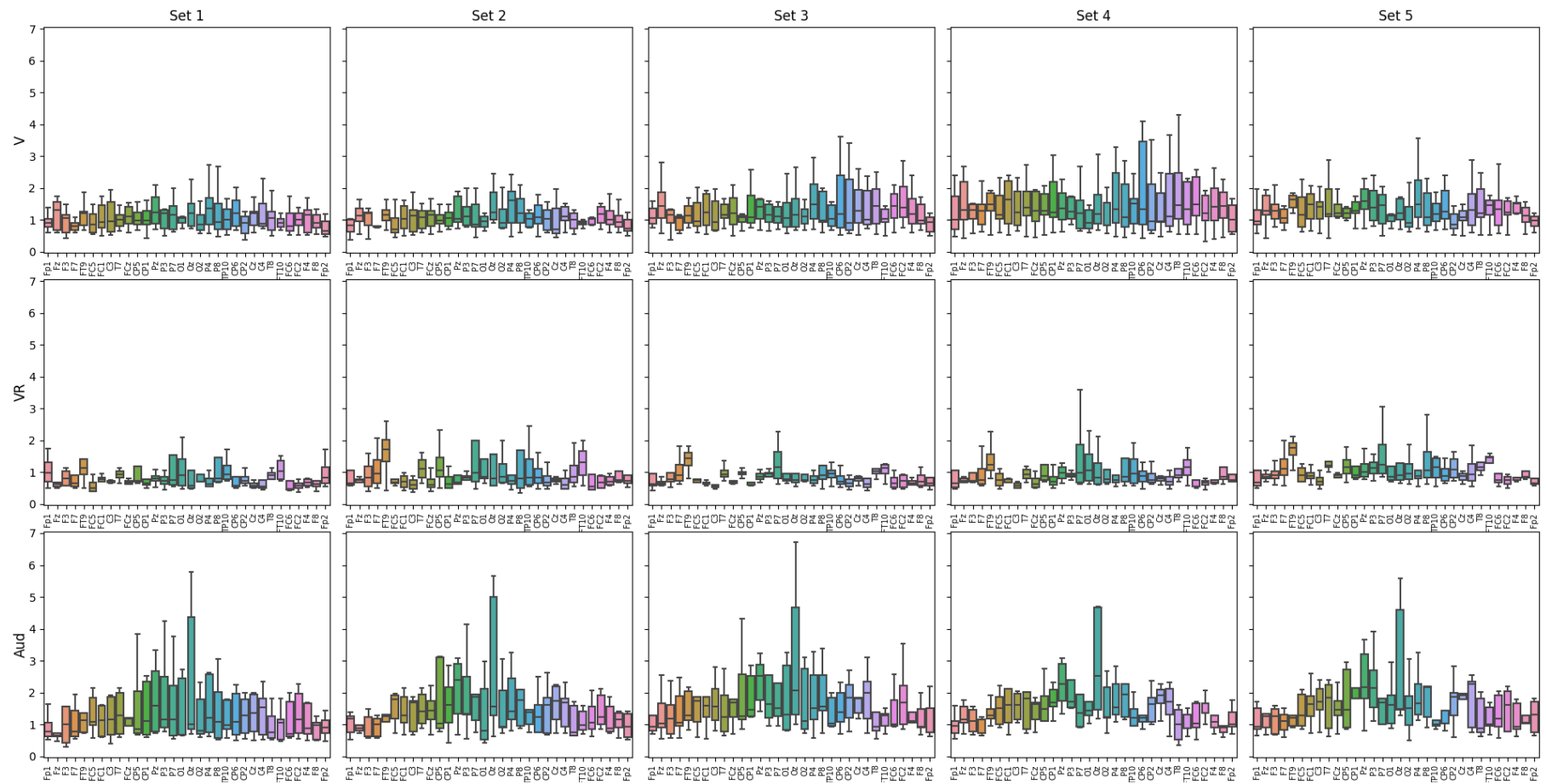


Figure 7.52 - Strength per Set for the Session 2 – SL3 data

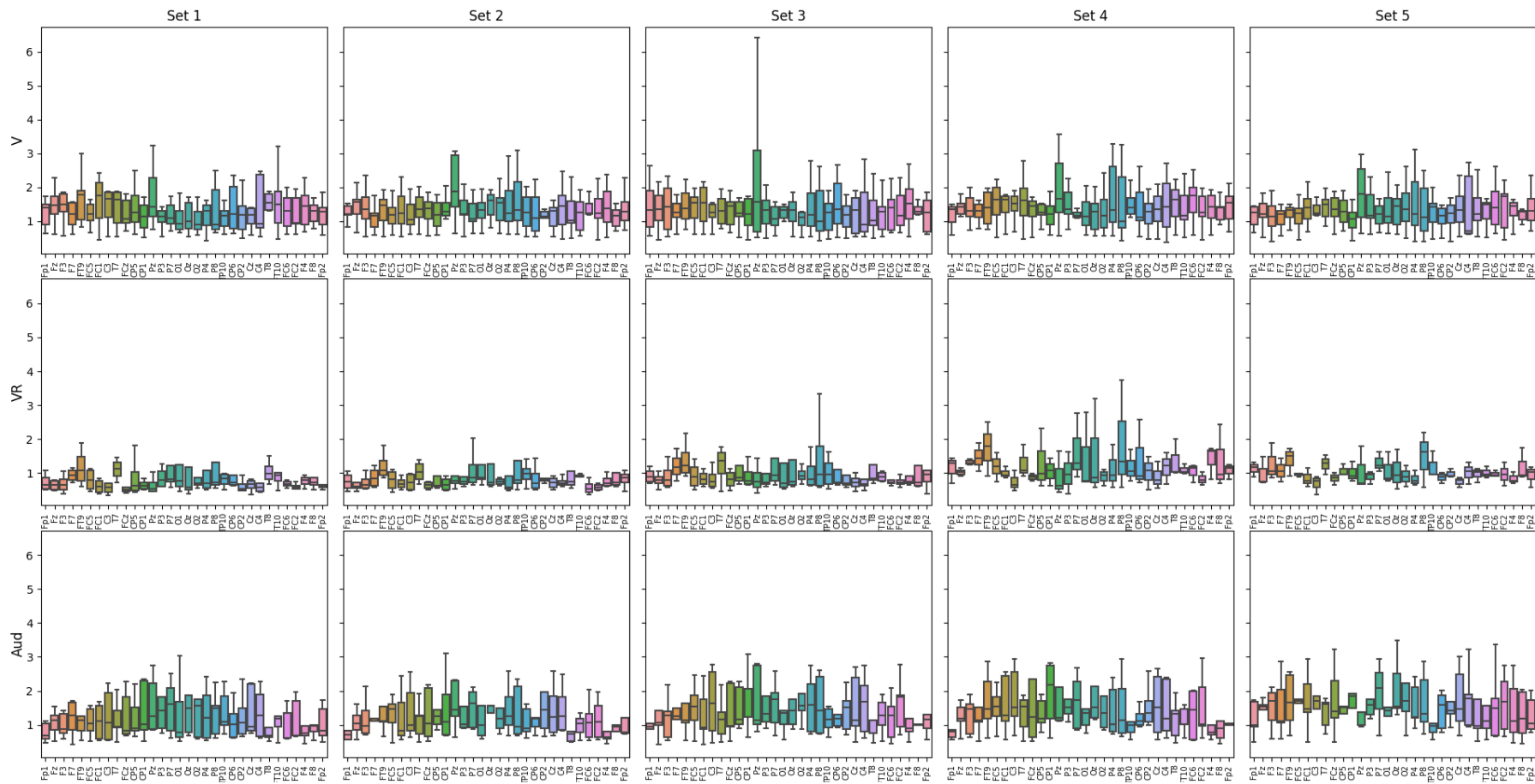


Figure 7.53 - Strength per Set for the Session 3 – SL3 data

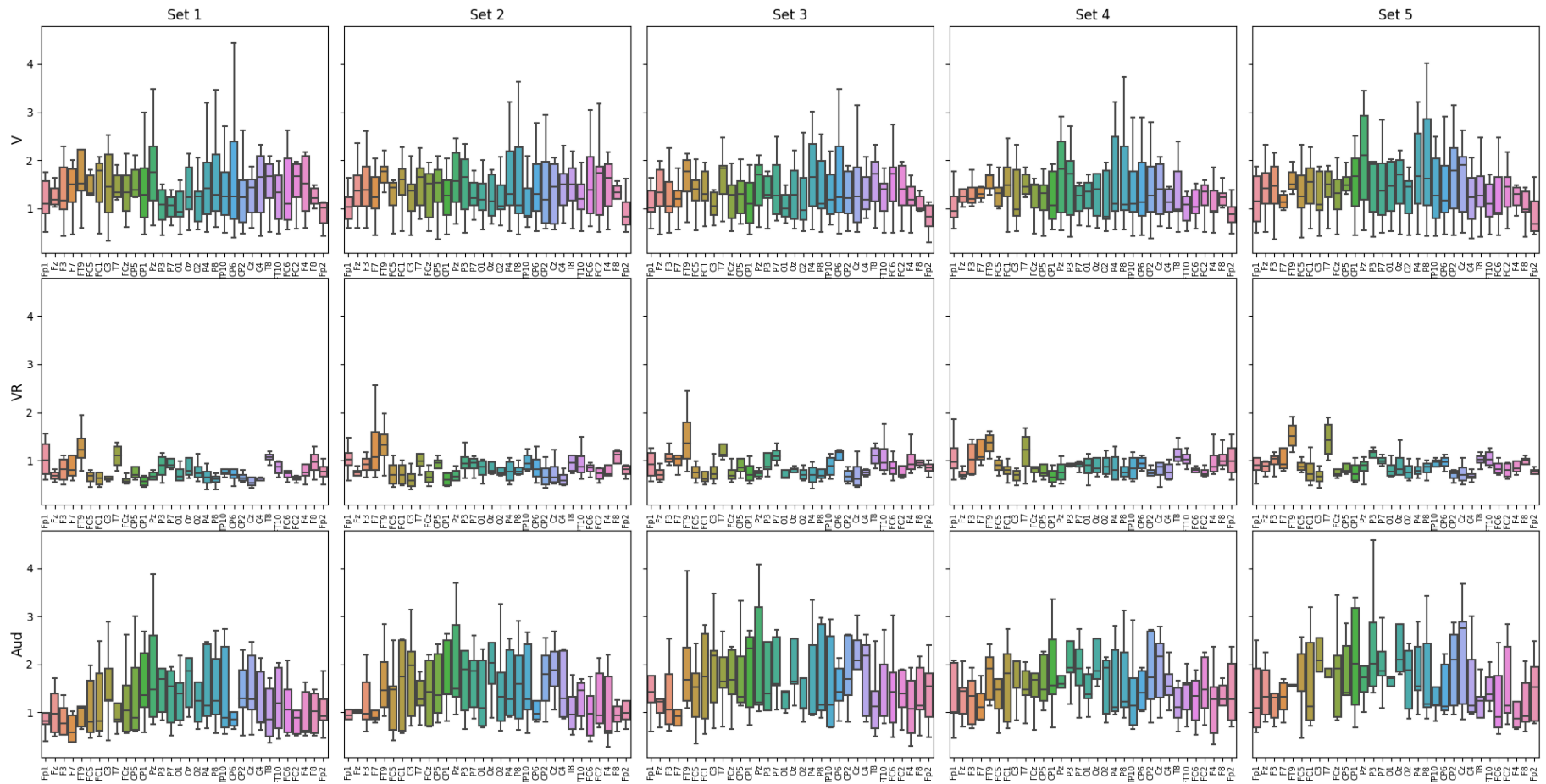


Figure 7.54 - Strength per Set for the Session 4 – SL3 data

7.3.2.3 Transitivity

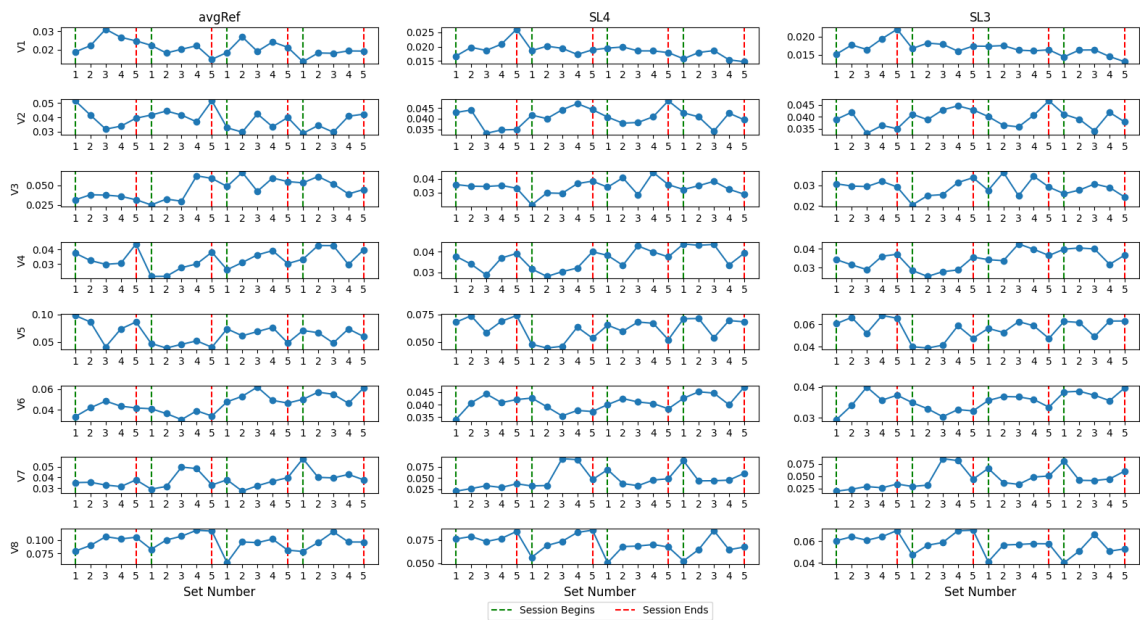


Figure 7.55- Per-Set Transitivity for the Visual NF-training group

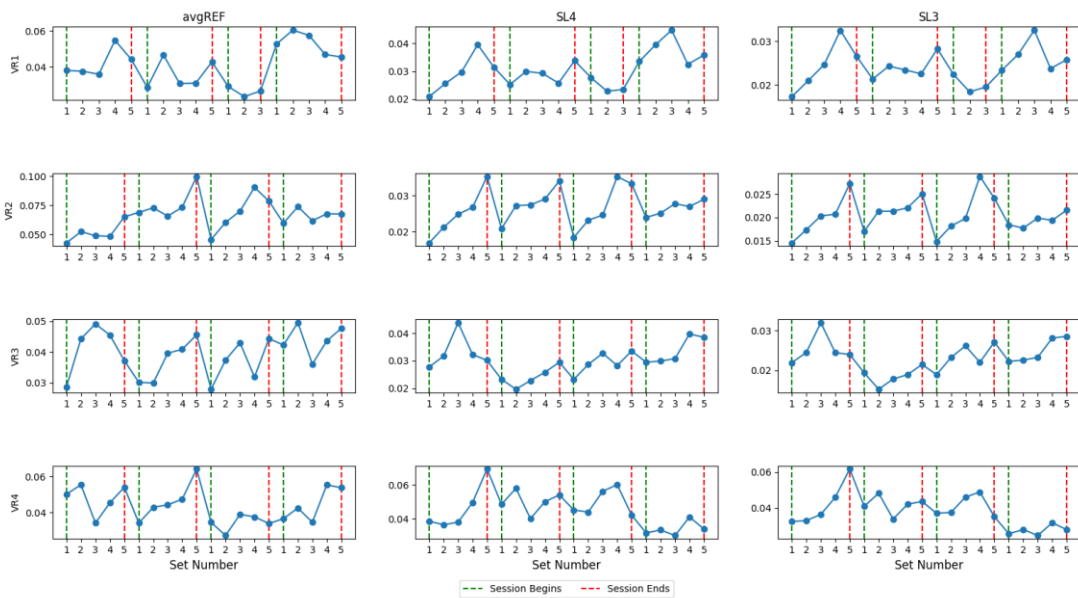


Figure 7.56 - Per-Set Transitivity for the VR NF-training group

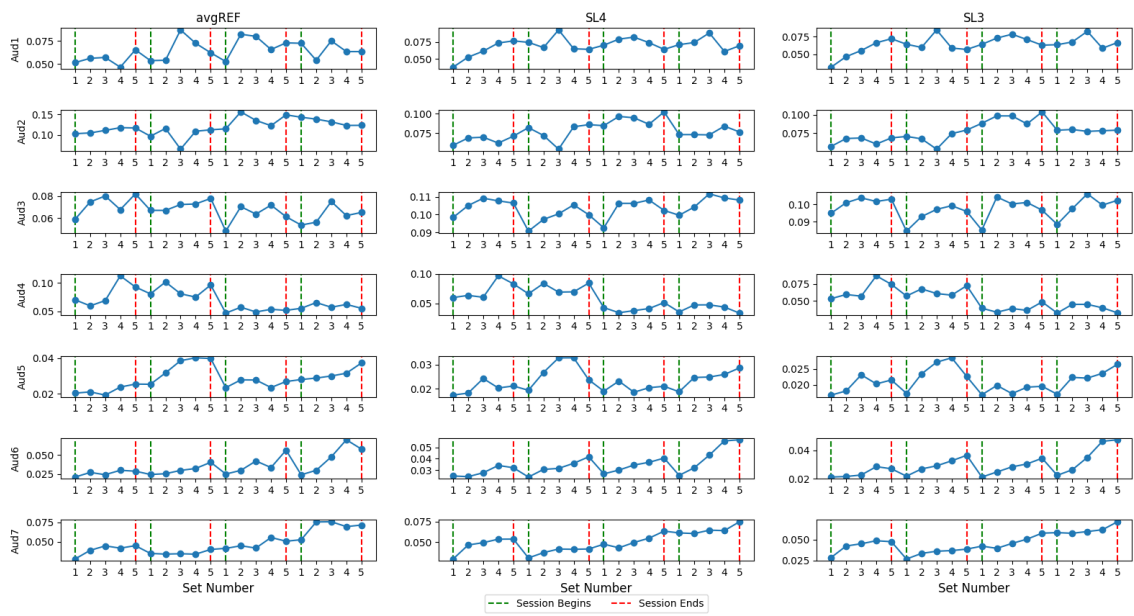


Figure 7.57 - Per-Set Transitivity for the Transitivity NF-training group

7.3.2.4 Charpath

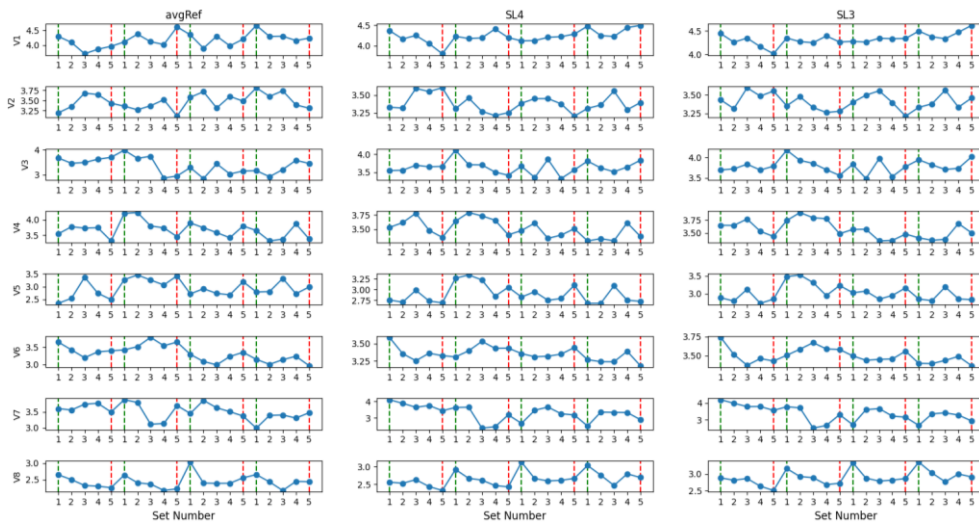


Figure 7.58 - Per-Set Charpath for the Visual NF-training group

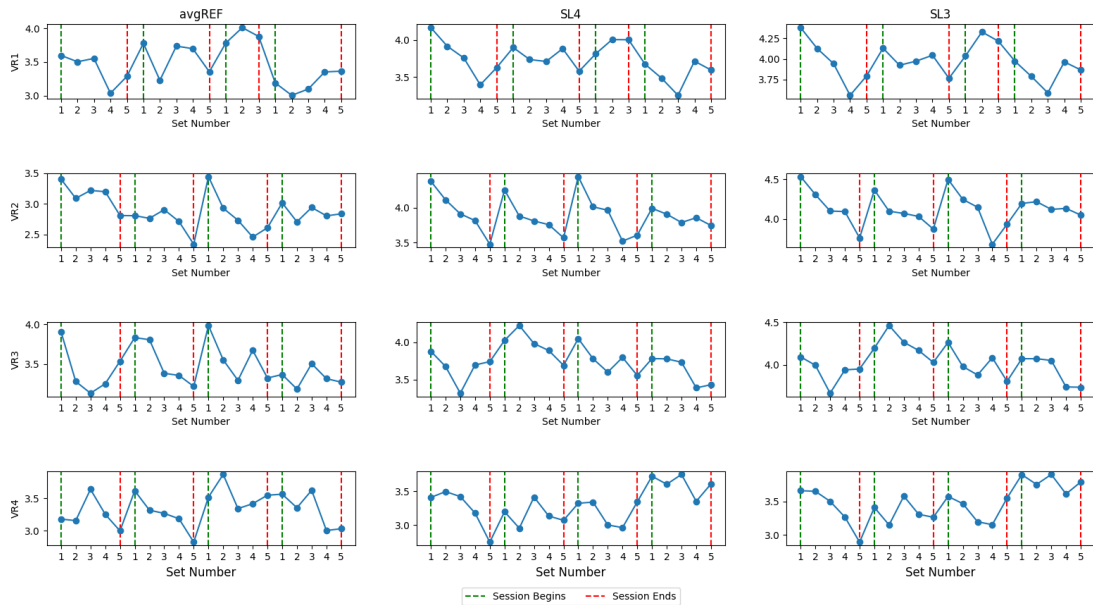


Figure 7.59 - Per-Set Charpath for the VR NF-training group

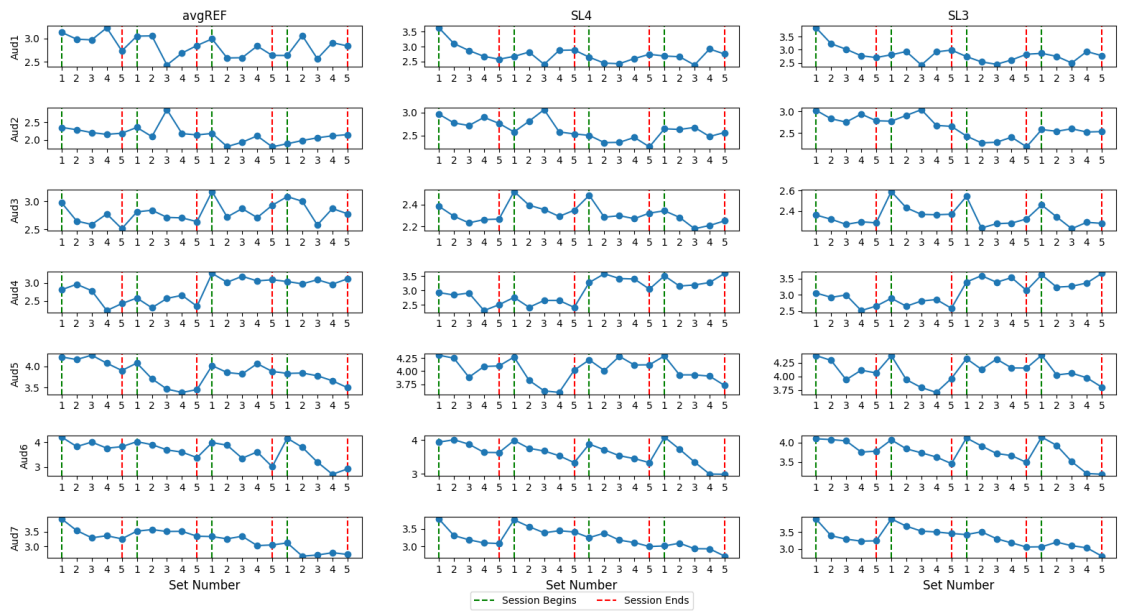


Figure 7.60-Per-Set Charpath for the Auditory NF-training group

7.3.2.5 GE

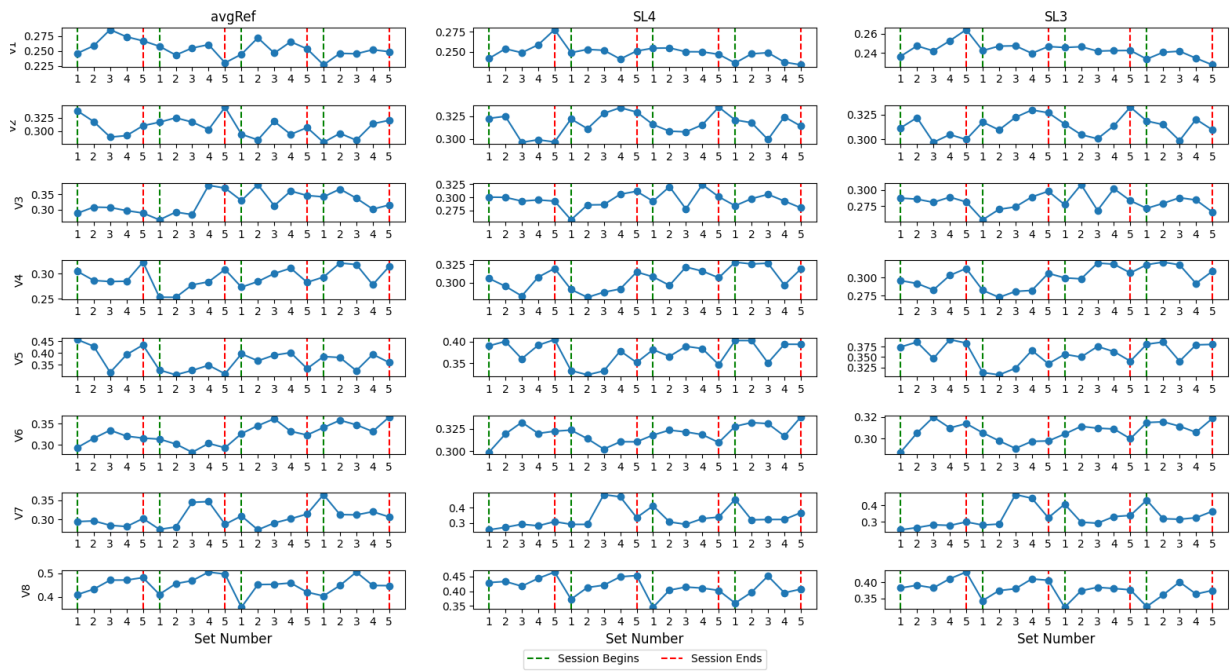


Figure 7.61 - Per-Set GE for the Visual NF-training group

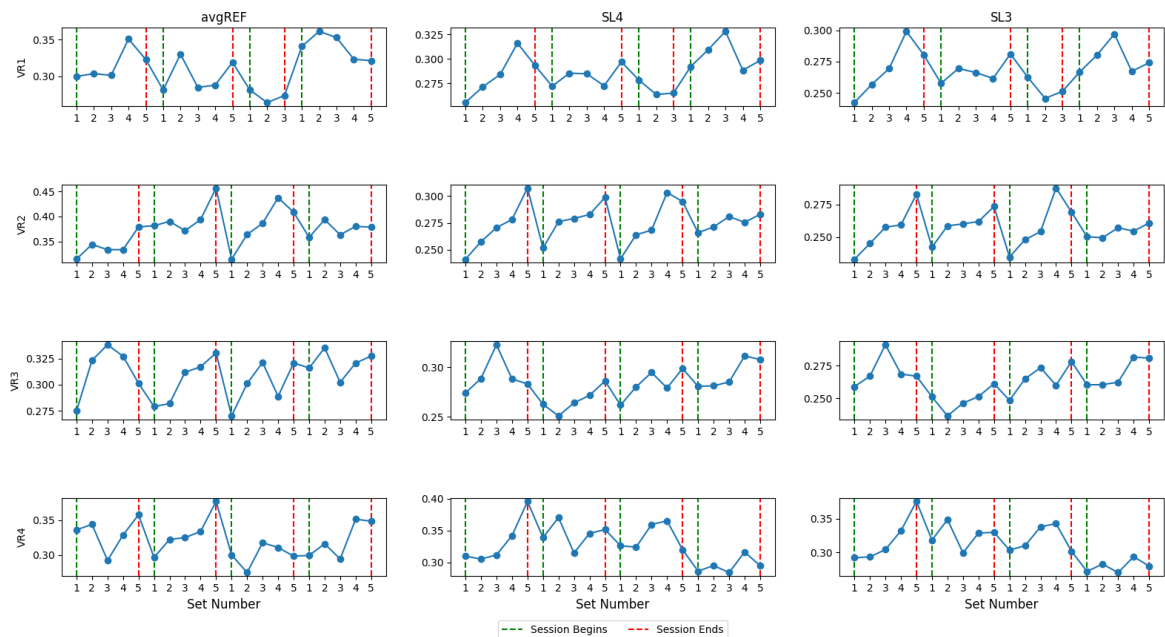


Figure 7.62 - Per-Set GE for the VR NF-training group

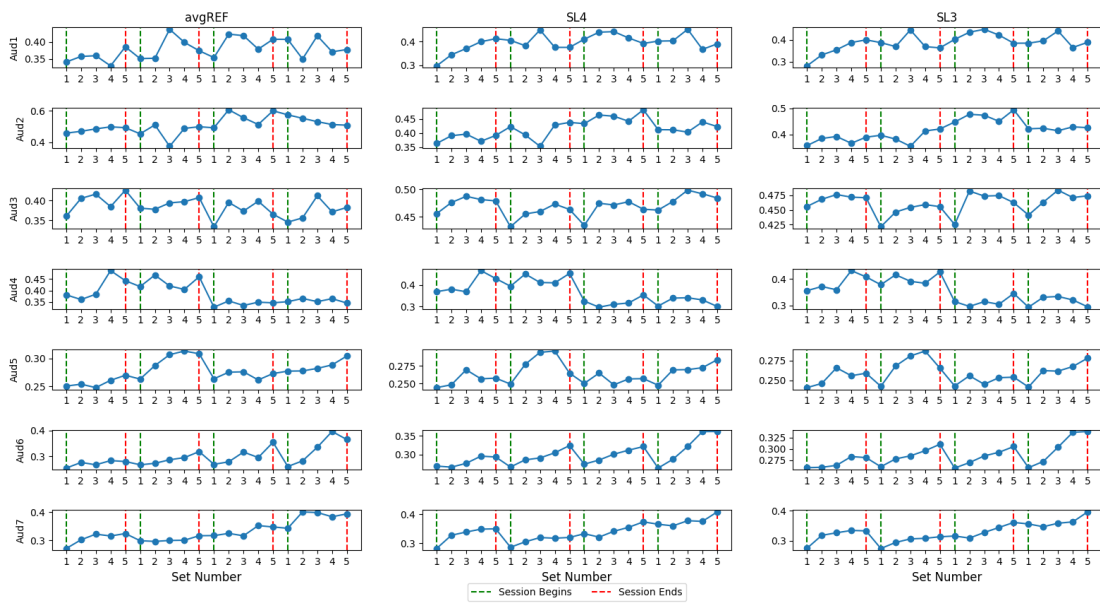


Figure 7.63 - Per-Set GE for the Auditory NF-training group